Study on Polyhedral Oligomeric Silsesquioxane (POSS) Methacrylate-based Copolymers for Biomedical Applications

Suchismita Chatterjee

(Degree)
博士（学術）

(Date of Degree)
2019-09-25

(Date of Publication)
2020-09-01

(Resource Type)
doctoral thesis

(Report Number)
甲第7606号

(URL)
https://hdl.handle.net/20.500.14094/D1007606

Study on Polyhedral Oligomeric Silsesquioxane (POSS) Methacrylate-based Copolymers for Biomedical Applications
(生医学材料応用に向けたかご型シルセスキオキサン(POSS)共重合体に関する研究)

By

Suchismita Chatterjee

Dissertation Submitted

To

Kobe University

In Partial Fulfillment of The Requirements for The Degree of

Doctor of Philosophy

Under Supervision and Guidance of

Prof. Dr. Tooru Ooya

Associate Professor

Graduate School of Engineering

Kobe University

Japan

July, 2019

Referee in Chief:	**Associate Professor**	**Dr. Tooru Ooya** Kobe University
Referees:	**Professor**	**Dr. Naoto Ohmura** Kobe University
	Professor	**Dr. Hideto Minami** Kobe University
	Professor	**Dr. Takashi Nishino** Kobe University

Table of Contents

Acknowledgements 1

Abstracts 3

Abbreviations 7

Chapter 1

General Introduction

1-1. Background of the Research 9

1-1. 1. The coating materials for cardiovascular device 11

1-1. 2. Biomaterials for drug delivery 13

1-1.3. Concept of "element block" and "element block"-copolymer 16

1-2. Scope of the Research 17

1-2.1. Self-assembling of polymeric biomaterials 19

1-2.2. Polymeric Micelle and application in drug delivery 20

1-2.3. Phospholipid 2-methacryloyloxyethyl phosphorylcholine (MPC) 23

1-2.4. Polyhedral oligomeric silsesquioxane (POSS): "element block" 24

1-2.5. Radical polymerization 25

1-2.6. Reversible/Addition-Fragmentation Chain Transfer (RAFT) polymerization 27

Reference 31

Chapter 2

Synthesis and characterization of POSS-based amphiphilic copolymers

2-1. Introduction **35**

2-2. Experimental Section **37**

2-2.1. Material 37

2-2.2. Synthesis of methacrylate POSS and MPC random copolymers by free radical polymerization technique 37

2-2.2.1. Synthesis of silsesquioxane partial cages (1a-c) 37

2-2.2.2. Synthesis of polyhedral oligomeric silsesquioxanes (POSS)-based methacrylate (MA) (2a-c) 37

2-2.2.3. Synthesis of POSS methacrylate (MA) - MPC random copolymers (R-POSS-MA-*ran*-MPC) (3a-c) 38

2-2.3. Synthesis of POSS and MPC copolymer by RAFT polymerization technique 40

2-2.3.1. Preparation of poly(2-(methacryloyloxy)ethyl phosphorylcholine)-based chain transfer agent ($PMPC_{61}$) 40

2-2.3.2. Preparation of MPC-*block*-R-POSS-MA block copolymer (3a'-c') 40

2-2.4. Characterization of POSS and MPC copolymers synthesized by free radical and RAFT polymerization technique 42

2-2.4.1. Characterization of POSS and MPC copolymers (3a-c) synthesized by free radical polymerization technique 42

2-2.4.2. Characterization of POSS and MPC di-block copolymers (3a'-c') synthesized by RAFT polymerization technique 43

2-3. Results and Discussion **44**

2-3.1. Synthesis and characterization of R-POSS MA and MPC copolymers (3a-c) synthesized by free radical polymerization technique 44

2-3.2. Synthesis and characterization of R-POSS and MPC di-block copolymers (3a'-c') synthesized by RAFT polymerization technique 51

2-4. Conclusion **55**

Reference **56**

Chapter 3

"Element Block" R-POSS and 2-(methacryloyloxy)ethyl phosphorylcholine-based random copolymers for a surface coating material

3-1. Introduction **59**

3-2. Experimental Section **60**

3-2.1. Material 60

3-2.2. Measurements of stress-strain behavior of copolymers (3a-c) 60

3-2.3. Film Coating by copolymers (3a-c) 61

3-2.4. Water contact angle measurements of the copolymers (3a-c) coated surface 61

3-2.5. Protein adsorption on the copolymers (3a-c) coated surface 61

3-2.6. Cell attachment on the copolymer (3a) coated surface 62

3-3. Results and Discussion **62**

3-3.1. Stress-strain behavior of the random copolymers (3a-c) 62

3-3.2. Morphology observation and characterization of the random copolymers (3a-c) coated surface 66

3-3.3. Surface property: wettability, protein adsorption and cellar attachment 67

3-4. Conclusion 71

Reference 73

Chapter 4

R-POSS and 2-(methacryloyloxy)ethyl phosphorylcholine-based random copolymers as a hydrophobic drug solubilizer in drug delivery

4-1. Introduction 76

4-2. Experimental Section 78

4-2.1. Material 78

4-2.2 Measurements 78

4-2.3 Cytotoxicity of the copolymers (3a-c) 79

4-2.4 Determination of paclitaxel solubility in copolymers (3a-c) solution 80

4-2.5 Preparation of PTX-loaded R-POSS and MPC-based random copolymers assembly (3a-c) 80

4-2.6 Characterization of the R-POSS and MPC-based copolymer assembly 81

4-2.7 Cell viability measurements of PTX-solubilized 3a copolymer 81

4-2.8 Cellular uptake of FITC-PTX solubilized copolymer (3a) 82

4-2.9 *In vitro* release of PTX from copolymer assembly (3a) 84

4-2.10 Statistical analysis 84

4-3. Results and Discussion 84

4-3.1 Characterization of R-POSS and MPC based random copolymers (3a-c) 84

4-3.2 Characterization of PTX-solubilized copolymer (3a-c) assembly 90

4-3.3 Solubility of PTX in copolymers (3a-c) solution 91

4-3.4 Cell viability study of PTX solubilized copolymer (3a) 93

4-3.5 Cellular uptake of FITC labelled PTX solubilized copolymer (3a) 95

4-3.6 *In vitro* release of PTX from the copolymers (3a-c) assemblies 98

4-4. Conclusion 101

Reference 102

Chapter 5

C_2H_5-POSS and 2-(methacryloyloxy)ethyl phosphorylcholine-based random copolymer as a drug carrier for solid formulation

5-1. Introduction 105

5-2. Experimental Section 107

5-2.1 Materials 107

5-2.2 Paclitaxel solid formulation preparation using 3a copolymer and PVP 107

5-2.3 Dissolution study 107

5-2.4 X-ray diffraction (XRD) 108

5-2.5 Fourier transform infrared spectroscopy (FT-IR) 108

5-2.6 Differential scanning calorimetry (DSC) 108

5-3. Results and Discussion 109

5-3.1 Characterization of the solid formulation (3a/PVP/PTX) 109

5-3.2 Dissolution profile of solid formulation (3a/PVP/PTX) 114

5-4. Conclusions 116

Reference 117

Chapter 6

R-POSS and 2-(methacryloyloxy)ethyl phosphorylcholine-based di-block copolymers for hydrophobic drug delivery

6-1. Introduction 121

6-2. Experimental Section 124

6-2.1 Materials 124

6-2.2 Measurements 124

6-2.2.1 Dynamic light scattering (DLS) 124

6-2.2.2 Static light scattering (SLS) 125

6-2.2.3 Electrophoretic light scattering (ELS) 126

6-2.2.4 Transmission electron microscopy (TEM) 126

6-2.2.5 Preparation of micelles and drug-loaded micelles 126

6-2.2.6 *In vitro* drug release studies 127

6-2.2.7 Biological Assays 128

6-2.2.7.1 Cell Viability 128

6-2.2.7.2 Cellular Uptake 128

6-2.2.7.3 Flow cytometry 129

6-3. Results and Discussion 129

6-3.1 Characterization of di-block (3a'-c') micelles 129

6-3.2 Characterization of drug-loaded di-block (3a'-c') copolymers micelles 133

6-3.3 *In vitro* drug release from (3a'-c') copolymers micelles 136

6-3.4 Cell viability (in (3a'-c') copolymers micelles) 137

6-3.5 Cellular uptake of (3a'-c') copolymers micelles 139

6-3.6 Quantitative assessment of cellular uptake of (3a'-c') copolymers: Flow cytometry 143

6-4. Conclusion 144

Reference 146

Chapter 7

R-POSS and 2-(Methacryloyloxy)ethyl phosphorylcholine-based copolymers as a simple modifier for liposome

7-1. Introduction 148

7-2. Experimental Section 149

7-2.1 Liposome preparation 149

7-2.2 Transmission electron microscopy (TEM) 150

7-2.3 Particle size and zeta potential measurement 150

7-2.4 Differential scanning calorimetry 151

7-2.5 Cellular Uptake 151

7-2.6 Flow cytometry 151

7-3. Results and discussion 152

7-3.1 Characterization of liposome 152

7-3.2 Stability of liposome 155

7-3.3 Effect of copolymer on the phase transition temperature of liposome membrane 158

7-3.4 Uptake study 159

7-3.4.1 Qualitative uptake study 159

7-3.4.2 Quantitative uptake study 165

7-4. Conclusion 167

Reference 168

Chapter 8

General Conclusion

Conclusion 169

Appendix

List of Publications and Presentations I

Acknowledgment

The present doctoral dissertation is the research work carried out at Kobe University, Kobe, Japan, during October' 2016 to September' 2019 under the supervision and guidance of Prof. Dr. Tooru Ooya.

First and foremost, the author should like to express her deepest gratitude to Prof. Dr. Tooru Ooya for his continuous guidance, valuable advice, scientific strategy, sharing remarkable knowledge and continuous hearty encouragement and support throughout this research work. The author also extend thanks to Prof. Dr. Tooru Ooya for his advice in matters others than research from time to time as a guardian and well-wisher of an international student.

The author also expresses her thankfulness to all the current and previous laboratory members for their advice and guidance on handling the laboratory instrument and making the laboratory working environment comfortable despite the language barrier.

The author would like to thank Graduate Student Miss Ayaka Kurondo, Kobe University for her help in conducting the experiment of the drug release study from the solid formulation.

The author is highly indebted to active collaborator Prof. Dr. Takashi Nishino, Kobe University and Prof. Dr. Shin-ichi Yusa, University of Hyogo and all their Laboratory Members for their encouragements, discussions on research topic, helpful advice and providing research facility.

The author expresses her gratitude to Prof. Dr. Hideto Minami, Kobe University and his all Laboratory Members, Prof. Dr. Akihiko Kondo, Kobe University and his all Laboratory Members, Prof. Dr. Hideto Matsuyama, Kobe University and his all Laboratory Members, Prof. Dr. Tatsuo Maruyama, Kobe University and his all Laboratory Members for providing research facility and for their kind cooperation.

The author would like to thank JAIST supported by the Nanotechnology Platform Program (Molecule and Material Synthesis) of the Ministry of Education, Culture, Sports, Science and Technology (MEXT), Japan for conducting STEM/ EDS measurements.

The author is deeply grateful for the financial support from a Grant-in-Aid for Scientific Research on Innovative Areas "New Polymeric Materials Based on Element-Blocks (no. 2401)" (JSPS KAKENHI grant number JP15H00748) and the Izumi Science and Technology

Foundation, Japan (2018-J-75) for conducting the research work and JASSO (November' 2016 to March' 2017), Toshimi Otsuka Scholarship Foundation (April' 2017 to March' 2019), Kawanishi Memorial ShinMaywa Education Foundation Scholarship (April' 2019 to September' 2019) for financially supporting the author's research work in the form of scholarship.

The author likes to thank the admirative staff of the Faculty of Engineering office and the Centre of the International Exchange , Kobe University for their support and supervision in any administrative work during three years of doctoral course.

The author expresses her deepest gratitude to her parents Mrs. Purnima Chatterjee and Mr. Sambhunath Chatterjee, brother Dr. Suddhasatwya Chatterjee and in-laws Mrs. Ava Talukdar and Mr. Rupendranath Talukdar for their continuous support and encouragement during the hard work in the doctoral course.

Last but not the least, the author expresses her deepest gratitude to her beloved daughter Ms. Aryadita Chatterjee Talukdar for her love, support and accompany in fulfilling all the requirements of the course despite bearing the continuous hardship, and to her husband Mr. Deboprasad Talukdar for continuous support and providing positive advices.

Suchismita Chatterjee
Prof. Dr. Tooru Ooya Laboratory
Graduate School of Engineering
Kobe University, Japan
September, 2019

Abstract

Phospholipid-based copolymers having zwitterionic phosphorylcholine (PC) group provide bioinert nature which has great importance in providing blood compatibility and reducing non-specific protein adsorption for application in biomedical science. So, these copolymers are important in designing synthetic biopolymer for application in coating cardiovascular implant and synthesizing polymeric micelles for drug delivery. Till date, most of the research focussed on the fabrication of MPC based amphiphilic copolymer using conventional or ready-made hydrophobic monomer such as poly [MPC-*co*-*n*-butyl methacrylate(BMA) and Cholesterol. The hydrophobic domain in the amphiphilic copolymer is one of the essential fundamental domains for hydrophobic drug interaction, encapsulation and stable micelle formation which was mainly investigated using BMA as hydrophobic moiety. Additionally, the biomaterial used for the cardiovascular application requires mechanical strength for sustainability, bio and hemocompatibility through attracting the endothelial progenitor cells from circulatory blood. The modification of MPC with focus on the above mentioned essential requirements for extending its application has not been studied yet. This doctoral research focused on the design of new polymeric biomaterial based on 'element block' concept (proposed by researchers from Japan) with phospholipid MPC and element block (polyhedral oligosilsesquioxane (POSS)). The 'element block' concept suggests the incorporation of inorganic component with domain size at the nano or molecular scale into the polymer matrix to produce organic-inorganic polymer hybrids. The structural unit of organic-inorganic polymer hybrids consisting of various group of elements is termed as "element block". Design and synthesis of new element blocks and polymerization of those blocks with polymeric material creates new copolymer with improved material properties. It is well-known that hydrophobic POSS moiety improves the mechanical, surface, thermal properties of the polymer. Additionally, the POSS cage structure can be easily modified depending on the functional requirement. The element block POSS and MPC based copolymer described in this thesis is the first report of combination of POSS and MPC. The research has been performed with an objective to explore application of synthesized copolymer as a surface coating material for a cardiovascular implant and hydrophobic drug carrier molecules for controlled delivery.

The element block (POSS) was synthesized in laboratory with focus on inducing hydrophobicity (vertex R-groups modified with ethyl (C_2H_5), hexyl (C_6H_{13}), octyl (C_8H_{17})) and was copolymerized (random and RAFT copolymerization techniques) with phospholipid MPC

to achieve the following desired functions a) controlled protein adsorption and cell attachment on the surface and b) formation of stable polymeric assembly in an aqueous environment which will help in encapsulating the hydrophobic drug and its controlled release.

The surface modification is essential to attract the endothelial progenitor cells from circulatory blood for enhancement of the bio and haemocompatibility of cardiovascular devices. Mechanical strength is another essential requirement for graft. The results of the study showed that only the C_2H_5-POSS based MPC random copolymer achieves significant improvement of mechanical and thermal properties and also showed protein adsorption and cell attachment on the surface. The results suggested that C_2H_5-POSS moiety is evenly distributed on the polymer matrix in nanometer scale and strong interaction with MPC restricted the mobility which results in the better Young's modulus. The observed phenomenon of cell attachment on the surface supported that the unique hydration layer of poly MPC which resists the protein adsorption and cell adhesion is affected by the incorporation of C_2H_5-POSS moiety. The obtained results suggested the potentiality of the designed C_2H_5-POSS based MPC random copolymer as a coating material.

Administration of poorly water-soluble drug like paclitaxel (PTX) is a major challenge both in the injectable and oral dosage form. So, the next focus was on micellar delivery of PTX and its dissolution from the solid dosage form. The designed C_2H_5-POSS based MPC random copolymer (along with PTX and polyvinylpyrrolidone (PVP) only for solid dosage form) showed a significant increase in the solubility of paclitaxel in water, and encapsulation of the drug inside the micelles also showed controlled drug release. The random copolymers form stable association in aqueous environment and their slight anionic surface charge favourable for acquiring good blood compatibility. The strong interaction of C_2H_5-POSS moiety with PTX in association effectively control the drug release. After drug loading, the strong hydrophobic interaction between PTX and the POSS moiety leads to the shrinkage in hydrodynamic diameter which also support the phenomenon of control drug release. The cell viability in PTX solubilized C_2H_5-POSS based MPC random copolymer was found around 87 ± 24 % and 21 ± 5 % after 24 and 48 h of incubation respectively. The phenomenon suggests that PTX remains incorporated into the copolymer association till 24 h. Due to the negligible release of PTX the cell viability was not significantly reduced. After 48 h the PTX accumulation inside the cell increased which leads to cytotoxicity. In vitro PTX release results also suggested that only 30 % (cumulative PTX release) of PTX was released in 47 h from PTX-solubilized C_2H_5-POSS based MPC random copolymer. The FITC labelled PTX loaded C_2H_5-POSS based MPC random copolymer was internalized by the cells within 2 h and induced cell death. The results suggested that C_2H_5-POSS based MPC random copolymer play a role for rapid cellular uptake.

Based on the findings, it can be inferred that C_2H_5-POSS based MPC random copolymer shows promising characteristics and C_2H_5-POSS moiety in the copolymer have significant importance as hydrphobic monomer for enhancement of drug solubilization and delivery.

The above study revealed that C_2H_5-POSS based MPC random copolymer enhanced the aqueous solubility of PTX. This promising result encourages for further investigation of the role of C_2H_5-POSS based MPC random copolymer in dissolution of PTX from solid formulation. The solid formulation of C_2H_5-POSS based MPC random copolymer, PVP and PTX formed a single-phase homogeneous formulation. The XRD, FT-IR spectroscopy and DSC analysis confirmed the presence of PTX in amorphous state. The solid formulation of C_2H_5-POSS based MPC random copolymer, PVP and PTX enhanced the dissolution rate and dissolved amount (approximately 90% within 40 min) of PTX without any visible precipitation. The presence of the C_2H_5-POSS based MPC random copolymer prevented the immediate recrystallization of amorphous PTX at the water interface. The formulation of C_2H_5-POSS based MPC random copolymer , PVP and PTX would be a promising approach to enhance the dissolution of PTX from solid formulation. Hence, the outcome of the two sperate studies indicated that the C_2H_5-POSS based MPC random copolymer could be a good carrier for PTX in both liquid and solid dosage form applicable in cancer therapy.

The RAFT polymerization technique with the focus of achieving POSS and MPC based well-defined architecture di-block copolymer which will form 3D supramolecular self-assembly structures in an aqueous environment was undertaken to study the encapsulation of hydrophobic drug and its controlled release. The copolymer formed highly stable small-size $(26-43\ nm)$ micelle in an aqueous environment, suitable for encapsulation of hydrophobic drug inside the core. All the micelles were able to encapsulate hydrophobic drugs inside the core, the stability of which was dependent on the chemical structure of the drugs: poorly soluble drugs bearing long alkyl chains such as α-TP were suitable for the R-POSS core. Also, the copolymer micelles were highly internalized by the cell. Cellular uptake of PTX-loaded micelles was governed by the PMPC-related cellular uptake phenomena. The excellent results pointed out that the C_2H_5-POSS and C_8H_{17}-POSS based MPC di-block copolymer can be a potential selective hydrophobic drug carrier.

The applications of MPC and alkylated POSS based random and di-block copolymers were extended to investigate their effect on the stabilization of liposome. The surface of the liposomes were modified with copolymers and the stability of copolymer modified liposomes were compared with DSPE-PEG-2000 modified liposomes. The stability of random and di-block modified liposomes were found to increase in 1:1 D-PBS and serum mixed solutions after 6 days. The cellular uptake after 6 h was observed to be more in case of random and di-

block copolymer modified liposome than that in DSPE-PEG-2000 modified liposome. The MPC and POSS based random and di-block copolymers could be a good amphiphilic surface modifier of liposome for overcoming limitations in liposomal drug delivery.

This study has been systemically performed starting from the stage of design of element block POSS to the investigation of POSS – MPC – based copolymer in application as surface coating material and drug delivery system. The research highlights that the element block POSS and phospholipid MPC based copolymer have the potential for opening a new path in the area of biomedical and pharmaceutical engineering.

Abbreviation

The following abbreviations are used in this dissertation

AIBN	α, α'- Azobisisobutyronitrile
BCA	Bicinchoninic acid
BMA	n-butyl methacrylate
BSA	Bovine serum albumin
CTA	Chain transfer agent
C_2H_5-POSS MA	Methacrylethyl polyhedral oligomeric silsesquioxane
C_6H_{13}-POSS MA	Methacrylhexyl polyhedral oligomeric silsesquioxane
C_8H_{17}-POSS MA	Methacryloctyl polyhedral oligomeric silsesquioxane
DMEM	Dulbecco's Modified Eagle Medium
DP	Degree of polymerization
DSPE-PEG-2000	1, 2-distearoyl-sn-glycero-3-phosphoethanolamine-N-[amino(polyethylene glycol)-2000]
EDTA	Ethylenediaminetetraacetic acid
FACS	Fluorescence-activated cell sorting
FITC	Fluorescein-4-isothiocyanate
GPC	Gel permeation chromatography
HPLC	High performance liquid chromatography
M_n	Number-average molecular weight
M_w	Weight-average molecular weight
NMR	Nuclear magnetic resonance
PBS	Phosphate buffered solution (saline)
PEG	Polyethylene glycol
PEO	Poly (ethylene oxide)
THF	Tetrahydrofuran
UV	Ultraviolet

Chapter 1

General Introduction

1-1. Background of the Research:

1-1. 1. The coating materials for cardiovascular device

1-1. 2. Biomaterials for drug delivery

1-1.3. Concept of "element block" and "element block"-copolymer

1-2. Scope of the Research

1-2.1. Self-assembling of polymeric biomaterials

1-2.2. Polymeric Micelle and application in drug delivery

1-2.3. Phospholipid 2-methacryloyloxyethyl phosphorylcholine (MPC)

1-2.4. Polyhedral oligomeric silsesquioxane (POSS): "element block"

1-2.5. Radical polymerization

1-2.6. Reversible/Addition-Fragmentation Chain Transfer (RAFT) polymerization

Reference

1-1. Background of the Research:

Biomaterials have been used since a long time and subsequently increased their applications in medical research due to the rapidly growing chronic diseases, traumatic accidents, surgical reconstructions and other health-related issues. The extensive research has been conducted on biomaterials and has shown an important role of it in medical science, especially in the field of tissue engineering and drug delivery applications. In 1960-70, the first generation of biomaterials was evolved with the fabrication of biomedical devices that have a balance between physical and mechanical properties with minimal cytotoxicity or carcinogenicity to living host tissues. The second-generation of biomaterials was a focus on the incorporation of bio-activity and resorbable behavior with the use of bioactive glass and ceramics material in orthopedic and dental implants. The third-generation of biomaterials was focused on to develop stimulating specific cell response for the living tissue. The concept of nanotechnology in biomaterial-based devices and drug delivery system help in achieving further improvement. Recently, the researchers are focusing on the incorporation of architectural nanoscale features in the development of biomaterials to achieve 3D microenvironment to mimic native extracellular matrix (ECM)[1-4]. The designing of biomaterials for targeted and controlled drug delivery and complex tissue regeneration is still a great challenge toward clinical applications. The successful treatment of cancer highly depends on the designing of the drug-carrier molecule that can encapsulate drugs and release the drug molecules in a controlled manner at the specific site.

Historically, purified collagen, gelatine, silk, or cotton were natural biomaterials. Advancement in polymer chemistry brings first-generation medical polymers which are currently used in a wide range of biomedical applications. Selection of appropriate biomaterials for a specific application is a key factor of successful implementation. The application of biomaterials are as follows[5]:

a) To support new tissue for growth where cell-cell communication and availability of nutrient, growth factors, pharmaceutically active component will be maximized.

b) To prevent cellular activity where tissue growth is undesirable.

c) To monitor tissue response like enhancement and inhibition of particular cellular response.

d) **To enhance cell attachment and cellular activation** such as fibroblast attachment, proliferation and extracellular matrix production for dermis repair.

e) **To inhibit cellular attachment and activation** such as platelet attachment to a vascular graft.

f) To prevent biological response such as blocking antibodies against homograft or xenograft in the case of organ transplantation.

The key step of the biomedical application of biomaterials is its accurate processing **(Figure 1-1)**. There are nine potential biomedical applications areas have been identified[5]:

1) Membranes in extracorporeal applications such as oxygenators.

2) **Bioactive material for controlled release delivery systems.**

3) Disposable equipment for blood bags and disposable syringes.

4) Sutures and adhesives material including biodegradable and nonbiodegradable.

5) **Cardiovascular devices for vascular grafts.**

6) Reconstructive and orthopedic implants material.

7) Ophthalmic devices material for corneas and contact lenses.

8) Dental restoration materials including dentures.

9) Degradable plastic material for commodity products.

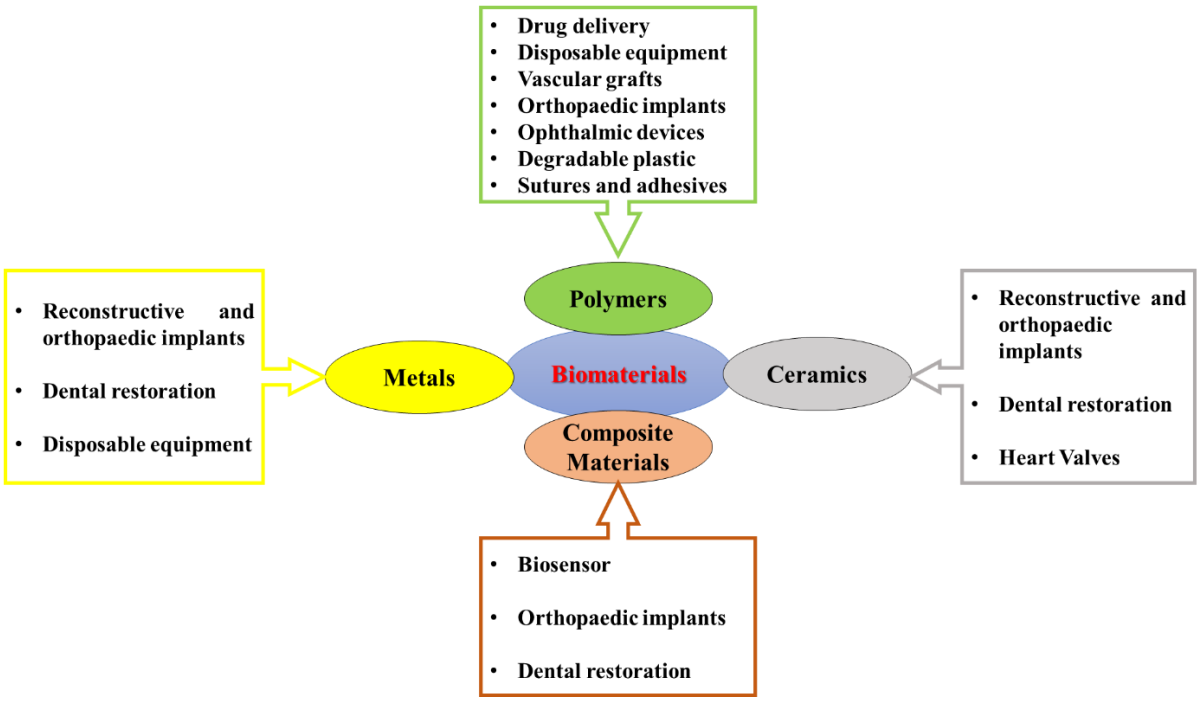

Figure 1-1. Biomedical applications of biomaterials

This thesis describes the application of polymeric biomaterial in the field of control delivery and polymer coating aiming for cardiovascular use. The selection of appropriate biomaterials was based on enhancement or inhibition of cellular attachment and cellular activity.

1-1. 1. The coating materials for cardiovascular device

When the natural heart valves or arteries fail to function properly, replacement materials are used to correct the functions. The replacement materials are used to restore the flow of blood in the body to function properly. The development of polymeric materials as a replacement for heart valves and for use in making stents draw great attention[5]. Hemocompatibility is an essential requirement of biomaterials used in cardiovascular applications as the implants are directly in contact with the blood. So, the material should not induce any thrombosis or damage the red blood cells[5,6]. To meet the essential requirement for these applications coating of the surface is necessary **(Figure 1-2)**. Natural polymers such as

heparin (a polysaccharide) have been used for the coating[5]. The resorbable polymers such as polycaprolactone, polyorthoester, and copolymers such as polyglycolic–polylactic acid, poly(hydroxybutyrate valerate), poly(ethylene oxide)–poly(butylene terephthalate) have been studied *in vivo* as resorbable coatings material[5,7]. Phosphorylcholine moiety showes to have great potential to prevent the thrombus formation on the surface. The nanocomposite polymers, bio-functionalized with growth-factor through surface modification, attract the endothelial progenitor cells from circulatory blood and enhance the bio- and haemo-compatibility of cardiovascular devices. The mechanical strength of the biomaterials is an essential requirement of the cardiovascular implant especially for heart valves, which should have properties like flexibility, toughness and durability[8].

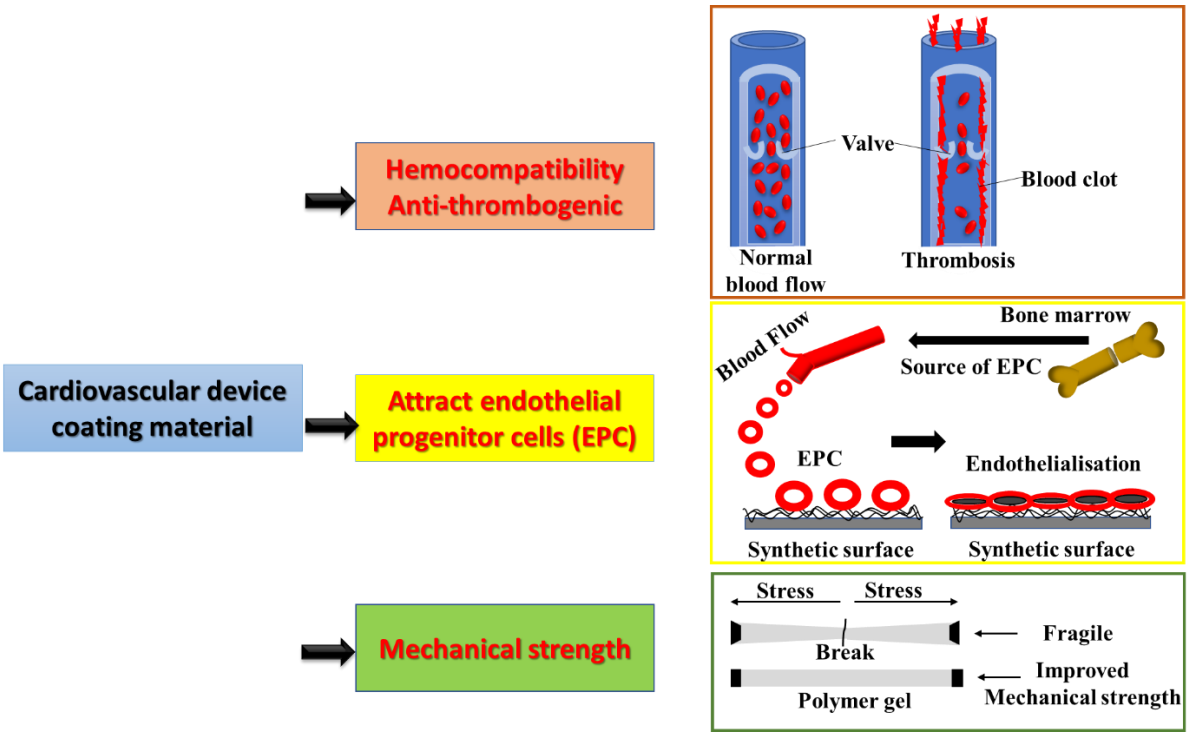

Figure 1-2. Essential requirement of cardiovascular coating material

1-1. 2. Biomaterials for drug delivery

Polymeric delivery systems are focus to achieve temporal or spatial control of drug delivery. Polymeric vehicles are capable to deliver the drug over an extended period of time and to the site of action. Polymeric vehicles can be designed to enhance drug safety, efficacy, reduce side-effect and can improve patient compliance. The polymeric vehicles can decrease the amount of drug molecule and dosage frequency of the drug[9]. The goals of drug delivery **(Figure 1-3)** are as follows[9,10,11]:

1. Controlled drug delivery: to control the duration of action of the drug and maintain the drug's level in the human body.

2. Targeting: to target the drug particular places or cells in the body.

3. Overcome tissue barriers: to overcome certain tissue barriers such as the lung, skin, or intestine.

4. Overcome cellular barriers: to overcome certain cellular barriers which are important in gene therapy.

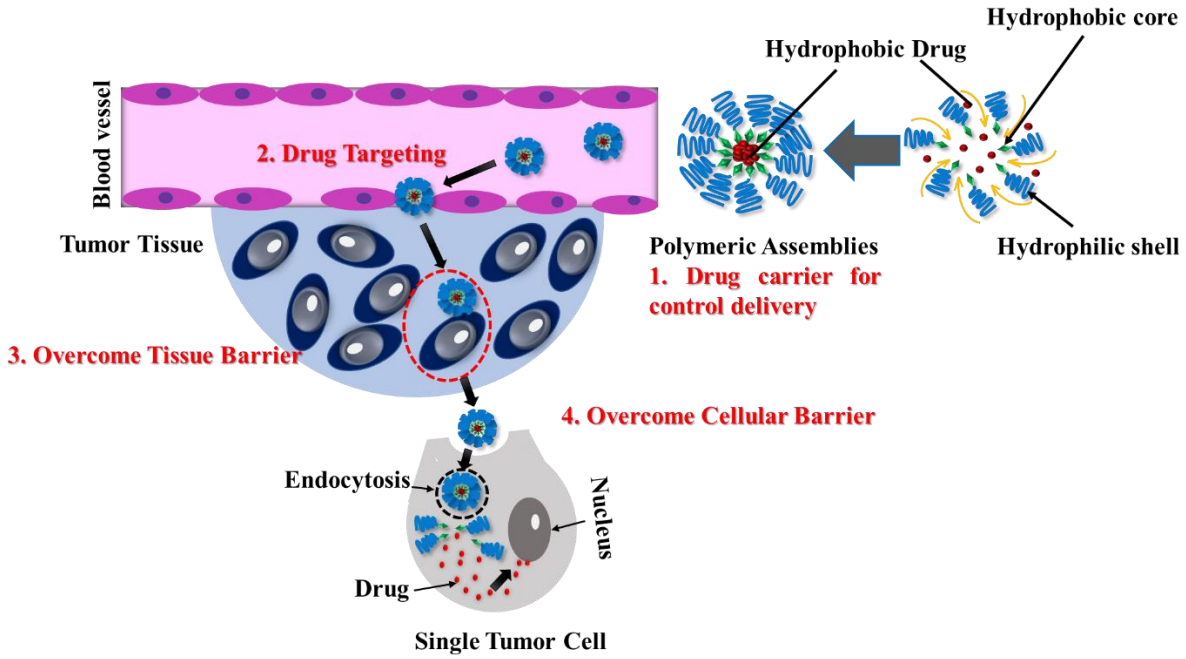

Figure 1-3. Goal of polymeric drug delivery

Innovations in materials chemistry have initiated the development of delivery system by creating new carriers that are biodegradable, biocompatible, targeting, and stimulus-responsive. And nanotechnology has helped in realizing the fact that the size and shape of nanoparticles (NPs) play an equal role to develop effective particulate for successful drug delivery (**Figure 1-4)**. The size of the NPs determines the biodistribution. The smaller particles (less than 20 nm) cleared from circulation via reticuloendothelial system (RES) within a few hours of injection, whereas larger ones trapped in the liver and the spleen within minutes[10]. Different fabrication techniques such as nanoprecipitation, emulsion-based phase inversion, microfluidics-based self-assembly, layer-by-layer synthesis, and nanoimprinting have been used to generate particle nano-carrier to deliver a wide range of drugs. Liposome has been the most successful candidate of DDS in clinical applications. Most of the FDA approved DDS are liposome or lipid-based[10].

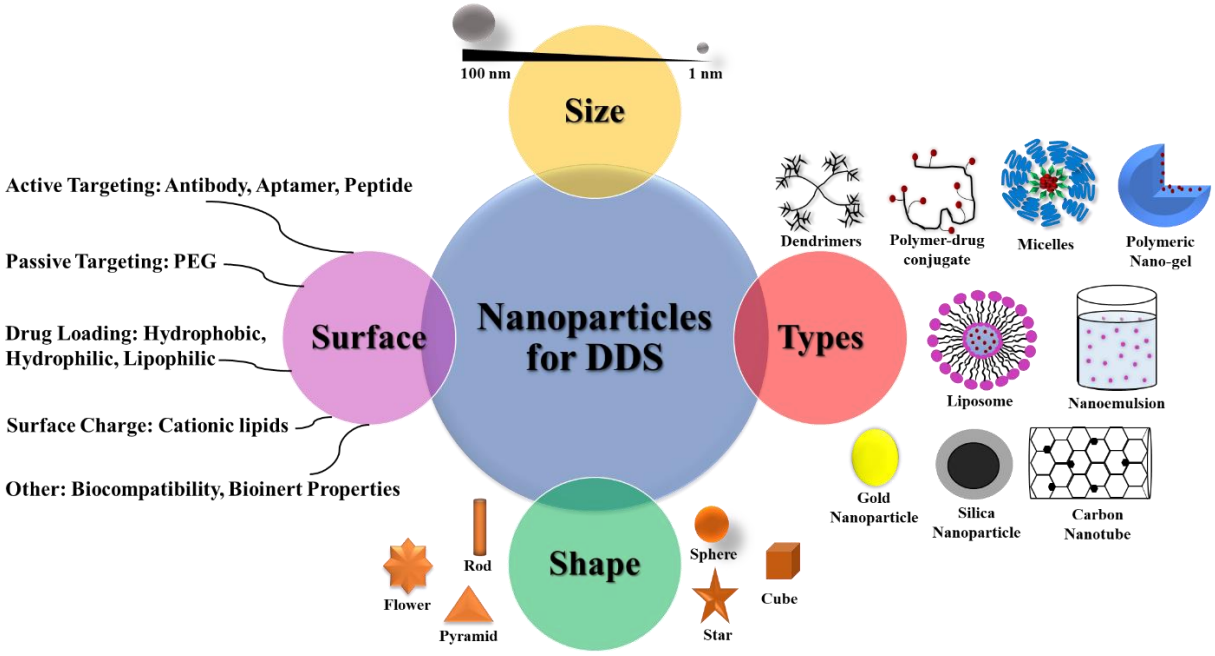

Figure 1-4. Nanoparticles for drug delivery

Biodegradable polymers are considered as an alternative to lipid-based delivery for their improved in vivo stability. The degradability of the polymer could be tuned to control the

release of the drug. The polymers, poly (lactic acid) (PLA), poly(glycol acid) (PGA) and their copolymers, poly (lactide-co-glycolide) (PLGA) are the most widely used for DDS development because of their biodegradability, biocompatibility and ease of processing[10,12,13]. Polyanhydride is another class of biodegradable polymers for application in DDS. To overcome the undesirable bulk-degrading behavior of polyesters, polyanhydrides are designed to undergo surface-degradation. As the different drugs used for various therapies demand the carriers of various properties to achieve optimal delivery[10].

Block copolymers draw great attention of researchers because of their remarkable chemical flexibility. The building blocks can be designed in such a way that they could assemble to nanostructures in the form of micelles, electrostatic complexes, or polymersomes. The stable nanoparticle can be used for passive tumor targeting utilizing the enhanced permeability and recognition (EPR) effect[14]. The A-B block type copolymer comprised of PEG and poly(aspartic acid) modified by 4-phenyl-1-butanol to enhance the hydrophobicity is under phase II clinical investigation with the aim of delivery of paclitaxel (NK105) and doxorubicin (NK911)[15]. The amphiphilic block copolymer of PEG-polycation is also of great interest due to their ability to condense nucleic acids into their nanosized polyplex with protective and biocompatible PEG shell[10].

The major drawback of polymeric micelles is the stability of micelle in blood stream after administration which leads to rapid dissociation and burst release of the drug. Some approaches have been taken to address this issue[10]:

a) Attachment of pendent group to the backbone such as fatty acid, benzyl groups, cholesterol to increase the hydrophobicity of the core[16,17,18].

b) Introducing hydrogen-bond interaction in the core. For example, amphiphilic PEO-PCL based polymer containing urea functional group in the side chain shows improved kinetic stability of micelles in the presence of a destabilizing agent[19].

c) Introduction of oppositely charged groups in the micelle core to promote electrostatic interactions. For example, PEO with poly (L-lysine) or poly(aspartic acid)[15].

d) Crosslinking of the micelle core by thermal or photo-induced polymerization. For example, PEO-PLA block copolymers having polymerizable methacryloyl pendant groups at the PLA

block can be crosslinked thermally or photochemically during micelle formation. It provides stability at high temperature and in an organic solvent[20,21].

The shell and core of polymeric micelles could also be modified depending on the applications. The hydrophilic shell of the micelles can be functionalized with various ligands such as antibodies, small organic molecules, carbohydrates, peptides or polymers to target binding to cancer cells[10]. The polymeric micelles with cationic surface allow the co-delivery such as nucleic acids and small organic drugs. The cationic amphiphilic block copolymers of poly(N-methyldietheneamine sebacate) (PMDS) and cholesterol have been studied for targeting and drug loading[22]. The cationic block PMDS act as siRNA and plasmid binding and the cholesterol pendant group increases the hydrophobicity of the core for efficient drug loading[10]. A triblock copolymer of poly (ethylene glycol)-β-poly (ε-caprolactone)-β-poly(2-aminoethyl ethylene phosphate) (mPEG-β-PCL-β-PPEEA) have been studied for co-delivery of pro-like kinase 1 gene (Plk1) siRNA and paclitaxel[23]. Many co-delivery systems have been investigated so far by various groups and the system showed a promising alternative to the liposomal co-delivery system for hydrophilic macromolecule and small lipophilic drugs[10].

The literature review indicated the challenges in the research area of the surface coating of implant and drug delivery system. Also, indicated the huge scope to encounter the challenges in these research areas. The designing of the biomaterials is key to encounter the challenges. In this thesis, I focused on the development of new polymeric material to be applied for the surface coating of the implant and for hydrophobic drug delivery.

1-1.3. Concept of "element block" and "element block"-copolymer

Recently, a new concept of polymer hybrids has been suggested by Chujo et. al. The concept is the incorporation of the inorganic component with domain size at the nano or molecular scale into the polymer matrix to produce organic-inorganic polymer hybrids. The inorganic structural unit consisting of various groups of elements is termed as "*element block*" and the organic-inorganic polymer hybrids is termed as "*element block*"-copolymer[24]. The concept involves the design and synthesis of the new element blocks and polymerization of those blocks to create new polymeric materials with improved and desired functional properties **(Figure 1-5)**. This bottom-up approach is expected to encourage the creation of new polymeric material which cannot be achieved with conventional designing and synthesis process of

organic polymeric material. The new element block with a variety of elements can be synthesized by different approaches such as an organic, inorganic and organometallic reaction and these element blocks can be polymerized by different polymerization techniques. This strategy was applied in the current study to develop the new element block based MPC copolymer for the biomedical applications[24].

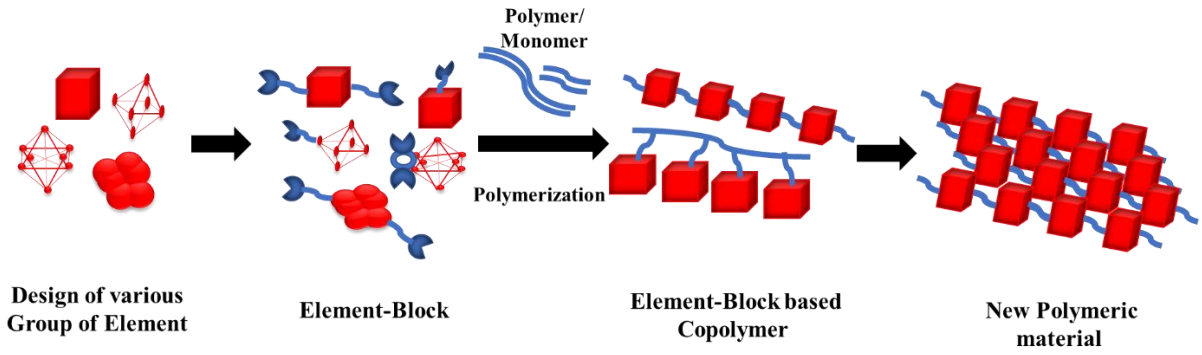

Figure 1-5. Concept of "element block" copolymer

1-2. Scope of the Research

The purpose of this study is the investigation of the properties of amphiphilic phospholipid copolymer with “element block”-based hydrophobic domain as surface coating materials and drug carrier molecules in an aqueous environment. Amphiphilic copolymers can be synthesized by copolymerization of hydrophilic and hydrophobic monomers, which form aggregates or nanoparticle in an aqueous environment. This amphiphilic copolymer system has a great interest in various biomedical applications (drug delivery). Conventional polymer aggregate was fabricated with conventional ready-made material. This study was based on the design of hydrophobic “element block” monomer for amphiphilic phospholipid-based copolymers and systemic research for its different application. The design of the molecules was fundamentally different from the conventional polymeric biomaterial and in this study “2-methacryloyloxyethyl phosphorylcholine (MPC)” was selected as phospholipid-based hydrophilic polymer as one of the monomers of the amphiphilic copolymer. The zwitterionic water-soluble polymer, 2-methacryloyloxyethyl phosphorylcholine (MPC) polymer (poly

MPC) has been used extensively in blood-contacting medical devices for a high level of biocompatibility and resistance to protein adsorption. Also, MPC monomer can copolymerize with hydrophobic monomers, and the obtained amphiphilic copolymers have been considered for solubilization and delivery of hydrophobic drugs. For example, $MPC_{100}-DPA_{100}$ micelle system, poly[MPC-co-*n*-butyl methacrylate (BMA)] (PMB30W)/ PLA micelle system, pMPC*m*-BMA*n* micelle system[25], cholesterol-end-capped poly(2-methacryloyloxyethyl phosphorylcholine) (CMPC) micelle system[26], poly(2-methacryloyloxyethylphosphorylcholine)-*b*-poly(butylene succinate)-*b*-poly(2 methacryloyloxyethyl phosphorylcholine) (PMPC-*b*-PBS-*b*-PMPC) micelle system etc. have been studied with the focus on drug delivery system. The research reported yet was a focus on the fabrication of MPC based amphiphilic copolymer using conventional or ready-made hydrophobic monomer (BMA, Cholesterol). In this study, the MPC based amphiphilic copolymer was designed and synthesized by element block concept which comprises a synthesis of new element blocks (Polyhedral oligomeric silsesquioxane (POSS)) and polymerization of those blocks with MPC (radical polymerization and reversible addition-fragmentation chain transfer (RAFT) polymerization). This amphiphilic MPC-POSS based copolymer having element block POSS as a hydrophobic unit is the first report. The scientific and biological evaluation revealed the interesting feature of copolymers. The results indicated the thermal and mechanical improvement of the copolymer after incorporation of element block POSS. The hydrophobicity of the surface increase and copolymer formed aggregate and micelle in an aqueous environment. The hydrophobic domain of aggregate can be applied in various field of pharmaceutical science. For example, in the field of drug delivery, it can act as a good solubilizer of a poorly water-soluble hydrophobic drug such as Paclitaxel. Stable polymeric micelle can encapsulate the hydrophobic drug in the hydrophobic domain and deliver to the targeted site. The interface of the biomaterial is important for surface coating and micelle nanoparticles as they are in close contact with the circulatory system. In this study MPC-POSS, the based copolymer was investigated which contain bioinert phosphorylcholine group which helps in preventing nonspecific adsorption. Additionally hydrophobic POSS moiety on the water-polymer interface (in the surface coating) help in protein adsorption and cell attachment which help in providing bio and hemocompatibility by attracting the endothelial progenitor cells from circulatory blood. This thesis describes several novel application of the synthesized MPC-POSS based amphiphilic copolymers in the field of bioscience.

1-2.1. Self-assembling of polymeric biomaterials

Self-assembling of polymer indicates self-assembly of the mono unit by noncovalent interactions has become a topic of increasing interest in recent years. In living organisms, the association of various biomolecules such as DNA, polysaccharides and proteins controlled by non-covalent interactions such as ionic bonding, hydrogen bonding and hydrophobic interaction. Amphiphilic polymers composed of at least one solvophobic moiety and at least one solvophilic moiety (hydrophilic and hydrophobic, respectively, if the solvent is water) self-assemble in selective solvents[27]. The crucial driving force associated with self-assembling is based on multiple intermolecular interactions such as hydrogen bonding, p–p stacking, metal-ligand coordination, hydrophobic interactions and host-guest interactions[28]. The reversible and tunable nature of these noncovalent interactions provides important properties of reversibility and stimuli-responsiveness. These tuneable natures allow to large physical or chemical changes in the response of weak stimulating signal in the environment such as pH, temperature, light, redox agents, enzymes, ions, gases, mechanical force, electric and magnetic fields. This material as a wide application in the different biomedical field. Self-assembling nature of amphiphilic polymer can construct different interesting one-, two- and three-dimensional morphologies, such as spherical micelles, cylinders, rods and vesicles **(Figure 1-6)**. These have a wide range application in the fields of bioimaging, drug delivery, sensing and electronics[27,29].

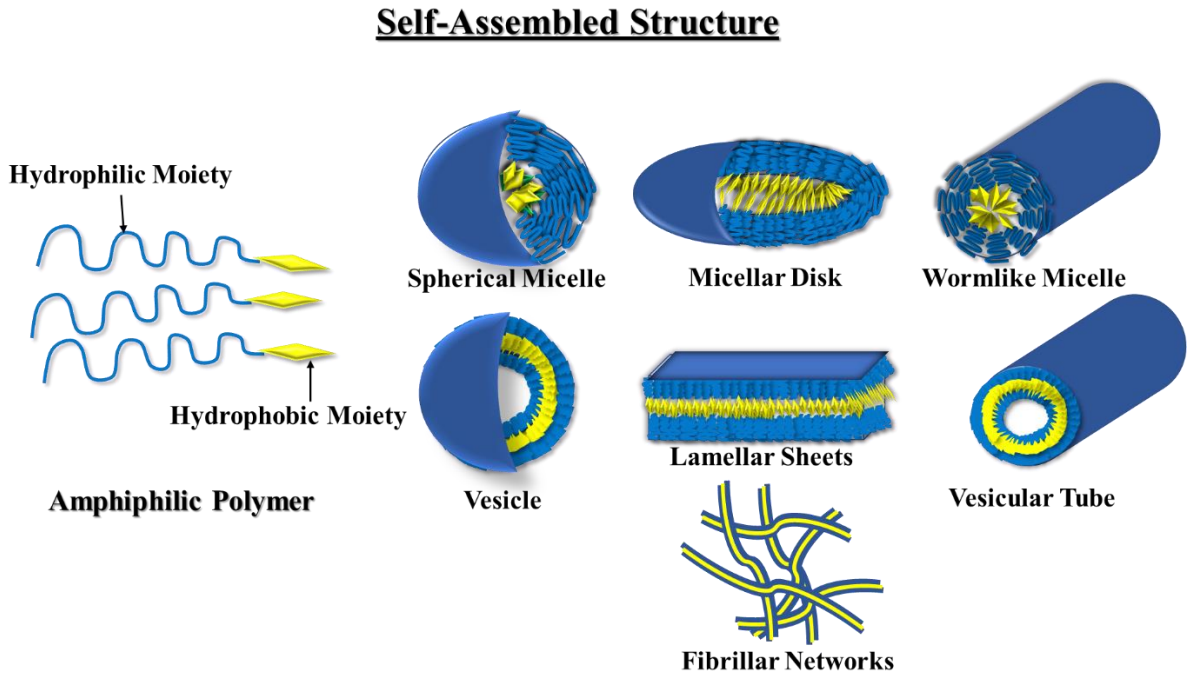

Figure 1-6. Self-assembled polymeric biomaterial for different application

The core-corona structure is the distinct feature of polymeric self-assembled particles. Both, the core and corona are able to accommodate active substances of appropriate nature and to serve as carriers. The core is composed of strongly entangled solvophobic chains, whereas the corona is built up of solvophilic chains, which can be nonionic or charged. The careful designing the copolymer composition is important to intelligently control the properties and the stability of the whole aggregate.

In this study, we design and synthesize the MPC (hydrophilic) and POSS (hydrophobic) based copolymer which formed a self-assembled structure in an aqueous environment. In this study, POSS was selected as hydrophobic moiety with the focus of achieving well balance stable core-corona structure based polymeric assembly.

1-2.2. Polymeric Micelle and application in drug delivery

Polymeric micelles are self-assembled core-shell nanostructures of amphiphilic block copolymers formed in an aqueous environment. Formation of micelles in aqueous solution

happens when the concentration of the block copolymer increases and reached to a certain concentration named the critical aggregation concentration (CAC) or critical micelle concentration (CMC) **(Figure 1-7)**. At the CAC or CMC, hydrophobic segments start to associate to minimize the contact with water molecules which leads to the formation of a vesicular or core-shell micellar structure[27,29]. The micelles formation is driven by the decrease of free energy. The micelles formation is associated with the removal of hydrophobic fragments from the aqueous environment and the re-establishment of the hydrogen bond network in water which decreases the free energy of the system. The unique core-shell structure of micelles has great potential to deliver the hydrophobic drug. The inner hydrophobic core formed by a hydrophobic block of copolymer enables incorporation of poorly water-soluble drugs by hydrophobic interaction and improve their stability and bioavailability. Besides, it can also form polyion complex (PIC) micelles, hydrogen bonding and metal-ligand coordination complex micelles. The outer hydrophilic shell of polymeric micelles plays an important role in the in vivo behavior, steric stabilization and ability to interact with the cells.

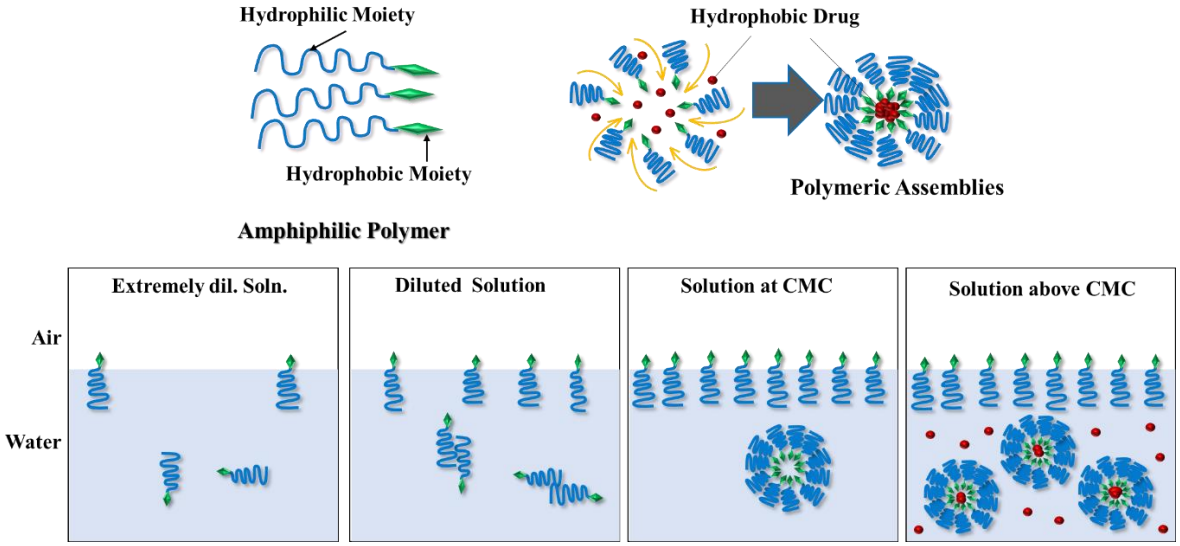

Figure 1-7. Polymeric micelles formation and drug encapsulation

The block copolymers can be of two type diblock copolymers or triblock copolymers. A-B type is the diblock copolymer, commonly used for designing polymeric micelles in which A

represents a hydrophilic block and B represents a hydrophobic block. The triblock copolymers consist of two types of polymers (A-B-A) or three types of polymers (A-B-C). Most drug carrier applications have been studied with A-B or A-B-A type block copolymers[30]. The physicochemical characteristics of the building blocks have an influence on the physical and biological properties of the polymeric micelles. The choice of hydrophobic core forming polymers has a major importance to determine the stability, drug loading capacity, and drug release profiles of polymeric micelles. Poly(propylene oxide) (PPO), poly(lactic acid) (PLA), hydrophobic poly(amino acids), copolymers of lactic acid and glycolic acids, and poly(caprolactone) (PCL) are commonly used core-forming blocks of polymeric micelles. These core-forming hydrophilic block will strongly affect the stealth properties and influence the circulation kinetics of the micellar assembly. Poly(ethylene glycol) (PEG) is most commonly used as the hydrophilic segment of the block copolymers due to its non-toxic nature. The poly(N-vinyl-2-pyrrolidone) (PVP) and poly(acrylic acid) (PAA) are also used as an alternative of PEG[30].

Polymeric micelles can be safely used for parenteral drug administration than conventional solubilizing agents such as polyethoxylated Castor oil (Cremophor EL) or polysorbate 80. They are kinetically stable, dissociate very slowly and prolonging the circulation times in blood. The hydrophobic cores can solubilize hydrophobic drugs. Polymeric micelles containing Polyethylene glycol (PEG) provide the “Stealth” effect and help in reducing uptake by the macrophages of the reticuloendothelial (RES) system and extend in vivo circulation times. In spite of these advantages, micellar delivery has some short-comings like the dissociation of the micelle structure after dilution in blood circulation[9,30]. This dissociation accelerated when unimeric component bind with the protein. This phenomenon can be overcome by stabilizing the micelle core by proper selection and size of the hydrophobic block and optimum hydrophobic/hydrophilic ratio.

In this study, we selected the MPC as a hydrophilic block which is bioinert in nature and reduce protein adsorption and cell attachment to overcome the problem associated with the stability of the micelles. We selected POSS (modified with different alkyl chain length) as a hydrophobic block for the stability of the core, drug loading and controlled release. The purpose of this thesis is to design the amphiphilic copolymer and evaluation of their properties for the application in the pharmaceutical field.

1-2.3. Phospholipid 2-methacryloyloxyethyl phosphorylcholine (MPC)

Phospholipids draw great attention in the application of biological science as it is one of the major components of the lipid bilayer in the cellular membrane **(Figure 1-8)**. Due to the biocompatibility of the phosphorylcholine group, the design of synthetic polymers includes this moiety to achieve biocompatibility for biomedical applications. One of the representatives is 2-(methacryloyloxy)ethyl phosphorylcholine (MPC) polymers which have been developed by Ishihara *et al*. The phosphorylcholine group of 2-(methacryloyloxy)ethyl phosphorylcholine (MPC) is one of the components of cell membranes. Phosphorylcholine (PC) group is zwitterionic nature which is responsible for its bioinert characteristic. The poly MPC is highly water soluble. The hydrophobic main chain of poly MPC does not come in contact with water molecules and the phosphorylcholine group has a unique hydration state. The functions and the physiochemical properties of MPC for modulating the surface and/or interface properties can be controlled by copolymerization with other monomers. Copolymers of MPC and other hydrophobic monomers have been widely applied for biomedical applications such as surface coating for blood-compatible materials, oxygen sensing membrane and polymeric micelles for controlled release of anticancer drugs. K. Ishihara *et al.* reported that poly[MPC-*co*-*n*-butyl methacrylate(BMA) (PMB30W)] with 70 mol % of the BMA unit is the most effective polymer to dissolve the Paclitaxel. Addition to this, cellular uptake was found to be superior in the case of poly MPC-based polymeric micelle than poly(ethylene oxide) (PEO)- and poly(*N*-(2-hydroxypropyl)methacrylamide) (PHPMA)-based polymeric micelle which indicates that poly MPC shall be advantageous to interact with cell membranes. The hydrophobic part is essential to interact with hydrophobic drug paclitaxel and mainly the investigation was conducted with hydrophobic BMA moiety. The other hydrophobic monomers have not been investigated yet to synthesize MPC based amphiphilic molecules.

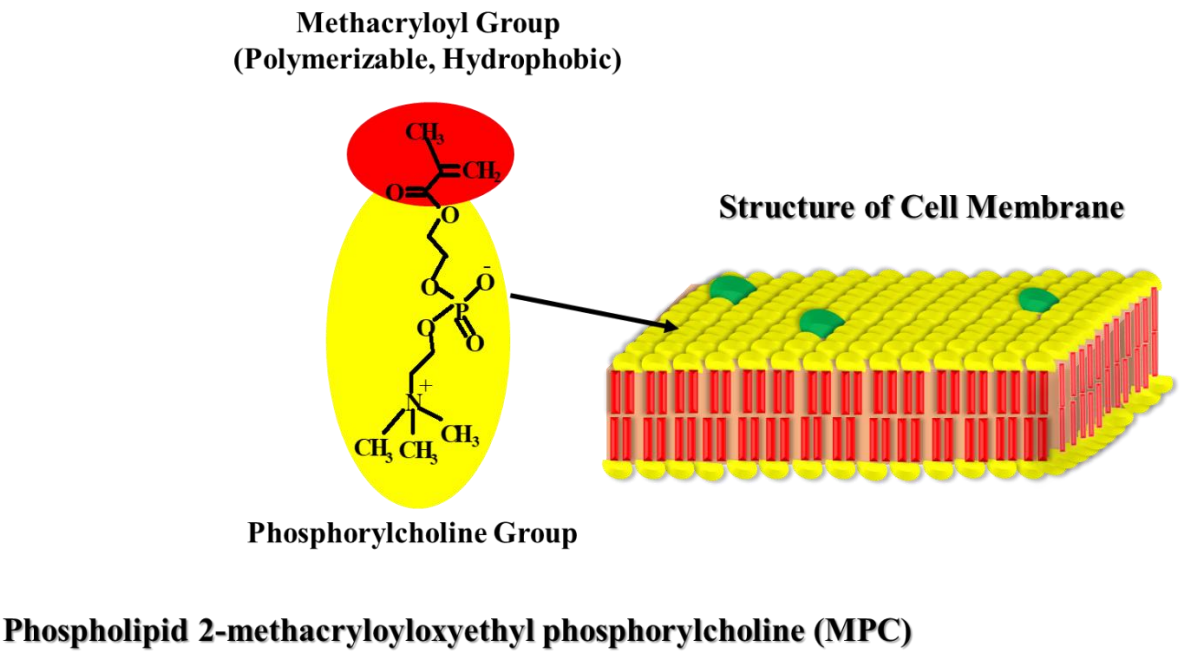

Figure 1-8. Zwitterionic MPC: component of cell membrane

1-2.4. Polyhedral oligomeric silsesquioxane (POSS): "element block"

Polyhedral oligosilsesquioxane (POSS) is an element block whose chemical structure follows the basic composition of $R_nSi_nO_{1.5n}$[31,32]. In the above-mentioned formula R represent the vortex group of POSS cage structure and it can be hydrogen, any alkyl, alkylene, aryl, arylene, or organofunctional derivative of alkyl, alkylene, aryl, arylene. With proper designing of the R group, the material properties can be controlled relatively as per requirement **(Figure 1-9)**. The POSS nano-cage structure is 1-3 nm in diameter. The vortex group can the design to polymerized with other biocompatible polymers. Incorporation of POSS moiety into polymeric material can lead to improving the mechanical property, surface property, thermal property, etc. of the polymer. The POSS silica cube is strongly hydrophobic in nature. As a result, it strongly interacts with the polymer and increases the local density of POSS core in the polymeric matrix. As reported that the introduction of POSS unit in hydrophilic polymer enhances the amphiphilicity of the material and increase the encapsulation of guest molecules. For example, the introduction of the POSS moiety to the ends of the hydrophilic chain such as PEO and poly (ethylene glycol) (PEG), results in the formation of self-assembled micelle and

vesicle in solutions and leading to solvent-sensitive self-association behavior. Kim *et al.* successfully encapsulated insulin inside PEG-POSS nanoparticles for drug delivery and their results suggested that the insulin was well protected inside PEG-POSS nanoparticles at gastric pH for 2 h. and start releasing at intestine pH 6-7. Yuan *et al*. synthesized poly(L-glutamic acid) dendrimers bearing POSS, conjugated with doxorubicin via pH-sensitive hydrazine bond and biotin as a targeting ligand. The hydrophobic nature POSS moiety suitable for application as drug carriers as well as artificial molecular chaperones and polymeric capsule for photodynamic therapy have been reported.

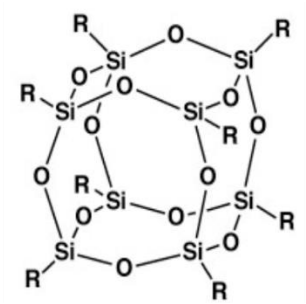

Figure 1-9. Structure of "Element Block": POSS

In this study, element block POSS was selected as hydrophobic moiety to polymerized with hydrophilic MPC polymer for the synthesis of the amphiphilic copolymer. The element block concept was applied for design and synthesis of element block POSS by modifying its R-group with different alkyl chain to fulfill the aim of inducing more hydrophobicity. This bottom-up approach (synthesis and design on the basis of functional need) will be a powerful tool to develop the advanced biomaterial according to the application.

1-2.5. Radical polymerization

Free radical polymerization (FRP) is a common way to synthesize macromolecular materials through a radical chain process. The high molecular weight polymer can be achieved

even under mild polymerization conditions with the monomer and a radical initiator. These features make FRP a very versatile process to obtain several polymer and copolymer compounds with peculiar properties. The major problem of FRP is that regulation of the chain length distribution and morphology of the resulting polymer not possible. The chain length distribution of the final product is associated with radical termination mechanisms which have great importance in determining the molecular weight distribution (MWD). The polymer microstructure and morphology depend on the network of reaction steps involve a large number of different species, including very reactive radicals.

Most free-radical polymerizations have three basic reaction steps:

- Initiation $\mathbf{I \rightarrow 2R^{\cdot}}$
- $\mathbf{R^{\cdot} + M_1 \rightarrow M_1^{\cdot}}$
- Propagation $\mathbf{M_n + M_1^{\cdot} \rightarrow M_{n+1}^{\cdot}}$
- Termination $\mathbf{M_n^{\cdot} + M_m^{\cdot} \rightarrow M_{n+m}}$

  $\mathbf{M_n^{\cdot} + M_m^{\cdot} \rightarrow M_n + M_m}$

In random copolymers, different monomeric components of the polymer are randomly arranged and the probability of getting a monomer unit at any location on the polymer is independent of the nature of the adjacent units **(Figure 1-10)**. The self-assembly behavior of random copolymers is largely dependent on their hydrophilic-hydrophobic balance. Morphologies of the self-assembled structure greatly vary with the ratio of hydrophilic side chains to hydrophobic groups. For example, amphiphilic random copolymers were synthesized by hydrophobic dodecyl (C12) chain and hydrophilic L-glutamic acid in which the ratio of co-monomers can be easily tuned. Vesicles formed when water was added into an ethanol solution of these polymers. The reason for the vesicle's formation is hydrogen bond in the side chains and the hydrophobic interactions between the long alkyl chains. The size of vesicles was found to be dependent on the hydrophobic alkyl chain. The polymersomes can be achieved from self-assembly of the amphiphilic random copolymer containing hydrophobic methacrylate and hydrophilic methacrylamide repeat units. The amphiphilic random copolymers were synthesized by esterification of hydrophilic poly(hydroxyethyl methacrylate) (PHEMA) and hydrophobic 2-diazo-1,2-naphthquinone (DNQ) molecules. The spherical assemblies form in water were not stable state above water content 35 wt%. It was observed that the relatively high molecular weight of poly(DNQMA-co-HEMA) and the suitable hydrophilicity of the polymer

backbone play an important role in the morphological transition[33]. The amphiphilic random copolymers, synthesized with hydrophilic triethylene glycol and hydrophobic alkyl chain connected with disulfide bond by free radical polymerization. This copolymer form micelle-like nano-assemblies in water and able to encapsulate hydrophobic guests inside their core. The nano-assemblies can release the encapsulated guest molecules in reducing environment.

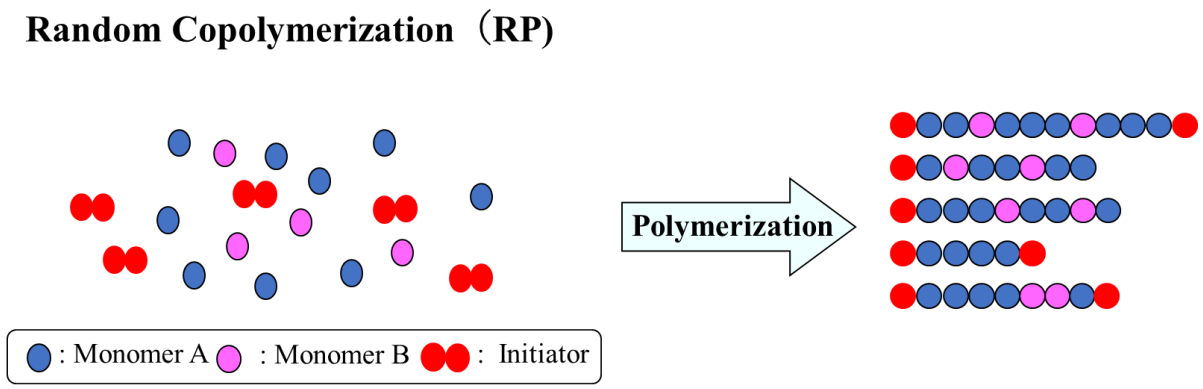

Figure 1-10. Random copolymerization technique and random copolymer

1-2.6. Reversible/Addition-Fragmentation Chain Transfer (RAFT) polymerization

In the free-radical polymerization process, the propagating species is a long-chain free radical initiated by the attack of free radicals derived from initiators. The living radical polymerization is also a free-radical polymerization containing living characteristic such as the process does not terminate or transfer and can be continued by adding more monomers if the initial one exhausted **(Figure 1-11)**. The control over molecular weight, molecular weight distribution and site-specific functionality can be possible that was impossible to achieve via free-radical polymerization. The major LRP techniques include nitroxide-mediated polymerization, RAFT polymerization and atom-transfer radical polymerization (ATRP).

RAFT polymerization is the most versatile process because of its occurrence in a wide variety of reaction conditions, functionalities and can be performed in conventional free-radical polymerization set-ups. The progress of the RAFT held via degenerative transfer process and chain-transfer (RAFT) agents play a major role. The chain-transfer agents are organic

compounds containing a thiocarbonylthio moiety. The R group involves in initiating the growth of polymeric chains, and the Z group activates the thiocarbonyl bond towards the radical addition and stabilization of resultant adduct radical[34].

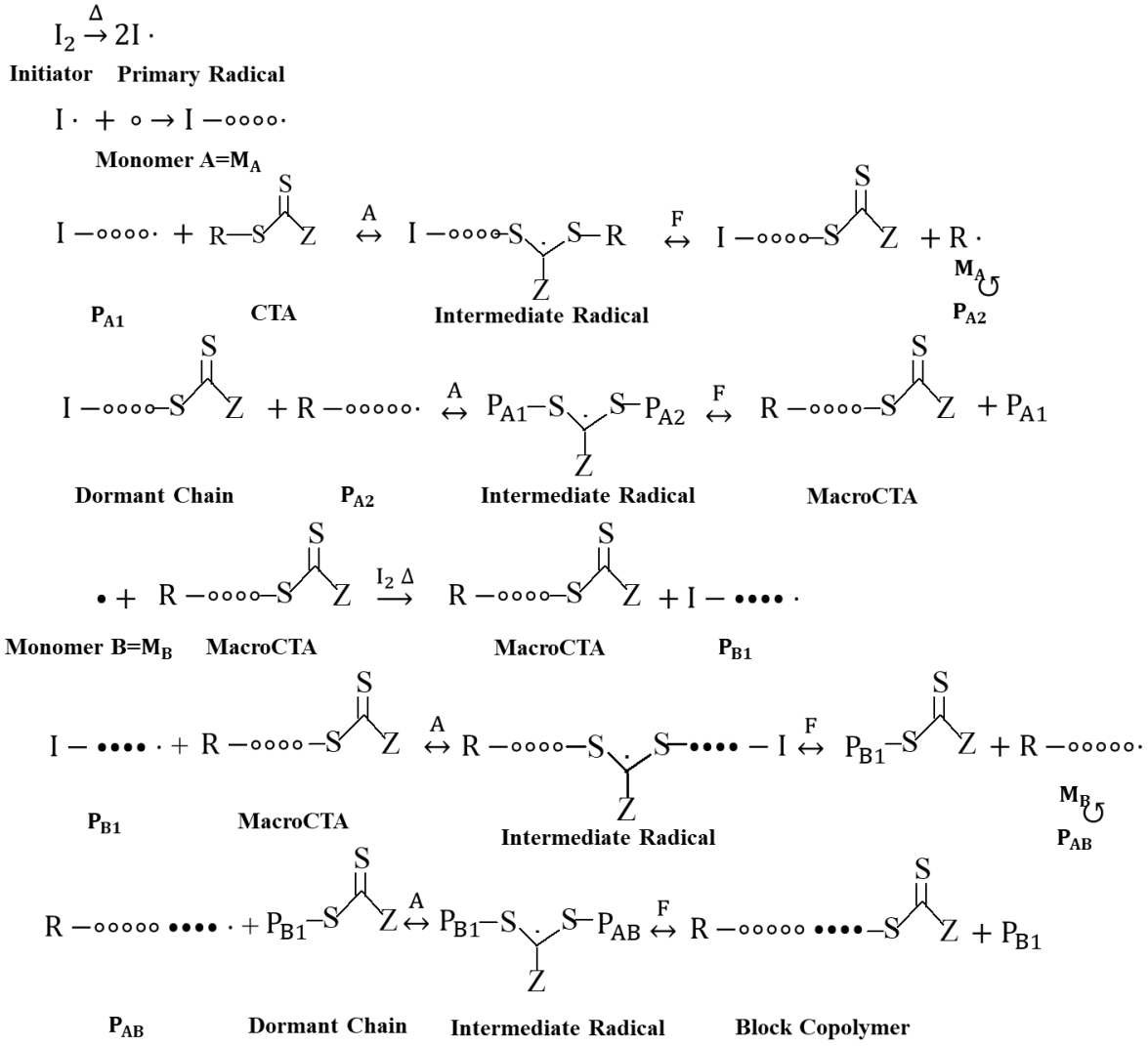

The RAFT polymers have high interest for its biomedical applications such as drug delivery via polymeric micelles. PEG and poly(N,N,N-trimethylammonium ethyl methacrylate) block copolymers were synthesized via RAFT polymerization method and self-assembly micelles formation was studied. It was observed that the micelles have the ability to encapsulate fatty acid salts. The poly- (2-methacryloyloxyethylphosphorylcholine)-b-poly(butyl methacrylate) amphiphilic block copolymer was investigated as a micellar carrier

of paclitaxel. its ability to form a micellar carrier for paclitaxel. The cationic polymers were investigated as genes and oligonucleotides delivery carrier due to their electrostatic interaction with negatively charged groups. Poly(dimethyl amino ethyl) methacrylate synthesized via RAFT polymerization was employed as gene delivery carrier. RAFT copolymer of poly(acryloyl glucosamine) and NIPAAm results in thermo-responsive micelles which can be disintegrated into unimers below the LCST. RAFT polymerization of poly(ethylene glycol)acrylate and butylacrylate results in pyridyl disulfide-terminated block copolymer which can quantitatively react with thiol-containing compounds such as bovine serum albumin (BSA).

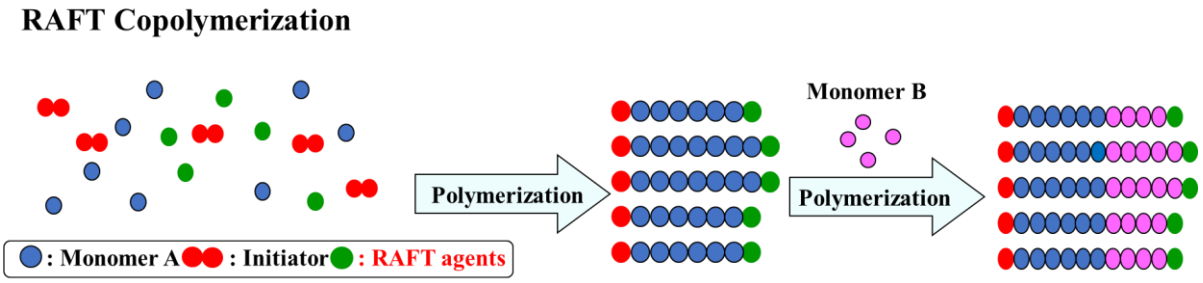

Figure 1-11. RAFT polymerization technique and di-block copolymer

In this study free radical and RAFT both polymerization technique was performed to synthesize the element block POSS-based MPC copolymer for their biomedical application.

This thesis is composed of eight chapters.

Chapter 1 is the general introduction describing the background and scope of the current research. The concept of the current research and implementation strategies are also elaborately described in this chapter.

Chapter 2 describes the design, synthesis and characterization of the POSS and MPC based copolymers. This chapter describe the fundamental characteristics of the designed copolymer to extend its application in different field.

Chapter 3 describes the new approach of enhancing and tuning of the thermal, mechanical and interface wettability of the MPC polymer by POSS moiety to extend it application as surface coating material.

Chapter 4 describes the self-assembled nature of the MPC and R-POSS based random copolymer and extend its application in hydrophobic drug solubilization and sustained release. This chapter discuss the role of the hydrophobic monomer in hydrophobic drug solubilization and release.

Chapter 5 describe the application of the synthesized MPC and R-POSS based random copolymer in formulation of solid doses form for quick dissolution of poorly soluble drug. This chapter discuss the role of the copolymer as a solubilizing molecular carrier of hydrophobic drug.

Chapter 6 describes the study about the novel amphiphilic di-block copolymer composed of R-POSS and MPC. The copolymer form stable tightly packet micelles in aqueous environment and encapsulate the hydrophobic drug inside the core of the micelles. The micelles are highly potential for intercellular drug delivery. In this chapter author describes the application and novelty of the synthesized copolymer in drug delivery system.

Chapter 7 describes the important advantages of the random and di-block copolymers for their application as a simple modifier of liposome for drug delivery.

Chapter 8 describes the overall conclusion of the current thesis.

In this thesis, the author has systemically and strategically design and synthesize the polymeric biomaterial focusing its application as surface coating and drug delivery to contribute for advancement of the biomedical research.

Reference

1. S. Bhat, A. Kumar, *Biomatter* **2013**, 3, e24717.
2. A. Kumar, S. S. Han, *Int J Polym Mater Polym Biomater* **2017**, 66, 159-182.
3. A. Kumar, Y. S. Negi, V. Choudhary, N. K. Bhardwaj, *Cellulose* **2014**, 21, 3409-3426.
4. A. Kumar, Y. S. Negi, V. Choudhary, N. K. Bhardwaj, S. S. Han, *Int J Polym Anal Charact* **2017**, 22, 139-151.
5. R. Francis, D.S. Kumar, Biomedical Applications of Polymeric Materials and Composites, **2016**, Wiley, ISBN 9783527690923, https://books.google.co.jp/books?id=rRotDQAAQBAJ.
6. G. M. Raghavendra, K. Varaprasad, T. Jayaramudu, Biomaterials: Design, Development and Biomedical Applications, **2015**, William Andrew Publishing, 21-44, ISBN 9780323328890, https://doi.org/10.1016/B978-0-323-32889-0.00002-9.
7. W.J. Van der Giessen, A.M. Lincoff, R.S. Schwartz, H.M.M. van Beusekom, P.W. Serruys, D.R. Holmes, S.G. Ellis, E.J. Topol, *Circulation* **1996**, 94, 1690–1697.
8. H. Ghanbari, A. de Mel, AM. Seifalian, *Int J Nanomedicine*. **2011,** 6, 775–786.
9. R. Langer, N. A. Peppas, AIChE J. **2003**, 49, 2990-3006.
10. Y. Zhang, H. F. Chan, K. W. Leong, *Advanced Drug Delivery Reviews* **2013**, 65, 1, 104-120.
11. M. W. Tibbitt, C. B. Rodell, J. A. Burdick, K. S. Anseth, *Proceedings of the National Academy of Sciences* **2015**, 112, 47, 14444-14451.
12. R. Jain, N.H. Shah, A.W. Malick, C.T. Rhodes, *Drug Dev. Ind. Pharm.* **1998**, 24, 703–727.
13. R.A. Jain, *Biomaterials* **2000**, 21, 2475–2490.
14. J. Gong, M. Chen, Y. Zheng, S. Wang, Y. Wang, *J. Control. Release* **2012**, 159, 312–323.
15. A. Harada, K. Kataoka, *Macromolecules* **1995**, 28, 5294–5299.
16. A. Lavasanifar, J. Samuel, S. Sattari, G.S. Kwon, *Pharm. Res.* **2002**, 19, 418–422.

17. A. Falamarzian, A. Lavasanifar, *Macromol. Biosci.* **2010**, 10, 648–656.

18. A. Falamarzian, A. Lavasanifar, *Colloids Surf. B Biointerfaces* **2010**, 81, 313–320.

19. S.H. Kim, J.P. Tan, F. Nederberg, K. Fukushima, J. Colson, C. Yang, A. Nelson, Y.Y. Yang, J.L. Hedrick, *Biomaterials* **2010**, 31, 8063–8071.

20. M. Iijima, Y. Nagasaki, T. Okada, M. Kato, K. Kataoka, *Macromolecules* **1999**, 32, 1140–1146.

21. J.H. Kim, K. Emoto, M. Iijima, Y. Nagasaki, T. Aoyagi, T. Okano, Y. Sakurai, K. Kataoka, *Polym. Adv. Technol.* **1999**, 10, 647–654.

22. Y. Wang, S. Gao, W.H. Ye, H.S. Yoon, Y.Y. Yang, *Nat. Mater.* **2006**, 5, 791–796.

23. T.M. Sun, J.Z. Du, Y.D. Yao, C.Q. Mao, S. Dou, S.Y. Huang, P.Z. Zhang, K.W. Leong, E.W. Song, J. Wang, *ACS Nano* **2011**, 5, 1483–1494.

24. Y. Chujo, K. Tanaka, *Bull. Chem. Soc. Jap.* **2015**, 88, 633-643.

25. T. Konno, J. Watanabe, K. Ishihara, *J Biomed Mater Res A* **2003,** 65a (2), 209-214.

26. J. P. Xu, J. Ji, W. D. Chen, J. C. Shen, *Journal of Controlled Release* **2005**, 107, 502–512

27. G. Mountrichas, P. Petrov, S. Pispas, S. Rangelov, Nano-sized Polymer Structures via Self-assembly and Co-assembly Approaches, **2016**, Springer, Cham.

28. F. Huang, R. O'Reilly, S. C. Zimmerman, *Chem. Commun.,* **2014**, 50, 13415.

29. Z. Ahmad, A. Shah, M. Siddiq, H. B. Kraatz, *RSC Adv.*, **2014**, 4, 17028.

30. W. Xu, P. Ling, T. Zhang, *Journal of Drug Delivery* **2013**, 340315, 15.

31. J. Wu, P. Mather, *J. of Macromol. Sci., Part C: Polm. Rev.* **2009**, 49:25-63.

32. S. Kuo, F. Chang, *Prog. Polm. Sci*. **2011**, 36, 1649-1696.

33. L. Li, K. Raghupathi, C. Song, P. Prasad, S. Thayumanavan, *Chem. Commun.***, 2014**, 50, 13417.

34. M. Semsarilar, S. Perrier, *Nature Chemistry* **2010,** 2, 811–820.

Chapter 2

Synthesis and characterization of POSS-based amphiphilic copolymers

2-1. Introduction:

2-2. Experimental Section:

2-2.1. Material

2-2.2. Synthesis of methacrylate POSS and MPC random copolymers by free radical polymerization technique

2-2.2.1. Synthesis of silsesquioxane partial cages (1a-c)

2-2.2.2. Synthesis of polyhedral oligomeric silsesquioxanes (POSS)-based methacrylate (MA) (2a-c)

2-2.2.3. Synthesis of POSS methacrylate (MA) - MPC random copolymers (R-POSS-MA-*ran*-MPC) (3a-c)

2-2.3. Synthesis of POSS and MPC copolymer by RAFT polymerization technique

2-2.3.1. Preparation of poly(2-(methacryloyloxy)ethyl phosphorylcholine)-based chain transfer agent ($PMPC_{61}$)

2-2.3.2. Preparation of MPC-*block*-R-POSS-MA block copolymer (3a'-c')

2-2.4. Characterization of POSS and MPC copolymers synthesized by free radical and RAFT polymerization technique

2-2.4.1. Characterization of POSS and MPC copolymers (3a-c) synthesized by free radical polymerization technique

2-2.4.2. Characterization of POSS and MPC di-block copolymers (3a'-c') synthesized by RAFT polymerization technique

2-3. Results and Discussion:

2-3.1. Synthesis and characterization of R-POSS MA and MPC copolymers (3a-c) synthesized by free radical polymerization technique

2-3.2. Synthesis and characterization of R-POSS and MPC di-block copolymers (3a'-c') synthesized by RAFT polymerization technique

2-4. Conclusion

Reference

2-1. Introduction

Phospholipids major components of the lipid bilayer in the cellular membrane, draw great attention in biomedical applications. The great biocompatibility of the phosphorylcholine group expands its application to the design of synthetic biopolymers. One of the representatives is 2-(methacryloyloxy)ethyl phosphorylcholine (MPC) polymers that have been developed by Ishihara *et al*.[1,2] The zwitterionic nature of this phosphorylcholine (PC) group in MPC is responsible for its bioinert nature[3]. The functions and physicochemical properties can be controlled by copolymerization of MPC with the other monomers, for modulating surface and/or interface properties. The copolymers of MPC polymers with other hydrophobic monomers have been widely applied for biomedical applications including surface coating for blood compatible materials[4, 5], a film exhibited the elastic properties with high tensile strength[6], oxygen sensing membrane[7], and polymeric micelles for controlled release of anticancer drugs[8]. The amphiphilic copolymers of MPC and other hydrophobic monomers can be achieved, which can solubilize and deliver paclitaxel (PTX)[9, 10, 11, 12, 13]. According to the report of K. Ishihara *et al.*, poly[MPC-*co*-*n*-butyl methacrylate(BMA) (PMB30W)] with 70 mol % of the BMA unit most effectively dissolve the PTX[10]. The cellular uptake reports revealed that poly MPC-based polymeric micelle showed superior uptake than poly(ethylene oxide) (PEO)- and poly(*N*-(2-hydroxypropyl)methacrylamide) (PHPMA)-based polymeric micelle, indicating the advantage of poly MPC to interact with cell membranes[14]. However, the hydrophobic part, which is essential to interact with the hydrophobic molecule, has been mainly constructed by BMA, and the other candidates of the hydrophobic monomers have not been investigated yet.

Polyhedral oligomeric silsesquioxane (POSS), the chemical structure follows the basic composition of $R_nSi_nO_{1.5n}$ is a well-defined organic/inorganic hybrid material. The small silica-like cage in POSS shows excellent compatibility with most of the organic polymers via blending, graft copolymerization and polymerization [9,15]. It was reported that incorporation of POSS moiety provides an enhancement in mechanical, thermal and anti-biodegradable property and biocompatibility. Due to the hydrophobic nature of POSS cage, amphiphilic copolymers can be synthesized by introducing the POSS moiety to the ends of hydrophilic chain. For example poly (ethylene oxide) (PEO) and poly (ethylene glycol) (PEG) [10,11] resulted in solvent-sensitive self-assembled micelle and vesicle in aqueous solutions[15]. Another approach of synthesizing POSS-based amphiphilic copolymers are polymerization

with other hydrophilic monomers. Since the reactivity for POSS monomers is high, various kinds of copolymers prepared with methyl methacrylate[12,13], *n*-butyl acrylate[16] and styrene[17,18]. The random POSS copolymers do not induce aggregation and crystallization because the POSS moiety can dispersed through the whole polymer matrix. The random POSS copolymers are able to decreased rubbery plateau modulus of the polymer with increasing the entanglement density[18], which is dependent on the vertex (R) groups of the POSS moiety, for example, isobutyl, cyclohexyl, and cyclopentyl groups[19]. Recently, the concept of a new concept of "*element block*" suggested the design and synthesis of new element blocks and polymerization of those blocks to create new polymeric materials with improved material properties. By considering POSS as an element block, organic-inorganic hybrid at the molecular level can be prepared and applied to improve the property of biomaterials.

The objective of this study is to develop amphiphilic copolymer of element block POSS (hydrophobic) and MPC (hydrophilic) polymer. The new approach of designing and synthesis will help in enhancing and tuning the properties of MPC-based copolymer. This new material with improved thermal and mechanical properties can be applied in the coating of biomaterial surface and self-assembling nature of the copolymers in an aqueous environment can encapsulate and deliver the hydrophobic drug. In this work, the amphiphilic copolymer was synthesized by chemically modifying POSS cage (vertex R-groups modified with ethyl (C_2H_5), hexyl (C_6H_{13}), octyl (C_8H_{17})) and polymerization of POSS cage with MPC polymer unit via free radical and RAFT polymerization to create POSS-based MPC amphiphilic copolymer. The self-assemble behaviour of random copolymers is dependent on hydrophilic-hydrophobic balance. Morphologies of the self-assembled structure greatly vary with the ratio of hydrophilic side chains to hydrophobic groups. On the other hand, RAFT polymerization allows the design and synthesis of copolymers with a well-defined architecture and controlled molecular weight (MW) with relatively low polydispersity which forms 3D supramolecular self-assembled structures in an aqueous environment when the adequate hydrophilic/ hydrophobic balance is reached [20]. The effect of chemical modification (vertex R-groups modified with ethyl (C_2H_5), hexyl (C_6H_{13}), octyl (C_8H_{17})) of POSS cage (consider to be effective for hydrophobicity of POSS cage) was investigated based on size, surface charge, hydrophobic drug encapsulation, drug releasing behaviour.

2-2. Experimental Section

2-2.1. Material

2-(Methacryloyloxy) ethyl phosphorylcholine (MPC) was kindly supplied by Prof. Kazuhiko Ishihara (University of Tokyo, Japan). Poly MPC was prepared by free radical polymerization[31]. AIBN was purified by recrystallization from methanol before use. Ethyltrimethoxysilane, hexyltrimethoxysilane, and trimethoxyoctylsilane were purchased from Tokyo Chemical Industry Co. Inc, (Tokyo Japan.). 3-Methacryloxypropyl trichlorosilane and cyanopentanoic acid dithiobenzoate (CPD) were purchased from Sigma-Aldrich (Tokyo, Japan). Those chemicals were used as received without any further purification. Water used in all experiment was purified with a Millipore Milli-Q system. Other reagents were used as received.

2-2.2. Synthesis of methacrylate POSS and MPC random copolymers by free radical polymerization technique

2-2.2.1. Synthesis of silsesquioxane partial cages (1a-c)

The silsesquioxane partial cages were synthesized according to the previous report[21]. For example, in the case of ethyltrimethoxysilane-based silsesquioxane partial cage (**Scheme 2-1 (i); 1a**), ethyltrimethoxysilane (0.69 g, 4.6 mmol), THF (5 mL), deionized water (0.106 g, 5.9 mmol) and sodium hydroxide (0.08 g, 2 mmol) were dissolved and refluxed for 5 h. After that, the reaction mixture was cooled down to room temperature with vigorous stirring for another 15 h. White solid was recovered by removing the solvent by evaporator (recovery of 59 %). Hexyltrimethoxysilane and trimethoxyoctylsilane-based silsesquioxane partial cages (**1b** and **1c**) were synthesized following the same procedure.

2-2.2.2. Synthesis of polyhedral oligomeric silsesquioxanes (POSS)-based methacrylate (MA) (2a-c)

POSS-MA was synthesized by the following procedure as described below (**Scheme 2-1 (ii); 2a**). In brief, **1a** (0.24 g, 0.36 mmol) and triethylamine (0.055 ml, 0.4 mmol) were dissolved in THF (8 mL) and the system was cool down to 0 ^{0}C. The 3-methacryloxypropyl trichlorosilane

(0.105 g, 0.4 mmol) was added to 0.8 ml of THF, and this solution was slowly drop by drop added to the mixture. The resulting solution was stirred at 0 ^0C for 4 h and then continued overnight at room temperature. After removal of insoluble salt by filtration, the solvent THF was removed using rotary evaporator. The obtained white solid was then washed with methanol for three times and dried *in vacuo*. Hexyltrimethoxysilane- and trimethoxyoctylsilane-POSS-based MA (**2b** and **2c**) were synthesized following the same procedure.

2-2.2.3. Synthesis of POSS methacrylate (MA) - MPC random copolymers (R-POSS-MA-*ran*-MPC) (3a-c)

POSS-MA-based MPC copolymers were synthesized considering 1 mol % of **2** (feeding ratio) in the copolymer by conventional free radical polymerization technique using AIBN as an initiator. In brief, MPC monomer (1.46 g, 4.95 mmol) and **2a** (0.037 g, 0.05 mmol) were dissolved in dry ethanol (5 mL). After degassing the mixture by N_2 bubbling for 15 min, the flask was then transferred to the polymerization chamber with the temperature set at 60 ^0C, and sthe tirring process was continued for overnight. The reaction mixture was poured into an excess amount of diethyl ether, and the obtained precipitate was dried *in vacuo* to recover **3a (Scheme 2-1 (iii))**. The **3b** and **3c** were synthesized following the same procedure.

Yield: **3a** (~92%), **3b** (~97%), and **3c** (~95%)

^{1}H NMR (400 MHz) spectra obtained from CD_3OH of **3a-c** and poly MPC: revealed signal δ: 0.94 [s, -C-CH_3], 1.91 [s, -CH_2-], 3.28 [s, -N(CH_3)$_3$], 4.05-4.3 [m, -OCH_2], 3.74 [s, -CH_2N], 0.59 [s, -Si-CH_2-] **(Figure 2-1; (i))**. FT-IR (cm^{-1}): 1725 (C=O Ester), 1249, 1166 and 1089 (-POCH_2-), 966 (-N^+(CH_3)$_3$) and 1120 (-Si-O-) **(Figure 2-1; (ii))**.

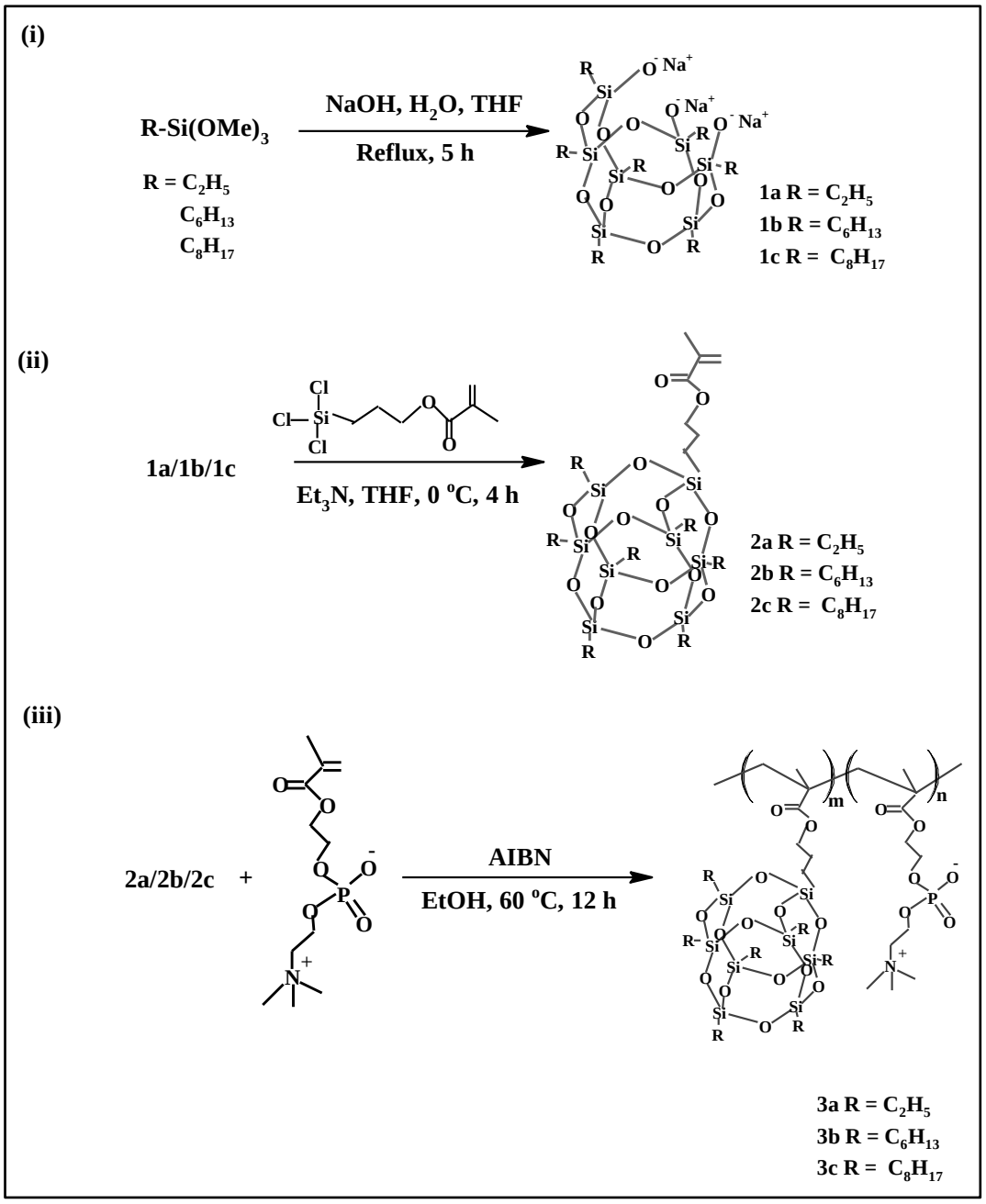

Scheme 2-1. Preparation of R-POSS-MA-*ran*-MPC copolymers (i) Preparation of silsesquioxane partial cages (R-POSS PC; **1a-c**). (ii) Preparation of POSS-based methacrylates (R-POSS-MA; **2a-c**) (iii) Preparation of POSS methacrylate-based MPC copolymers (R-POSS-MA-*ran*-MPC; **3a-c**)

2-2.3. Synthesis of POSS and MPC copolymer by RAFT polymerization technique

2-2.3.1. Preparation of poly(2-(methacryloyloxy)ethyl phosphorylcholine)-based chain transfer agent ($PMPC_{61}$)

MPC (0.01 mol, 2.95 g) monomer was dissolved in dried 10 ml Ethanol. Cyanopentanoic acid dithiobenzoate (CPD) (0.0002 mol, 0.0559 g), AIBN (0.00005 mol, 0.0082 g) were added to the solution. The mixed solution was deoxygenated by purging N_2 gas was for 30 min. It was then transferred to the polymerization chamber with the temperature set at 60 ^0C and continuous stirring process for 24 h (**Scheme 2-2 (i)**)**.** After cooling, the solution was dialyzed against pure water for 3 days. Poly MPC macro-CTA was recovered by freeze-drying. The number-average molecular weight ($M_w(\mathrm{NMR}) = 18{,}275$) and degree of polymerization (DP = 61) of poly MPC macro-CTA was determined from ^{1}H NMR peak areas observed at 7.3-7.9 ppm (phenyl, 5H) and 3.7 ppm (N-CH_2,2H).

2-2.3.2. Preparation of MPC-*block*-R-POSS-MA block copolymer (3a'-c')

Poly MPC macro-CTA ($PMPC_{61}$) (182.8 mg, M_w = 18,275 (NMR)), C_2H_5-POSS MA (224 mg, 0.3 m mol), C_6H_{13}-POSS MA (316 mg, 0.3 m mol) and C_8H_{17}-POSS MA (401 mg, 0.3 m mol) [**2a**, **2b**, **2c** respectively from **Scheme 2-1 (ii)**] and AIBN (0.33 mg, 0.002 m mol) were dissolved in 3 ml of ethanol and THF 1:1 mixture. The solution was outgassed and filled with N_2 by five freeze-pump-thaw cycles. The polymerization was carried out at 60 ^0C for 24 h (**Scheme 2-2 (ii)**). The reaction mixture was poured into an excess amount of diethyl ether to precipitate the polymer. The polymer was purified by reprecipitating it from methanol into a large amount of diethyl ether two times.

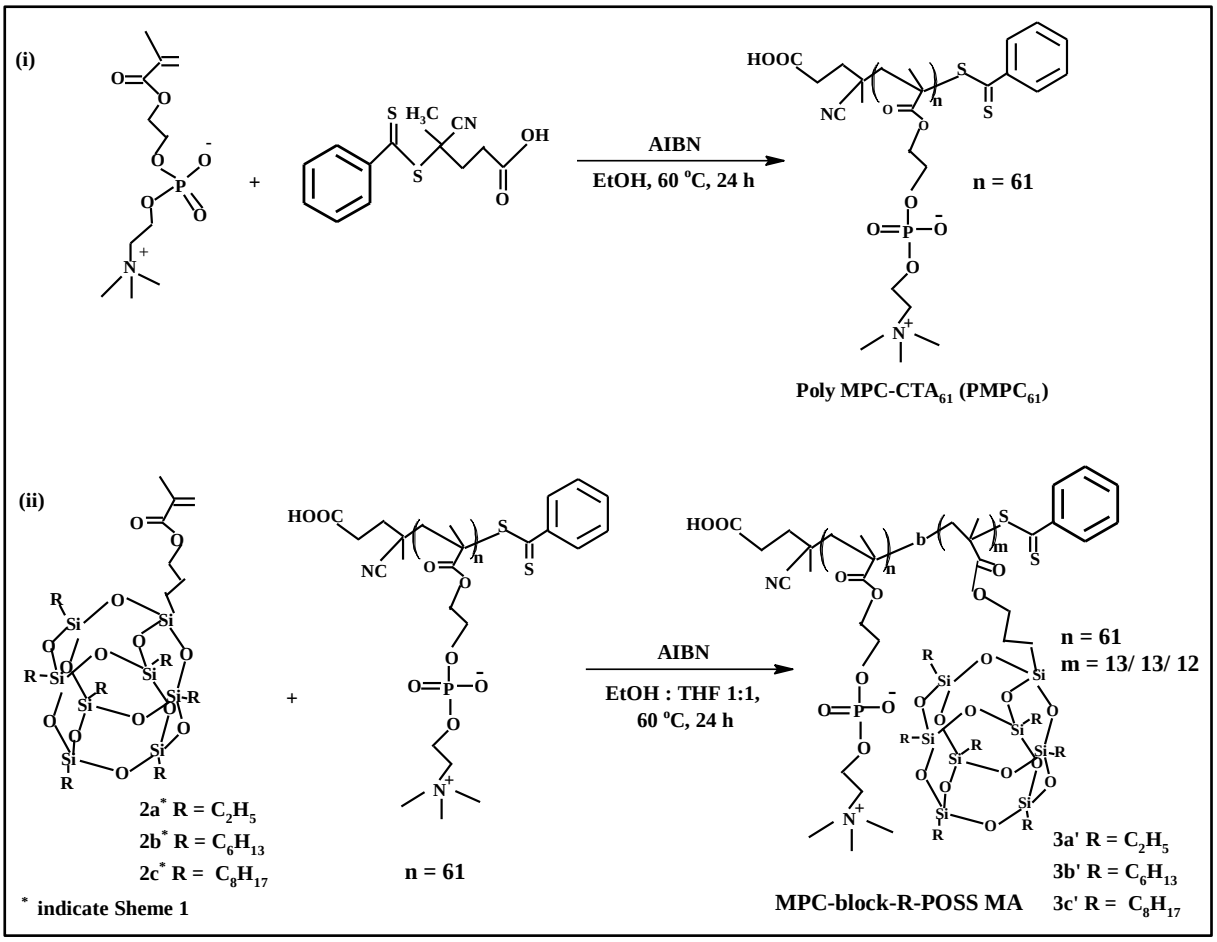

Scheme 2-2. Synthesis route of R-POSS MA-based MPC block copolymer (i) Homopolymerization of Poly(2-(methacryloyloxy)ethyl phosphorylcholine)-based chain transfer agent [Poly MPC-CTA$_{61}$ (PMPC$_{61}$)] by RAFT polymerization using AIBN as initiator and CPD as chain transfer agent (ii) Di-block copolymerization of Poly MPC-CTA$_{61}$ (PMPC$_{61}$) with R-POSS MA in the presence of AIBN as initiator [MPC-*block*-R-POSS MA].

2-2.4. Characterization of POSS and MPC copolymers synthesized by free radical and RAFT polymerization technique

2-2.4.1. Characterization of POSS and MPC copolymers (3a-c) synthesized by free radical polymerization technique

Solubility testing of the prepared copolymers **(3a-c)** were performed using six different solvents; pure water (H_2O), methanol (MeOH), ethanol (EtOH), THF, chloroform ($CHCl_3$) and Dimethyl sulfoxide (DMSO). The solubility of copolymers was measured at 25 ^0C with continuous stirring for 24 h (for pure water, methanol and ethanol more than 30 h). The solutions were filtered using a 0.45 µm pore size filter to remove the insoluble samples. The solvents were removed and the solubility was measured by measuring the weight of the soluble solid. The solubility measurements were conducted triplicate.

GPC measurements were performed by Prof. S. Yusa at University of Hyogo, Japan using a Tosoh DP-8020 pump equipped with a Tosoh RI-8020 refractive index detector, and a Shodex 7.0 µm bead size GF-7 M HQ column (exclusion limit ~10^7) operated at 25 °C under a flow rate of 0.6 mL/min. A phosphate buffer at pH 9 containing 10 vol% acetonitrile was used as the eluent. M_n and M_w/M_n were determined using standard sodium polystyrene sulfonate samples. Sample solutions were filtered with a 0.45 µm pore size filter before the GPC measurements.

^{1}H NMR spectra were measured by dissolving the copolymers in *d*-methanol (CD_3OH) with a concentration of 5 mg/ml (approximate) using a JEOL JNM-ECZS400FT NMR System.

The chemical structures of the copolymers were examined by Fourier transform infrared (FTIR) spectroscopy (JASCO FT/IR-460plus). KBr was used for the attenuated total reflectance crystal. The scanning wave numbers ranged from 4,000 to 400 cm^{-1}. The spectrum resolution was 4 cm^{-1}, and the 2 mm/sec scans were accumulated to determine one spectrum.

Powder X-ray diffraction was carried out using X-Ray Diffractometer (RINT2000, Rigaku Co., Japan) with monochromatic CuKα radiation and the generator working at 40 kV and 20 mA. Intensity was measured in the range of $2 < 2\theta < 40^o$ with scan steps of 1^o min^{-1}.

The composition of elements was determined by X-ray photoelectron spectroscopy (XPS) (Automated XPS Microprobe, PHI X-tool). The samples measurements were performed

on the dry powder sample. High-resolution scans for C1s, O1s, N1s, P2p and Si2p were acquired at a takeoff angle of 45° for the photoelectrons.

The thermal analyses of the copolymers were carried out by differential scanning calorimetry (DSC) (Seiko Instruments Inc. EXSTAR 6000/DSC6200). The scan rate was 10 °C/min (1^{st} cooling, 2^{nd} cooling and 1^{st} heating) and 5 °C/min (2^{nd} heating) within the temperature range of -50 - 80 °C. The glass transition temperature was obtained at the midpoint of change in the baseline of DSC thermograms.

The thermogravimetric analysis (TGA) of the copolymers were carried out using a thermogravimetric analyzer (Rigaku, TG 8121/ Thermo plus EV02) at a heating rate of 20 ^0C /min from 25 to 500 ^0C under a continuous nitrogen purge (100 mL/min). Temperature was increased from 25 to 120 ^0C with holding time for 20 min and then from 120 to 500 ^0C and with holding time for 10 min [22]. The composition of char yield was determined by XPS following the same procedure stated above.

2-2.4.2. Characterization of POSS and MPC di-block copolymers (3a'-c') synthesized by RAFT polymerization technique

^{1}H NMR spectra were measured by dissolving copolymers **(3a'-c')** in methanol-d_3 : tetrahydrofuran-d_8 (50:50) mixed solvent with a concentration of 3 mg/ml using a JEOL JNM-ECZS400FT NMR System.

The chemical structures of the copolymers were examined by FTIR spectroscopy (JASCO FT/IR-460plus). The scanning wave numbers ranged from 4000 to 400 cm^{-1}. The spectrum resolution was 4 cm^{-1}, and the 2 mm/sec scans were accumulated to determine one spectrum.

2-3. Results and Discussion:

2-3.1. Synthesis and characterization of R-POSS MA and MPC copolymers (3a-c) synthesized by free radical polymerization technique

Ethyltrimethoxysilane-based POSS-MA (**2a**), hexyltrimethoxysilane-based POSS-MA (**2b**) and trimethoxyoctylsilane-based POSS-MA (**2c**) were prepared by using silsesquioxane partial cages (**1a-c**) and 3-methacryloxypropyl trichlorosilane (**Scheme 2-1**). The POSS and MPC copolymers **(3a-c)** were prepared by free radical polymerization using AIBN as an initiator. The solubility of the copolymers (**3a-c)** in various solvents were compared to check the influence of aliphatic chain length (R-group) in the POSS moiety (**Table 2-1**). The solubility of copolymers **3a**, **3b** and **3c** in water, methanol and ethanol reduced abruptly (compare to Poly MPC) after incorporation of R-POSS moiety into the MPC polymeric matrix. Presumably, the R-POSS moiety strongly interacted with the phosphorylcholine (PC) group, which is responsible for the solubility of the MPC polymer in water and the hydrophobic region (R-POSS) is exposed on the solid polymer surface even in water [23].

Table 2-1. Solubility of R-POSS and MPC Copolymers **(3a-c)**

Sample Name	H_2O* (mg/ml)	MeOH* (mg/ml)	EtOH* (mg/ml)	THF (mg/ml)	$CHCl_3$ (mg/ml)	DMSO (mg/ml)
Poly MPC	84 ± 0.6	107 ± 4.0	74 ± 6.0	< 0.01	< 0.01	< 0.01
3a	10 ± 0.1	10 ± 0.1	1 ± 0.02	< 0.01	< 0.01	< 0.01
3b	5 ± 0.1	19 ± 1.0	10 ± 0.2	< 0.01	< 0.01	< 0.01
3c	7 ± 0.1	16 ± 0.4	11 ± 0.1	< 0.01	< 0.01	< 0.01

* Stirring continued for more than 30 h.

The molecular weight of the copolymers **(3a-c)** measured by GPC summarized in **Table 2-2**. The number-average molecular weight (M_n) of all copolymers is in the range of 1×10^4. In case of **3a**, the molecular weight (M_n) obtained was lower than other two copolymers, suggesting the increased copolymerization ratio of **2a**, which was calculated from ^{1}H-NMR spectra (**Figure 2-1; (i))**, affected the propagation and termination steps of radical polymerization.

Table 2-2. Chemical Composition and Thermal Properties of POSS and MPC copolymers **(3a-c)**

Samples		**% Mol (Feed)**	**% Mol ^{1}H NMR**	**Mole. Wt. in a phosphate buffer/AcCN (9:1)**			**T_g**	**Char Yield**
		MPC/ R-POSS	**MPC/ R-POSS**	**M_n ×10^4**	**M_w × 10^4**	**M_w/ M_n**	**°C**	**%**
Poly MPC		100	100	5.69	22.49	3.3	3	30
3a		99/1	98/ 2	2.79	9.81	3.5	11	30
3b	①[a)]	99/1	99/1	141	255	1.8	6	29
	②[a)]			4.19	14.1	3.3		
	Avg.			5.1	58.59	11.5		
3c		99/1	N. D.[b)]	6.1	41.1	6.8	7	29

[a)] Two peaks were observed in GPC charts; [b)] % Mol. could not be determined from NMR spectra

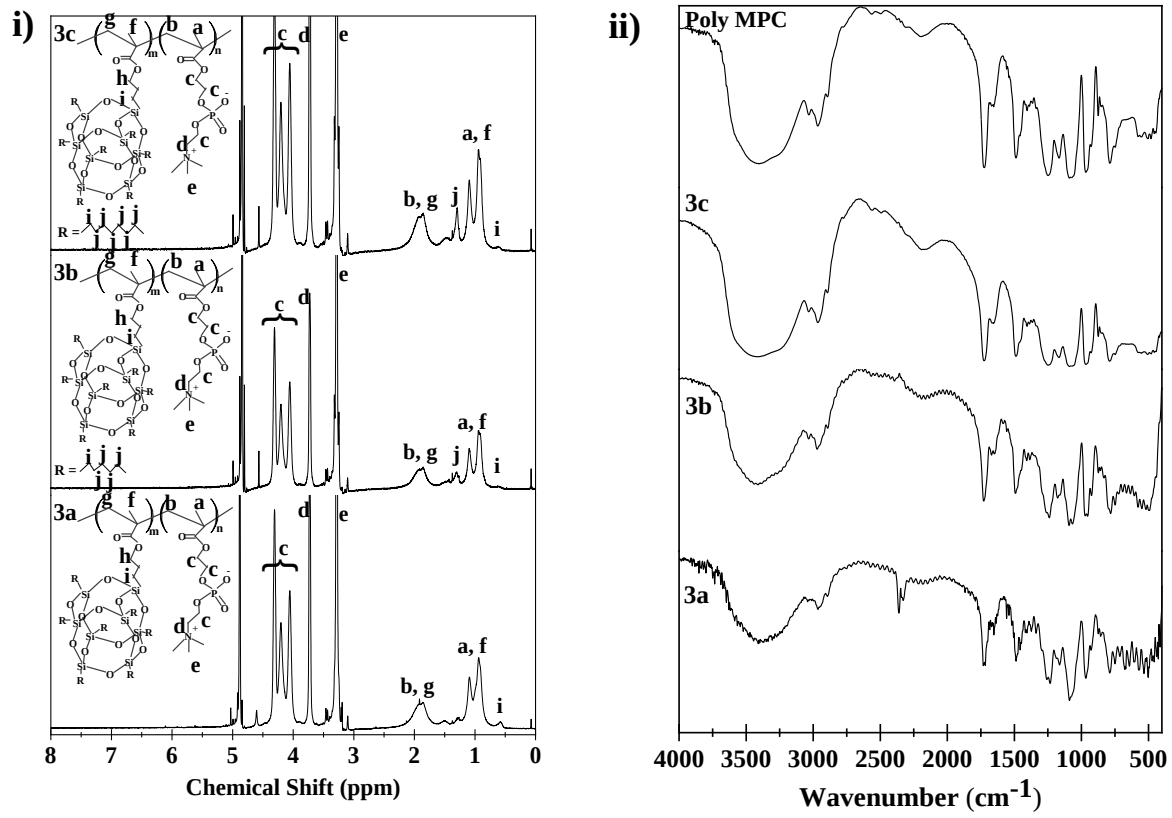

Figure 2-1. i) ^{1}H NMR spectra and **ii)** FT-IR spectra of R-POSS and MPC based copolymer **(3a-c)**

Compositions of POSS and MPC copolymers **3a-c** was analyzed by the XPS spectra (**Table 2-3**). The peaks of the carbon atom region (C_{1s}) was observed at 285 eV in all the copolymers, correspond to neutral carbon. The peak of the phosphorus (P_{2p}) atom region (correspond to the phosphate group) was detected at 133 eV and the nitrogen (N_{1s}) atom region correspond to protonated ammonium group was detected at 403 eV [24, 25]. The appearance of the Si 2_p (101 eV) and Si 2_s (152 eV) were confirmed which indicate the presence of Si. From the results of XPS, the successful incorporation of R-POSS moiety in the copolymers **3a-c** was confirmed.

Table 2-3. XPS Analysis of POSS and MPC copolymer Powder Samples **(3a-c)**

Sample	Atomic Conc. % from XPS				
	C_{1s}	N_{1s}	O_{1s}	P_{2p}	Si_{2p}
Poly MPC	59	4	33	4	0
3a	60	3	31	5	1
3b	67	1	28	2	2
3c	71	0	24	1	4

The POSS and MPC copolymers **(3a-c)** were characterized by thermal analysis (**Table 2-2**). With the incorporation of 1mol. % of R-POSS, the glass transition temperature (T_g)of **3a-c** increased in the order of **3a** > **3**c ≈ **3b (Figure 2-2; (i))**. In the case of **3a**, the T_g increased to 11 ^0C, which was 8 ^0C higher than poly MPC. Since, the thermal property of the polymer is primarily associated with their structural orientation, incorporation of R-POSS moiety to the MPC chains is likely to hinder the molecular motion of the MPC chain in the polymer matrix. This might be the reason of remarkable improvement in T_g [26]. In all the three copolymers **3a-c**, 1 mol. % R-POSS was used, and all the three copolymers have shown remarkable improvement in T_g. To further investigate the mechanism behind the T_g increase, FTIR characterization of the three copolymers **3a-c** and poly MPC were carried out **(Figure 2-2; (ii))**.

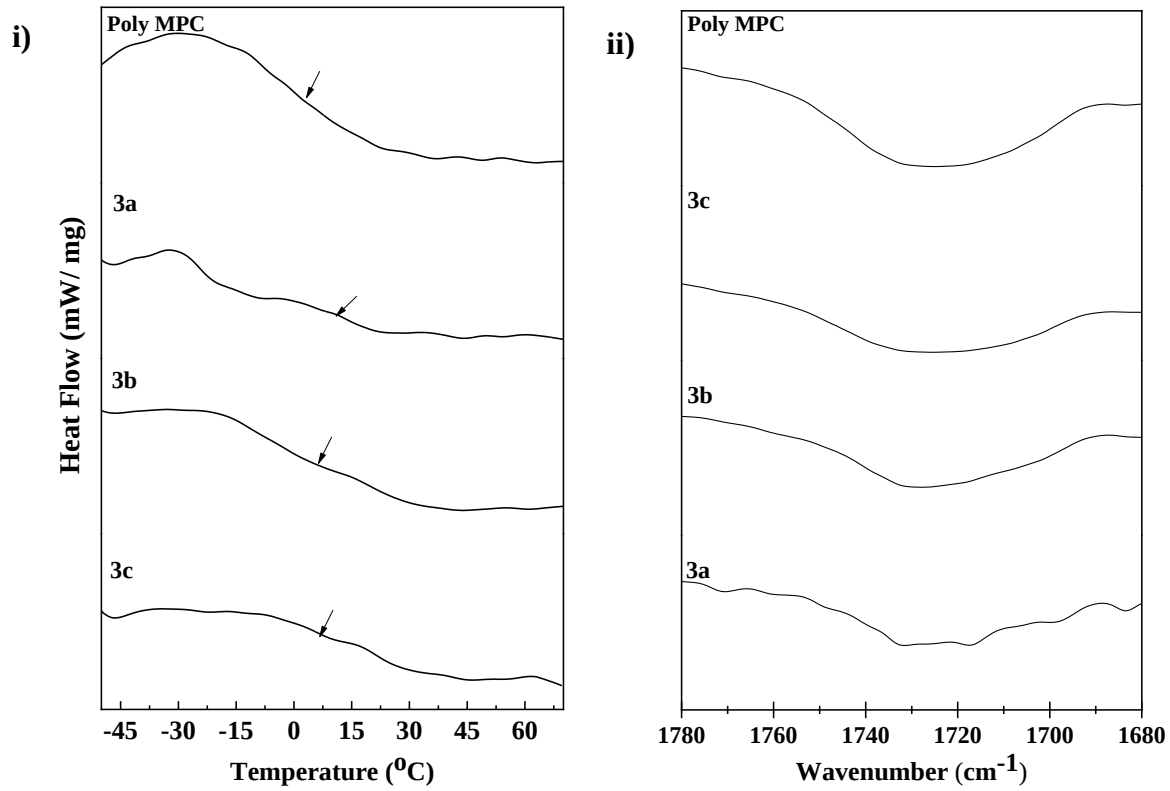

Figure 2-2. i) DSC thermogram and **ii)** FT-IR spectra of the regions from 1680 to 1780 cm^{-1} of R-POSS and MPC based copolymer **(3a-c)**

The carbonyl (C=O) and choline ($-N^{+}(CH_3)_3$) absorption in poly MPC observed at ~1725 cm^{-1} and 965 cm^{-1} respectively. In the case of **3a,** strong shoulder peak was observed at low frequency (1717 cm^{-1}) **(Figure 2-2; (ii))** which indicated the existence of new strong dipole-dipole interaction between the POSS and the carbonyl group of MPC polymer. This dipole-dipole interaction helps in suppressing the diluting effect of POSS and help in contributing positive T_g [19,26,27] of **3a**. In the case of **3c** when R-POSS was incorporated into the MPC polymer, a broad absorption shoulder appeared around 1725 cm^{-1} which indicates the interaction between R-POSS and MPC polymer and responsible for increasing T_g of **3c**. In the case of **3b**, after incorporation of R-POSS moiety in MPC polymer the absorption maximum shift toward the higher frequency (~1728 cm^{-1}) which indicate that interaction between the R-POSS and MPC is weaker than the diluent effect of R-POSS to the self-association interaction

of MPC. In the case of **3b** and **3c,** POSS has a small influence on T_g value due to the high molecular weight (> 2,00,000 g mol^{-1}) (**Table 2-2),** as there is a relationship between the high molecular weight and topological restriction on chain movement [28].

TGA thermograms of copolymers **3a-c**, indicate the four-step degradations at ~138.9, ~241.1, ~348.9 and ~396.9 ^0C (**Figure 2-3)**. The temperature of the first degradation ($T_{Initiation}$) observed in poly MPC ~137 ^0C to 161 ^0C (**3a**), 144 ^0C (**3b**), 141 ^0C (**3c**) [26] which suggested that incorporation of inorganic R-POSS help in increasing the thermal stability of the copolymers. XPS analysis of TGA char yield (**Table 2-2)** was performed, and the result indicated no trace of Si in the three copolymers after 500 ^0C.

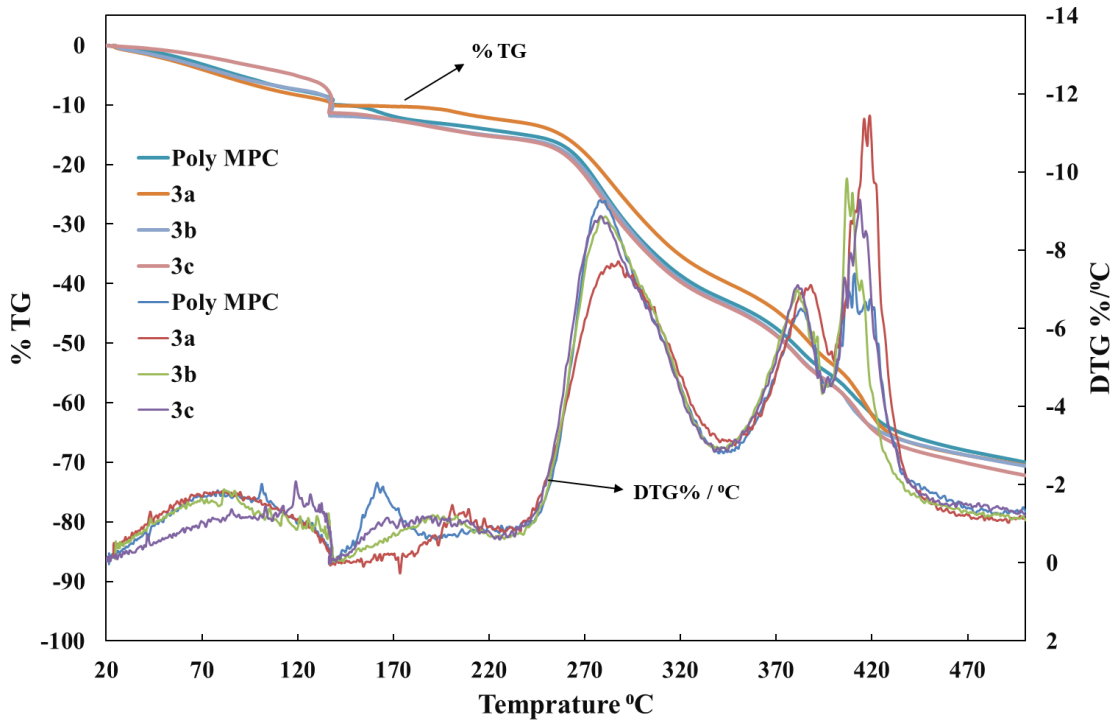

Figure 2-3. TGA thermogram of R-POSS and MPC based copolymer **(3a-c)**

X-ray diffraction of Poly MPC and **3a-c** were performed at room temperature (**Figure 2-4**). The XRD pattern of poly MPC indicated the amorphous broad peak pattern. As a reference,

the XRD of **1a** (partial cage) was performed, and the main reflections obtained at around 8-11°, which correspond to lattice spacing of 11-8 Å, very similar to the recently reported paper [29]. In the case of **3a-c**, the main reflections attributed to POSS moiety was not observed, and the pattern was similar to poly MPC. The results indicated no crystallization of POSS moiety in **3a-c**. Also, the intensity of the peak at $2\theta \approx 20^{o}$, attributed to the amorphous nature of poly MPC was decreased due to the enlargement of interchain correlation distance and inter-side-group correlation [30].

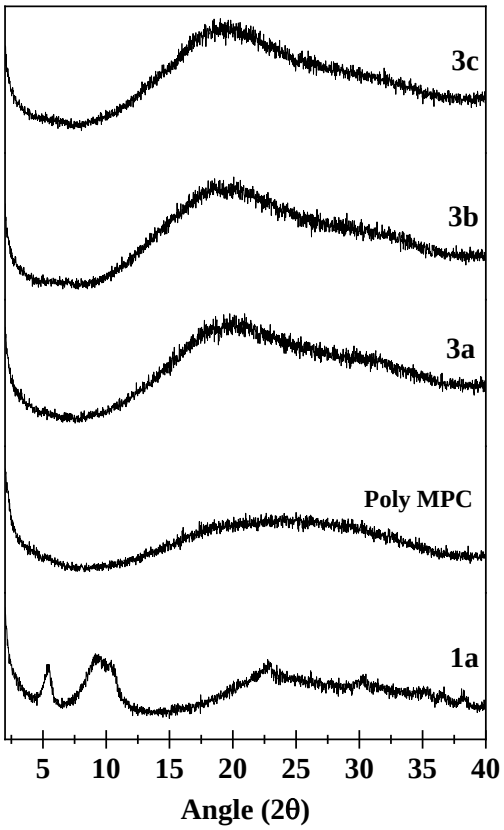

Figure 2-4. Powder X-Ray pattern of R-POSS and MPC based copolymer **(1a, 3a-c)**

2-3.2. Synthesis and characterization of R-POSS and MPC di-block copolymers (3a'-c') synthesized by RAFT polymerization technique

The di-block **(3a'-c')** copolymers were synthesized by RAFT polymerization using $PMPC_{61}$ as the CTA were characterized by ^1H NMR and FT-IR measurements (**Figure 2-5(i)-(iii) & Figure 2-6)**. From the ^1H NMR spectra, the resonance bands observed at 3.3-4.5 ppm were attributed to the phosphorylcholine (PC) moiety. The band observed at 1.7-2.31 ppm are attributed to the methylene protons of the main chain. The band observed at 0.8-1.25 ppm are attributed to the α-methyl proton which split due to the tacticity[6]. The resonance peak observed at 0.92, 1.11, 0.62, 1.91 and 4.32 were assigned to methyl and methylene protons of POSS moiety in the R-POSS units. The degree of polymerization (DP) was calculated from the integral intensity ratio of resonance bands at 3.3 and 0.62 ppm for phosphorylcholine moiety and R-POSS moiety, respectively. From the IR spectra, the absorption band appeared at1721 cm^{-1} ((C=O)-O-, ester), 1251, 1172, 1089 cm^{-1} (-P-OCH_2-) and 960 cm^{-1} (-$N^+(CH_3)_3$) corresponding to the poly MPC block and the absorption band at around 1120 cm^{-1} (-Si-O-) is the characteristic Si-O-Si stretching vibration peak of silsesquioxane cages from R-POSS (**Figure 2-6)**. Accordingly, the degree of polymerization of R-POSS unit was calculated to be 12-13, which was governed by the same monomer to initiator ratio. From the results, the segment length of three di-block copolymers were determined and abbreviated to MPC_{61}-*block*-C_2H_5-$POSS_{13}$, MPC_{61}-*block*-C_6H_{13}-$POSS_{13}$ and MPC_{61}-*block*-C_8H_{17}-$POSS_{12}$ **(3a'-c')**. Thus, the influence of the R-groups of POSS moiety on the micelle formation can be discussed the same block length of R-POSS moiety (DP of R-POSS 13/13/12).

^1H NMR (400 MHz) spectra of R-POSS and MPC based block copolymers obtained (**Figure 2-5 (i), (ii), (iii))** from methanol-d_3: tetrahydrofuran-d_8 (50:50) δ: 0.96 [s, -C-CH_3], 1.78-2.24 [s, -CH_2-], 3.29 [s, -N$(CH_3)_3$], 4-4.39 [m, -OCH_2], 3.77 [s, -CH_2N], 0.62 [s, -Si-CH_2-], 6.8-7.15 [phenyl, 5H]

FT-IR (cm^{-1}): 1721 (C=O Ester), 1250, 1173 and 1089 (-$POCH_2$-), 963 (-$N^+(CH_3)_3$) and 1121 (-Si-O-) (**Figure 2-6)**.

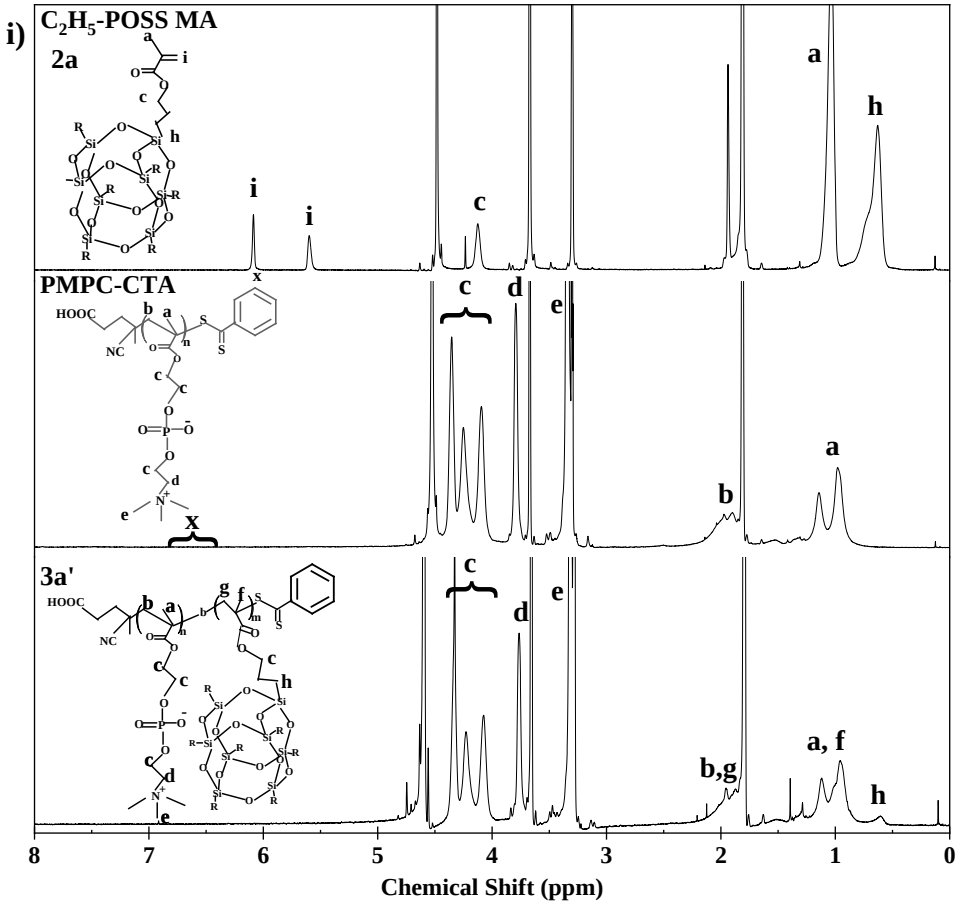
i)
C2H5-POSS MA
2a
PMPC-CTA
3a'
Chemical Shift (ppm)

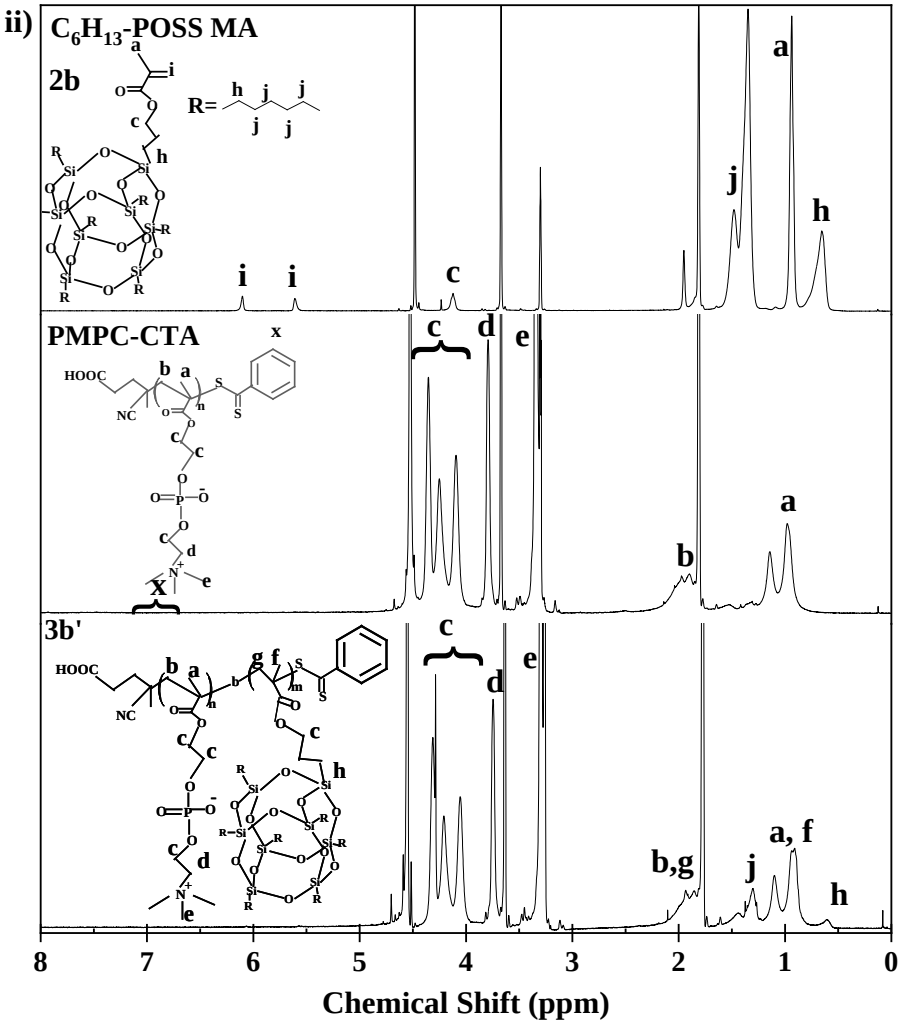
ii)
C6H13-POSS MA
2b
R=
PMPC-CTA
3b'
Chemical Shift (ppm)

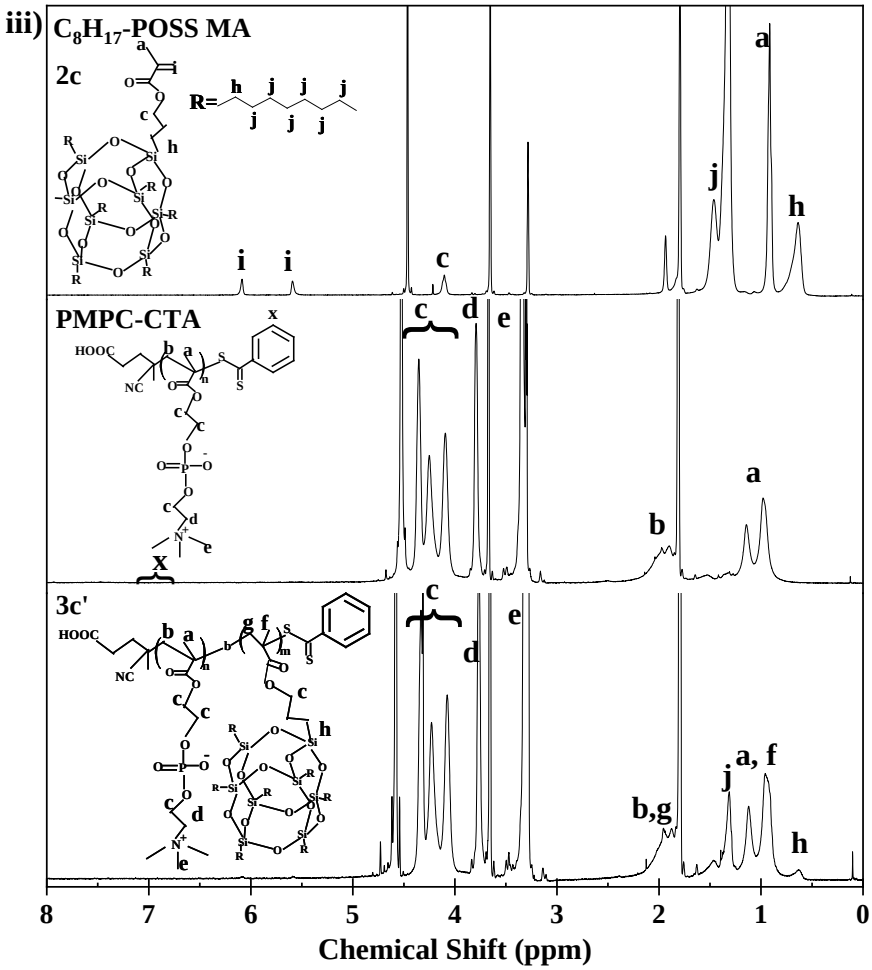

Figure 2-5. ^{1}H NMR spectrum of (i) MPC_{61}-*block*-C_2H_5- $POSS_{13}$ **(3a')**, (ii) MPC_{61}-*block*-C_6H_{13}- $POSS_{13}$ **(3b')** and (iii) MPC_{61}-*block*-C_8H_{17}- $POSS_{12}$ **(3c')** in methanol-d_3 : tetrahydrofuran-d_8 (50:50).

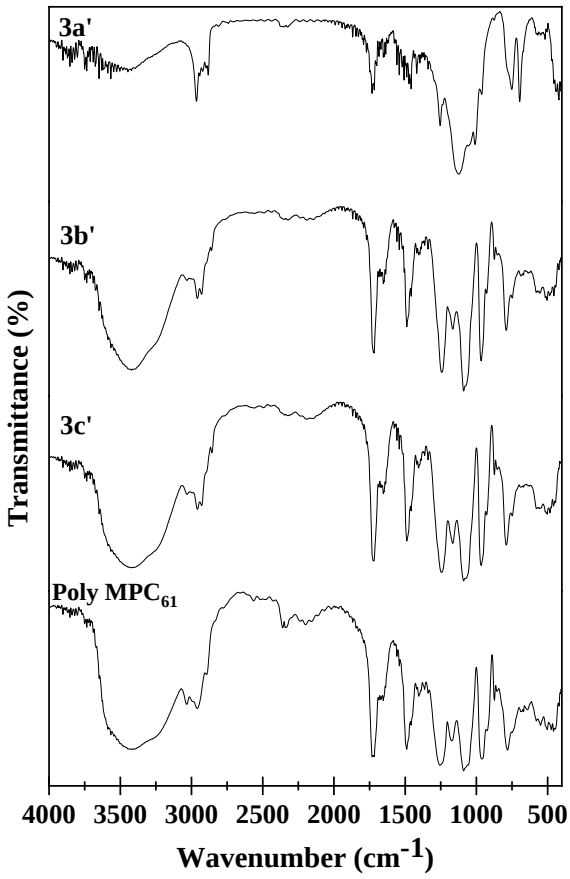

Figure 2-6. The FT-IR spectra of MPC_{61}-*block*-C_2H_5- $POSS_{13}$ **(3a')**, MPC_{61}-*block*-C_6H_{13}-$POSS_{13}$**(3b'),** MPC_{61}-*block*-C_8H_{17}- $POSS_{12}$ **(3c')** and polyMPC_{61}

2-4. Conclusion

The R-POSS and MPC based copolymers were synthesized by two polymerization techniques (free radical and RAFT polymerization). The characterization results ^1H NMR, FI-IR and XPS results indicated the successful synthesis of the copolymers using two polymerization technique. The copolymers has been further studied focusing its application in drug delivery system.

Reference

1. Y. Iwasaki, K. Ishihara, *Anal. Bioanal. Chem.* **2005**, 381, 534-546.
2. K. Ishihara, H. Nomura, T. Mihara, K. Kurita, Y. Iwasaki, N. Nakabayashi, *J. Biomed. Mater. Res., Part A* **1998**, 39, 323-330.
3. T. Goda, K. Ishihara, Y. Miyahara, *J. Appl. Polym. Sc.* **2015**, 132, 41766.
4. T. Ueda, H. Oshida, K. Kurita, K. Ishihara, N. Nakabayashi, *Polym. J.* **1992**, 24, 1259–1269.
5. S. P. Ho, N. Nakabayashi, Y. Iwasaki, T. Boland, M. LaBerge, *Biomaterials 24.* **2003**, 5121-5129.
6. W. Sirithep, Y. Narita, Y. Nagase, *Trans. Mat. Res. Soc. Japan 38.***2013**, 473-476.
7. K. H. Chae, Y. M. Jang, Y.H. Kim, O. Sohn, J. I. Rhee, *Sensors and Actuators B 124* **2007**, 153-160.
8. J. Xu, J. Ji, W. Chen, D. Fan, Y. Sun, J. Shen, *Eur. Polym. J., 40* **2004**, 291-298.
9. S. Kuo, F. Chang, *Prog. Polm. Sci.* **2011**, 36, 1649-1696.
10. G. Li, L. Wang, H. Ni, C. Pittman Jr., *J. Inorg. Organometa. Polym.* **2001**, 11, 3.
11. H. Ghanbari, B. G. Cousins, A. M. Seifalian, *Macromol. Rapid Commun.* **2011**, 32, 1032-1046.
12. E.T. Kopesky, T.S. Haddad, R.E. Cohen, G.H. McKinley, *Macromolecules*, **2004**, 37, 8992–9004.
13. Xu, H.Y., Yang, B.H.,Wang, J.F., Guang, S.Y., Li, C. *J. Polym. Sci. Polm. Chem.***,2007**, 45, 5308–5317.
14. J. Pyun, K. Matyjaszewski, J. Wu, G. M. Kim, S.B. Chun, P.T. Mather, *Polymer*, **2003**, 44, 2739–2750.
15. J. Wu, P. Mather, *J. of Macromol. Sci., Part C: Polm. Rev.* **2009**, 49:25-63.
16. J. Pyun, K. Matyjaszewski, J. Wu, G. M. Kim, S.B. Chun, P.T. Mather, *Polymer*, **2003**, 44, 2739–2750.
17. A. Romo-Uribe, P.T. Mather, T.S. Haddad, J.D. Lichtenhan, *J. Polym. Sci., Part B: Polym. Phys.*, **1998**, 36, 1857–1872.
18. J. Wu, T.S. Haddad, G.M. Kim, P.T. Mather, *Macromolecules*, **2007**, 40, 544–554.
19. J. Wu, T.S. Haddad, P.T. Mather, *Macromolecules*, **2009**, 42, 1142-1152.
20. S. I. Yusa, K. Fukuda, T. Yamamoto, K. Ishihara, Y. Morishima, *Biomacromolecules* **2005**, 6 (2), 663-670.

21. D. W. Lee, Y. Kawakami, *Polymer Journal* **2007**, *39*, *3*, 230-238.
22. K. Peacock, S. I. Cauet, A. Taylor, P. Murray, S. R. Williams, J. V. M. Weaver, D. J. Adams, M. J. Rosseinsky, *Chem. Commun.* **2012**, *48(75)*, 9373-5.
23. Y. Inoue, Y. Onodera, K. Ishihara, *Colloids and Surfaces B: Biointerfaces* **2016**, 141, 507–512.
24. Y. Inoue, T. Nakanishi, K. Ishihara, *React. & Funct. Polym.* **2011,** 71, 350–355.
25. H. Xu, B. Yang, J. Wang, S. Guang, C. Li, *J. Polym. Sci.: Part A: Poly. Chem.* **2007**, 45, 5308–5317.
26. H. Xu, S. Kuo, J. Lee, F. Chang, *Macromolecules,* **2002**, 35, 23.
27. B. X. Fu, W. H. Zhang, B. S. Hsiao, M. Rafailovich, J. Sokolov, G. Johansson, B. B. Sauer, S. Phillips, R. Balnski, *High Perform. Polym*. **2000**, 12, 565.
28. Pramudya, C. G. Rico, C. Lee, H. Chung, *Biomacromolecules.* **2016**, 17, 3853−3861.
29. Y. Du, M. Yu, X. Chen, P. X. Ma, B. Lei, *ACS Appl. Mater. Interfaces* **2016**, 8, 3079−3091.
30. Md. Rabby, S. Jeelani, V. K. Rangari, *J. Nanomat.* **2015**, Art. ID 894856, 13.
31. S. Chatterjee, T. Matsumoto, T. Nishino, T. Ooya, *Macromol Chem Phys* **2018,** 219 (8), doi: 10.1002/macp.201700572.

Chapter 3

"Element Block" R-POSS and 2-(methacryloyloxy)ethyl phosphorylcholine-based random copolymers for a surface coating material

3-1. Introduction

3-2. Experimental Section

3-2.1. Material

3-2.2. Measurements of stress-strain behavior of copolymers (3a-c)

3-2.3. Film Coating by copolymers (3a-c)

3-2.4. Water contact angle measurements of the copolymers (3a-c) coated surface

3-2.5. Protein adsorption on the copolymers (3a-c) coated surface

3-2.6. Cell attachment on the copolymer (3a) coated surface

3-3. Results and Discussion

3-3.1. Stress-strain behavior of the random copolymers (3a-c)

3-3.2. Morphology observation and characterization of the random copolymers (3a-c) coated surface

3-3.3. Surface property: wettability, protein adsorption and cellar attachment

3-4. Conclusion

Reference

3-1. Introduction

Hemocompatibility is the major requirement of organic/ inorganic material for those application in the preparation and coating of the cardiovascular implant. Nano-composite materials have shown unique characteristics for application as blood biomaterial interface. Nano-composite polymers can be bi-functionalized with growth-factor through a surface modification to attract the endothelial progenitor cells from circulatory blood which could help in the enhancement of bio and hemocompatibility of the cardiovascular devices coated by these polymers. Recently, the study has been shown that small diameter coronary artery bypass grafts composed of POSS-PCU with improved mechanical strength eliminated the apparent disadvantages associated with handling and longevity. Guo et al. developed a biodegradable drug-eluting stents coating material using POSS-TPU[1]. Their results demonstrated that biodegradable PTX loaded POSS-TPU coating allow control drug release with a variation of T_g and the degradation rate was tunable by the thickness of the coating under physiological conditions [1]. Maeda et al. fabricated the MPC fiber using the electrospinning process and drug releasing characteristics from the electro-spun MPC fiber was examined. Their studied suggested that MPC-based nanofiber could be a promising candidate as cardiovascular graft material with effective control over drug releasing [2].

POSS and poly MPC have already been studied individually for the application in the field of cardiovascular implant fabrication and their coating. Their individual studies have demonstrated promising result and their high need in this particular area. In this chapter, R-POSS-methacrylates (bearing different vertex (R-) groups such as ethyl, hexyl and octyl) and MPC-based random copolymers synthesized in chapter 2 has been consider for further study. The effect of the R-group in the POSS moiety was evaluated in terms of thermal, mechanical, physical and surface properties of synthesized copolymers focusing their application in the field of the surface coating. The results showed that thermal and mechanical strengths of copolymers have increased by employing only the ethyl (R= C_2H_5)-POSS. Solubility characteristics of the copolymers in various polar and non-polar solvents were evaluated, and observation has provided the knowledge about the influence of this R-group in the POSS moiety on wettability and hydrophilicity of the copolymer when coating the surface. The current study suggested a new approach of enhancing and tuning the properties of MPC, with improved thermal and mechanical property for its application as surface coating materials.

3-2. Experimental Section

3-2.1. Material

The R-POSS-MA MPC random copolymers (R = C_2H_5, C_6H_{13}, and C_8H_{17}) were synthesized as described in **Chapter 2** (**Scheme 2-1; 3a-c)**. The mol. % of R-POSS in the copolymers were found to be 1-2 mol. %. Dulbecco's Modified Eagle Medium (DMEM), Dulbecco's phosphate-buffered saline (DPBS), 0.25 %-Trypsin/1mM-EDTA solution, penicillin-streptomycin mixed solution and sodium carbonate was purchased from Nacalai Tesque, Inc. (Kyoto, Japan). Fetal Bovine Serum (FBS) was purchased from Sigma-Aldrich Co. LLC. (St. Louis, U.S.A). The other reagents and solvents were used without further purification. NIH 3T3 fibroblast cells (kindly supplied by Prof. Tsutomu Tanaka, Kobe University) were cultured in DMEM supplemented with 10% FBS and 100 U/mL penicillin-streptomycin. Cells were grown in a humidified incubator at 37 ℃ under 5% CO_2.

3-2.2. Measurements of stress-strain behavior of copolymers (3a-c)

To prepare the samples for mechanical testing, **3a-c** and polyMPC were dissolved in methanol (5 w/v %), and the solutions were cast on a molded poly(tetrafluoroethylene) sheet (6 cm x 5 cm x 1.5 cm). The samples were kept at 40 ^0C inside a dryer for 24 h and then at room temperature (25 ℃) in a dry condition for 3 days. The dried films were cut into rectangular strips (40×5×0.01~0.03 mm) using a razorblade. Stress-strain curves were obtained by Autograph AG-XPlus, (Shimadzu Corporation, Japan), considering the gauge length 20 mm and crosshead speed 2 mm/min.

Additionally, compression testing was also performed by Autograph AGS-J, (Shimadzu Corporation, Japan). Samples for the measurements were prepared by pressing the dry copolymers in steel mold using 10 N force. The size of the sample used for the measurements was ~ 10 mm × 10 mm × (2.7 ~ 3.3 mm). The amount of copolymer used for samples preparation was 400-500 mg/ sample. The samples were pressed at 0.3 mm/min compression rate. Young's modulus was calculated by measuring the slop in the stress-strain curve over 10% displacement. Five measurements were recorded for each sample [3].

3-2.3. Film Coating by copolymers (3a-c)

The copolymers **3a-c** were coated by spin coating on an aliphatic polyether-based thermoplastic polyurethane film (Tecoflex®) with three different concentration copolymer solution (1%, 5% and 10% w/v) using spinning speed of 400 rpm for 10 sec (1st run) and 1200 rpm for 20 sec (2nd run). The coated films were dried inside the vacuum dryer for 6 h at 40 ^0C [4]. The XPS analysis was performed to determine the composition of elements on the surface of the coated film, and the scanning electron microscopy (SEM) (JEOL, JSM-6510) was performed to observe the surface morphology.

3-2.4. Water contact angle measurements of the copolymers (3a-c) coated surface

The wettability of copolymers **3a-c** and poly MPC coated surface were evaluated by the measurement of the static contact angles by distilled water and 0.1 M PBS (pH 7.4) (4.5 µL droplet). The contact angle measurements were conducted by contact angle meter (Kyowa Interface Science Co. Ltd., DMs-401) and the measurement was carried out at five different positions of each specimen at room temperature.

3-2.5. Protein adsorption on the copolymers (3a-c) coated surface

The amount of BSA adsorbed on the surface of the copolymers **(3a-c)** coated and uncoated films were quantified by micro-BCA method. The 450 µg/ml BSA in 0.1M phosphate buffered saline (PBS) (pH 7.4) solution was used. Before the measurement, the surface of the coated film (size of 10 mm × 10 mm) was cleaned by high N_2 gas flow. The film surface was immersed into 8 ml of BSA solution at 37 ^0C for 1 h. The samples were rinsed with 50 ml of 0.04 M PBS (pH 6.8) at a flow rate of 8 ml/min. The BSA adsorbed on the surface was recovered by washing it with 2 ml of 1 wt.% sodium dodecyl sulphate (SDS) solution in 0.1 M PBS for 5 min at room temperature [5]. The concentration of protein adsorbed on the surface was determined from the BSA standard curve. Stability of the surface coating in PBS for 2 h was confirmed by XPS measurement (the composition of elements on the surface of the coated film).

3-2.6. Cell attachment on the copolymer (3a) coated surface

To determine the cell attachment on the surface, polystyrene tissue culture dishes were coated with **3a** using a spin coating technique. NIH 3T3 fibroblast cells were seeded on the coated tissue culture dish with a density of 10,000 cells/ dish using DMEM cell medium. After incubation for 24 and 48 h at 37 ^0C in 5 % CO_2 atmosphere, the cell morphology was observed under a digital inverted microscope (EVOS FL, Life Technologies). The existence of **3a** on tissue culture dish after 48 h in the cell culture medium was confirmed by the XPS measurements. The culture dish was washed three times with distilled water and dried inside the vacuum dryer before the measurement.

3-3. Results and Discussion

3-3.1. Stress-strain behavior of the random copolymers (3a-c)

In order to assess the bulk properties of **3a-c** in relation to the T_g increase, a tensile test was performed. The preparation of bulk films of copolymers **3a-c** for the measurement of mechanical properties was hard. **Figure 3-1 (i)-(ii)** represent Young's modulus and tensile strength calculated from the stress-strain curve of the copolymers. The Young's modulus and tensile strength of **3a** was observed significantly higher in comparison with the other copolymers **3b-c**. The compression test results (**Figure 3-2 (i)-(ii)**) also indicated that incorporation of C_2H_5-POSS help in increasing Young's modulus of **3a.** For the copolymer **3b** and **3c,** the results indicated that incorporation of C_6H_{13} and C_8H_{17}-POSS moieties decreased the mechanical strength of the copolymers. The tensile strength of **3b** could not be measured due to weak mechanical strength. The previous study[15] revealed that the mechanical property of the copolymer influenced by the degree of dispersion of the R-POSS in the polymer matrix, the concentration of R-POSS and type of pendant group. The POSS-POSS and POSS-polymer interaction strongly affect the mechanical property of the copolymers. The **Figure 3-3** represented the expanded FT-IR spectra from 1680 to 1780 cm^{-1}. The FT-IR spectra indicated that in the case of **3a** a strong shoulder peak appeared at low frequency (~1717 cm^{-1}) which represented the existence of a new strong dipole-dipole interaction between the C_2H_5-POSS and the carbonyl group of MPC. This strong dipole-dipole interaction might be the reason of

increased mechanical strength of **3a**. In the case of **3c,** a broad absorption shoulder appears (~1725 cm^{-1}) which indicates the interaction between C_8H_{17}-POSS and MPC polymer. In the case of **3b,** the absorption maximum tends to shift toward the higher frequency (~1728 cm^{-1}) after incorporation of C_6H_{13}-POSS which may play an inert diluent role to decrease the self-association interaction of MPC molecule. The reason for the improvement of mechanical strength of **3a** may be (i) the introduction of POSS moiety restricted the mobility of the polymer chains due to its strong interaction with MPC polymer, and (ii) evenly distribution of C_2H_5-POSS moiety on the polymer matrix in nanometer scale resulting better Young's modulus [3, 6-10]. Form these results it can be concluded that long alkyl side chain of R-POSS might not be favorable to tangle with MPC polymeric chains in terms of the decreased elasticity of the material [7, 11].

i)

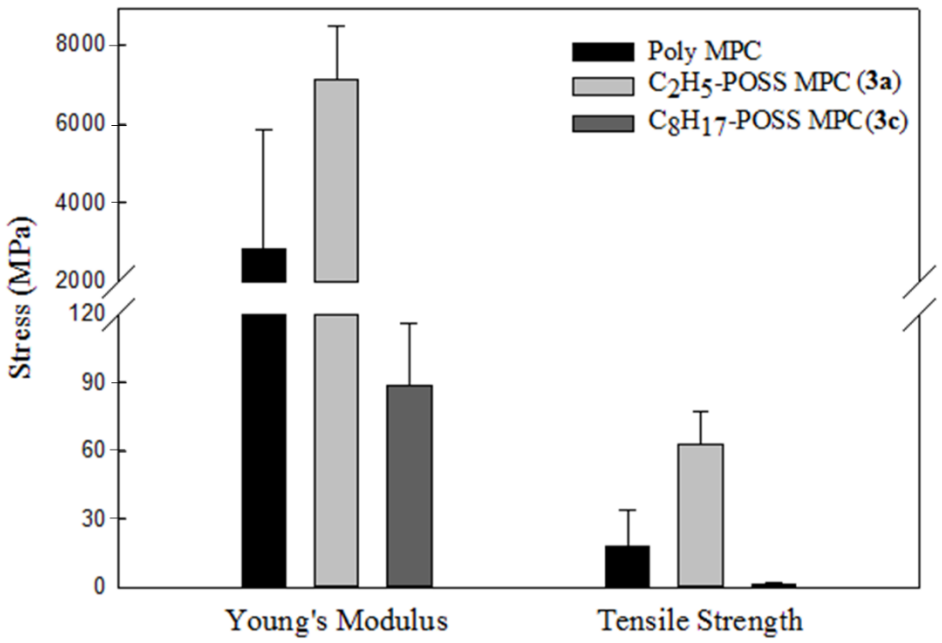

ii)

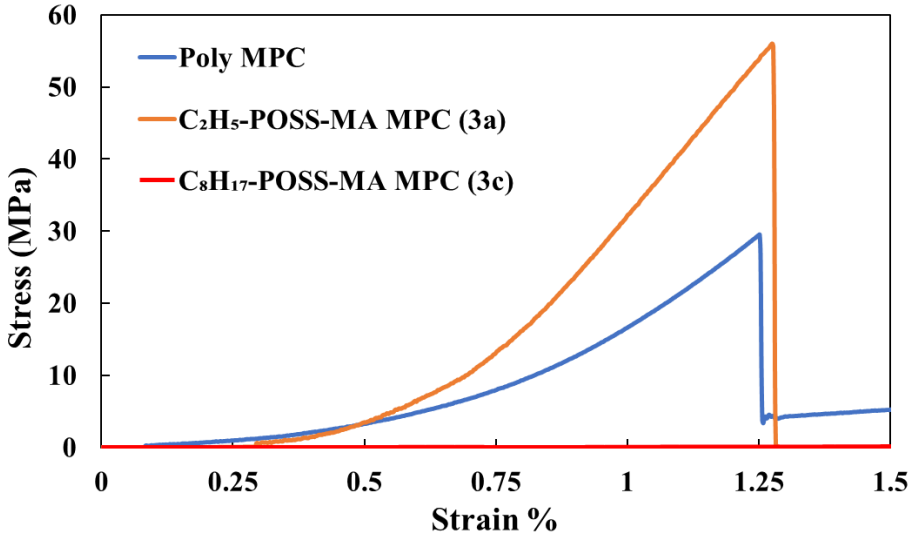

Figure 3-1. Results of Tensile testing of R-POSS and MPC based copolymers **(3a-c)**: **i)** Young's modulus and tensile strength **ii)** Tensile stress-strain curves

i)

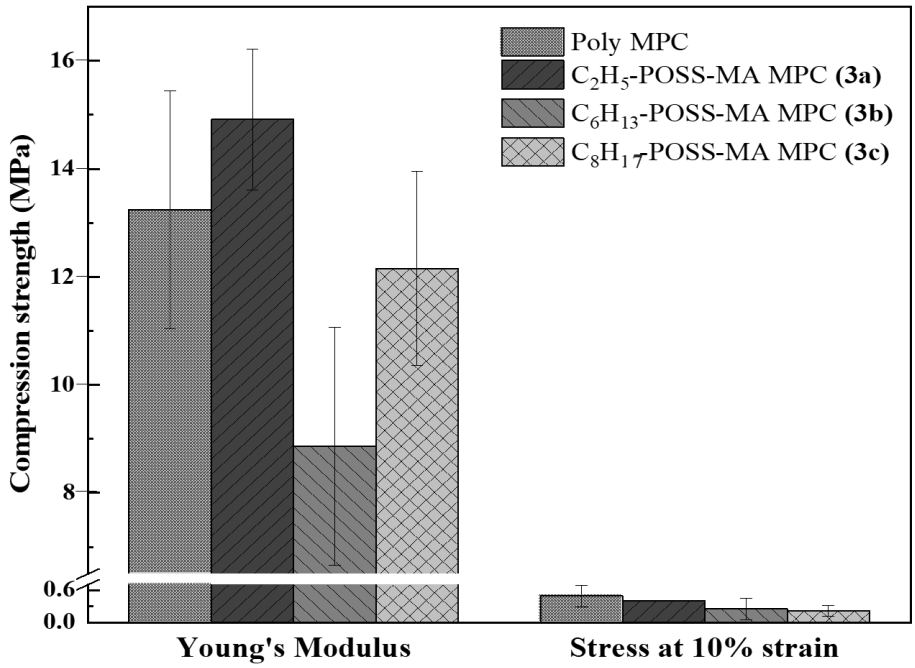

ii)

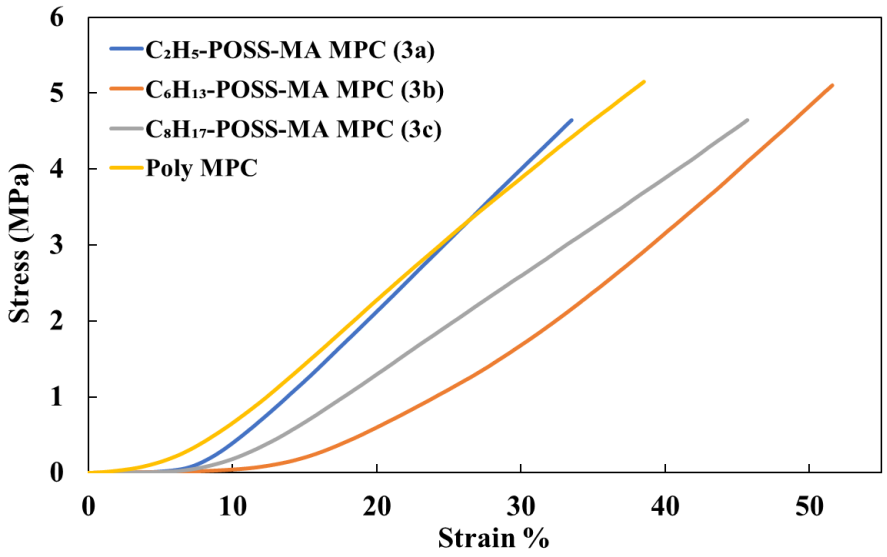

Figure 3-2. Results of Compression testing of R-POSS and MPC-based random copolymers **(3a-c)**: **i)** Young's modulus and compression strength at 10 % strain **ii)** Compression stress-strain curves

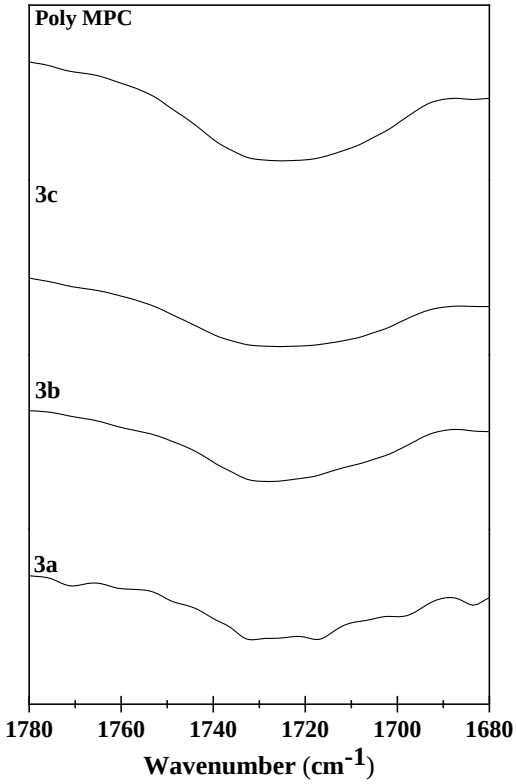

Figure 3-3. FT-IR spectra of the regions from 1680 to 1780 cm^{-1} of R-POSS and MPC based copolymer **(3a-c)**

3-3.2. Morphology observation and characterization of the random copolymers (3a-c) coated surface

Surface characterization of the copolymer **3a-c** coated surfaces were performed using the XPS measurements (**Table 3-1**). Peaks for Si 2p (101 eV) and Si 2s (152 eV) were observed for all the copolymers-coated surface. The atomic concentration % analysis showed a higher concentration of Si on the surface of **3a** coated film which indicates the presence of C_2H_5-POSS moiety on the coating surface. Surface morphology of the copolymer **3a-c** coated surface was observed using SEM measurement. The SEM image showed that when 1% w/v **3a** solution concentration was used for coating the surface, the smooth wave-like surface appeared, but when higher % solution like 10% w/v concentration solution used liner uniform cracked surface was observed (**Figure 3-4**).

Table 3-1. XPS Analysis of R-POSS and MPC-based copolymer coated surface **(3a-c)**

Sample	Atomic Conc. % from XPS analysis				
	C1s	**N1s**	**O1s**	**P2p**	**Si2p**
Poly MPC	63.1	4.0	29.9	4.1	0.1
3a	69.9	4.0	27.0	1.9	3.1
3b	62.0	4.1	28.9	3.1	2.9
3c	73.1	0.9	23.1	2.1	1.0

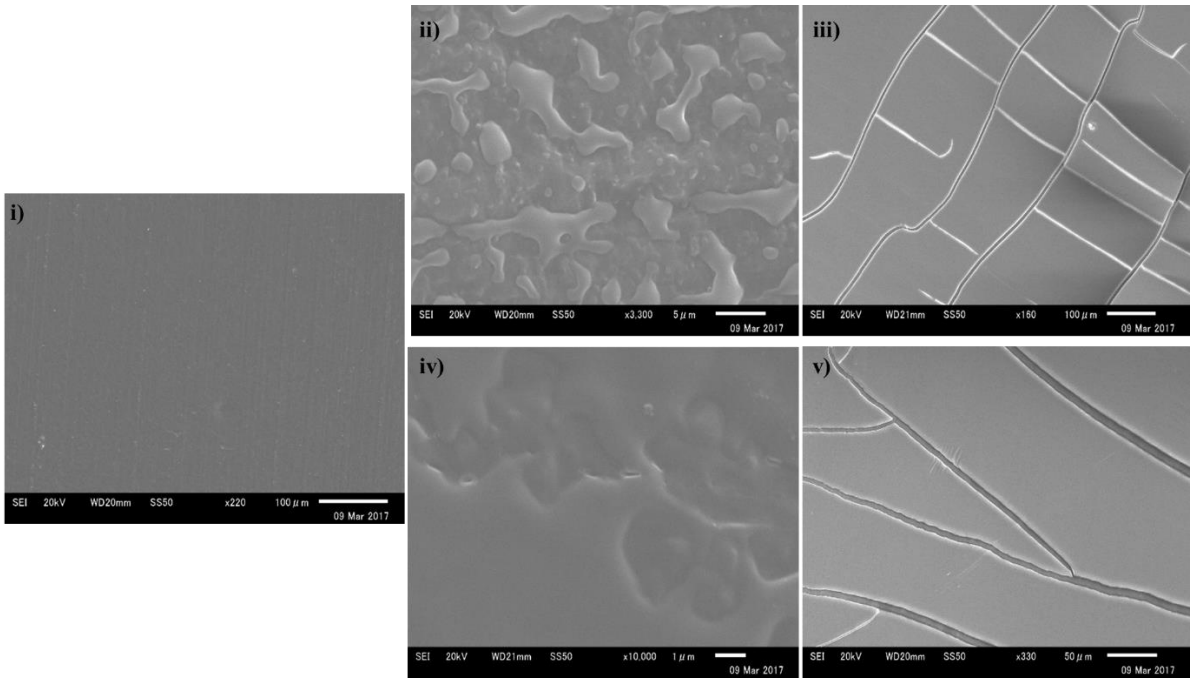

Figure 3-4. SEM Image of R-POSS and MPC-based copolymers **(3a)** coated surface. **(i)** blank surface, **(ii)** poly MPC-coated surface (1% w/v), **(iii)** poly MPC-coated surface (10 % w/v), **(iv) 3a**-coated surface (1% w/v), and **(v) 3a**-coated surface (10 % w/v).

3-3.3. Surface property: wettability, protein adsorption and cellar attachment

The results of the solubility study suggested the presence of C_2H_5-POSS moiety on the surface of **3a** which is responsible for the reduction of solubility of the copolymer in water

(**Table 3-1**). So, in the above-mentioned respect, we hypothesized that **3a** possess much hydrophobic surface due to the restriction of the motion of MPC moiety. The results of static contact angle (SCA) measurement **(Figure 3-5 (a)1)** suggested that the copolymer solution concentration for the spin coating should be over 5% w/v, as the SCA value of only poly MPC-coated surface decreased significantly over 5% w/v. From the results, it can be concluded that the copolymer solution concentration over 5% w/v completely covers the whole surface. The obtained results suggested that the highest contact angle observed in copolymer **3a** coated surface supported our hypothesis: The C_2H_5-POSS moiety was preferably located on the surface of the film due to the restricted motion of MPC moiety. The SCA was also measured using a PBS solution to evaluate the effect of wettability of copolymer-coated surface in a physiological environment. The results **(Figure 3-5 (a)2)** showed that static contact angle of poly MPC was almost same in both water and PBS irrespective of the coating thickness (in this study it was considered that increase in the concentration of copolymer solution, deposit more copolymer on the surface which increases the thickness of the coating). The results showed that the value of the contact angle of **3a** coated surface measured using PBS (with 5 % w/v solution concentration) was more than the value measured using pure water. The presence of inorganic salt in PBS might help in forming the hydrophobic domain (C_2H_5-POSS moiety) on the surface, which helps in increasing the surface hydrophobicity [12]. The value of the contact angle was found to be decreased when the coated with **3a** with 10 % w/v solution concentration. During the time of static contact angle measurement, the increased surface roughness was observed, which might be the reason for decreasing the value contact angle. A sudden increase in the value of the contact angle was observed in case **3b** and **3c**-coated surfaces (coated with 10 % w/v solution concentration). The increased amounts of **3b** and **3c** copolymers on the coated surface increases the presence of C_6H_{13} and C_8H_{17}-POSS moieties which forms the hydrophobic domain in the presence of inorganic salt in PBS might be the reason for the high value of contact angle.

In order to assess the correlation between the surface wettability and protein adsorption on the copolymer **3a-c** coated surfaces (with 1 and 5% w/v concentration solutions), protein adsorption measurements were conducted, and the adsorption of BSA was quantified. The BSA adsorption was only observed in **3a**-coated surface and the adsorption was increased with an increase in coating thickness **(Figure 3-5 (b))**. This observation suggested that the hydration layer formed surrounding the phosphorylcholine (PC) group of poly MPC in an aqueous

medium, which was responsible for the resistance to the protein adsorption, might be disrupted by the incorporation of C_2H_5-POSS moiety at the water-polymer interface [11-14]. The results of surface wettability and protein adsorption studies suggested the presence of C_2H_5-POSS moiety on the interface of **3a**-coated film which was responsible for providing the surface hydrophobicity. The current results also strongly correlated with the surface wettability results performed using 0.1 M PBS (pH 7.4) solution **(Figure 3-5 (a)2)**. The results of the XPS measurements suggested the presence of copolymer on the surface during the protein adsorption study.

Cell attachment study on the **3a**-coated surface was performed using NIH 3T3 cell line, in order to investigate the effect of exposed C_2H_5-POSS moiety on cellular interaction with the surface. After 24 and 48 h incubation at 37 ^0C, the morphology of the NIH 3T3 cells were observed under a digital inverted microscope **(Figure 3-5 (c))**. The observation suggested that the number of cells were increased after 24 h although the cells spreading on the surface was not observed. After 48 h, the cell spreading with cell membrane extension morphology were observed. The observed phenomenon supported that the unique hydration layer of poly MPC which resists the protein adsorption and cell adhesion affected by the incorporation of C_2H_5-POSS moiety into the polymeric matrix.

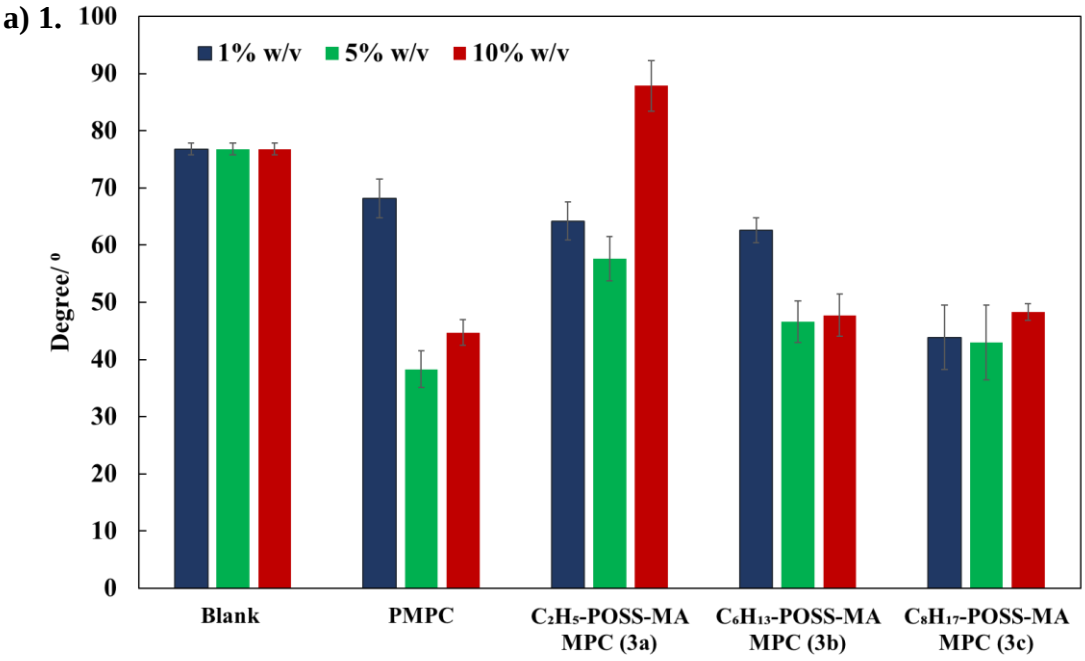

a) 2.

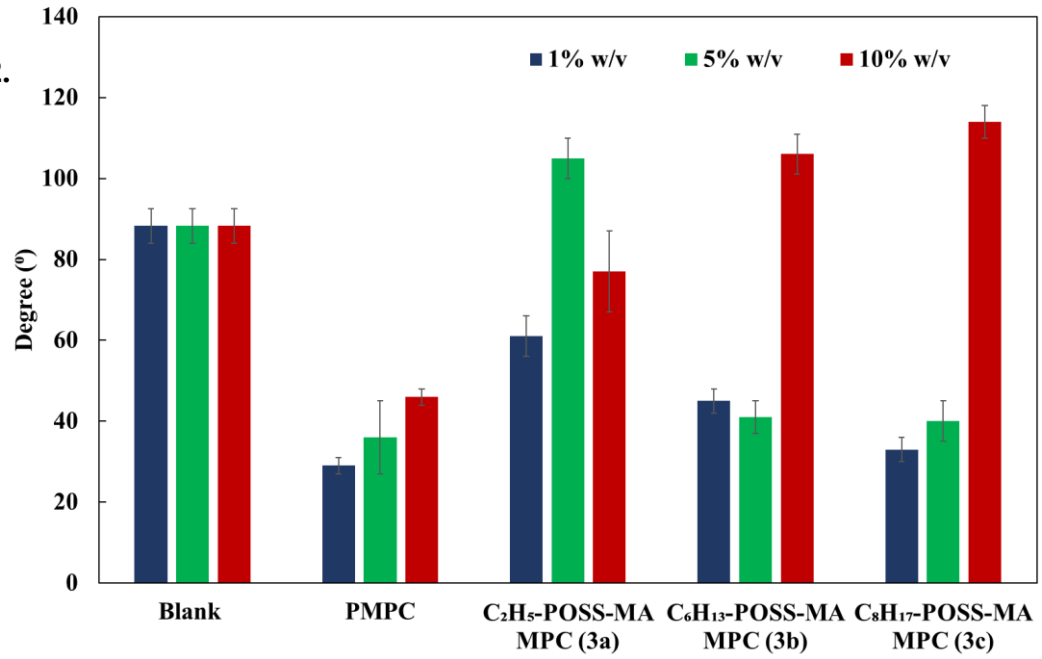
140
120
100
80
60
40
20
0
Degree (°)
1% w/v
5% w/v
10% w/v
Blank
PMPC
C2H5-POSS-MA MPC (3a)
C6H13-POSS-MA MPC (3b)
C8H17-POSS-MA MPC (3c)

b)

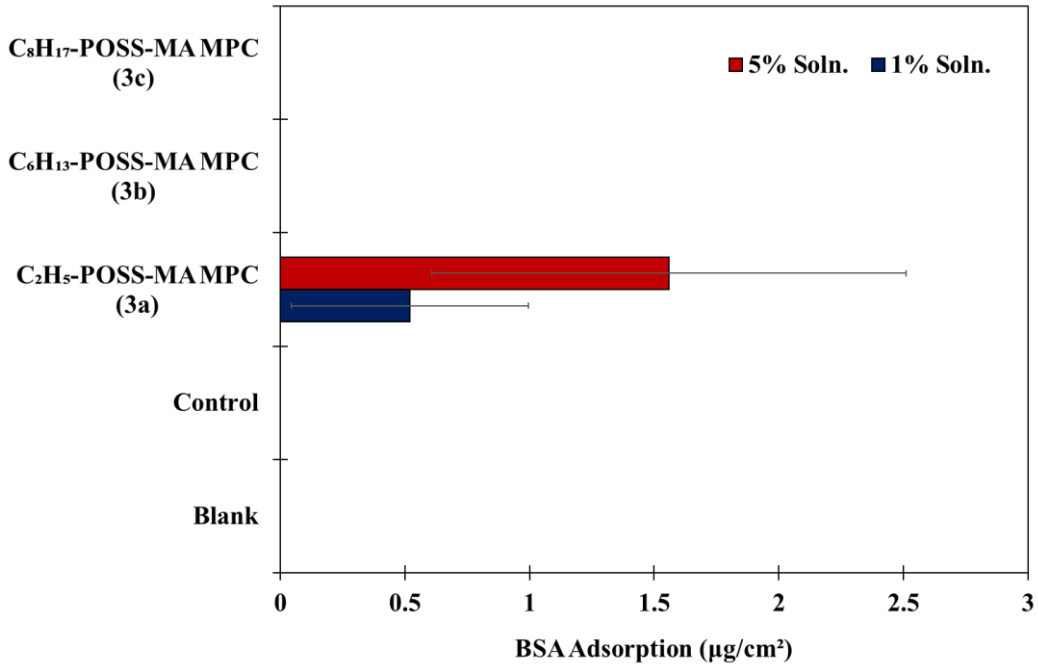
C8H17-POSS-MA MPC (3c)
C6H13-POSS-MA MPC (3b)
C2H5-POSS-MA MPC (3a)
Control
Blank
5% Soln.
1% Soln.
0
0.5
1
1.5
2
2.5
3
BSA Adsorption (µg/cm²)

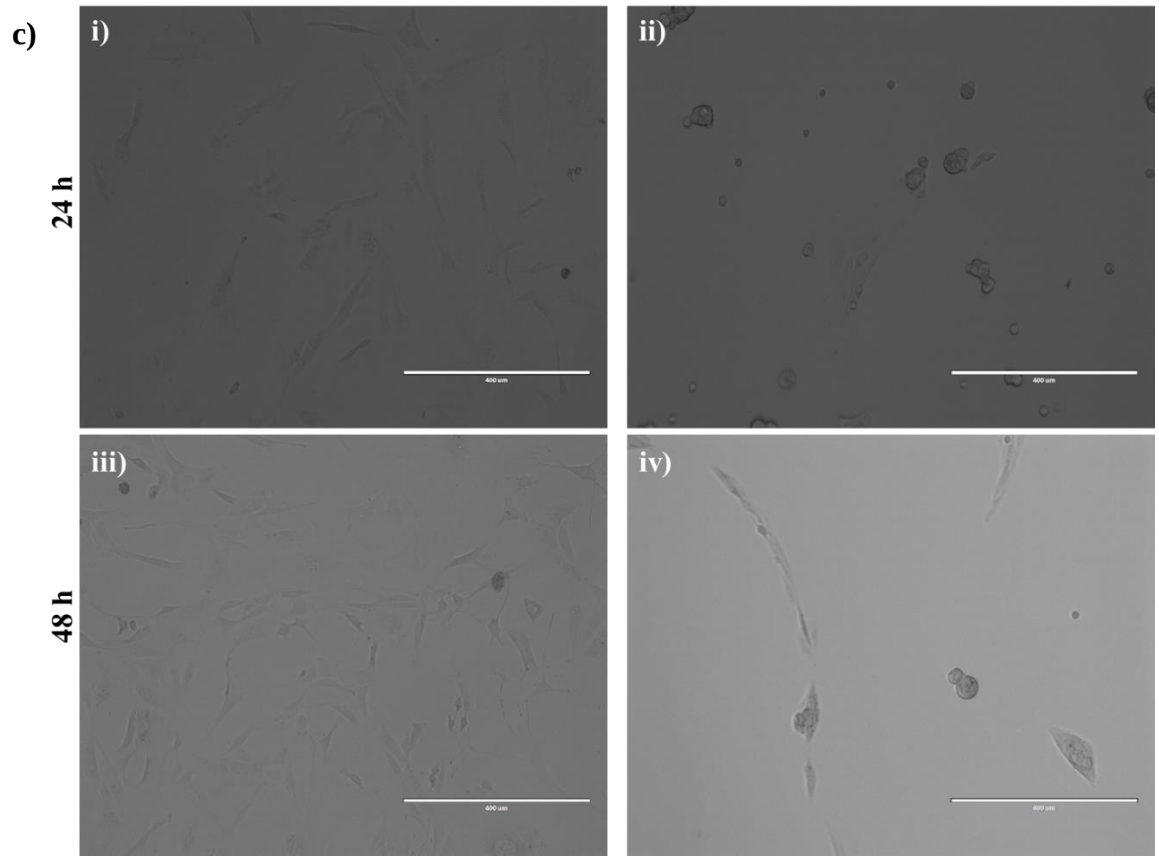

Figure 3-5. Surface wettability, protein adsorption and cell attachment on the random copolymers **3a-c** coated surface. **(a)** Results of static contact angle (SCA) measurement coated with **3a-c** with different concentration solutions (1 %, 5 % & 10 % w/v). **a) 1.** SCA in water & **a) 2.** SCA in PBS, **(b)** Results of BSA protein adsorption on the **3a-c** coated surface with different concentration solution (1 % & 5 % w/v) **(c)** Image of cell attachment on surface coated with copolymer **3a** after 24 and 48 h (**ii** and **iv**) and cell attachment on polystyrene tissue culture plate after 24 and 48 h (**i** and **iii**).

3-4. Conclusion

The C_2H_5-POSS-based random copolymer in combination with MPC showed unique surface and bulk properties. The C_2H_5-POSS help in increasing the mechanical property of the MPC based copolymer. The hydrophobic region (C_2H_5-POSS moiety) dispersed in the poly MPC matrix provides the controlled protein adsorption and cell attachment on the surface. In a contest of the investigation, it can be concluded that C_2H_5-POSS-based MPC copolymer

fulfills all required characteristics needed to develop it for further biomedical application especially as coating material of the cardiovascular implant.

Reference

1. H. Ghanbari, B. G. Cousins, A. M. Seifalian, *Macromol. Rapid Commun.* **2011**, *32*, 1032-1046.
2. T. Maeda, K. Hagiwara, S.Yoshida, T. Hasebe, A. Hotta, *J. Appl. Polym. Sci.* **2014,** *131*, 40606.
3. I. Pramudya, C.G. Rico, C. Lee, H. Chung, *Biomacromolecules* **2016**, *17*, 3853-3861.
4. K. H. Chae, Y. M. Jang, Y.H. Kim, O. Sohn, J. I. Rhee, *Sensors and Actuators B* **2007**, *124*, 153-160.
5. J. Sibarani, M. Takai, K. Ishihara, *Colloids and Surfaces B: Biointerfaces* **2007**, *54*, 88-93.
6. W. Sirithep, Y. Narita, Y. Nagase, *Trans. Mat. Res. Soc. Japan* **2013**, 38, 473-476.
7. S. Kuo, F. Chang, *Prog. Polm. Sci*. **2011**, 36, 1649-1696.
8. Y. Du, M. Yu, X. Chen, P. X. Ma, B. Lei, *ACS Appl. Mater. Interfaces* **2016**, 8, 3079−3091.
9. Md. Rabby, S. Jeelani, V. K. Rangari, *J. Nanomat.* **2015**, Art. ID 894856, 13.
10. R. Drake, A. W. Vogl, A. W. M. Mitchell, Gray's Anatomy E-Book: The Anatomical Basis of Clinical Practice, Nerve Biomechanics, 3 rd ed., Churchill Livingstone, **2014**.
11. K. Tanaka, S. Adachi, Y. Chujo, *J. Polym. Sci.: Part A: Polym. Chem.* **2009**, *47*, 5690–5697.
12. K. Ishihara, M. Mu, T. Konno, Y. Inoue, K. Fukazawa, *J. Biomater. Sci. Polym. Ed.* **2017**, *28*, 884-899.
13. Y. Inoue, Y. Onodera, K. Ishihara, *Colloids and Surfaces B: Biointerfaces* **2016**, *141*, 507–512.
14. Y. Inoue, T. Nakanishi, K. Ishihara, *React. & Funct. Polym.* **2011,** *71*, 350–355.
15. S. Chatterjee, T. Matsumoto, T. Nishino, T. Ooya, *Macromol Chem Phys* **2018,** 219 (8), doi: 10.1002/macp.201700572.

Chapter 4

R-POSS and 2-(methacryloyloxy)ethyl phosphorylcholine-based random copolymers as a hydrophobic drug solubilizer in drug delivery

4-1. Introduction

4-2. Experimental Section

4-2.1. Material

4-2.2 Measurements

4-2.3 Cytotoxicity of the copolymers (3a-c)

4-2.4 Determination of paclitaxel solubility in copolymers (3a-c) solution

4-2.5 Preparation of PTX-loaded R-POSS and MPC-based random copolymers assembly (3a-c)

4-2.6 Characterization of the R-POSS and MPC-based copolymer assembly

4-2.7 Cell viability measurements of PTX-solubilized 3a copolymer

4-2.8 Cellular uptake of FITC-PTX solubilized copolymer (3a)

4-2.9 *In vitro* release of PTX from copolymer assembly (3a)

4-2.10 Statistical analysis

4-3. Results and Discussion

4-3.1 Characterization of R-POSS and MPC based random copolymers (3a-c)

4-3.2 Characterization of PTX-solubilized copolymer (3a-c) assembly

4-3.3 Solubility of PTX in copolymers (3a-c) solution

4-3.4 Cell viability study of PTX solubilized copolymer (3a)

4-3.5 Cellular uptake of FITC labelled PTX solubilized copolymer (3a)

4-3.6 *In vitro* release of PTX from the copolymers (3a-c) assemblies

4-4. Conclusion

Reference

4-1. Introduction

Paclitaxel (PTX) is a hydrophobic, poorly water-soluble anti-cancer drug for the treatment of breast, ovarian and lung cancers. Because of poor water solubility of PTX, special solvents are required to solubilize it in water like 50:50 v/v mixture of polyoxyethylated castor oil, dehydrated ethanol[1] etc. The use of the solvents often results in serious hypersensitivity reaction, and also the solvent causes erythema and swelling at the injection sites. So, the alternative dosage form is essential to reduce the side effects. The applications of liposomes[2, 3] , polymeric assemblies[4], and cyclodextrin complexes[5] mediated delivery of PTX have been reported, but there is no report yet of clinically effective delivery. The water-soluble polymers have been extensively studied for the effective therapeutic use of the poorly water-soluble drug. Among them, a zwitterionic water-soluble polymer like 2-methacryloyloxyethyl phosphorylcholine (MPC) polymer (poly MPC) has been used extensively studied for its application in blood-contacting medical devices because of its high level of biocompatibility and resistance to protein adsorption [6,7]. The MPC monomer can be easily copolymerized with different hydrophobic monomers and the obtained amphiphilic copolymers can be effectively used for the solubilization and delivery of PTX[8-12]. According to the report by K. Ishihara *et al.*, the most effective copolymer to dissolve the paclitaxel was poly[MPC-*co*-*n*-butyl methacrylate(BMA) (PMB30W)] containing 70 mol % of the hydrophobic BMA unit[9]. In addition, cellular uptake of a poly MPC-based polymeric micelle was found to be superior to poly(ethylene oxide) (PEO) and poly(*N*-(2-hydroxypropyl)methacrylamide) (PHPMA)-based polymeric micelle system because of the interaction of poly MPC with cellular membrane[13]. However, the hydrophobic part thus is essential for the interaction with the hydrophobic drug molecule like PTX has been mainly constructed by hydrophobic BMA unit. The other hydrophobic monomer in combination with MPC has not elaborately investigated yet.

Polyhedral oligomeric silsesquioxane (POSS) is an organic/inorganic hybrid molecule. It is soluble in many solvents and is highly compatible with various polymeric materials due to the synergy between inorganic core and organic side groups. The hydrophobic nature of POSS can generate an amphiphilic molecule when incorporated in the hydrophilic polymer chain. The aggregation and order stacking nature of hydrophobic POSS cage are responsible for the generation of self-assembled amphiphilic molecules. The various studies related to the synthesis of POSS-containing hybrid polymers and characterization of their self-assembly behavior in selective solvents have been reported recently. The studies have revealed some

novel interesting self-assemble morphologies of POSS-containing polymers like ellipsoidal aggregates, giant capsules, complex spheres, dendritic cylinders etc. The introduction of POSS moiety at the ends of PEO and poly (ethylene glycol) (PEG) hydrophilic chain resulted in the formation of self-assembled micelle and vesicle in solutions and solvent-sensitive self-association behavior have been observed[13]. Kim *et al.* reported the successful encapsulation of insulin by PEG-POSS for delivery. They observed that insulin was well protected inside PEG-POSS nanoparticles at gastric pH for 2 h and start releasing at intestine pH 6-7[15]. Yuan *et al*. reported the successful synthesis of poly(L-glutamic acid) dendrimers bearing POSS nanocubic-core conjugated with doxorubicin (via pH-sensitive hydrazine bond) and biotin used as a targeting ligand[16]. Thus, the hydrophobic nature of POSS moiety suitable for its application as drug carriers as well as artificial molecular chaperones[17] and polymeric capsule for photodynamic therapy[18].

R-POSS and MPC based random copolymers (where R-groups are modified with ethyl (C_2H_5), hexyl (C_6H_{13}), octyl (C_8H_{17}) alkyl group) were designed, synthesized and subsequent mechanical, thermal and surface properties were studied (see **Chapter 2** and **Chapter 3**). It has been observed that incorporation of only the C_2H_5-POSS moiety increases the hydrophobicity at water polymer interface in poly MPC matrix. This study is the first report of synthesis and biomedical application of element block (see **Chapter 2** and **Chapter 3**) R-POSS-based MPC copolymer. Therefore, the study has been extended towards the application of the amphiphilic nature of R-POSS-based MPC random copolymers for solubilization of hydrophobic anti-cancer drugs like PTX and their delivery as a carrier molecule.

In this chapter, the self-assembled nature of different copolymer is characterized by fluorescence spectroscopy using pyrene as a fluorescence probe to determine critical association concentration (CAC), dynamic light scattering (DLS) measurements and transmission electron microscopy (TEM) observation. Among the different copolymer, only C_2H_5-POSS-based MPC copolymer (**3a)** (see **Chapter 2, Scheme 2-1 (iii)**) has increased the solubility of paclitaxel which was related to the formation of the assembled structure. The relationship between the C_2H_5-POSS and MPC-based copolymer concentration and PTX solubility was discussed. The cytotoxicity, cellular uptake of the copolymer using a fluorescein-4-isothiocyanate (FITC)-labelled PTX was evaluated using the HeLa cell line. The release of PTX from C_2H_5-POSS and MPC based copolymer assembly was demonstrated to discuss the role of C_2H_5-POSS moiety as a hydrophobic monomer.

4-2. Experimental Section

4-2.1. Material

The R-POSS and MPC based copolymers (R = C_2H_5, C_6H_{13}, and C_8H_{17}) are synthesized as mentioned in **Chapter 2** (**Scheme 2-1; 3a-c)**. The mol. % of R-POSS in the synthesized copolymers were found to be 1-2 mol. %. The PTX was purchased from FUJIFILM Wako Pure Chemical Corporation, Japan**.** Dulbecco's Modified Eagle Medium (DMEM), Dulbecco's phosphate-buffered saline (DPBS), 0.25 %-Trypsin/1mM-EDTA solution, penicillin-streptomycin mixed solution and sodium carbonate was purchased from Nacalai Tesque, Inc. (Kyoto, Japan). Fetal Bovine Serum (FBS) was purchased from Sigma-Aldrich Co. LLC. (St. Louis, U.S.A). The other reagents and solvents were used without any further purification. The HeLa cells (Health Science Research Resources Bank, Osaka, Japan) were cultured in media DMEM supplemented with 10% FBS and 100 U/mL penicillin-streptomycin. The HeLa cells were grown in a humidified incubator at 37 ℃ under 5% CO_2.

4-2.2 Measurements

The critical association concentration (CAC) measurement was performed by fluorescent spectroscopy using a hydrophobic fluorescent probe pyrene[19-20]. The pyrene stock solution was prepared (15 μM) in acetone and added to the aqueous solution of copolymers (**3a-c)** with different concentrations (ranging from 0.0001 to 50 mg/ml) to get final samples containing 6.0×10^{-7} M pyrene. As the C_2H_5-POSS and MPC based copolymer was partially soluble in water, the aqueous solution was prepared by first dissolving it in methanol, followed by the addition of water along with stirring the solution. The methanol was completely removed by rotary evaporator and subsequently keeping the solution inside the vacuum dryer for 1 h at 40 ℃. The solution was diluted with water to prepare the required concentration. The samples were kept overnight in dark at room temperature to allow complete evaporation of acetone. Fluorescence spectra were recorded at room temperature using a fluorescence spectrophotometer (JASCO Spectrofluorometer FP-8200). The CAC was determined by measuring the excitation spectra of pyrene in different concentration solution. The emission wavelength was at 390 nm.

Dynamic light scattering (DLS) measurements were carried out using a light scattering instrument (Malvern, Zetasizer Nano ZS) with 90º as scattering angle. The measurement was performed at 25 ℃ in pure water with the copolymer (**3a-c)** concentration varying between 1 and 100 mg/ml.

Transmission electron microscopy (TEM) images were collected using JEOL JEM-1230 at an accelerating voltage of 100 kV. Samples were prepared using 200 mesh copper grids. Before the measurements, the samples were vacuum dried and kept overnight *in vacuo*. An energy-dispersive X-ray analysis (EDS) attached to the scanning TEM-high angle annular dark field (STEM-HAADF) was performed with JEOL JEM-ARM200F at 200 kV.

4-2.3 Cytotoxicity of the copolymers (3a-c)

The cytotoxicity of the copolymers (**3a-c)** was determined by cell counting kit-8 (CCK-8). The copolymer (1 mg) was dissolved in 1 ml of 0.1 M phosphate buffer saline (pH 7.4). The copolymer **3a (**high concentration range 5, 10, 50, and 100 mg/ml), was considered to evaluate the concentration-dependent cytotoxicity. The copolymers were purified by dialysis process (MWCO: 1,000) against ultra-purified water before cytotoxicity measurements. During the dialysis process, no visible precipitation of copolymers was observed. The HeLa cells were seeded in 96-well plate with volumes of 90 µl (5000 cells/ well in DMEM media, supplemented with 10% FBS) and incubated overnight at 37 ℃. The copolymer **3a-c** solutions were sterilized for 30 min under UV light. The 10 µl of sample **3a-c** solution were added to each well and incubated for 24 h at 37 ℃. Only media and only cell were considered as blank (BL) and positive control (C), respectively. The 10 µl of CCK-8 reagent was added to each well and incubated for 2 h at 37 ℃. The absorbance was measured using Corona Grationg Microplate Reader SH-9000 Series (Corona Electric Co., Ltd, Japan) at 450 nm. The cell viability (%) was calculated by the following formula:

$$\text{Cell viability (\%)} = (I_{450}^{S} - I_{450}^{BL}) / (I_{450}^{C} - I_{450}^{BL}) \times 100 \ldots (1)$$

where I_{450}^{S}, I_{450}^{BL} and I_{450}^{C} represent the absorbance of the copolymer samples (S), blank (BL) and positive control (C) respectively.

4-2.4 Determination of paclitaxel solubility in copolymers (3a-c) solution

One mg of PTX was dissolved in 1 ml of methanol. Three different concentrations copolymers (**3a-c)** solutions were prepared in water (5, 10 and 50 mg/ml). The 100 µl of PTX solution (in methanol) was added to 900 µl of **3a-c** aqueous solution, followed by vortexing. Methanol was removed from the solution by keeping it under reduced pressure. The PTX crystal appeared in all concentration poly MPC solution, but for other copolymers (**3a-c)**, the crystal appeared only in 5 mg/ ml concentration solution. The solid PTX crystal phase was separated by centrifugation (3000 rpm) for 15 min. All the samples were filtered before HPLC measurement[21] using 0.45 µm pore size filter. HPLC measurements were performed using GILSON HPLC system (UV-vis detector : Gilson 119 UV/VIS Detector, Autosampler : GILSON 231XL, Pump : GILSON 805 Manometric Module, GILSON 811c dynamic mixer and GILSON 306 Pump, Injector : GILSON DILTOR401) with a COSMOSIL $5C_{18}$-MS-II (Φ 4.6 nm × 150 mm) column (Nacalai Tesque Inc., Japan) as stationary phase at room temperature. The detection was performed at a wavelength of 227 nm. The mixture of acetonitrile (60 %) and water (40 %) was used as mobile phase with a flow rate of 1 ml/min. The PTX concentration in **3a-c** solution was calculated by comparing the peak area with the standard curve. Since the PTX solubility in **3a;** solution was found to be higher than the other, the solubility was further measured by increasing the concentration to 100 mg/ml.

4-2.5 Preparation of PTX-loaded R-POSS and MPC-based random copolymers assembly (3a-c)

The **3a-c;** copolymers (20 mg) and PTX (1 mg) were dissolved in 1ml of methanol and the solution was drop by drop added into 10 ml water with vigorous stirring for overnight. The mixture was dialyzed against water (MWCO = 6,000-8,000) for 24 h to eliminate the methanol. The inner phase was collected after centrifugation (4000 rpm) for 30 min, and the supernatant was filtered by 0.45 µm filter. The solution was used for further characterization and stability study. The **3a-c** copolymer blank micelles (without PTX-loading) was also prepared following the similar procedure.

4-2.6 Characterization of the R-POSS and MPC-based copolymer assembly

The morphology of **3a-c** copolymer assembly structure in the dry state was observed in day 1 and 4 by transmission electron microscopy (TEM) measurements using JEOL JEM-1230 at an accelerating voltage of 100 kV. Samples were prepared using 200 mesh copper grids. Before the measurements, the samples were dried and kept overnight *in vacuo*. In addition, an energy-dispersive X-ray analysis (EDS) attached to the scanning TEM-high angle annular dark field (STEM-HAADF) was performed with JEOL JEM-ARM200F at 200 kV (at JAIST, Japan).

Dynamic light scattering (DLS) measurements were carried out to determine the average hydrodynamic diameter and size distribution of both with or without PTX-loaded **3a-c**. The measurement was performed using a light scattering instrument (Malvern, EXSTER DSC600) with 90° as a scattering angle. The stability measurement was performed after standing the sample at room temperature for 4 days. The DLS measurement was performed at 25 ℃ in the water of 1 mg/ml concentration sample. The sample was filtered using a 0.45 µm-pore size filter before measurements and every sample was measured three times to analyse the mean diameter.

4-2.7 Cell viability measurements of PTX-solubilized 3a copolymer

PTX (1 mg/ml in ethanol) and **3a** (100 mg/ml) aqueous solution was prepared following the same procedure as solubility measurement (see **Chapter 2**). This **3a** copolymer and PTX mixed solution were divided into three parts: one for solubility measurement by HPLC, second for preparing pH 7 neutral copolymer solution and third for preparing pH 5 solution using 0.5 M HCl. The PTX (1 mg) was dissolved in 1 ml ethanol to use as a control. The HeLa cells were seeded into 96-well plate considering the volumes of 90 µl (5000 cells/ well in DMEM media supplemented with 10% FBS) and incubated overnight at 37 ℃. The **3a** copolymer solution was sterilized under UV light for 30 min before the measurement. The 10 µl of solutions were added to the well plate and incubated for 24 and 48 h at 37℃ to measure the cell viability (the final concentration of PTX in the copolymer solution and control was 7.6 and 100 µg/ml respectively). Only media and cell were considered as blank and positive control respectively. 10 µl of CCK-8 reagent was added after 24 and 48 h and incubated for 2 h at 37 ℃. The

absorbance at a wavelength of 450 nm was measured using a microplate reader. The cell viability (%) was calculated using the Eq. (1).

4-2.8 Cellular uptake of FITC-PTX solubilized copolymer (3a)

The visualization of cellular uptake of PTX solubilized **3a** was performed by FITC-labelled PTX (FITC labelled PTX; **Scheme 4-1; 4**) which was synthesized according to the literature [22, 23] with some modifications (**Scheme 4-1**). The FITC-labelled PTX has encapsulated inside the **3a** by dialysis approach. The HeLa Cells were seeded into a 4-well slide and chamber plate (Watson Bio Lab, Kobe, Japan) with a cell density of 12,750 cells/ well in 0.8 ml DMEM media supplemented with 10% of FBS and incubated overnight at 37 ℃. After 24 h incubation, the media was removed and the cells were treated with serum-free medium containing FITC-labelled PTX solubilized **3a** (concentration of FITC-labelled PTX: 2 µg/ml) solution. As a control, only FITC-labelled PTX (2 µg/ml) was used. After incubation for 2, 5 and 24 h, the medium was removed and 3 times washed with D-PBS. The cells were fixed with cold acetone and washed 3 times with D-PBS. The cells were imaged by confocal laser scanning electron microscope (CLSM) Fluo View^{TM} FV1000 Confocal Microscope (Olympus Co., Tokyo, Japan).

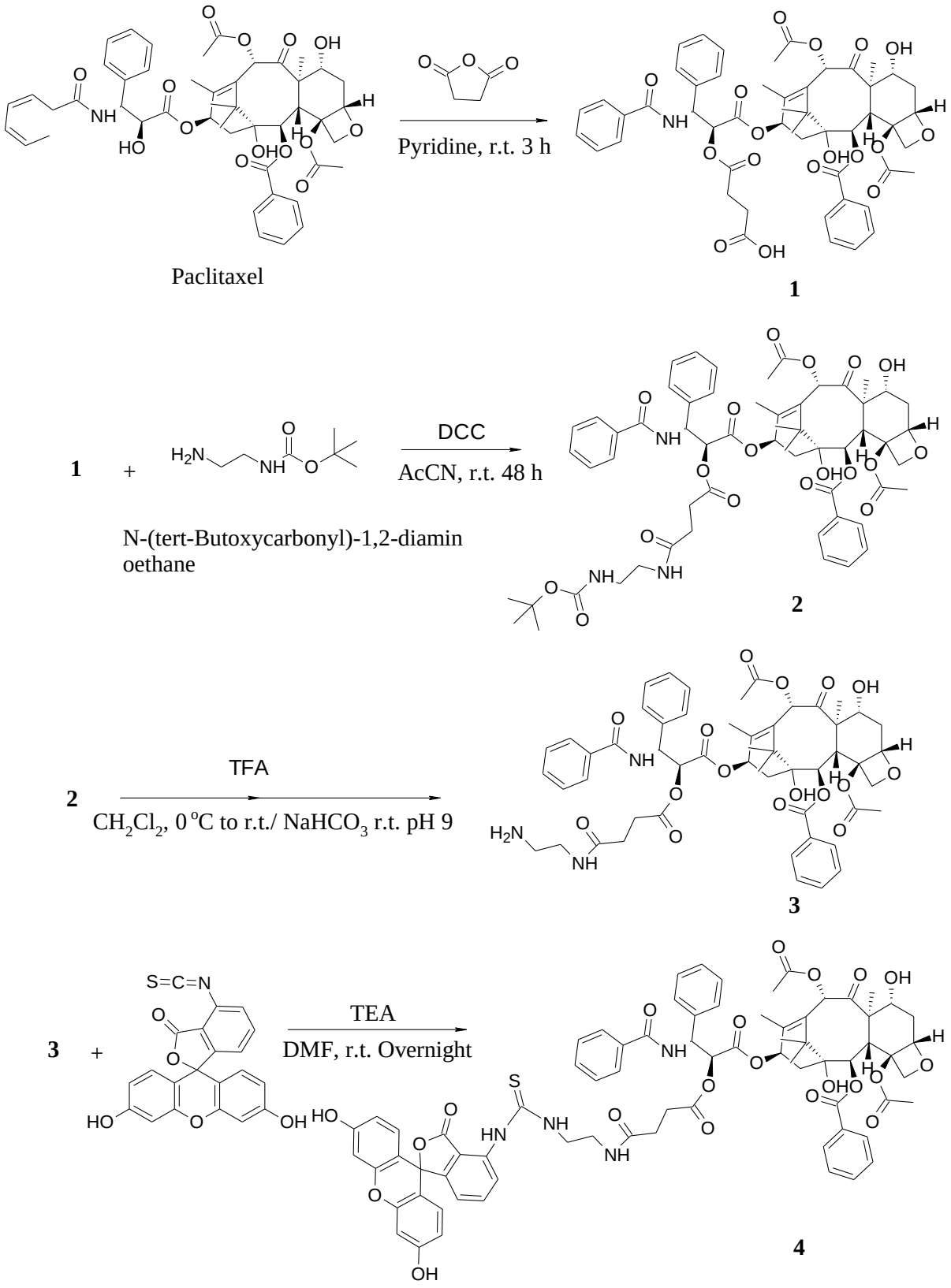

Scheme 4-1. Synthetic route of synthesis of FITC labelled paclitaxel (FITC labelled PTX, **4**)

4-2.9 *In vitro* release of PTX from copolymer assembly (3a)

The PTX-solubilized copolymer **(3a)** assembly (2.4 mg of lyophilized solid powder) was dissolved in 1 ml of D-PBS (pH 7.4). The mixture was then poured into a dialysis tube with a molecular cut-off of 6,000 – 8,000 Da, followed by introducing it in the vial containing 25 ml of D-PBS (pH 7.4) and 1 % Tween 80 mixed solution. The system was kept in a shaking bed with shaking speed of 100 rpm at 37 ℃. One ml of the release medium was collected at the predetermined interval for concentration measurement and an equal volume was replaced with of D-PBS (pH 7.4) plus 1 % Tween 80 mixed solution to keep the volume of the release medium constant. The concentration of PTX release was monitored by HPLC measurements (GLISON HPLC system, see section 2.4) at a detection wavelength at 228 nm. The sample was diluted with an equal volume of acetonitrile and filtered with 0.45 µm pore-size filter before measurement. A mixture of acetonitrile (60%) and water (40%) was used as the mobile phase with a flow rate of 1 ml/min. The concentration of PTX was determined by comparing the peak area with the PTX standard curve prepared under the same measurement conditions. The amount of PTX remaining in the assembly was also measured after collecting the inner phase of the dialysis tube following a similar procedure.

4-2.10 Statistical analysis

Statistical analysis was performed applying the one-way analysis of variance (ANOVA) followed by Fischer's test as post-hoc comparison at a significance level set at $p<0.05$.

4-3. Results and Discussion

4-3.1 Characterization of R-POSS and MPC based random copolymers (3a-c)

As discussed in **Chapter 2**, the number-average molecular weight (M_n) of copolymers **3a-c** was in the range of 10^4 and the copolymers are soluble in water. Characterization of **3a-c** copolymers was performed by ^{1}H NMR and FT-IR measurements and was discussed in **Chapter 2**. The effect of R-POSS domain in terms of hydrophobicity was determined by fluorescence technique using pyrene as a hydrophobic probe. The critical association

concentration (CAC) was calculated from the fluorescence excitation spectra of pyrene, participate between aqueous and micellar environment. A shift in excitation spectra of pyrene was observed with increase in the concentration of **3a-c** in an aqueous medium. The intensity ratio (I_{339}/I_{334}) vs. logarithmic value of concentration (Log C) was plotted (**Figure 4-1**). The curves were flat at the low concentration of **3a-c**, but started decreasing at high concentration except in the case of poly MPC. The phenomenon indicated the association formation in water. The CAC values of **3a-c** were determined by drawing the intersection of two straight lines. The calculated value of CAC of **3a-c** were 4.8×10^{-2} mg/ml, 6.3×10^{-2} mg/ml and 8.1×10^{-2} mg/ml respectively. The results indicated that the CAC value of the **3a-c** increased with increasing the aliphatic chain in the R groups (C_2H_5, C_6H_{13}, C_8H_{17}) of POSS moiety. As mentioned in **Chapter 3**, C_2H_5-POSS moiety was responsible for increasing the hydrophobicity in poly MPC matrix at water-polymer interface. Due to the increased hydrophobicity, the CAC value at **3a** was found to be lower than the other copolymers **3b** and **3c**. The other factors affecting the CAC values were the molecular weight (M_n). The M_n of the **3a-c** were in the order of **3a** ($M_n = 9.8 \times 10^4$) < **3c** ($M_n = 4.1 \times 10^5$) < **3b** ($M_n = 5.9 \times 10^5$). Since the hydrophobic part (R-POSS moiety) of the copolymers was the same (~1-2 mol. %), the hydrophilic chain length was responsible for increasing the molecular weight (M_n). The increased hydrophilic chain length of **3b** and **3c** decreased the association tendency of the hydrophobic R-POSS segment. Additionally, the appropriate balance between hydrophilic (MPC chain) and hydrophobic (R-POSS) segment required to achieve lower CAC value[24,25].

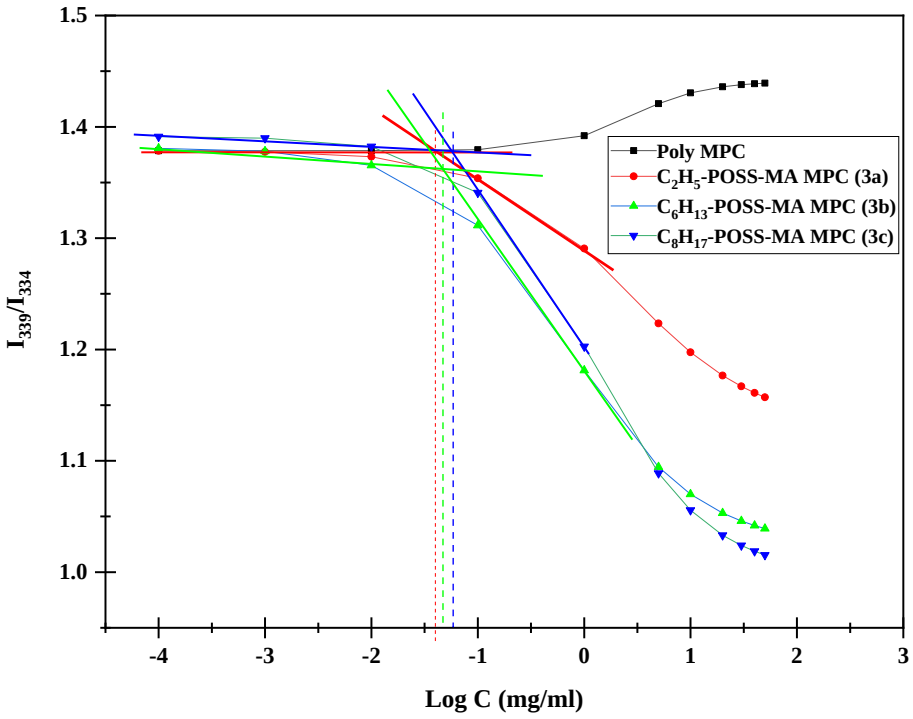

Figure 4-1. Intensity ratio (I_{339}/I_{334}) in pyrene excitation spectra in the presence of poly MPC and the **3a-c** copolymers as a function of logarithmic concentration (Log C). The emission wavelength was 390 nm.

The z-average sizes of **3a-c** copolymers were estimated by DLS measurements (**Figure 4-2**). The z-average diameter of the **3a-c** copolymers was in the range 65 – 80 nm (solution concentration 1 mg/ml) and showed a wide size distribution. In **3a** copolymer, two peaks were observed at around 10 and 100 nm. The peak observed around 10 nm likely to be unimolecular assembly. Since the R-POSS moiety in the **3a** copolymer matrix was only 1-2 mol. %, the random incorporation of R-POSS moieties induced the association states. The z-average diameter after 4 days was found similar in the case of **3a** which indicate the stability of the assembled structure in water (**Figure 4-2**). The similar phenomenon was observed in the case of **3b** and **3c**. ζ-Potentials of **3a-c** were measured in water and the values found in the range of - 0.5 to – 4 mV (**Figure 4-2**). The slightly anionic charge which was observed in the current

study was considered to be beneficial for acquiring good blood compatibility as reported by the researcher in case of MPC-based nanoparticles[26].

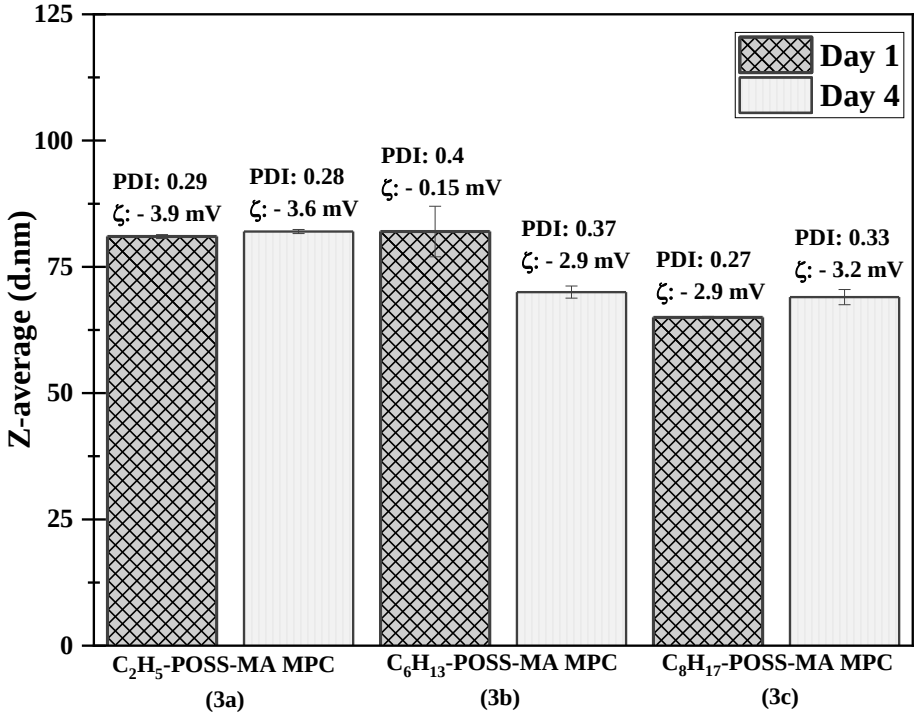

Figure 4-2. Particle size (Z-average diameter (nm)) (day 1 & 4) and ζ-potential (mV) of **3a-c**

Morphology of **3a-c** assembly (concentration of solution 1 mg/ml) was investigated by TEM observation (**Figure 4-3 (D)**) after 4 days. The shapes of the **3a-c** assembly were found to be spherical and the size was consistent with the size found in DLS measurements. After 4 days, the morphology and size found similar in the case of **3a** and **3b** (**Figure 4-3 (D)**). The distribution of R-POSS moiety in the assemble structure (at 1st day) was determined by high-resolution dark field STEM/EDS observation[27] (**Figures 4-3 (A)-(C)**). The dark phase represents the region with lower electron density, so the copolymer assemblies are likely to be located in the bright phase. From the elemental map of nitrogen (N), oxygen (O), phosphorous (P) and silicon (Si), the R-POSS and MPC molecule are likely to be located in the assemblies, and all the elements were found homogeneously distributed in the matrix. The results suggested

that the randomly incorporated R-POSS moiety help in the formation of stable (4 days) assemble structure in water.

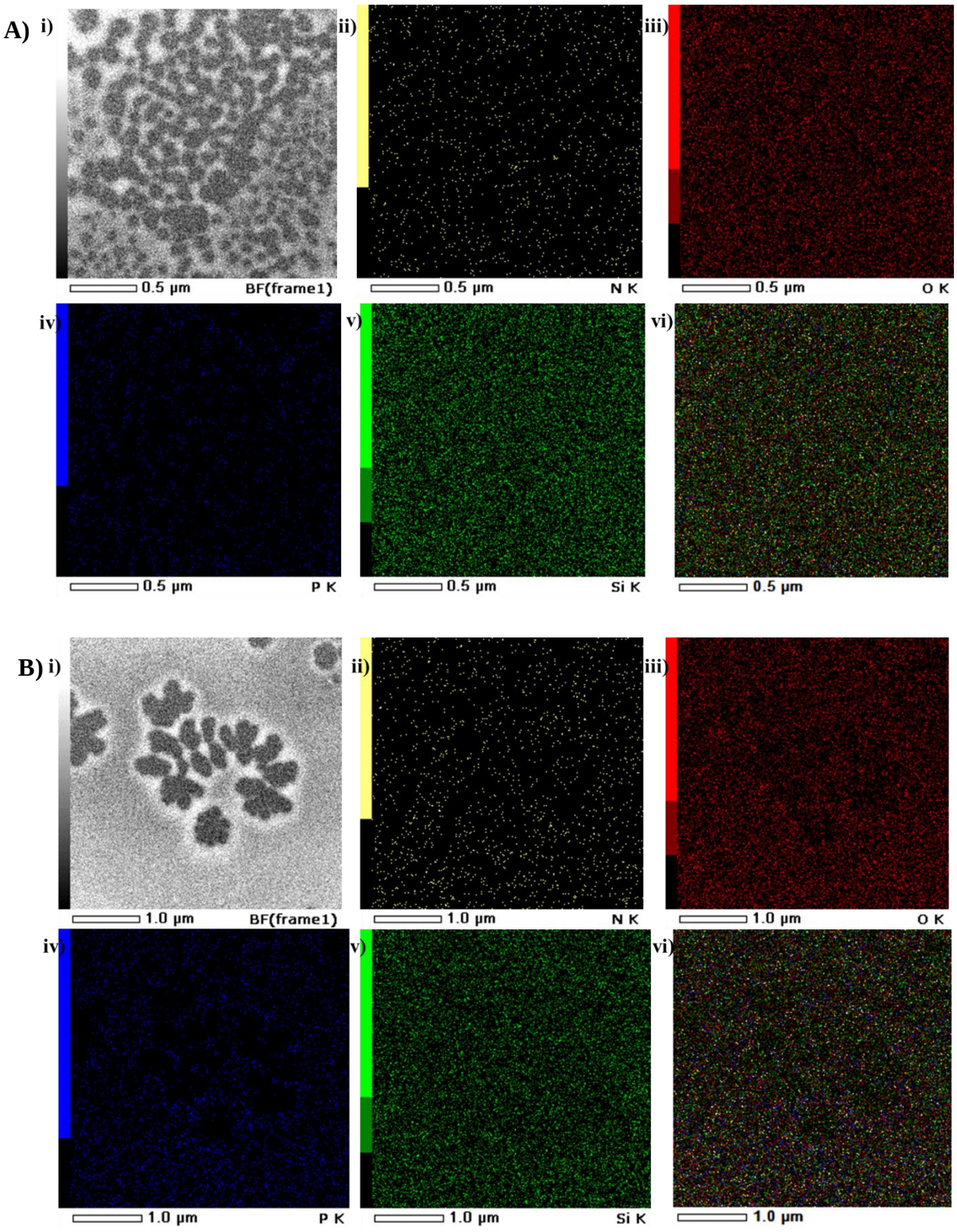

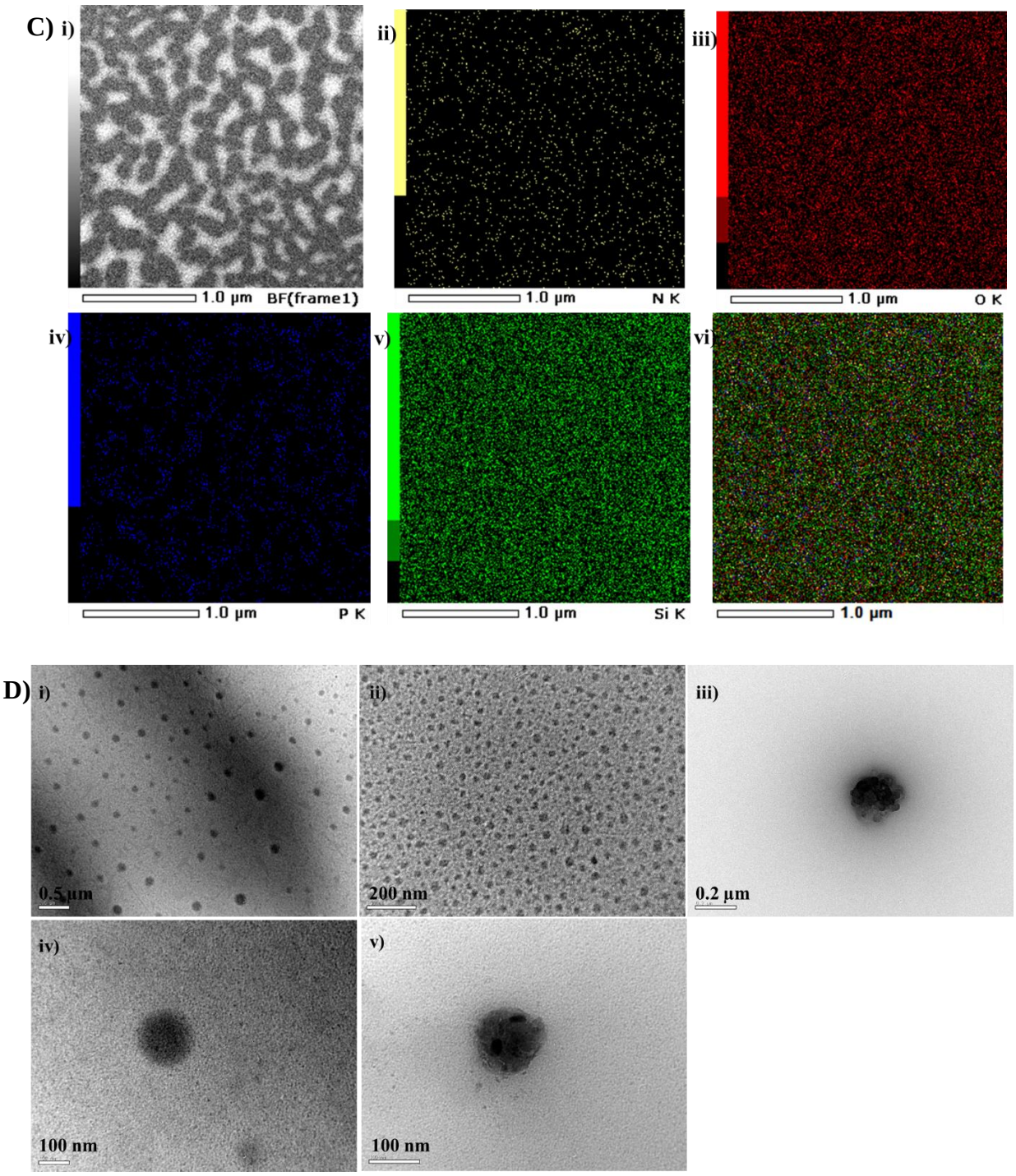

Figure 4-3. STEM images of (**3a-c)** copolymer **A) 3a, B) 3b** and **C) 3c** at day 1: i) dark-field STEM image and elemental map of ii) nitrogen (N) iii) oxygen (O) iv) phosphorous (P) v) silicon (Si) vi) composite map of all elements (N= yellow, O= red, P= blue, Si= green) **D)** TEM images of i) **3a** (30K) ii) **3b** (120K) iii) **3c** (100K) iv) **3a** (150K) and v) **3b** (250K) after 4 days (Stability study).

The cytotoxicity of **3a-c** assemblies (concentration of 1 mg/ml) after 24 h incubation was determined by CCK-8 assay. The cell viability was observed ~ 100 % and in some case more than 100 % (**Figure 4-4**).

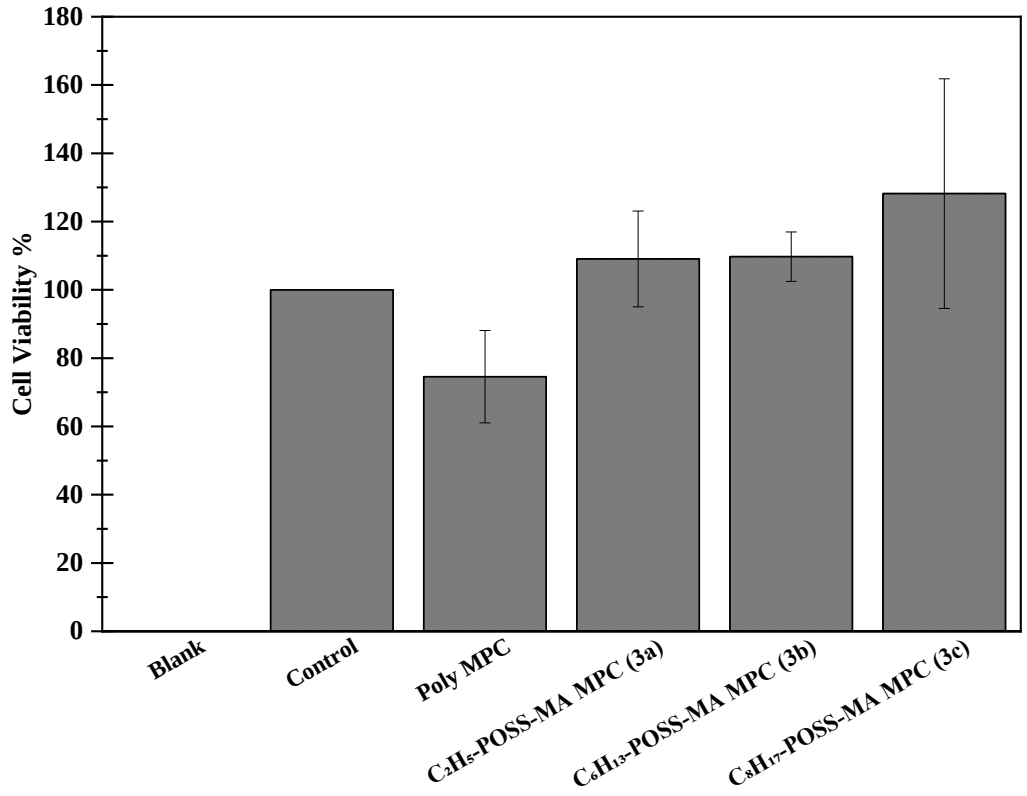

Figure 4-4. The cell cytotoxicity of **3a-c** assemblies (1 mg/ml) at pH 7. Each of the copolymer solution (10 µl) was added to HeLa cells seeded on the well plate (90 µl) and incubated for 24 h at 37 ^{0}C to measure the cell viability. Values are mean ± s.d. (n = 6). Cell viability was determined using the CCK-8 Kits and the absorbance was detected at 450 nm.

4-3.2 Characterization of PTX-solubilized copolymer (3a-c) assembly

The PTX can be loaded in **3a-c** copolymer assemble structure which helps in increasing the solubility of PTX. After the PTX loading, the z-average diameter was measured by DLS (**Figure 4-5)**. The z-average diameter of both **3a** and **3b** decreased after the PTX loading

(**Figure 4-5**). The strong hydrophobic interaction between PTX and the R-POSS moiety leads to the shrinkage in hydrodynamic diameter. After 4 days, PTX loaded **3a** and **3c** copolymer maintained its original hydrodynamic size, while **3b** copolymer showed an increase in size due to aggregation. The results suggested that **3a** copolymer association structure are stable in water after 4 days.

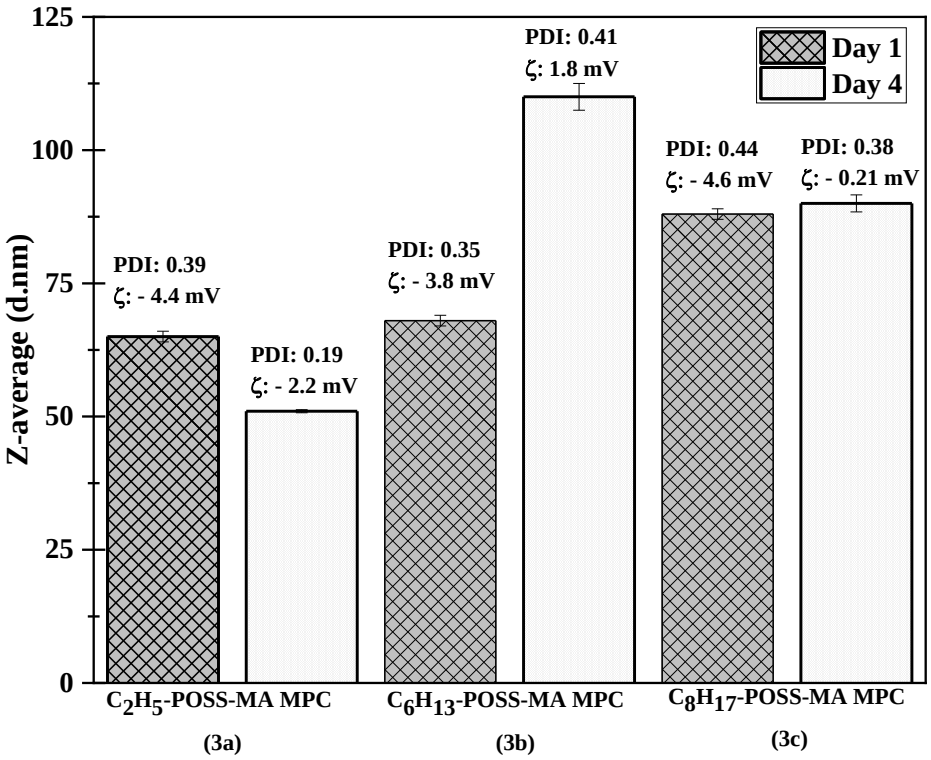

Figure 4-5. Particle size (Z-average diameter (nm)) and ζ-potential of PTX-solubilized **3a-c** assemblies in the water at 25℃ at the concentration of 1 mg/ml. The particle size was measured after 1 day and 4 days.

4-3.3 Solubility of PTX in copolymers (3a-c) solution

The solubility of PTX solubility in **3a-c** copolymers and poly MPC different concentration solutions (5, 10 and 50 mg/ml) were evaluated by HPLC measurements (**Figure 4-6 (a)**). The solubility of PTX in poly MPC aqueous solution was found less than the

detectable range (considered to be around 0 µg/ml). The **3a-c** enhanced the solubility of PTX in an aqueous environment, especially at concentration 50 mg/ml. The PTX solubility was found in the order of C_2H_5 > C_6H_{13} > $C_8H_{17,}$ which indicates that shorter alkyl chain (R-group in POSS moiety) enhanced the hydrophobic interaction of copolymer with PTX. The results were also consistent with the CAC value observed in the study. The solubility of PTX in 100 mg/ ml concentration aqueous solution of **3a** was also measured to evaluate the concentration-dependent solubility (**Figure 4-6 (b)**). The solubility of PTX at 100 mg/ml (**3a** copolymer solution) was found to be 75.5 ± 8.8 µg/ml. From the results, **3a** copolymer was selected for further study and cell viability study.

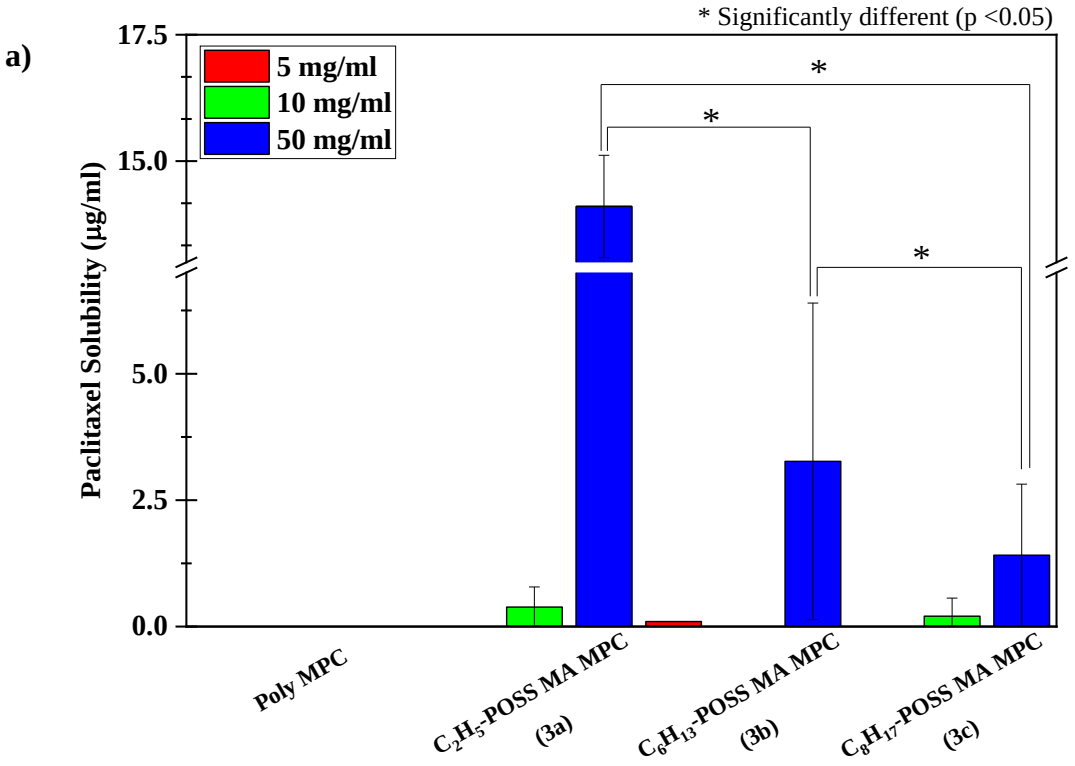

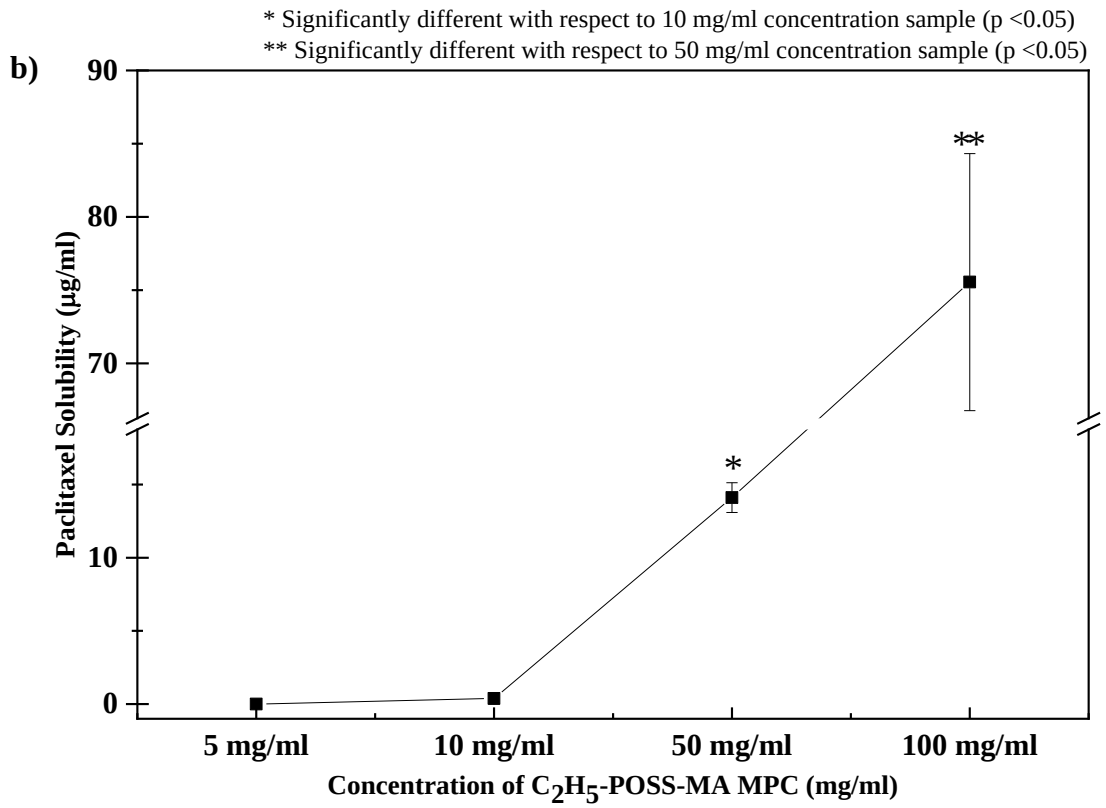

Figure 4-6 (a) PTX solubility of in the presence of **3a-c** and poly MPC in 5, 10, and 50 mg/ml concentration solution (b) **3a** concentration-dependent (5, 10, 50 and 100 mg/ml concentration solution) PTX solubility. Initial PTX concentration was 1 mg/ml. Values are mean ± S.D. (n = 3).

4-3.4 Cell viability study of PTX solubilized copolymer (3a)

The cell viability in PTX solubilized **3a** copolymer aqueous solution of two different pH (pH 7 and pH 5) was measured and compared with free PTX as control (**Figure 4-7**). The final concentration of PTX dissolved in **3a** was ~ 7.6 μg/ml and the free PTX was 100 μg/ml. The cell viability in free PTX was observed 38 ± 18 and 17 ± 10 % after 24 and 48 h respectively. Xu *et al* reported that HeLa cell viability in the presence of free PTX (concentration 10 μg/ml) after 24 and 48 h was about 50 and 30 % respectively[28]. According to that, the cell viability observed in free PTX with a concentration of 100 mg/ml in this study was identical. The cell viability of PTX solubilized **3a** solution of pH 7 was observed 87 ± 24 % after 24 h incubation.

On the other hand, cell viability in free PTX was found significantly low. This indicates that the PTX solubilized in **3a** was strongly bounded inside the copolymer association until 24 h. After 48 h, a significant decrease in cell viability was observed at 21 ± 5 %. The result suggested that PTX bounded with the **3a** copolymer association was released in the cellular medium after 24 h. The similar phenomena were also observed when solution pH was adjusted to 5 (**Figure 4-7**) which suggested the release of PTX from the copolymer association facilitate under the intracellular pH condition. The cellular uptake study of the **3a** was performed to understand the mechanism of cytotoxicity due to the release of PTX.

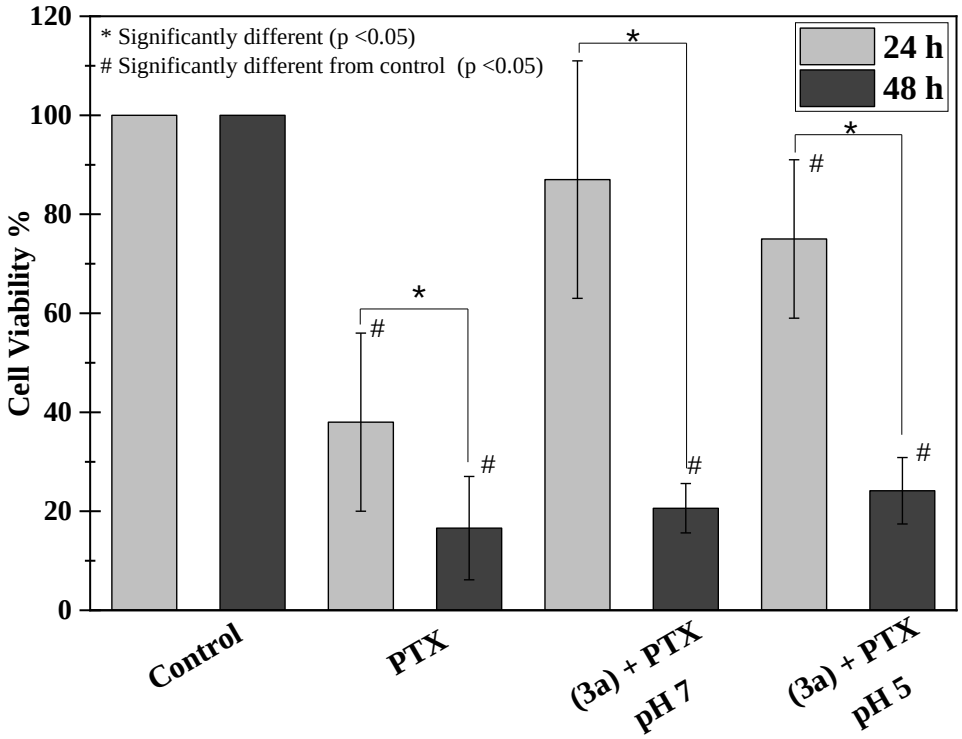

Figure 4-7. The cytotoxicity results of free PTX (initial conc.: 1 mg/ml) and PTX solubilized **3a** copolymer solution (100 mg/ml) at two different pH (pH 7 and pH 5). Each of the solutions (10 µl) were added to HeLa cells seeded on a well plate (90 µl) and incubated for 24 and 48 h at 37 ^{0}C to measure the cell viability. The final concentration of PTX in **3a** solution and control was 7.6 and 100 µg/ml, respectively. Values are Mean ± S.D. (n = 6) (*: P < 0.05 #: P < 0.05

vs control, one-way ANOVA, Fischer's test). Cell viability was determined using the CCK-8 Kits and the absorbance was detected at 450 nm.

4-3.5 Cellular uptake of FITC labelled PTX solubilized copolymer (3a)

The cellular uptake of PTX-solubilized **3a** copolymer was observed by FITC-labelled PTX (**4**) which was synthesized and confirmed by ^{1}H NMR and ECI-MS spectroscopy. FITC labelled PTX was solubilized in the **3a** solution following the same procedure as PTX. The green fluorescence intensity inside the cells was observed in **Figure 4-8 (i)** after 2 h incubation with **4** solubilized **3a**. The cells treated with only **4** did not show any fluorescence color after the same incubation time. After 24 h incubation, the green fluorescence color was observed inside the cells treated with both free **4** and **4** solubilized **3a**, although most of the cells were found died due to the cytotoxicity of **4** (**Figure 4-8 (ii)**). The results suggested that **4** solubilized **3a** was internalized by the HeLa cells through cellular uptake mechanism within 2 h incubation. Therefore, from the results, it can be concluded that **3a** assembly plays a major role in rapid cellular uptake process, followed by the release of paclitaxel in the targeted cells.

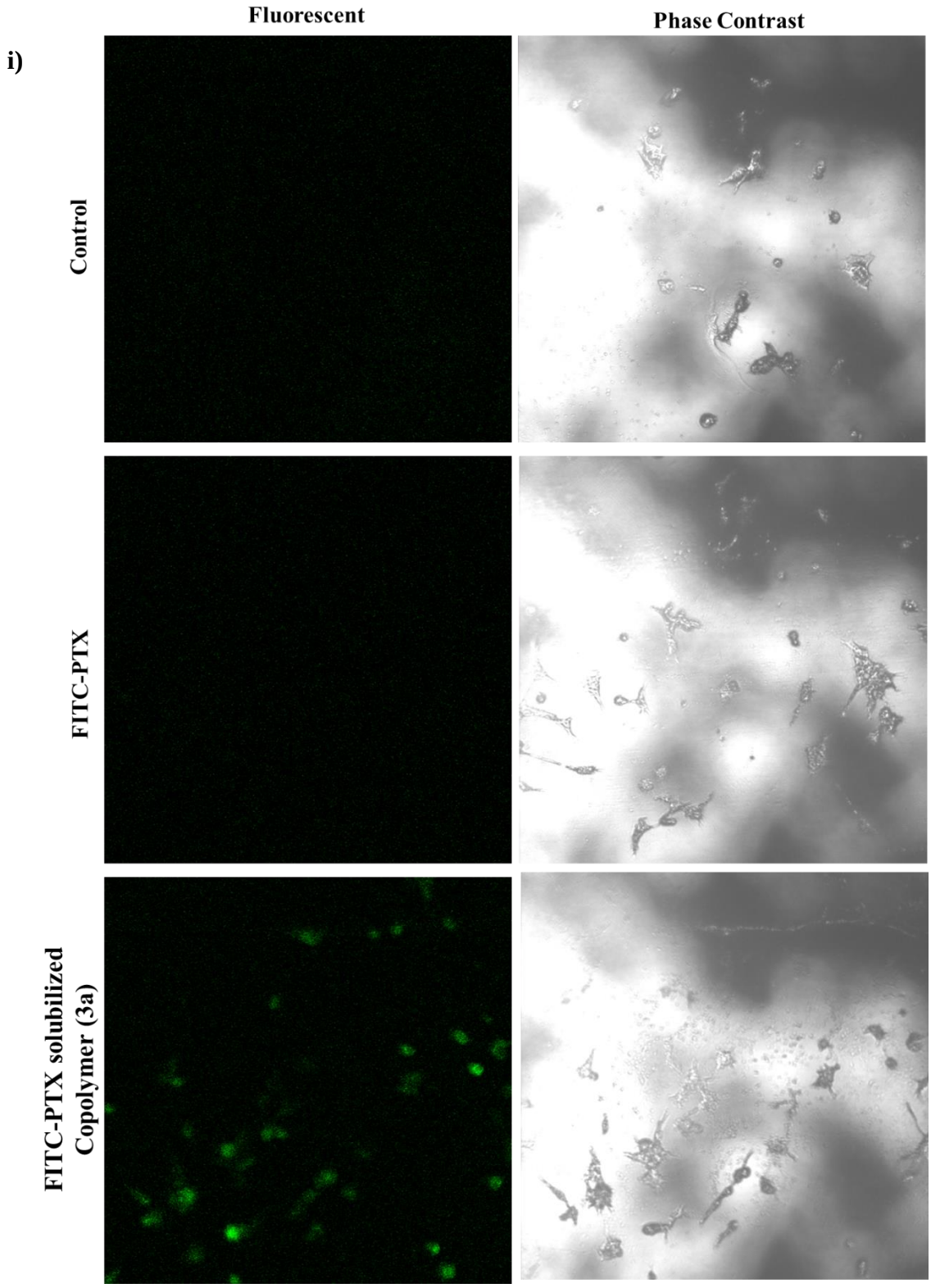
i)
Fluorescent
Phase Contrast
Control
FITC-PTX
FITC-PTX solubilized Copolymer (3a)

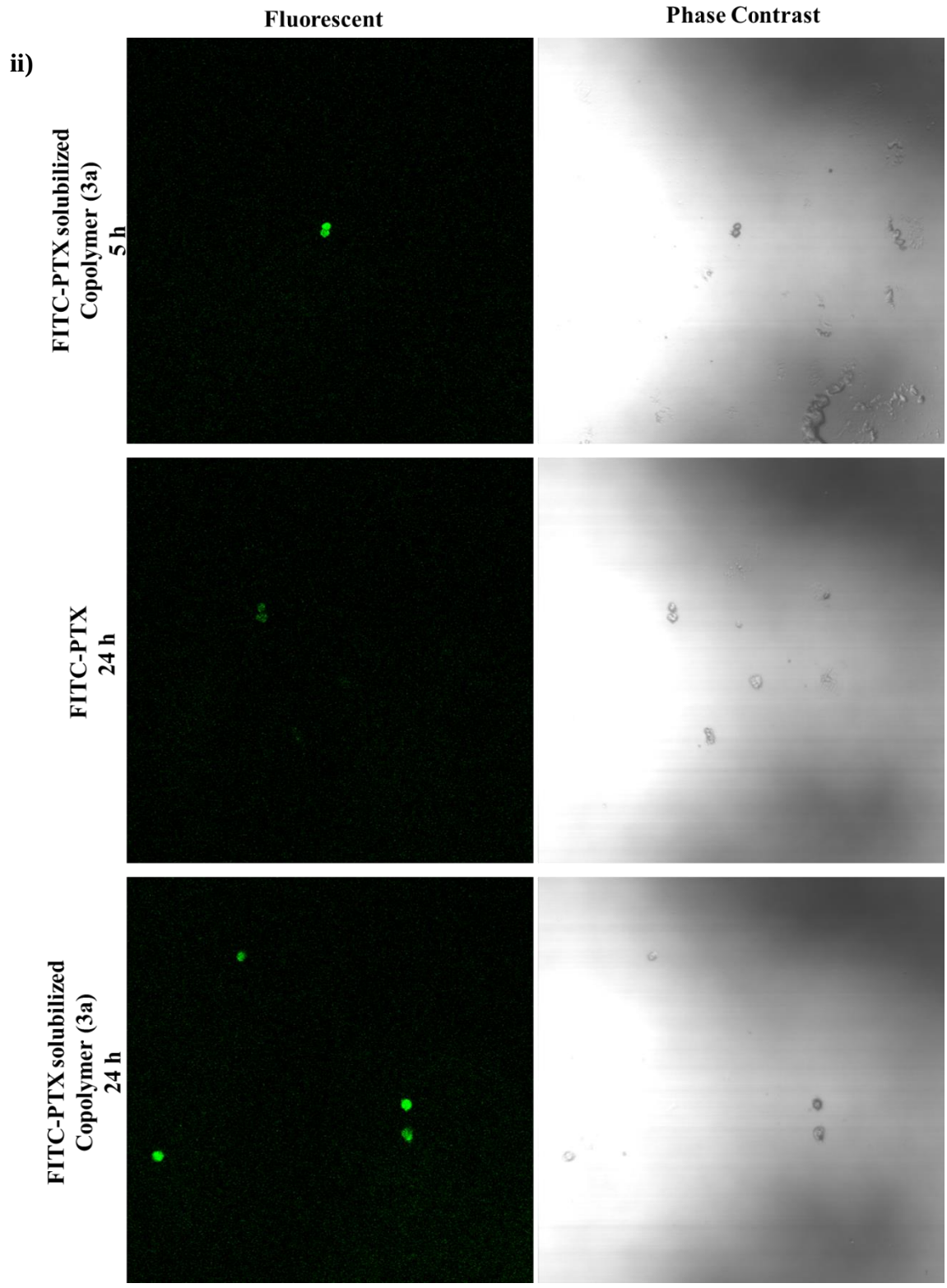

Figure 4-8. The CLSM images of HeLa cells i) control without FITC-PTX (upper), with free FITC-PTX (middle) and solubilized **3a** (bottom) after 2 h incubation ii) free **4** and **4** solubilized **3a** after 5 and 24 h incubation.

4-3.6 *In vitro* release of PTX from the copolymers (3a-c) assemblies

In vitro release profile of PTX from the PTX solubilized **3a-c** copolymers was studied using D-PBS (pH 7.4) and 1 % Tween 80 mixed solution as dissolution medium. **Figure 4-9** indicated different release pattern of three PTX solubilized **3a-c** copolymer. The initial burst release was not observed in case of all the PTX solubilized **3a-c** copolymer which confirmed the absence of free PTX on the surface of the copolymer association. The cumulative release of PTX from the PTX solubilized **3a** copolymer assembly was reached to 30 %, while that from the other **3a** and **3c** copolymer was over 40 % at 47 h. According to the STEM/EDS results (**Figures 4-3 (A)-(C)**), the R-POSS seem to be homogeneously distributed in the copolymer association. The slow release of PTX might be the effect of strong hydrophobic interaction between the hydrophobic region in the **3a** copolymer association and PTX. From the results, it can be concluded that C_2H_5-POSS moiety in **3a** copolymer effectively controlled the slow release of PTX. The results were also supported by the results of DLS (**Figure 4-2** and **Figure 4-5)** where the size of **3a** copolymer association (~ 80 nm) was observed to be decreased after the PTX solubilization (~ 62 nm) and the structure remain stable for 4 days.

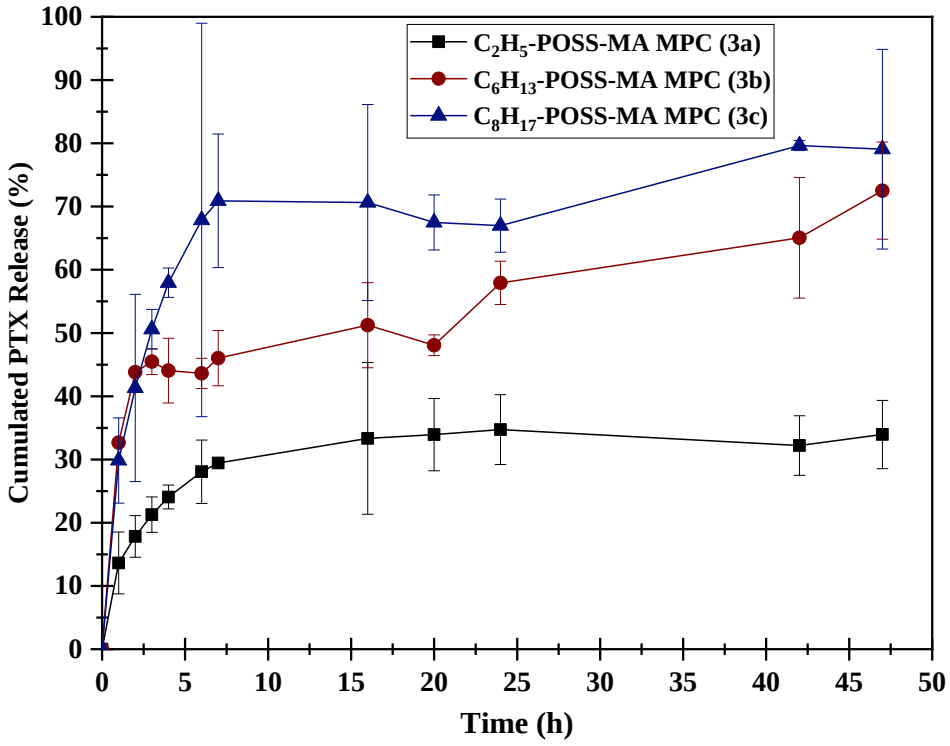

Figure 4-9. Released of PTX from PTX solubilized **3a-c** copolymer vs. time curves of (square) PTX solubilized **3a**, (circle) PTX solubilized **3b** and (triangle) PTX solubilized **3c**. Values are mean ± S.D. (n = 3).

The *in vitro* PTX release profile during the first 7 h was fitted in different mathematical models, and was interpreted from the graphical representation as shown in **Figure 4-10.** The highest degree of correlation coefficient (r^2) represent the suitability of the mathematical model for drug release kinetics. The PTX release from **3a** follows the zero-order model (r^2 = 0.9749) and **3c** follows the first-order model (r^2 = 0.9596) (**Table 4-1)**. The Korsmeyer-Peppas model (eq 1) states the type of diffusion which can be evaluated by the value of *n*[29].

$$\frac{M_t}{M_\infty} = k \cdot t^n \qquad \text{(eq. 1)}$$

Where M_t/M_∞ is the fraction of drug released at time *t*, k is the rate constant and *n* is the release exponent. In case of **3a**, the value of *n* was calculated to be 0.49. Since the n value of the Higuchi model is approximated to 0.5, the calculated n value for **3a** implies that the PTX release from the system follows Fickian diffusion. The drug release profile of **3a** micelle system indicated the release of PTX followed the zero order and Higuchi model (r^2 = 0.9094) which implies the controlled drug diffusion. The drug release profile and kinetics indicates controlled

and sustained drug release from **3a**. The n = 0.53 in **3c** implies that the PTX release follow the non-Fickian transport[29]. The **3c** follows first-order kinetic model and did not maintain constant release rate. The release behavior of **3c** implies rapid-to-slow release of PTX. The PTX release profile of **3b** does not match with any mathematical model (**Table 4-1**) considered in the current study. These mathematical models play an important role in the prediction of mechanism of drug release, drug release rate and diffusion behavior from the system.

Table 4-1. The results of different model in terms of r^2, slop and intercept

Model Name	3a			3b			3c		
	r^2	Slope	Intercept	r^2	Slope	Intercept	r^2	Slope	Intercept
Zero-order model	0.9749	2.15	14.41	-0.1254	0.18	43.49	0.9132	7.53	27.22
First-order model	0.8555	0.04	92.76	0.4046	0.06	75.97	0.9596	0.17	86.87
Higuchi model	0.9094	18.09	0.00	-50.61	36.26	0.00	0.8258	39.87	0.00
Korsmeyer-Peppas model	-19.10	0.49	31.44	-181.67	0.018	45.05	-25.78	0.53	76.75

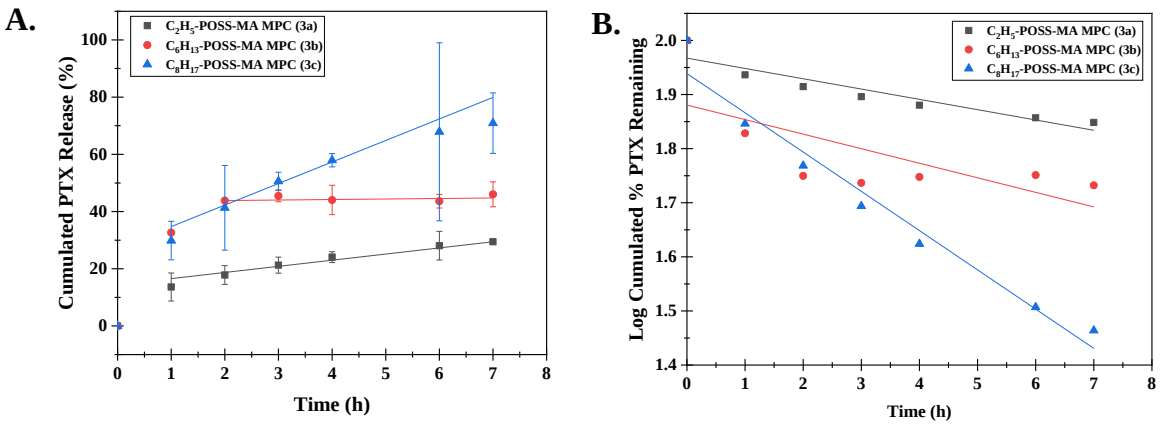

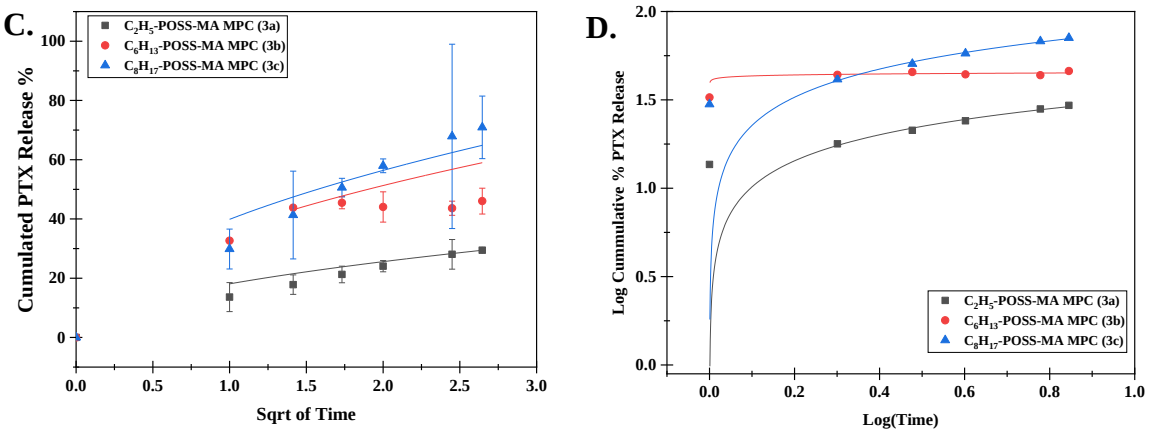

Figure 4-10. Interpretation of PTX release profile with various mathematical models: (A) Zero order model (B) First order model (C) Higuchi model (D) Korsmeyer-Peppas model

4-4. Conclusion

The R-POSS and MPC based random copolymers (R-groups in POSS moiety modified with alkyl chain ethyl (C_2H_5), hexyl (C_6H_{13}), octyl (C_8H_{17})) were evaluated as a solubilizing biocompatible carrier molecule of hydrophobic drug paclitaxel. Among the series of R-POSS molecule consider in the current study, C_2H_5-POSS based MPC copolymer have shown promising contribution in terms of enhancement of paclitaxel solubility in an aqueous environment with high cellular uptake and release of paclitaxel at the intracellular environment. The hydrophobic C_2H_5-POSS moiety strongly interacted with paclitaxel controlled the release rate in an aqueous environment. Based on the findings of the current investigation it can be concluded that C_2H_5-POSS and MPC based copolymer possess promising characteristics to be considered as polymeric biomaterials for enhancing the solubility of poorly water-soluble component like a drug, imaging prob, etc.

References

1. A. K. Singla, A. Garg, D. Aggarwal, *Int J Pharm* **2002,** 235 (1-2), 179-192.
2. X. S. Hu, L. Lin, P. Y. Xing, C. G. Zhang, L. Wang, Y. Q. Liz, *J Thorac Oncol* **2017,** 12 (1), S902-S902.
3. S. Yamashita, H. Katsumi, N. Hibino, Y. Isobe, Y. Yagi, Y. Tanaka, S. Yamada, C. Naito, A. Yamamoto, *Biomaterials* **2018,** 154, 74-85.
4. C. Y. Deng, C. Xu, X. M. Zhang, J. Yao, Y. X. Zhang, B. Yu, R. J. Lee, C. J. A Jiang, *Anticancer Res* **2018,** 38 (1), 219-225.
5. J. L. Zhang, X. F. Zhao, Q. Chen, X. Y. Yin, X. Xin, K. X. Li, M. X. Qiao, H. Y. Hu, D. W. Chen, X. L. Zhao, *Acta Biomater* **2017,** 50, 381-395.
6. K. Ishihara, H. Nomura, T. Mihara, K. Kurita, Y. Iwasaki, N. Nakabayashi, *J Biomed Mater Res* **1998,** 39 (2), 323-330.
7. Y. Iwasaki, K. Ishihara, *Anal Bioanal Chem* **2005,** 381 (3), 534-546.
8. K. Ishihara, M. W. Mu, T. Konno, *J Biomat Sci-Polym E* **2018,** 29 (7-9), 844-862.
9. T. Konno, J. Watanabe, K. Ishihara, *J Biomed Mater Res A* **2003,** 65a (2), 209-214.
10. M. W. Mu, T. Konno, Y. Inoue, K. Ishihara, *Colloid Surface B* **2017,** 158, 249-256.
11. M. Wada, H. Jinno, M. Ueda, T. Ikeda, M. Kitajima, T. Konno, J. Watanabe, K. Ishihara, *Anticancer Res* **2007,** 27 (3b), 1431-1435.
12. S. I. Yusa, K. Fukuda, T. Yamamoto, K. Ishihara, Y. Morishima, *Biomacromolecules* **2005,** 6 (2), 663-670.
13. C. E. de Castro, C. A. S. Ribeiro, A. C. Alavarse, L. J. C. Albuquerque, M. C. C. da Silva, E. Jager, F. Surman, V. Schmidt, C. Giacomelli, F. C. Giacomelli, *Langmuir* **2018,** 34 (5), 2180-2188.
14. J. Wu, P. T. Mather, *Polym Rev* **2009,** 49 (1), 25-63.
15. K. O. Kim, B. S. Kim, I. S. Kim, *Journal of Biomaterials and Nanobiotechnology* **2011,** 2 (3), 201-206.
16. H. Yuan, K. Luo, Y. S. Lai, Y. J. Pu, B. He, G. Wang, Y. Wu, Z. W. Gu, *Mol Pharmaceut* **2010,** 7 (4), 953-962.
17. Z. B. Li, B. H. Tan, G. R. Jin, K. Li, C. B. He, *Polym Chem* **2014,** 5 (23), 6740-6753.
18. Z. H. Zhang, Y. D. Xue, P. C. Zhang, A. H. E. Muller, W. A. Zhang, *Macromolecules* **2016,** 49 (22), 8440-8448.

19. M. Wilhelm, C. L. Zhao, Y. C. Wang, R. L. Xu, M. A. Winnik, J. L. Mura, G. Riess, M. D. Croucher, *Macromolecules* **1991,** 24 (5), 1033-1040.
20. K. M. Huh, J. Hashi, T. Ooya, N. Yui, *Macromol Chem Phys* **2000,** 201 (5), 613-619.
21. M. Kimura, T. Ooya, *J Drug Deliv Sci Tec* **2016,** 35, 30-33.
22. L. L. Cai, L. He, Y. Wang, J. Zhong, C. J. Zhao, S. Zeng, J. Y. Yu, Y. Bian, Y. Q. Wei, W. Cai, E. W. Long, P. C. Jiao, J. F. Yan, Q. Xu, *RSC Adv* **2017,** 7 (22), 13458-13466.
23. C. Y. Gong, Y. M. Xie, Q. J. Wu, Y. J. Wang, S. Y. Deng, D. K. Xiong, L. Liu, M. L. Xiang, Z. Y. Qian, Y. Q. Wei, *Nanoscale* **2012,** 4 (19), 6004-6017.
24. J. P. Xu, J. Ji, W. D. Chen, J. C. Shen, *J Control Release* **2005,** 107 (3), 502-512.
25. Y. Lu, Z. G. Yue, J. B. Xie, W. Wang, H. Zhu, E. S. Zhang, Z. Q. Cao, *Nat Biomed Eng* **2018,** 2 (5), 318-325.
26. T. Konno, K. Kurita, Y. Iwasaki, N. Nakabayashi, K. Ishihara, *Biomaterials* **2001,** 22 (13), 1883-1889.
27. I. Villaluenga, S. Inceoglu, X. Jiang, X. C. Chen, M. Chintapalli, D. R. Wang, D. Devaux, N. P. Balsara, *Macromolecules* **2017,** 50 (5), 1998-2005.
28. Q. Xu, Y. X. Liu, S. S. Su, W. Li, C. Y. Chen, Y. Wu, *Biomaterials* **2012,** 33 (5), 1627-1639.
29. R. Gouda, H. Baishya, Z. Qing, *J Develop Drug* **2017,** 6, 171

Chapter 5

C_2H_5-POSS and 2-(methacryloyloxy)ethyl phosphorylcholine-based random copolymer as a drug carrier for solid formulation

5-1. Introduction

5-2. Experimental Section

5-2.1 Materials

5-2.2 Paclitaxel solid formulation preparation using 3a copolymer and PVP

5-2.3 Dissolution study

5-2.4 X-ray diffraction (XRD)

5-2.5 Fourier transform infrared spectroscopy (FT-IR)

5-2.6 Differential scanning calorimetry (DSC)

5-3. Results and Discussion

5-3.1 Characterization of the solid formulation (3a/PVP/PTX)

5-3.2 Dissolution profile of solid formulation (3a/PVP/PTX)

5-4. Conclusions

Reference

5-1. Introduction

Paclitaxel (PTX) is known as one of the excellent regimens for the treatment of different types of cancer such as breast, ovary, stomach, lung, etc. The major limitation of the application of paclitaxel is its low aqueous solubility (~0.4 μg/mL) due to its hydrophobic nature. The mixture of Cremophor EL (polyoxyethylated castor oil) and dehydrated ethanol need to be used for intravenous administration to solubilized paclitaxel in the circulatory system. The solvents often are the reasons for a serious hypersensitivity reaction [1]. In order to avoid the problem, various formulation of paclitaxel (use of biocompatible materials, polymer) and different mode of administration has been investigated. The various study on solid dispersion technology using biocompatible materials has been reported for the improvement of the solubility and dissolution of poorly water-soluble drugs like PTX [2,3]. For example, the incorporation of PTX into poly(ϵ-caprolactone)-based film [4]. The liposome delivery system was investigated to improve the aqueous solubility, stability and clinical efficacy of paclitaxel [5,6]. The nanoparticles (Abraxane®) and micelles (Genexol®, Nanoxel® and Paclical®) nanoplatforms have been investigated for clinical studies [7,8]. The cyclodextrin complexes system as a formulation to increase the water solubility has been reported [9,10], which has observed a decrease in toxicity. The promising clinical effects have not achieved yet.

Oral administration of PTX is one of the important methods for successful implementation of low-dose metronomic (LDM) chemotherapy. The LDM chemotherapy focus on low doses frequent administration of the drug with no drug-free periods in the system. For successful implementation of this LDM chemotherapy oral doses form of PTX is important in term of patient convenience and compliance. The major limitation of the oral administration of paclitaxel is its poor aqueous solubility which leading to reduce the bioavailability [11]. The recent studies reported that glycyrrhizic acid (GA) micelle encapsulate the PTX and help in improving the oral bioavailability [12]. So, to develop the solid dispersion suitable polymer need to be designed depending on nature and chemical structure of the poorly water-soluble drug. For example, 2-methacryloyloxyethyl phosphorylcholine (MPC) and butyl methacrylate (BMA) based copolymer poly[MPC-*co*-BMA] has been synthesized [13], which could solubilize the PTX by encapsulating it (hydrophobic paclitaxel) in the hydrophobic domain and form a micelle-like structure in an aqueous environment [14]. The poly[MPC-*co*-BMA] was also applied for the preparation of solid dispersion of tranilast, [*N*-(3,4-dimethoxycinnamoyl) anthranilic acid], an anti-allergic BSC class II drug [15]. The study suggested that poly[MPC-

co-BMA] improved the dissolution rate by the interaction between the polymer and tranilast. The polyvinylpyrrolidone (PVP) has been extensively studied for solid dispersions study to improve the dissolution rate poorly water-soluble drug without recrystallization [16]. The solid dispersion formulation containing PVP, sodium lauryl sulfate (SLS) and paclitaxel (PTX) have been studied and shown to increase the solubility and dissolution rate of PTX and the solid dispersion formulation was the first clinical trial of oral LDM chemotherapy [11]. From the literature review, it can be inferred that the design of water-soluble polymers which will interact and keep the paclitaxel in an amorphous state is one of the crucial factors for improving the solubility and dissolution rate of paclitaxel [17].

Based on the literature review, focus was given on MPC as a hydrophilic monomer and R-POSS hydrophobic monomers as the BMA segment in poly[MPC-*co*-BMA] which as mentioned above was not optimized for the interaction and controlled release of PTX. In the current study, a random copolymer of MPC (hydrophilic unit) and ethyl (C_2H_5) group-modified polyhedral oligomeric silsesquioxane (POSS) (hydrophobic unit) was synthesized (**Chapter 2, Scheme 2-1**). The obtained copolymer **3a** was observed to be non-cytotoxic [18], and form hydrophobic domain in water through hydrophobic interaction. Additionally, the copolymer solubilizes the paclitaxel and the strong interaction between the C_2H_5-POSS and paclitaxel strongly correlated with the slow release of PTX from a micelle-like association (**Chapter 4**) This finding encourages for further application of the copolymer **3a** toward the preparation of homogeneous PTX solid formulation. The current study suggested that **3a** is a potential carrier of PTX in the formulation of drug/polymer mixture. The solid formulation of **3a** and PTX was prepared by simple evaporation technique. The hydrophilic carrier PVP was added to the formulation to evaluate the role of PVP in the **3a** copolymer matrix. The solid states of PTX in the PVP and **3a** polymeric matrix was characterized by X-ray diffraction (XRD), Fourier transforms infrared spectroscopy (FT-IR), and differential scanning calorimetry (DSC). The dissolution behavior of paclitaxel from the formulation of **3a** copolymer/ PVP/PTX was investigated and the effect of the **3a** copolymer on the dissolution of PTX was also discussed in this study. The enhancement in PTX dissolution without any precipitation was observed, which can be correlated with the amorphous state of PTX in the copolymer / PVP matrix.

5-2. Experimental Section

5-2.1 Materials

The 2-(Methacryloyloxy) ethyl phosphorylcholine (MPC) was purchased from NOF Corporation (Tokyo, Japan). The **3a** copolymer was synthesized in the laboratory as described in the **Chapter 2**. The mol. % of C_2H_5-POSS in the **3a** copolymer was calculated by the ^1H NMR spectrum and value found to be 2 mol. %. The PTX was purchased from FUJIFILM Wako Pure Chemical Corporation, Japan**.** The PVP K30 (M_n = 50,000) was purchased from Sigma-Aldrich Co. LLC. (St. Louis, U.S.A). The other reagents and solvents were used without any further purification.

5-2.2 Paclitaxel solid formulation preparation using 3a copolymer and PVP

The solid formulation was prepared by the solvent method. The **3a** copolymer, PTX and PVP were dissolved in dehydrated ethanol with a ratio of **3a** : PVP : PTX = 44 : 44 : 12 wt. % and mixed with continuous stirring. The solvent was removed under reduced pressure inside vacuum dryer at 25 ℃. The **3a**/PTX (**3a** : PTX = 88 : 12 wt. %) and PTX/PVP (PVP : PTX = 88 : 12 wt. %) formulations were also prepared following the same procedure.

5-2.3 Dissolution study

The dissolution of the solid formulation was studied following the European Pharmacopoeia, using a type 2 (paddle) dissolution apparatus (NTR-6100A, Toyama Sangyo Co., Ltd., Japan). The dissolution study was conducted in a 500 ml dissolution medium containing 2nd Fluid mixed with 1 % Tween 80 mixed solution. The 1 % Tween 80 maintained the sink condition and acted as solubilizing agent of drug. The temperature 37 ºC and a stirring speed of 100 rpm were maintained during the study. The 10 mg solid formulation was considered for dissolution study containing 1.1 mg equivalent of PTX. The 25 ml sample solutions were collected in the different time interval (5, 10, 20, 30, 40, 50, 60, 90, 120 and 180 min) and an equivalent amount of fresh media was added to keep the volume constant. The dissolution of PTX was determined by measurement of concentration of PTX in dissolution medium using HPLC equipped with UV-vis detector (Gilson 119 UV/VIS Detector), two pumps (GILSON 805 Manometric Module and 306 Pump), a mixer (GILSON 811c dynamic

mixer), a column (TSKgel ODS-100S (Φ 4.6 nm × 150 mm) (TOSOH Co., Japan)). All the samples were filtered by 0.45 µm pore size PVDF membrane filters before each measurement. The mixed solution of methanol and water (with a ratio of 70:30 v/v) was used as the mobile phase and the flow rate of 1 ml/min was maintained during the measurement. The wavelength of 227 nm was fixed for the detection of PTX peak. The PTX dissolution was calculated using the PTX standard curve. The PTX standard curve was prepared by plotting the area under the peak vs. different concentration (considering the different concentration 100, 50, 10, 1, 0.1 µg/ml in methanol). The resulting standard curve was linear with $R^2 = 0.9949$. All the dissolution experiments were conducted triplicate.

5-2.4 X-ray diffraction (XRD)

Powder X-ray diffraction was carried out using an X-Ray Diffractometer (RINT2000, Rigaku Co., Japan) with monochromatic CuKα radiation and the generator working at 40 kV and 20 mA. Scattering intensity was measured in the range of $2 < 2\theta < 60^{o}$ with scan steps 1^{o} min^{-1}.

5-2.5 Fourier transform infrared spectroscopy (FT-IR)

The chemical bonds of the solid formulation were characterized by Fourier transform infrared spectroscopy (FT-IR) using apparatus (JASCO FT/IR-460plus). The scanning wave numbers ranged from 4,000 to 400 cm^{-1}. The KBr was used for the attenuated total reflectance crystal. The spectra were recorded from KBr pellets, prepared by mixing the solid formulation with KBr at room temperature. The spectrum resolution was 4 cm^{-1}, and the 2 mm sec^{-1} scans were accumulated to determine one spectrum.

5-2.6 Differential scanning calorimetry (DSC)

Thermal analyses of the solid formulation were carried out by differential scanning calorimetry (DSC) using apparatus (EXSTAR 6000/DSC6200, Seiko Instruments Inc., Japan). The scan rate was considered 10 °C min^{-1} (1^{st} cooling, 2^{nd} cooling, 1^{st} heating and 2^{nd} heating) within the temperature range between 20 and 185 °C. The glass transition temperature (T_g) was obtained at the midpoint of change in the baseline of DSC thermograms of 2^{nd} heating. The

$T_{g\,mix}$ of the solid formulation (blend) [11] of amorphous polymer blend was calculated by using the Fox-equation,

$$1/T_{g\,mix} = \sum_i w_i/T_{g\,i} \quad \text{..... (1)}$$

where w_i is the weight fraction of the ith pure component and $T_{g\,i}$ is the glass transition temperature (in Kelvin) of the ith pure component.

5-3. Results and Discussion

5-3.1 Characterization of the solid formulation (3a/PVP/PTX)

In the current study, three different solid formulations were prepared considering the PTX weight % same: **3a** : PVP : PTX = 44 : 44 : 12 wt. % (**3a**/PVP/PTX), **3a** : PTX = 88 : 12 wt. % (**3a**/PTX) and PVP : PTX = 88 : 12 wt. % (PV/PTX). The crystalline and amorphous states of PTX and polymers were characterized by XRD, DSC and FT-IR measurement.

XRD spectra of the **3a**, PVP, PTX, and the three different solid formulations were represented in **Figure 5-1 (i)**. The PTX showed semi-crystalline diffraction peaks at 5.5°, 8.7° and 12.6° (**Figure 5-1 (i)-C**). The observed peaks were consistent with the previous report [20]. The characteristic peaks of PTX as observed in **Figure 5-1 (i)-C** were not seen in solid formulations of **3a**/PTX, PVP/PTX, and **3a**/PVP/PTX (**Figure 5-1 (i)-D, E & F**), suggesting the amorphous state of PTX in the formulation [4]. From the results, it can be concluded that PTX was homogeneously distributed over the **3a**/PVP/PTX formulation [11, 19].

The T_g of the solid formulations and constituent polymers (**3a** and PVP) were calculated from DSC thermograms (**Figure 5-1 (ii)**), which supported the results observed in XRD. The T_g of **3a**, PVP and PTX were observed at 69.9 ºC (~343 K), 156.1 ºC (~429 K) and 105.9 ºC (~379 K), respectively (**Figure 5-1 (ii)-A, B and C**). The T_g obtained in case of PVP was consistent with the previous report [20]. From this observation, it can be stated that the calculation of T_g values from the 2nd heating curves in case of PVP was reliable. It is known that paclitaxel exhibits a melting point around 213-217 ºC as a semi-crystal phase [21] and also bears a T_g value as an amorphous phase [22]. In the solid formulation of **3a**/PVP/PTX single T_g was observed at 91.1 ºC (~364 K) (**Figure 5-1 (ii)-F**).

According to the Fox-equation (1), $T_{g\,mix}$ of the **3a**/PVP/PTX was calculated to be 98.1 ºC (~381 K), approximately. The Fox-equation (1) only applicable to the prediction of the

properties of pure components. The contribution of asymmetric entropic and enthalpic does not reflected in this equation. Also, the Fox-equation (1) does not reflect the strength of intercomponent and intracomponent interaction, entropic effect, structural heterogeneity term and composition dependent energetic contribution from hetero-contact. The limitations of the Fox-equation (1) has been considered in the study which suggested that T_g and $T_{g\ mix}$ are not directly comparable.

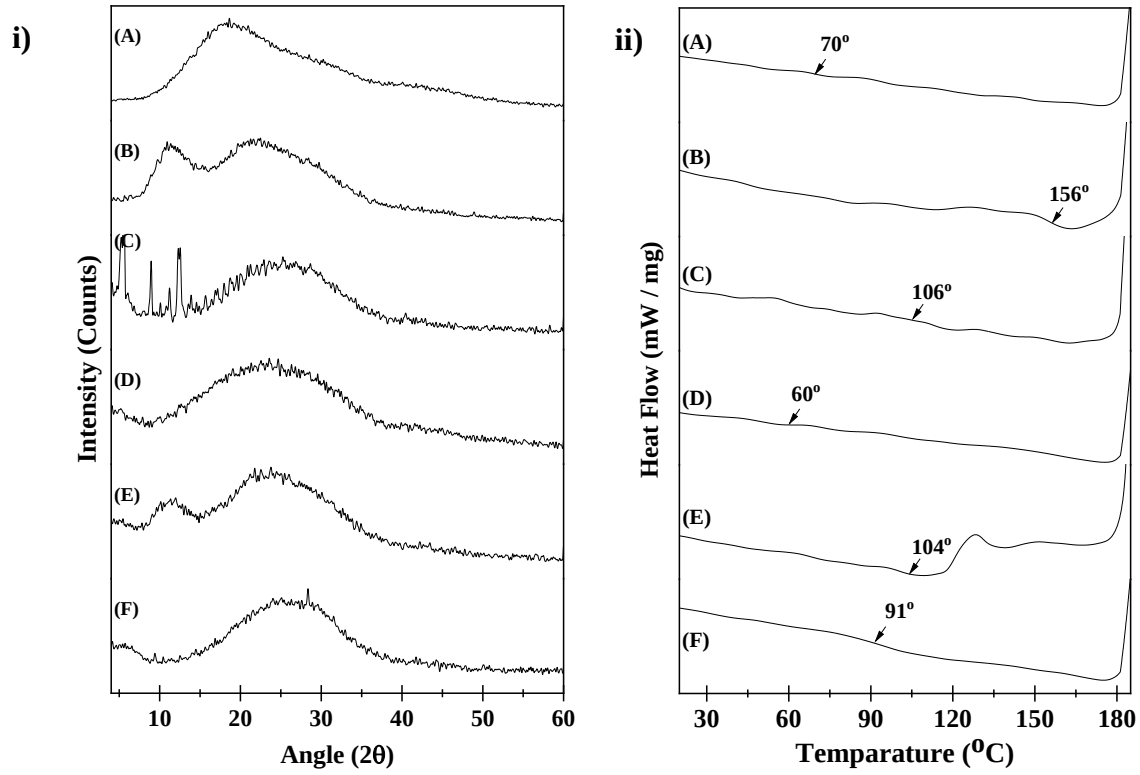

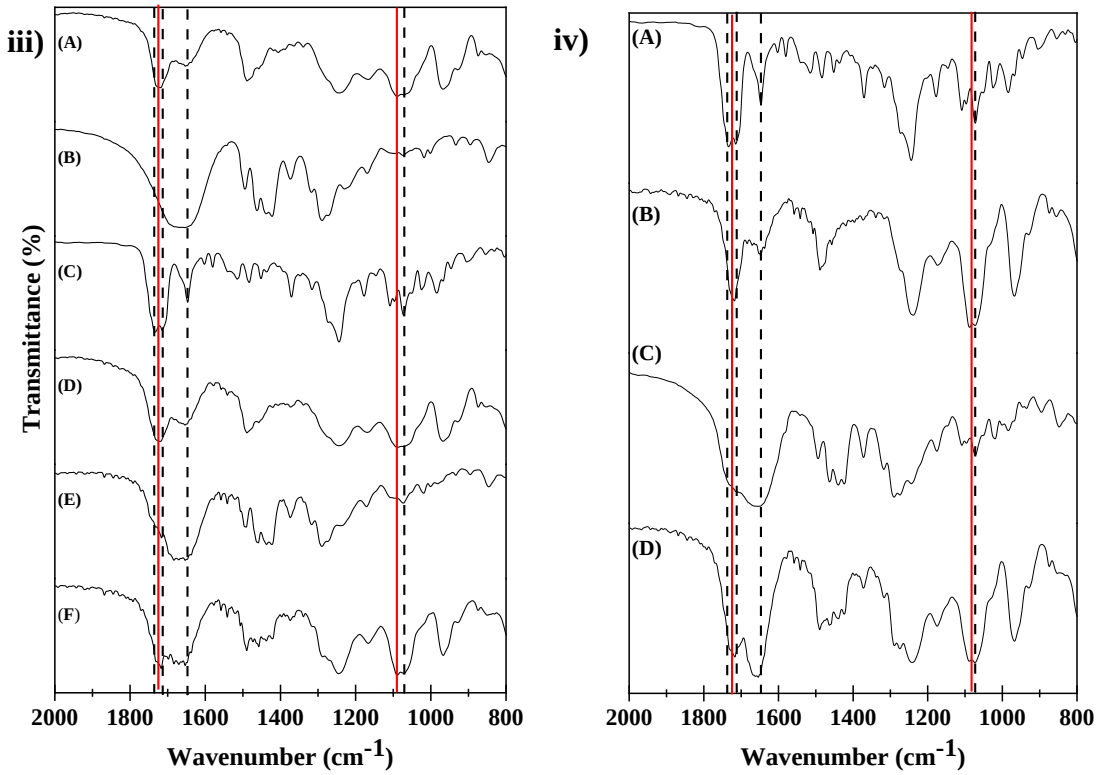

Figure 5-1. X-ray diffraction (XRD) spectra (i), DSC thermogram (ii), FT-IR spectra (iii) of A: **3a**; B: PVP; C: PTX; D: **3a**/PTX; E: PVP/PTX; F: **3a**/PVP/PTX and FT-IR spectra (iv) of A: PTX; B: **3a**/PTX physical mixture; C: PVP/PTX physical mixture; D: **3a**/PTX /PVP/PTX physical mixture.

In amorphous binary systems, the glass transition temperature and microstructure are closely related. The microstructural characteristics are evident of miscibility in binary polymer and drug/polymer mixture (**3a**/PVP/PTX system) [25, 26]. The analytical equation proposed by Brostow et. al. (Brostow, Chiu, Kalogeras and Vassilikou-Dova (BCKV) equation) for the prediction of glass transition temperature (T_g) that characterizes the binary systems of polymer blends or copolymers depending on their composition [24]:

$$T_g = \Delta T_g + x_1 T_{g1} + (1-x_1) T_{g2} \text{ …….. (2)}$$

$$\Delta T_g = x_1(1-x_1)[a_0 + a_1(2x_1-1) + a_2(2x_1-1)^2] \text{ …… (3)}$$

where ΔT_g the term is the deviation from the linear function (additional term in FOX equation), x_i is the mass fraction of component *i*, a_i is the parameters of the polynomial (a quadratic polynomial for binary systems). In the above equations (2) and (3), a_i parameters need to be determined to correlate with the experimental data and it highlight the complexity of the binary systems [24]. The higher deviation observed from the experimental and predicted T_g values calculated from the Fox equation (1) represent the increased system complexity. The parameters a_i in the equation reflected the strength of intercomponent and intracomponent interactions, entropic effects, structural heterogeneities, composition-dependent energetic contributions from hetero-contacts [23]. The BCKV equation has been used to correlate the experimental data of drug plus polymer mixture (poly(vinyl pyrrolidone-*co*-vinyl acetate)) and the results indicated that the results from the equation was a good agreement with the experimental data[25].

The ΔT_g which represent the system complexity in the BCKV equation to the formulation of **3a**/PVP/PTX was determined. The T_{gDSC} was determined from the DSC thermogram (**Figure 5-1 (ii)**) and $T_{g\,mix}$ was calculated using the FOX equation. The difference between T_{gDSC} and $T_{g\,mix}$ represent the ΔT_g which was calculated -14, -45 and -17 K for **3a**/PTX, PVP/PTX and **3a**/PVP/PTX respectively **(Table 5-1)**. According to the equation (3), the ΔT_g values include a_0-a_2 parameters (in the case of **3a**/PVP/PTX, a_0-a_3 due to the trinary systems). Since the parameters a_i indicate the interaction energies and structural heterogeneities, the energetic term related to the interaction between **3a,** PVP and PTX in solid formulations will exhibit in this value. The smaller ΔT_g values of the **3a**/PTX and **3a**/PVP/PTX than PVP/PTX solid formulation suggested that **3a** copolymer has some contribution toward increasing the miscibility of PTX.

Table 5-1 The T_{gDSC} , $T_{g\,mix}$ and ΔT_g values of the solid formulations, **3a** copolymers and PTX

Sample	T_{gDSC} [a] (K)	T_{gmix} [b] (K)	ΔT_g (= T_{gDSC}-T_{gmix}) (K)
3a	343	-	-
PVP	429	-	-
PTX	379	-	-
3a/PTX	333	347	-14
PVP/PTX	377	422	-45
3a/PVP/PTX	364	381	-17

[a] Experimental T_g values from DSC thermogram

[b] Calculated from FOX equation (1)

The T_g value is dependent on the mass fraction in case of binary polymer and drug/polymer mixture. In the current study single T_g at 91 ºC was observed and it was higher than the T_g of **3a** copolymer (69.9 ºC). The observation is similar to the conventional miscible organic blends [23]. It can be stated that the presence of single T_g value represents the miscibility and strong interaction between PTX, PVP and **3a** copolymers in single homogeneous phase [11]. Additionally, the increased T_g value of **3a** copolymer from 70 ºC to 91 ºC suggests the increased stability of PTX due to strong interaction in **3a**/PVP/PTX homogeneous formulation [22].

The FT-IR spectrum of PTX (**Figure 5-1 (iii)-C**) represented strong carbonyl bands around 1714 cm^{-1} (C=O, ketone),1735 cm^{-1} ((C=O)-O-, ester), 1643 cm^{-1} (aromatics), 1071 cm^{-1} (C-O-C). In case of **3a** copolymer, the corresponding ester bonds appeared at 1724 cm^{-1} ((C=O)-O-, ester) and 1080 cm^{-1} (P-O) from MPC segment [26] (**Figure 5-1 (iii)-A**). In **3a**/PTX (**Figure 5-1 (iii)-D**), the similar spectrum of **3a** was observed which suggested that incorporation of PTX in the **3a** copolymer matrix was difficult to confirm from the IR spectrum. The FT-IR spectrum of **3a**/PTX was governed by the **3a** copolymer. When PVP was incorporated in the formulation (**3a**/PVP/PTX), many jagged peaks around 1705-1740 cm^{-1} were appeared (**Figure 5-1 (iii)-F**). This observation suggested the restricted molecular interaction between individual components. This result was consistent with the DSC data which indicated high $T_{g\,mix}$ of the solid formulation. This result also indicated the contribution of PVP toward the reduction of crystallinity in the solid formulation. FT-IR measurements of the

physical mixtures of **3a**/PTX, PVP/PTX and the **3a**/PVP/PTX were performed to confirm the detection of 12 wt. % PTX in FT-IR spectra (carbonyl bands at 1714 cm^{-1} (C=O, ketone) and 1735 cm^{-1} ((C=O)-O-, ester) in addition to 1643 cm^{-1} (aromatics) and, 1071 cm^{-1} (C-O-C)) (**Figure 5-1 (iv)**). The FT-IR spectra of the physical mixture of the component were observed to be the summation of the spectra of an individual component. This result suggested the negligible interactions between the components in the physical mixture. In case of the formulation, PTX was found more homogeneously distributed over the **3a** and PVP matrix than physical mixture [11]. Considering all the results (XRD, DSC and FT-IR spectra) it can be concluded that PTX exist as an amorphous state in the homogeneous single-phase formulation.

5-3.2 Dissolution profile of solid formulation (3a/PVP/PTX)

The dissolution profile of PTX from the solid formulation of **3a**/PVP/PTX, **3a**/PTX and PVP/PTX was studied by in vitro dissolution tests. **Figure 5-2** indicate that the dissolution rate of PTX from **3a**/PVP/PTX was higher than the **3a**/PTX and PVP/PTX solid formulation in the first 10 min. Here, the dissolution rate was considered as the slope of the first liner curve section between 0 and 10 min. The cumulative release amount of PTX from **3a**/PVP/PTX was saturated until 20 min and then the dissolution was observed to be accelerated. The accelerated dissolution rate dissolved ~90% PTX at 40 min. As the similar complicated dissolution behavior was not observed in the case of the **3a**/PTX and the PVP/PTX, the first stage of the dissolution (until 20 min) might be due to the synergistic effects of the **3a** and PVP in the solid formulation. In the second stage (from 20 min to 40 min) the dissolution might be governed by the **3a** as the apparent dissolution behavior observed to be similar to the **3a**/PTX. The maximum dissolution of PTX from **3a**/PVP/PTX was around 2 µg ml^{-1} (almost complete dissolution of PTX) during 40 min. The similar phenomenon was also observed in the **3a**/PTX, where the solubility of PTX was observed around 1.5 µg/ml in 40 min. After reaching the maximum dissolution %, the dissolved concentration % was observed to be decreased. The decreased in PTX concentration was due to the rise of crystal nucleation rate of PTX which represent the ratio of the supersaturated solubility to the solubility of the crystal [27]. This is the general phenomenon observed in the case of the homogeneous solid formulation.

The *in-vitro* drug release profile (first 0 to 0.5 h time) was fitted in different mathematical model**.** The highest degree of correlation coefficient (r^2) represent the suitability of the mathematical model for drug release kinetics. The PTX release from **3a**/PVP/PTX follows

the Higuchi square root model (r^2 = 0.96996) and **3a**/PTX (r^2 = 0.96008) and PVP/PTX (r^2 = 0.94711) follows the zero-order model. In case of **3a**/PVP/PTX and **3a**/PTX the release exponent n is lower than 0.5 which indicate that the drug release from the system follow Fickian diffusion. In case of PVP/PTX the value of the n = 0.52 which indicate that the drug release follow the non-Fickian transport.

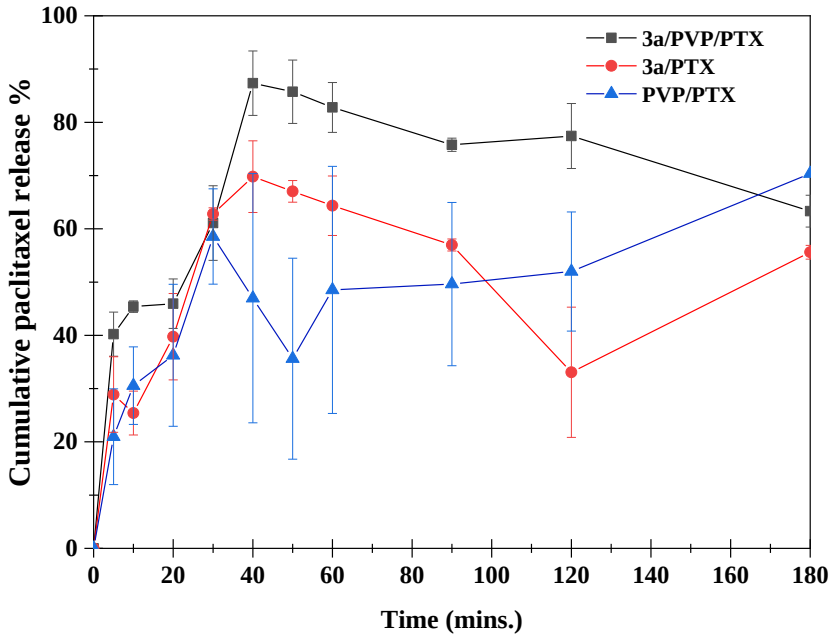

Figure 5-2. Dissolution profiles of PTX from solid formulations in mixed solution of 2nd fluid and 1 % Tween 80 at 37 ºC; (■): **3a** / PVP / PTX; (●): **3a**/ PTX; and (▲)): PVP / PTX. Values are Mean ± S.D. (n = 3).

The higher apparent dissolution of PTX from **3a**/PVP/PTX was caused by various factors like i) the amorphous state of PTX in the formulations **(Figure 5-1 (i)-F & D)**, ii) enhanced solubilizing effect of **3a** (solubility of PTX 75.5 ± 8.8 µg in **3a** 100 mg mL^{-1} solution) [19], iii) inhibition of recrystallization of amorphous PTX by PVP. The amphiphilic nature **3a** [19] prevent the immediate recrystallization of amorphous PTX at the water interface and reduce the interfacial tension between PTX and water [28]. The amount of PTX dissolution was observed to be lower in case of PVP/PTX than **3a**/PVP/PTX and **3a**/PTX which suggested that hydrophilic PVP matrix (absence of hydrophobic moiety) induced the recrystallization of PTX. Thus, from the results, it can be concluded that incorporation of the **3a** in the solid formulation

plays a crucial role in modulation of the dissolution behavior of PTX which help in providing PTX supersaturation around the media [29].

5-4. Conclusions

The **3a** amphiphilic copolymer was used to prepare the solid formulation of PTX and PVP. The **3a**/PVP/PTX solid formulation formed a single phase homogeneous formulation and enhance the dissolution rate of PTX. The improved wettability and amphiphilic nature of **3a** copolymer facilitated the rapid and complete release of paclitaxel (~ 90% within 40 min.). The interaction between PTX and **3a** copolymeric matrix in **3a**/PVP/PTX solid formulation reduced the mobility of amorphous PTX, which help in the enhancement of PTX dissolution. Therefore, it can be concluded that the formulation of **3a**/PVP/PTX would be a promising combination to enhance the physicochemical nature of PTX.

Reference

1. H. Gelderblom, J. Verweij, K. Nooter, A. Sparreboom, *Eur J Cancer* **2001**, 37, 1590-1598.
2. M.A. Alam, R. Ali, F.I. Al-Jenoobi, A.M. Al-Mohizea, *Expert Opin Drug Del* **2012**, *9*, 1419-1440.
3. D.N. Bikiaris, *Expert Opin Drug Del* **2011**, 8, 1501-1519.
4. Y.Q. Shen, F. Lu, J.W. Hou, Y.Y. Shen, S.R. Guo, *Drug Development and Industrial Pharmacy* **2013**, 39, 1187-1196.
5. T. Yang, F.D. Cui, M.K. Choi, H.X. Lin, S.J. Chung, C.K. Shim, D.D. Kim, *Drug Deliv* **2007**, 14, 301-308.
6. X.S. Hu, L. Lin, P.Y. Xing, C.G. Zhang, L. Wang, Y.Q. Liz, *J Thorac Oncol* **2017**, 12, S902-S902.
7. E. Bernabeu, M. Cagel, E. Lagomarsino, M. Moretton, D.A. Chiappetta, *Int J Pharmaceut* **2017**, 526, 474-495.
8. B. Louage, O. De Wever, W.E. Hennink, B.G. De Geest, *J Control Release* **2017**, 253, 137-152.
9. W. Bouquet, W. Ceelen, B. Fritzinger, P. Pattyn, M. Peeters, J.P. Remon, C. Vervaet, *Eur J Pharm Biopharm* **2007**, 66, 391-397.
10. H. Hamada, K. Ishihara, N. Masuoka, K. Mikuni, N. Nakajima, *J Biosci Bioeng* **2006**, 102, 369-371.
11. J. Moes, S. Koolen, A. Huitema, J. Schellens, J. Beijnen, B. Nuijen, *Eur J Pharm Biopharm* **2013**, 83, 87-94.
12. F.H. Yang, Q. Zhang, Q.Y. Liang, S.Q. Wang, B.X. Zhao, Y.T. Wang, Y. Cai, G.F. Li, *Molecules* **2015**, 20, 4337-4356.
13. S.I. Yusa, K. Fukuda, T. Yamamoto, K. Ishihara, Y. Morishima, *Biomacromolecules* **2005**, 6, 663-670.
14. T. Konno, J. Watanabe, K. Ishihara, *J Biomed Mater Res A* **2003**, 65a, 209-214,
15. S. Onoue, Y. Kojo, H. Suzuki, K. Yuminoki, K. Kou, Y. Kawabata, Y. Yamauchi, N. Hashimoto, S. Yamada, *Int J Pharmaceut* **2013**, 452, 220-226.
16. L.S. Taylor, G. Zografi, *Pharmaceut Res* **1997**, 14, 1691-1698.
17. C.L.N. Vo, C. Park, B.J. Lee, *Eur J Pharm Biopharm* **2013**, 85, 799-813.
18. X. Liu, L. Lei, J.W. Hou, M.F. Tang, S.R. Guo, Z.M. Wang, K.M. Chen, *J Mater Sci-Mater M* **2011**, 22, 327-337.

19. H.K. Han, B.J. Lee, H.K. Lee, *Int J Pharmaceut* **2011**, 415, 89-94.
20. S.Y. Chan, Y.Y. Chung, X.Z. Cheah, E.Y.L. Tan, J. Quah, *Asian J Pharm Sci* **2015**, 10, 372-385.
21. J. Lee, J.Y. Choi, C.H. Park, *Int J Pharmaceut* **2008**, 355, 328-336.
22. R.E. Richard, M. Schwarz, S. Ranade, A.K. Chan, K. Matyjaszewski, B. Sumerlin, *Biomacromolecules* **2005**, 6, 3410-3418.
23. I.M. Kalogeras, H.E. Hagg Lobland, *J Mater Educ* **2012**, 34, 69-94.
24. W. Brostow, R. Chiu, I.M. Kalogeras, A. Vassilikou-Dova, *Mater Lett* **2008**, 62, 3152-3155.
25. R.J. Babu, W. Brostow, O. Fasina, I.M. Kalogeras, S. Sathigari, A. Vassilikou-Dova, *Polym Eng Sci* **2011**, 51, 1456-1465.
26. T. Tateishi, M. Kyomoto, S. Kakinoki, T. Yamaoka, K. Ishihara, *J Biomed Mater Res A* **2014**, 102, 1342-1349.
27. C.L. Que, Y. Gao, S.A. Raina, G.G.Z. Zhang, L.S. Taylor, *Cryst Growth Des* **2018**, 18, 1548-1559.
28. A.K. Aggarwal, S. Singh, *Drug Development and Industrial Pharmacy* **2011**, 37, 1181-1191.
30. J.M. Miller, A. Beig, R.A. Carr, J.K. Spence, A. A Dahan, *Mol Pharmaceut* **2012**, 9, 2009-2016.

Chapter 6

R-POSS and 2-(methacryloyloxy)ethyl phosphorylcholine-based di-block copolymers for hydrophobic drug delivery

6-1. Introduction

6-2. Experimental Section

6-2.1 Materials

6-2.2 Measurements

6-2.2.1 Dynamic light scattering (DLS)

6-2.2.2 Static light scattering (SLS)

6-2.2.3 Electrophoretic light scattering (ELS)

6-2.2.4 Transmission electron microscopy (TEM)

6-2.2.5 Preparation of micelles and drug-loaded micelles

6-2.2.6 *In vitro* drug release studies

6-2.2.7 Biological Assays

6-2.2.7.1 Cell Viability

6-2.2.7.2 Cellular Uptake

6-2.2.7.3 Flow cytometry

6-3. Results and Discussion

6-3.1 Characterization of di-block (3a'-c') micelles

6-3.2 Characterization of drug-loaded di-block (3a'-c') copolymers micelles

6-3.3 *In vitro* drug release from (3a'-c') copolymers micelles

6-3.4 Cell viability (in (3a'-c') copolymers micelles)

6-3.5 Cellular uptake of (3a'-c') copolymers micelles

6-3.6 Quantitative assessment of cellular uptake of (3a'-c') copolymers:

Flow cytometry

6-4. Conclusion

Reference

6-1. Introduction

The nanoparticle-mediated drug delivery has revealed great progress in the field of cancer therapy where the side effects of chemotherapeutic drugs can be reduced by nanoparticle-mediated delivery into tumors site. The appropriate size of the nanoparticle can deliver the drug to the specific tumor tissues via passive enhanced permeability with negligible toxicity to the other organs. The appropriate size also can help the nanoparticles (NPS) to escape the macrophage phagocytosis and rapid clearance from the blood circulation system. The micellar nanoparticle system, which formed by the self-assembling of amphiphilic copolymers, have been extensively studied for their great role in the enhancement of the solubility of hydrophobic anticancer drugs (poorly soluble in water). This nanoparticle (micelles) contain a lipophilic core which solubilizes hydrophobic drugs and a hydrophilic shell which help in solubilizing the entire micelle system in water. The small dimensions of polymeric micelles (> 200 nm) advantageous for escaping the renal excretion and also for avoiding the recognition of the reticular endothelial system (RES) [1, 2].

The amphiphilic di-block copolymers containing a hydrophilic and hydrophobic segment form a micellar structure in an aqueous environment. The hydrophobic drug can be easily entrapped into the hydrophobic core of micelle using various techniques like solution/precipitation etc. The amphiphilic di-block copolymers composed of poly(ethylene glycol) (PEG), polyacrylamide, dextran, polyvinyl alcohol, polyvinylpyrrolidone, PEG-based hydrogels, etc. have been widely studied as a hydrophilic chain. Among them, PEG is commonly used as a hydrophilic chain. The study has reported that low molecular weight (> 3000) PEG is cytotoxic to the body [2]. The phosphorylcholine (PC) group has reported being a promising replacement of PEG as it possesses biomimetic biocompatibility, which was come from its mimicking nature with phospholipid membrane bilayers. Principally the presence of PC group reduces the protein adsorption and cell activation, which help in avoiding macrophage-mediated RES removal [3]. The 2-methacryloyloxyethyl phosphorylcholine (MPC) has a polar phosphorylcholine (PC) group, which help in providing the excellent biocompatibility in copolymer containing MPC and another hydrophobic unit. The amphiphilic di-block copolymers micelle system of MPC (as a hydrophilic chain) have been widely studied such as poly(2-methacryloyloxyethyl phosphorylcholine)-b-poly(2-(diisopropylamino)ethyl methacrylate ($MPC_{100}-DPA_{100}$) have been shown to possess biomimetic and pH-responsive properties [4], poly[MPC-co-*n*-butyl methacrylate (BMA)] (PMB30W)/ PLA nanoparticles

have been shown to possess high dispersive stability which restrained the adsorption of blood components [5], pMPC*m*-BMA*n* micelle have been shown to increase the water solubility of PTX [6], cholesterol-end-capped poly(2-methacryloyloxyethyl phosphorylcholine) (CMPC) micelle have been shown to reduce in size (less than 200 nm) after drug loading with no cytotoxicity [2]. The copolymers of poly(2-methacryloyloxyethylphosphorylcholine)-*b*-poly(butylene succinate)-*b*-poly(2 methacryloyloxyethyl phosphorylcholine) (PMPC-*b*-PBS-*b*-PMPC) formed micelles with sizes ranging from 108 to 170 nm. The DOX-loaded micelles showed high cytotoxicity to and internalized by HeLa cells. The PMPC-*b*-PBS-*b*-PMPC micelles minimized the clearance of the reticuloendothelial system and prolonged the circulation time [3]. The $PMPC_{40}$-*b*-$PDPA_{70}$ assemblies were internalized by the cells more than PEO_{122}-*b*-$PDPA_{43}$ or $PHPMA_{64}$-*b*-$PDPA_{72}$ system. The assemblies were internalized by cancer (HeLa) more, compared to the healthy (Telo-RF) cells due to the stronger binding of PMPC to cell membranes [7].

The amphiphilic di-block copolymer, PHEMA-POSS-*b*-P(DMAEMA-*co*-CMA), synthesized via reversible addition-fragmentation chain transfer (RAFT) polymerization, form spherical micelles in an aqueous environment with POSS core and stimuli-responsive shell [8]. The tetraphenylporphyrin tetrasulfonic acid hydrate (TPPS)-loaded polymeric capsules containing light illumination produced cytotoxic singlet oxygen to kill the tumor cells. The MePEG-b-P(MAPOSS-co-DPA) was synthesized by atom transfer radical polymerization (ATRP), which produced spherical micelles with core-shell structure and possess a pH-responsive property [9]. The poly(L-glutamic acid) dendrimers containing POSS nanocubic core conjugated with doxorubicin was prepared via pH-sensitive hydrazine bond and biotin used as targeting ligand. The faster release of doxorubicin at pH 5.0 (than at pH 7.0) was observed due to the acid cleavage of the hydrazine bonds [10]. The poly (ethylene glycol) (PEG)-polyhedral oligosilsesquioxane (POSS) nanostructured core-shell nanoparticles were synthesized and insulin was encapsulated in the core. The study found that insulin was protected at gastric pH for 2 h and released at intestinal pH 6 - 7 where the absorption and activation of insulin are necessary [11]. Thus, POSS-containing inert vertex groups attached to the silicon-oxygen cage promote the formation of a well-patterned micelle structure for its hydrophobic nature and controlled the drug release. The aggregation of POSS- moiety forms regular stable hydrophobic micelle core that encapsulates the hydrophobic drug.

The objective of this chapter is to develop amphiphilic copolymer which can form micelle in an aqueous environment and has an important implication in encapsulation of hydrophobic drug molecules inside and can be internalized by the cells. In this work, amphiphilic di-block copolymers were synthesized by chemically modifying POSS cage (vertex R-groups modified with ethyl (C_2H_5), hexyl (C_6H_{13}), octyl (C_8H_{17})) and polymerization of POSS cage with MPC polymer unit via RAFT polymerization to create POSS-based MPC amphiphilic block copolymers. RAFT polymerization process was selected as it needs a lower temperature (70 ℃) for polymerization and does not need any metal complex. Also, RAFT polymerization allows the design and synthesis of polymers with a well-defined architecture and controlled molecular weight (M_w) with relatively low polydispersity which forms 3D supramolecular self-assembly structures in an aqueous environment when the adequate hydrophilic/ hydrophobic balance is reached [6]. The effect of chemical modification (vertex R-groups modified with ethyl (C_2H_5), hexyl (C_6H_{13}), octyl (C_8H_{17})) of POSS cage (keeping the hydrophilic chain length same) was investigated based on size, surface charge, hydrophobic drug encapsulation, drug releasing behavior. The cellular uptake and intracellular distribution of FITC-PT- loaded polymeric association in HeLa cell line were investigated by fluorescence microscopy and flow cytometry analysis. The encapsulation and releasing behavior of α − Tocopherol (α-TP) (**Figure 6-1**) were additionally studied (along with PTX) to understand the interaction between hydrophobic drugs and the hydrophobic domain (POSS cage with different vertex R-group) of copolymers. The combination of DLS (particle size 20-50 nm), fluorescence microscopy and flow cytometry results suggested that R-POSS-based MPC copolymer could be a promising candidate for hydrophobic drug encapsulation and intracellular drug delivery. From the viewpoint of literature review, R-POSS based MPC block copolymer micelle system with the potential for application in intracellular hydrophobic drug delivery has not been investigated earlier.

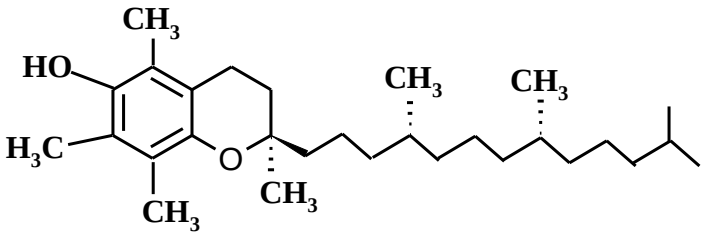

Figure 6-1. Chemical structure of α − Tocopherol (α-TP)

6-2. Experimental Section

6-2.1 Materials

The block copolymers **3a'-c'**were synthesized in the laboratory as described in the previous **Chapter 2, Scheme 2-2 (ii)**. The molecular weight (M_n) of copolymers were calculated by the ^{1}H NMR spectrum and the values summarized in the tabular form. The Dulbecco's Modified Eagle Medium (DMEM), Dulbecco's phosphate-buffered saline (DPBS), 0.25 %-Trypsin/1mM-EDTA solution, penicillin-streptomycin mixed solution and sodium carbonate were purchased from Nacalai Tesque, Inc. (Kyoto, Japan). The Fetal Bovine Serum (FBS) was purchased from Sigma-Aldrich Co. LLC. (St. Louis, U.S.A). The water used in all experiments was purified with a Millipore Milli-Q system. The other reagents and solvents were used without any further purification. The HeLa cells (Health Science Research Resources Bank, Osaka, Japan) were cultured in DMEM supplemented with 10% FBS and 100 U/mL penicillin-streptomycin mixed solution. The cells were cultured in a humidified incubator at 37 ºC under 5% CO_2 atmosphere.

6-2.2 Measurements

6-2.2.1 Dynamic light scattering (DLS)

Dynamic light scattering (DLS) measurements of nanoparticles were carried out using a light scattering instrument (Zetasizer Nano ZS, Malvern Instruments, UK). The measurement was performed at 25℃ in water with the **3a'-c'** copolymer concentration of 1 mg/ml. Samples were filtered by 0.45 µm pore size filter before measurements. The hydrodynamic radius (R_H) of the copolymer was determined by using the Stokes-Einstein relation Eq. (1) with $D = \tau^{-1}q^{-2}$:

$$R_H = \frac{k_B T q^2}{6\pi\eta}\tau \ldots . (1)$$

Where k_B is Boltzmann constant, T is the absolute temperature, q is the scattering vector, η is the viscosity of the solvent and $\tau$is the mean relaxation time. The polydispersity indexes

were determined using cumulant analysis of the autocorrelation functions monitored at 90° as Eq. (2)

$$\ln g_1(t) = \ln C - \Gamma t + \frac{\mu_2}{2} t^2 \ldots . (2)$$

Where *C* is the amplitude of autocorrelation function and Γ is the relaxation frequency (τ^{-1}). The parameter μ_2 (the second order cumulant) was used to calculate the polydispersity index of the samples (PDI = μ_2/Γ^2).

CAC was measured using DLS to the aqueous **3a'-c'** copolymer solutions of concentration varying from 0.0001 to 1 mg/ml. Above the CMC, the intensity of scattering light increases due to the presence of micelles and the intercepts obtained in the correlation functions are much higher.

6-2.2.2 Static light scattering (SLS)

Static light scattering (SLS) measurements were performed using Otsuka Electronic Photal (Osaka, Japan) DLS-7000 at 20 °C. A He–Ne laser (10.0 mW at 632.8 nm) was used as a light source. Each (**3a'-c')** copolymer was dissolved in a 10 mM PBS (pH 7.4) with polymer concentration (*Cp*) = 0.5 g/L and stirred overnight and then filtered using a membrane filter of 0.45 μm pore size. The **3a'** copolymer was stirred overnight at 60 °C, but it wasn't soluble completely. The difference between the Rayleigh ratio (R_θ) of the solution and that of the solvent due to the angular dependence can lead to the estimation of the weight-average molecular weight (M_w) and z-average radius of gyration (R_g) from the following relationship Eq. (3):

$$\frac{KC_p}{R_\theta} = \frac{1}{M_w}\left(1 + \frac{1}{3} R_g^{\,2} q^2\right) \ldots . (3)$$

where *K* is the optical constant and *q* is the magnitude of the scattering vector. The *K* value was calculated using $K = 4\pi^2 n^2 (dn/dC_p)^2 / N_A \lambda^4$, where *n* is the reflective index of the solvent, dn/dC_p is the refractive index increment against C_p, N_A is Avogadro's number, and λ is the wavelength of the light source. The *q* value was calculated using $q = (4\pi n/\lambda)\sin(\theta/2)$, where θ is the scattering angle. Values of dn/dC_p at 633 nm were determined using an Otsuka Electronics Photal DRM-3000 at 20 °C.

6-2.2.3 Electrophoretic light scattering (ELS)

The electrophoretic light scattering (ELS) measurements were performed using a Zetasizer Nano ZS instrument (Malvern Instruments, UK). The measurement was performed at 25℃ in water with the **3a'-c'** copolymer concentration of 1 mg/ml. Samples were filtered by 0.45 µm pore size filter before measurements. The value of electrophoretic mobility (U_E) were converted to the value of ζ-potential (mV) through Henry's equation (4):

$$U_E = \frac{2\varepsilon\zeta f(ka)}{3\eta} \ldots . (4)$$

Where ε is the dielectric constant of the medium and η is the viscosity. The Henry's function $f(ka)$ was calculated through the Smoluchowski approximation $f(ka) = 1.5$.

6-2.2.4 Transmission electron microscopy (TEM)

Transmission electron microscopy (TEM) images were collected using a TEM apparatus (JEOL JEM-1230, JEOL, Japan) at an accelerating voltage of 100 kV. Samples were prepared on 200 mesh copper grids. Before the measurements, the **3a'-c'** samples were vacuum dried and kept overnight *in vacuo*.

6-2.2.5 Preparation of micelles and drug-loaded micelles

Polymeric micelles were prepared by dialysis approach. 10 mg of **3a'-c'** copolymers were dissolved in 1 ml ethanol using ultrasonication for 30 min. The solutions were dropped by drop added into 10 ml of pure water with vigorous stirring for 24 h. The mixture was then transferred into a dialysis tube (MWCO = 2,000) and dialyzed against water for 24 h to eliminate organic solvent. The inside phase of the dialysis tube was filtered by 0.45 μm pore size filter. The copolymeric micelle solutions were then used for stability study by DLS and ζ-potential measurements (0, 5, 8, 11, 12 days keeping at 25 ºC).

PTX and $\alpha - \text{Tocopherol}$ (α-TP)-loaded polymeric micelles were prepared following the method mentioned above. The **3a'-c'** to drug weight ratio was considered 10:1. One part of drug-loaded polymeric micelle solution was then used for stability study by DLS and ζ-

potential measurements (0, 2, 5 days keeping at 25 ºC) and another part was lyophilized for drug release study.

Drug loading content (DLC) and Drug loading efficiency (DLE) was measured using HPLC (acetonitrile : water (60 : 40) (PTX)/ methanol : water (70 : 30) ($\alpha - \mathrm{Tp}$) mobile phase, flow rate of 1 ml/min) by dissolving the drug (PTX and $\alpha - \mathrm{Tp}$)-loaded polymer into methanol. DLC and DLE % were calculated according to the following equations (5) & (6):

$$\mathrm{DLC}\ (\%) = \frac{\text{Mass of drug in micelle}}{\text{Mass of drug} - \text{loaded micelle}} \times 100 \ldots . (5)$$

$$\mathrm{DLE}\ (\%) = \frac{\text{Mass of drug in micelle}}{\text{Mass of drug in feeding}} \times 100 \ldots . (6)$$

6-2.2.6 *In vitro* drug release studies

The PTX-loaded copolymer **(3a'-c')** micelles (3 mg of lyophilized solid powder) were dissolved in 1 ml of D-PBS (pH 7.4). The solutions were then placed into a dialysis membrane bag with a molecular cut-off of 6,000 – 8,000 Da. The dialysis membrane bag was then placed in a vial containing 25 ml of D-PBS (pH 7.4) and 1 % Tween 80 mixed solution. The vials were placed in shaking bed maintaining the temperature 37℃ with the shaking speed of 100 rpm. At predetermined time interval, 1 ml of the release medium was withdrawn for concentration measurement and an equal volume of fresh D-PBS (pH 7.4) and 1 % Tween 80 mixed solution was added to keep the volume constant. The concentration of paclitaxel release in the releasing medium and end PTX-loaded micelle sample (unreleased PTX inside dialysis tube) was monitored by HPLC measurement (GLISON HPLC system, see section 2.4) at a detection wavelength of 228 nm. Before measurement, the sample was filtered with a 0.45 μm pore-size filter. Mixture of acetonitrile (60%) and water (40%) were used as the mobile phase with a flow rate of 1 ml/min. In vitro $\alpha - \mathrm{Tocopherol}$ release study was additionally performed following the same procedure for better understanding of the drug release profile and hydrophobic drug-copolymer interaction.

6-2.2.7 Biological Assays

6-2.2.7.1 Cell Viability

The biocompatibility of the **(3a'-c')** copolymer samples and cell viability of drug-loaded polymeric micelles were determined using Cell Counting Kit-8. The cells (HeLa) were seeded into 96-well plate in volumes of 90 µl (5000 cells/ well in DMEM media supplemented with 10% FBS) and incubated overnight at 37 ºC. The drug-loaded copolymer (**3a'-c')** was dissolved in 1 ml of D-PBS solution (pH 7.4) using ultrasonication (for 10 mins). 10 µl of drug-loaded copolymer micelles solutions were added to each well to give a final concentration of Paclitaxel 2 µg/ ml and α-Tocopherol 108 µg/ml (paclitaxel and α-Tocopherol concentration in copolymer micelles were calculated from DLC %) and incubated for 24 & 48 h at 37 ºC. The biocompatibility of the copolymer (without drug loaded) was measured following the same procedure mentioned above and the final concentration of copolymer was considered the same as PTX-loaded copolymer micelle concentration used in cell viability study. Only media and only cell in the well were considered as blank (bl) and positive control (c+) respectively in this experiment. 10 µl of CCK-8 reagent was added to each well and incubated for 2 h at 37 ºC. The absorbance of each well was measured using microplate reader (Microplate Reader SH-9000 Lab, Corona Electric Co., Ltd, Japan) at a wavelength of 450 nm. The % Cell viability was calculated using the Eq. 7. Where $I_{450}{}^{s}$, $I_{450}{}^{bl}$ and $I_{450}{}^{c+}$ represents the absorbance of copolymer Samples, Blank and Positive Control respectively.

$$\% \text{ Cell Viability} = \frac{I_{450}{}^{s} - I_{450}{}^{bl}}{I_{450}{}^{c+} - I_{450}{}^{bl}} \times 100 \ldots . (7)$$

6-2.2.7.2 Cellular Uptake

FITC labelled paclitaxel (FITC-PTX) was encapsulated inside the copolymeric micelle (by dialysis approach) to visualize the cellular uptake. FITC-PTX was synthesized according to the literature [12]. The HeLa cells were seeded into a 24-well plate with a cell density of 20,000 cells/ well in 1 ml DMEM media supplemented with 10% FBS and incubated overnight at 37℃ before the experiment. After 24 h incubation, the growth media removed and the cells were treated with serum free medium containing free FITC- PTX (2 µg/ml) and FITC-PTX

loaded copolymeric **(3a'-c')** micelles (equivalent FITC-PTX= 2 μg/ml) for 2, 6 h. The media were removed and washed with D-PBS for 3 times. The cellular uptake was observed and imaged immediately (each well containing 0.5 ml D-PBS) using a fluorescence inverted microscope (EVOS Digital Inverted Microscope, Life Technologies, Carlsbad, CA, USA).

6-2.2.7.3 Flow cytometry

Cellular uptake of FITC labelled PTX loaded **(3a'-c')** copolymers were further quantified by flow cytometry using BD FACS Canto II flow cytometer (CA, U.S.A.). The experimental procedure was similar to cellular uptake experiment except that after 2 h of incubation the cells were collected, washed three times with D-PBS and resuspended in D-PBS for the measurement. 10,000 events were collected for each experiment and acquisitions were perform in triplicate.

6-3. Results and Discussion

6-3.1 Characterization of di-block (3a'-c') micelles

The di-block **(3a'-c')** copolymers were synthesized by RAFT polymerization using $PMPC_{61}$ as the CTA were characterized by ^1H NMR and FT-IR measurements (**Chapter 2, Figure 2-5(i)-(iii))**. The results of SLS and DLS were summarized in the **Table 6-1**. The CMC values of all the copolymers **(3a'-c')** were found in the range of 49-92 μg/ml, so that the SLS and DLS measurements of the copolymers were conducted at a concentration of 0.5 mg/ml. Since the copolymers are di-block copolymers, the copolymer above CMC are likely to form a core-shell type micelle structure with hydrophobic R-POSS blocks forming the cores and hydrophilic poly(MPC) blocks forming the shells. The aggregation number (N_{agg}) was calculated from the ratio of the apparent molecular mass of the micelle (M_w (SLS)) and the number-average molecular weight (M_n (NMR)) of the unimer (**Table 6-1**). The values of N_{agg} for **3a'**, **3b'**and **3c'** were 41, 4.1 and 1.5, respectively (**Table 6-1**). These results suggested that the aggregation ability of the copolymers decreased with increasing the long alkyl chain length of R-POSS in the copolymer. Our previous study also supported this phenomenon: the C_2H_5-POSS part in a random copolymer enhanced the hydrophobicity of a copolymer coated film

interface in the presence of water[13]. In order to evaluate how the alkyl chain length, affect the compaction of micelle formation, the R_g and R_h values of those copolymers were estimated (Table). The R_g values of **3a'**, **3b'**and **3c'** were 44.9, 50.4 and 32.6, respectively. Also, the R_h values of **3a'**, **3b'**and **3c'** were 36.1, 43.0 and 26.1, respectively. These results suggest that **3b'** exhibited somewhat expanded states, because both R_g and R_h values showed the highest ones although the N_{agg} value was just 4.1. Since the R_g/R_h values provide the shape of molecular aggregates, the R_g/R_h values of the copolymers were compared with each other. The R_g/R_h values of **3a'**, **3b'**and **3c'** were 1.24, 1.17 and 1.25, respectively. It is known that the ideal R_g/R_h value of hard spherical particle is 0.778. If the packing state of the aggregates decreases or the polydispersity of the aggregates increases, then the R_g/R_h value increases around 1.5−1.7 for flexible linear chains in a good solvent[14]. Therefore, the polymeric micelles of **3a'**, **3b'**and **3c'** were close to a spherical shape with somewhat polydisperse in size. The polydisperse states of the micelles could be confirmed by the size distribution data obtained by DLS measurements (**Figure 6-2**). Since the size distribution of **3a'** was extremely small (**Figure 6-2**), **3a'** forms tightly packed association in conjunction with the high N_{agg} value (**Table 6-1**). On the other hand, **3b'** and **3c'** exhibited relatively broad two peaks representing the micelles and/or oligomers (**Figure 6-2**). Considering the low N_{agg} values of **3b'** and **3c'**, longer alkyl chains of C_6H_{13}- and C_8H_{17}- on the POSS part induced loosely packed association to form the micelle.

Transmission electron microscopy (TEM) images also supported the packing states (**Figure 6-3)**. From the TEM images of **3a'**, **3b'**and **3c'**, spherically shaped images were observed, while they are quite polydisperse in size. Especially, the TEM image of **3b' (Figure 6-3)** showed that the clear and monodispersed particles (diameters 30-50nm) were uniformly distributed in a broadly distributed large aggregate. Thus, the size of the copolymers found in the TEM images was found to be consistent with the size that was obtained from DLS results.

ζ-Potentials of **3a'**, **3b'**and **3c'** were - 0.12, -7.5 and -0.91 mV, respectively. Only the **3b'** micelles showed the highest negative values: the loosely packed association and the polydisperse states of **3b'**, as seen in **Figure 6-2** and **Figure 6-3**, might disrupt the intermolecular interaction.

Table 6-1. Dynamic and static light scattering (DLS & SLS) results of **3a'-c'** copolymer in 10 mM PBS (pH 7.4)

Sample	M_w[a] × 10^5 (g/mol)	M_n × 10^5 (NMR) (g/mol)	N_{agg}[c]	R_g[a] (nm)	R_h[b] (nm)	R_g/R_h	dn/dC_p (mL/g)	ξ-Potential (mV)	CMC (DLS) (μg/ml)
MPC_{61}-*block*-C_2H_5-$POSS_{13}$ (**3a'**)	10.7	0.261	41	44.9	36.1	1.24	0.0141	-0.12±0.26	49.1
MPC_{61}-*block*-C_6H_{13}-$POSS_{13}$ (**3b'**)	1.29	0.312	4.1	50.4	43.0	1.17	0.1889	-7.5±0.60	24.5
MPC_{61}-*block*-C_8H_{17}-$POSS_{12}$ (**3a'**)	0.497	0.325	1.5	32.6	26.1	1.25	0.1269	-0.91±0.29	91.8

[a] Estimated by SLS in PBS buffer. [b] Estimated by DLS in PBS. [c] Aggregation number of a polymer micelle calculated from M_w of the micelle determined by SLS and M_w of the corresponding unimers determined by M_n(NMR). [d] Estimated by DLS measurements.

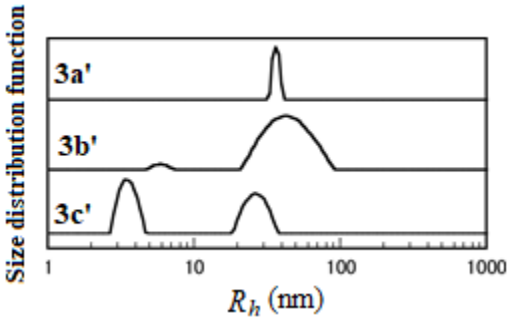

Figure 6-2. Size distribution of **3a'** (MPC_{61}-*block*-C_2H_5-$POSS_{13}$), **3b'** (MPC_{61}-*block*-C_6H_{13}-$POSS_{13}$) and **3c'** (MPC_{61}-*block*-C_8H_{17}-$POSS_{12}$) copolymer in 10 mM PBS (pH 7.4).

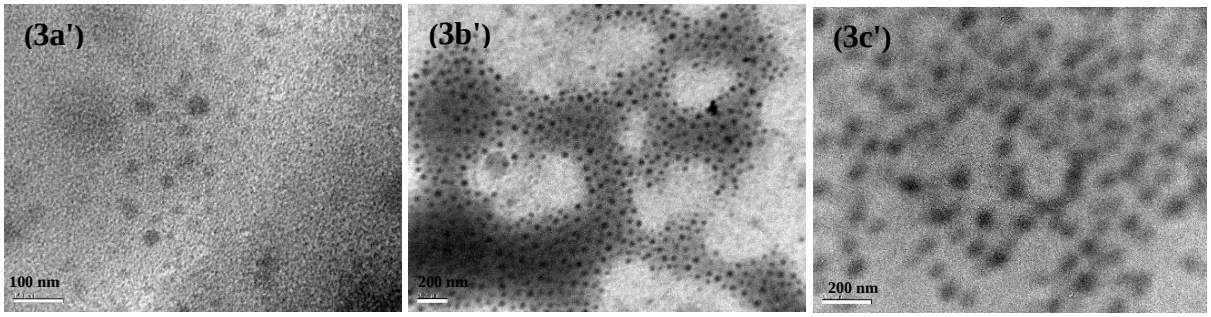

Figure 6-3. The TEM image of **3a'** (MPC_{61}-*block*-C_2H_5-$POSS_{13}$), **3b'** (MPC_{61}-*block*-C_6H_{13}-$POSS_{13}$) and **3c'** (MPC_{61}-*block*-C_8H_{17}-$POSS_{12}$) copolymer

The stability of the obtained **3a'-c'** copolymer micelles was determined by DLS measurements (**Figure 6-4)**. After standing up to 12 days at 25 ºC, the hydrodynamic diameter of **3a'** (**Figure 6-4 (A)**) and **3c'** (**Figure 6-4 (C)**) did not increase. The spherical micelles formed in aqueous environments by the C_2H_5-$POSS_{13}$ –based tightly packed association contributed to the good stability. In case of the **3c'**, even though the formation of the micelle was loosely packed manner but hydrophobic interaction due to the C_8H_{17} alkyl chain maintained the micelle formation. Besides, **3b'** (**Figure 6-4 (B)**) showed growth in size after 5 days, suggesting that the C_6H_{13}- moiety is thermodynamically unfavourable for the micelle formation.

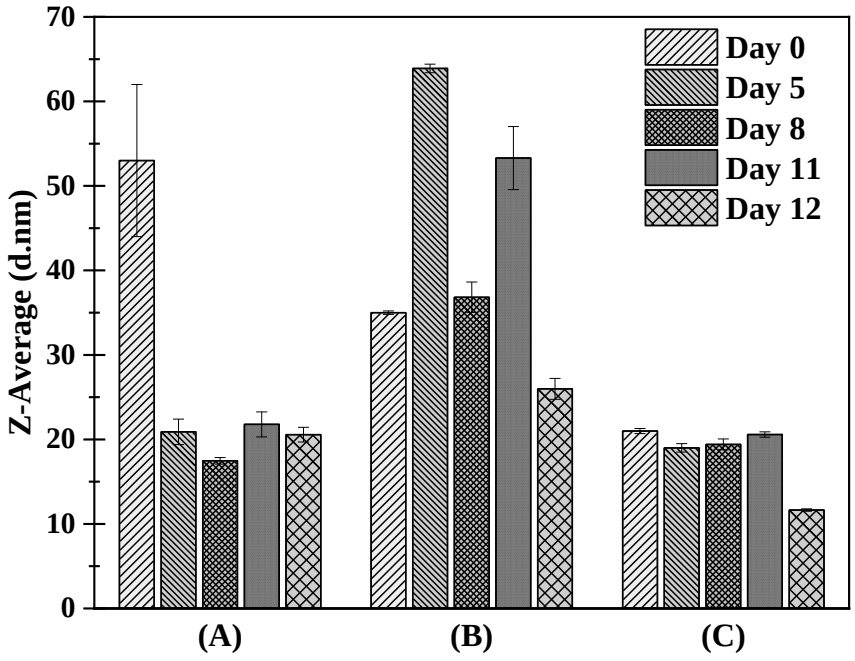

Figure 6-4 Particle size (Z-average diameter) change of (A) **3a'**, (B) **3b'** and (C) **3c'** copolymer micelles in water at 25℃ at the concentration of 1 mg/ml. The solutions were measured at different time interval 0, 5, 8, 11 and 12 days.

6-3.2 Characterization of drug-loaded di-block (3a'-c') copolymers micelles

As described in **section 6-3.1**, **3a'**, **3b'**and **3c'** formed polymeric micelles, but the association states were governed by the R-groups in POSS moiety. In order to evaluate how the polymeric micelle formation, affect poorly soluble drugs, we performed encapsulation of PTX and α-TP into the micelles.

Table 6-2 summarized the *Z*-average size (nm) change of polymeric micelles with or without PTX loading. The diameter of **3a'** was found to decrease after loading of PTX (day 0), indicating the strong interaction between PTX and C_2H_5- POSS moiety, which leads to the shrinkage and well consistent with our previous data[12]. In the case of **3c'**, the diameter was not changed after PTX loading: the long alkyl chain (C_8H_{17}) induced the hydrophobic interaction with PTX. This phenomenon also indicates that the PTX was encapsulated in the core of the micelle. On the contrary, the hydrodynamic diameter was observed to increase for **3b'** micelle after PTX loading, which suggests that the huge aggregation was induced by the PTX encapsulation. Considering the unstable state of **3b'**as seen in **Figure 6-2** (DLS) and

Figure 6-3 (TEM), the micelle-like formation was rearranged by the interaction with PTX. The PTX-loaded **3a'** and **3c'** micelles were found to be stable after 5 days at 25 ºC. After 5 days, **3b'** showed an increase in hydrodynamic size due to the enhanced aggregation formation.

Table 6-2. Z-average size (nm) change of PTX-loaded **3a'-c'** copolymer micelles in distilled water at 25℃

Sample [a]	Without PTX-loaded [b]		PTX-loaded [b]	
	Day 0	**Day 5**	**Day 0**	**Day 5**
MPC_{61}-*block*-C_2H_5-$POSS_{13}$ (**3a'**)	53 ± 9.1	21 ± 1.5*	24 ± 0.9	25 ± 1.8
MPC_{61}-*block*-C_6H_{13}- $POSS_{13}$ (**3b'**)	35 ± 0.2	64 ± 0.5*	106 ± 2.7	198 ± 14.8*
MPC_{61}-*block*-C_8H_{17}- $POSS_{12}$ (**3c'**)	21 ± 0.3	19 ± 0.5*	21 ± 4.4	16 ± 1.1

[a] The concentration was 1 mg/ml. [b] Z-average diameter (nm) (Mean ± SEM) (n = 3)

(*) indicates significantly different ($p<0.05$) from day 0 (Student *t*-test)

Similar experiments were performed using α-TP (**Table 6-3)**. The diameter of all the α-TP loaded copolymers **(3a'-c')** were in the range of 49-52 nm, and those were found to be stable after 5 days. Abrupt reduction of polydispersity index (0.09 - 0.15) was observed after α-TP loading, indicating the uniform size distribution. This observation indicates that α-TP molecules were encapsulated inside the micelle core, presumably due to the preferable intermolecular interaction between the aliphatic carbon chain in α-TP and the peripheral alkyl groups of POSS moiety in the micelle core and help in forming stable micelle structure[15].

Table 6-3. Z-average size (nm) change of α-tocopherol (α-TP) loaded **3a'-c'** copolymeric micelles in distilled water at 25℃

Sample [a]	Without α-TP-loaded [b]		α-TP-loaded [b]	
	Day 0	**Day 5**	**Day 0**	**Day 5**
MPC_{61}-*block*-C_2H_5-$POSS_{13}$ (**3a'**)	53 ± 9.1	21 ± 1.5*	51 ± 0.7	54 ± 0.6*
MPC_{61}-*block*-C_6H_{13}- $POSS_{13}$ (**3b'**)	35 ± 0.2	64 ± 0.5*	49 ± 0.7	54 ± 0.3*
MPC_{61}-*block*-C_8H_{17}- $POSS_{12}$ (**3c'**)	21 ± 0.3	19 ± 0.5*	52 ± 0.5	58 ± 0.8*

[a] The concentration was 1 mg/ml. [b] Z-average diameter (nm) (Mean ± SEM) (n = 3)

(*) indicates significantly different ($p<0.05$) from day 0 (Student *t*-test)

DLC and DLE of PTX loaded micelle were calculated using Eq. (5) and (6), respectively. The DLC of PTX for **3a'**, **3b'**and **3c'** were found to be 0.033 %, 0.024 % and 0.031 % respectively, while DLE of them were 0.44 %, 0.30 % and 0.20 %. The DLC and DLE were found to be relatively low in this case. Generally, the DLC and DLE depend not only on hydrophobicity and core size of the amphiphilic molecules but also the chemical structure of the drug. Since PTX does not bear normal aliphatic chains, the peripheral alkyl chains of the POSS moiety in the micelle core are not likely to fit the PTX chemical structure due to the enhancement of the intermolecular interaction. Additionally, DLC and DLE of α-TP were also investigated to gain a better understanding of the phenomenon. It was observed that DLC of α-TP for **3a'**, **3b'**and **3c'** were 3.6 %, 5.6 % and 3.6 %, respectively. Similarly, DLE of α-TP for each copolymer was 35 %, 53 % and 35 %, respectively. Since α-TP contains 4,8,12-trimethyltridecyl chain, the long aliphatic chain has the potential to provide good compatibility with the aliphatic core region of the polymeric micelles via hydrophobic interactions, resulting in high DLC and DLE values. Thus, loading capacity and efficiency of the **3a'-c'** copolymeric micelles were influenced by the selection of drug molecules.

6-3.3 *In vitro* drug release from (3a'-c') copolymers micelles

PTX release from the **3a'**, **3b'**and **3c'** copolymer micelles was monitored by a dialysis method for 52 h. However, the PTX concentration in the outer medium at each sampling time could not be determined because the PTX concentration was below the detection limit of the HPLC measurements. This indicates the strong interaction between PTX and micelle inside the core, which leads to a negligible level of PTX release from the **3a'**, **3b'**and **3c'** copolymer micelles. Additionally, the α-TP release was also investigated to compare the PTX release (**Figure 6-5)**. It was found that even after 61 h, the α-TP release from **3a'**, **3b'**and **3c'** copolymer micelles was 37 %, 12 % and 20 %, respectively. Because of higher DLC and DLE of α-TP than those of PTX, the amount of α-TP released slowly to the outer medium was determined. Both the phenomena can be explained that, once the drugs were encapsulated to the micelle core, most of the drugs were maintained in the copolymer micelles.

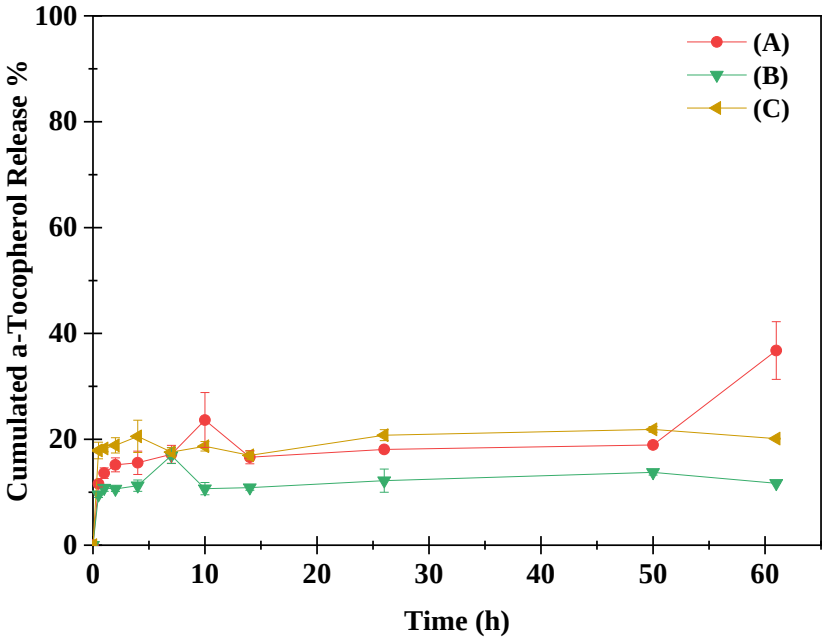

Figure 6-5. α-TP release from α-TP -loaded **3a'-c'** copolymer micelles: vs. time curves (A) (●) **3a'** (MPC_{61}-*block*-C_2H_5-$POSS_{13}$), (B) (▼) **3b'** (MPC_{61}-*block*-C_6H_{13}-$POSS_{13}$**)** and (C) (◀) **3c'** **(**MPC_{61}-*block*-C_8H_{17}-$POSS_{12}$) micelles. Values are mean ± S.D. (n = 3).

6-3.4 Cell viability (in (3a'-c') copolymers micelles)

Cell viability of the **3a'-c'** copolymers were evaluated using HeLa cells. All the copolymers showed excellent cell viability after 24 and 48 h (**Figure 6-6)**. The cytotoxic activity of PTX-loaded copolymeric micelles was evaluated (initial PTX concentration: 2 μg/ml) (**Figure 6-7)**. After 24 h, the cell viability was almost 90 % in all the PTX-loaded copolymers and free PTX. After 48 h, the cell viability reduced to around 50 % in all the copolymers and free PTX. This means that, if the efficacy of cellular uptake of the copolymers was assumed to be similar to the free PTX, those copolymers can release PTX in the intracellular environments rapidly, or the PTX-loaded micelles themselves acted as the anticancer compounds. Xu *et al* reported that HeLa cell viability of free PTX at 10 μg/ml was about 50 and 30 %, for 24 and 48 h of incubation respectively[16]. In our case, PTX concentration was 2 μg/ml, which is much less than the reported concentration to decrease the cell viability after 24 h. This is why it took 48 h to decrease cell viability. However, it is difficult to understand why there was no difference between the free PTX and the PTX-loaded micelles, and therefore, cellular uptake study was performed.

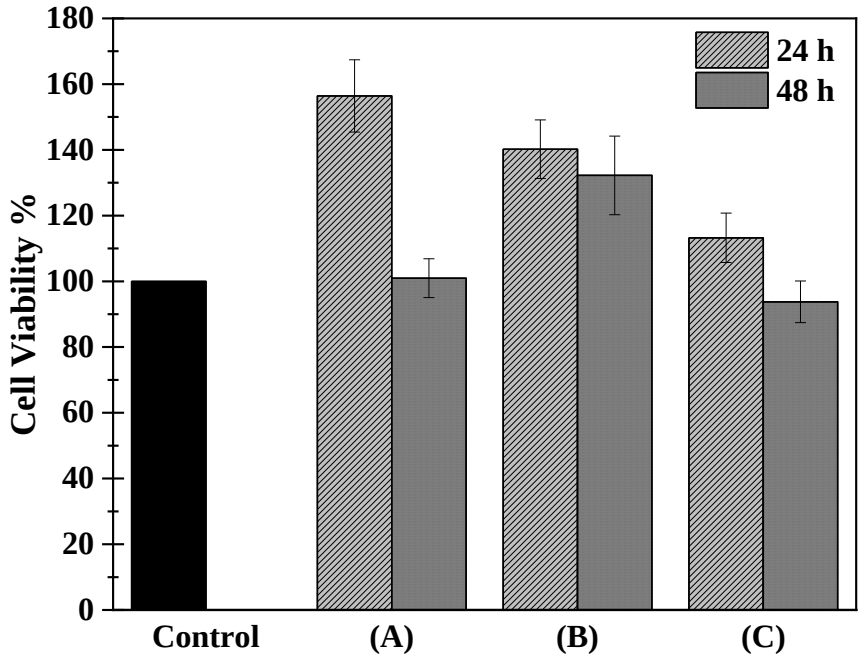

Figure 6-6. The cell viability of (A) **3a'** (MPC_{61}-*block*-C_2H_5-$POSS_{13}$), (B) **3b'** (MPC_{61}-*block*-C_6H_{13}-$POSS_{13}$**)** and (C) **3c'** (MPC_{61}-*block*-C_8H_{17}-$POSS_{12}$) (~11 mg/ml in cell-seeded plate). Each of the solutions (10 µl) were added to HeLa cells seeded well plate (90 µl) and incubated for 24 h and 48 h at 37ºC to measure the cell viability. Values are mean ± s.d. (n = 6). Cell viability was determined using the CCK-8 Kits and the absorbance was detected at 450 nm.

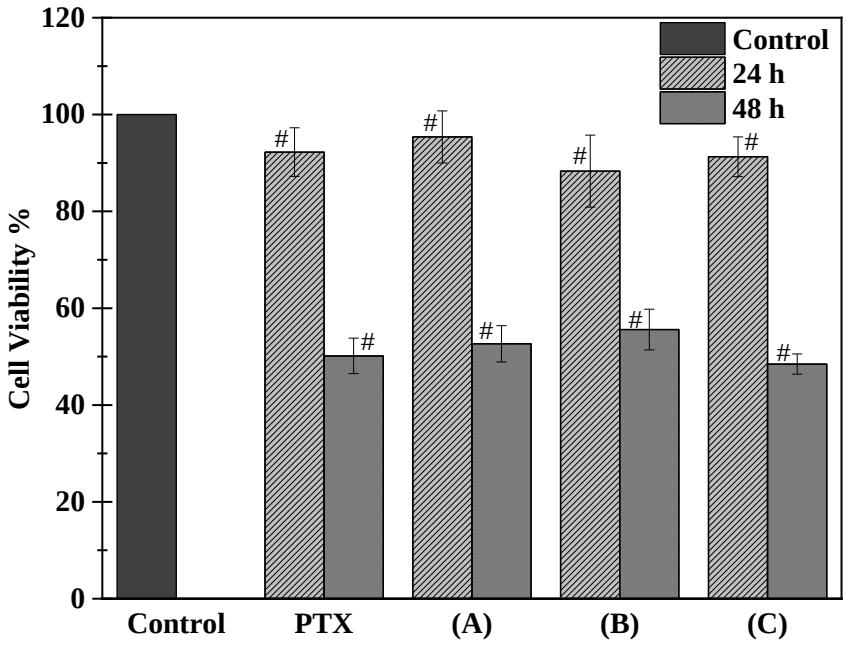

Figure 6-7. The cell viability % in presence of PTX-loaded copolymer micelle: (A) **3a'** (MPC_{61}-*block*-C_2H_5-$POSS_{13}$), (B) **3b'** (MPC_{61}-*block*-C_6H_{13}-$POSS_{13}$) and (C) **3c'** (MPC_{61}-*block*-C_8H_{17}-$POSS_{12}$) (each micelle contains PTX concentration 2 µg/ml seeded cell plate). Each of the solutions (10 µl) were added to HeLa cells seeded well plate (90 µl) and incubated for 24 h and 48 h at 37 ºC to measure the cell viability. Values are mean ± s.d. (n = 6). Cell viability was determined using the CCK-8 Kits and the absorbance was detected at 450 nm. (#) indicate significantly different ($p<0.05$) from the control sample (Two sample t-Test).

6-3.5 Cellular uptake of (3a'-c') copolymers micelles

Cellular uptake of the copolymers and its intracellular localization were investigated by using FITC-PTX-loaded copolymer[12,17]. FITC-PTX (**Figure 6-8)** was used as a green fluorescent probe, and the green fluorescent intensity was considered to be attributed by the FITC-PTX that was loaded in the copolymer micelles. **Figure 6-9 (a)** shows the fluorescent microscope images of HeLa cells after 2 h incubation with free FITC-PTX and FITC-PTX-loaded micelles. The fluorescent intensity of free FITC-PTX in the cells is likely to increase as compared to control. Similarly, the green fluorescent colour of the FITC-PTX-loaded **3a'** and **3b'** was found inside the cells after 2 h. It is to note that the intensity of FITC-PTX-loaded **3c'** seemed to be enhanced as compared with the other two copolymers. The fluorescent intensity

of FITC-PTX in the cells increased with incubation time (6 h) **Figure 6-9 (b))**. These results suggest that the **3c'** might modulate the cellular uptake. However, since this hypothesis is just based on the qualitative observation, we conducted FACS measurements of the same sample series after 2 h incubation.

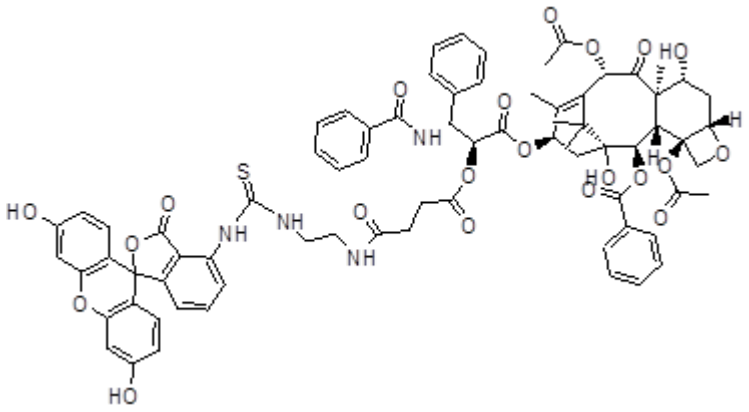

Figure 6-8. Structure of FITC-PTX

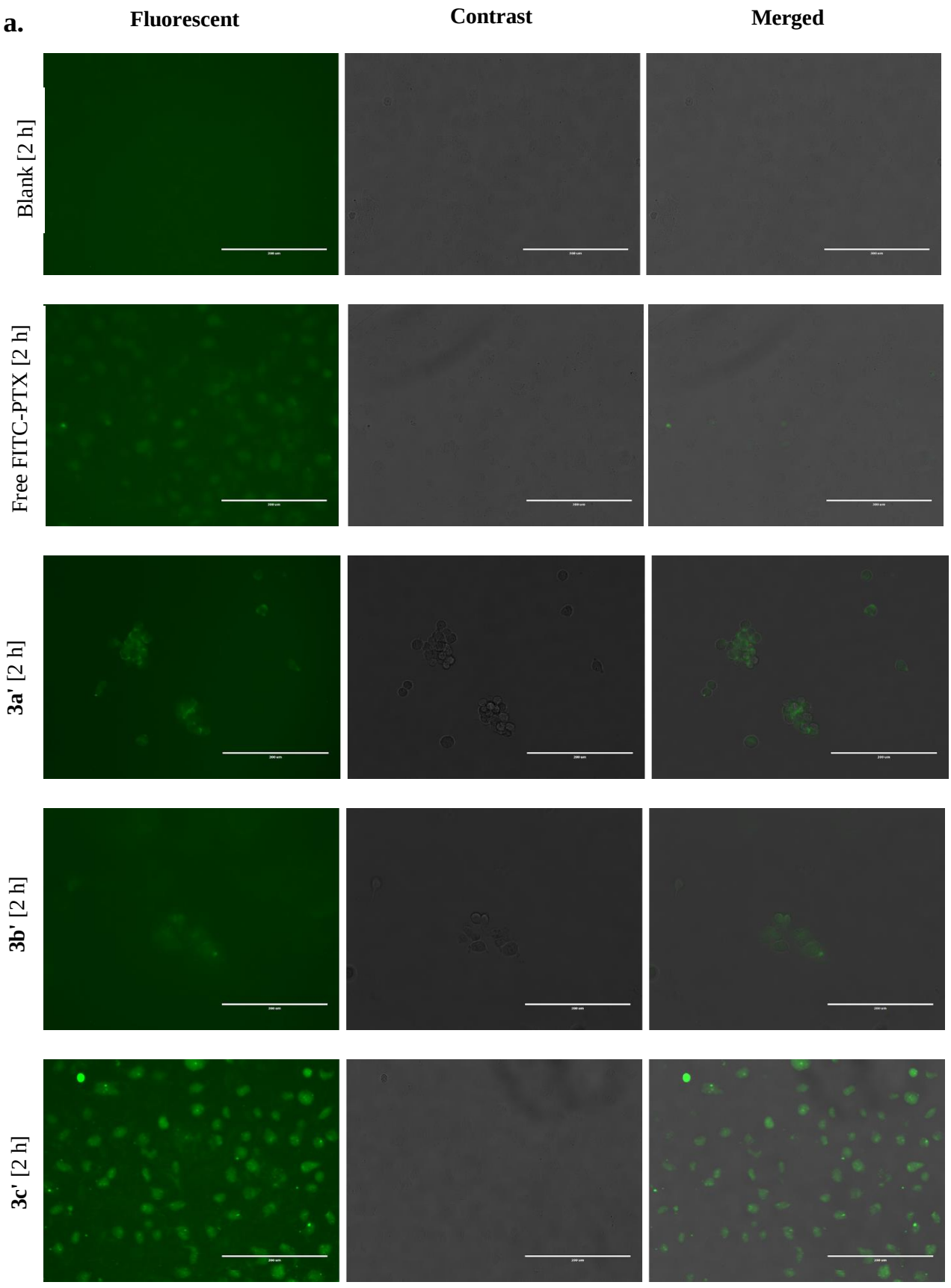
a.
Fluorescent
Contrast
Merged
Blank [2 h]
Free FITC-PTX [2 h]
3a' [2 h]
3b' [2 h]
3c' [2 h]

b.

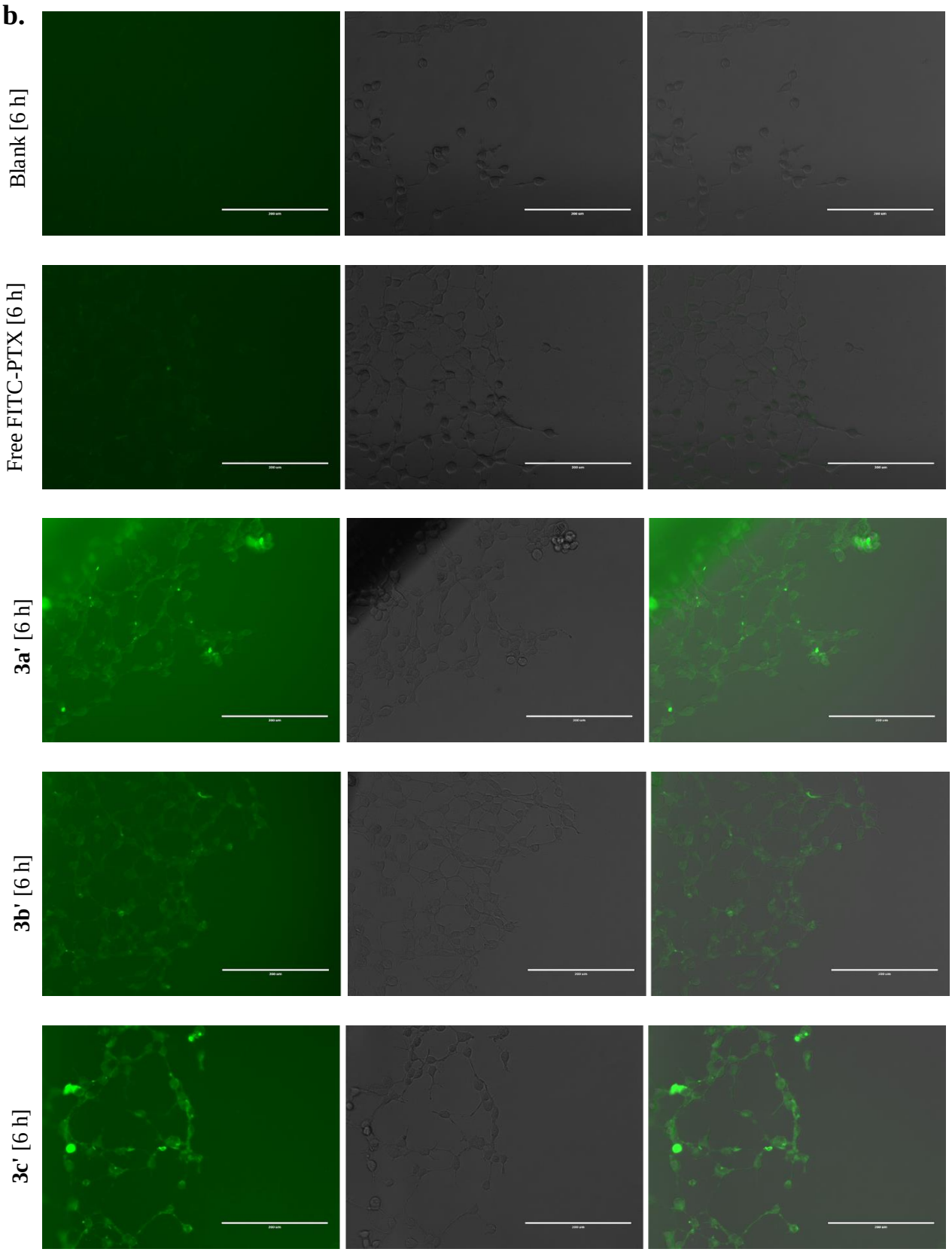

Figure 6-9. The Fluorescence microscopy images of HeLa cells treated with medium without a fluorescent prob, free FITC-PTX and FITC-PTX-loaded copolymer micelles **3a'**, **3b'**and **3c'** (each micelle contains paclitaxel concentration 2 μg/ml seeded cell plate) after (**a)** 2 h and (**b)** 6 h incubation.

6-3.6 Quantitative assessment of cellular uptake of (3a'-c') copolymers: Flow cytometry

The flow cytometry results were summarized in **Figure 6-10**. As shown in **Figure 6-10 (i)**, both the free FITC-PTX and the FITC-PTX-loaded copolymers increased the intensity level as compared to control, indicating the cellular uptake of both the free FITC-PTX and the FITC-PTX-loaded copolymers after 2 h. In order to quantitatively discuss the cellular uptake, mean fluorescence intensity (MFI) was calculated and summarized in **Figure 6-10 (ii)**. The MFI of the FITC-PTX-loaded **3b'**and **3c'** micelles were found to no different from free FITC-PTX, while only the MFI of FITC-PTX-loaded **3a'** micelle was significantly smaller than that of the free FITC-PTX. Considering the tightly packed association state of **3a'** micelle (**Table 6-1 and Figure 6-2**), it can be considered that the relatively harder morphology of **3a'** micelle might reduce the cellular uptake. Among the copolymer micelles, the cellular uptake of the FITC-PTX-loaded **3b'** was higher than that of the **3a'** and **3c'**. Previous reports suggest that the particle size and the distribution play an important role in cellular uptake which achieves a maximum in the size range of ~25-35 nm. Cellular uptake goes down for larger particles. The cellular uptake also depends on the surface charge (negative zeta potential caused electrostatic repulsion and hamper particle membrane interaction), hydrophobic nature of the core of the particle. It is noted that the size of PTX-loaded **3b'** was around 106 nm (**Table 6-2**: higher than the other copolymers), and the zeta potential was -10 mV (the highest negative charge among the copolymers) after PTX loading. Taking the unstable micelle formation of **3b'** into account (**Table 6-2**), the amphiphilic unimer or oligomers of **3b'** might disrupt cellular membrane to enhance the uptake. Overall, cellular uptake level of FITC-PTX-loaded copolymer micelles was similar to the free FITC-PTX, suggesting the PMPC shell of the micelles did not disturb the cellular uptake. Recently, de Castro *et al.* reported that PMPC has a strong affinity towards specific receptors that are expressed by most of the cells due to the phosphorylcholine group[7]. Therefore, the PMPC shells of the copolymers are likely to enhance the uptake similar to the free FITC-PTX, although the mechanism of uptake was independent.

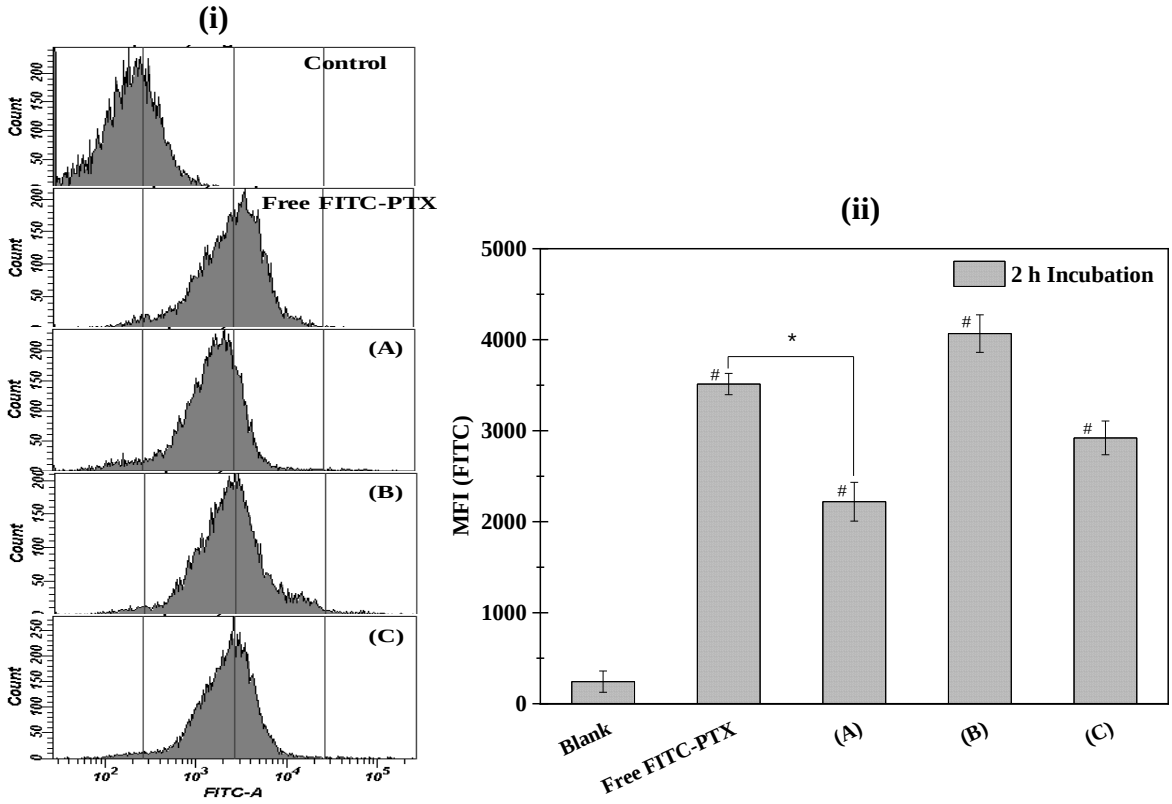

Figure 6-10. Flow cytometry data of **(i)** histograms (count vs fluorescence intensity) and the **(ii)** mean fluorescent intensity for FITC-PTX-loaded copolymer micelles (A) **3a'**, (B) **3b'** and (C) **3c'** (each micelle contains FITC-PTX concentration 2 μg/ml seeded cell plate) in HeLa cells after 2 h incubation. The mean fluorescence intensity was calculated by total 10000 events. (*) Statistically significant different compared to free FITC-PTX and (#) statistically significantly different compared to control.

6-4. Conclusion

In this chapter, amphiphilic di-block copolymers of 2-(methacryloyloxy)ethyl phosphorylcholine (MPC) and methacrylate R-POSS (vertex R-groups of POSS cage modified with ethyl (C_2H_5), hexyl (C_6H_{13}), octyl (C_8H_{17}) alkyl chain) were synthesized via RAFT polymerization. All the di-block copolymers formed spherical micelles in an aqueous environment within the range of 26-43 nm. By changing the alkyl chain length of R-POSS block, solution properties of the polymeric micelles were modulated: C_2H_5 induced tightly

packed association, in which ca. 41 **3a'** (MPC_{61}-*block*-C_2H_5-$POSS_{13}$) molecules were aggregated. By changing the R-groups to C_6H_{13} and C_8H_{17}, they induced loosely packed association, in which ca. 2-4 di-block copolymer molecules were aggregated. We found that only **3b'** (MPC_{61}-*block*-C_6H_{13}-$POSS_{13}$**)** micelle was unstable due to the polydisperse nature. All the micelles were able to encapsulate hydrophobic drugs inside the core, the stability of which was dependent on the chemical structure of the drugs: poorly soluble drugs bearing long alkyl chains such as α-TP were suitable for the R-POSS core. Cellular uptake of PTX-loaded micelles was governed by the PMPC-related cellular uptake phenomena. Therefore, the amphiphilic copolymers of MPC and R-POSS prepared by RAFT polymerization could be a promising candidate for controlled micelle formation and the selective hydrophobic drug encapsulation and potential as a carrier for drug delivery.

References

1. S. Luo, Y. X. Zhang, J. Cao, B. He, S. Li, *Colloid Surface B*, **2016**, 148, 181-192.
2. J. P. Xu, J. Ji, W. D. Chen, J. C. Shen, *J Control Release*, **2005**, 107, 502-512.
3. Y. Zhang, M. Yi, Y. Bao, S. Zhang, *PolymInt* **2018**, 67,155–165
4. J. P. Salvage, T. Smith, T. Lu, A. Sanghera, G. Standen, Y. Tang, A. L. Lewis, *Appl Nanosci* **2016**, 6, 1073-1094.
5. T. Konno, K. Kurita, Y. Iwasaki, N. Nakabayashi, K. Ishihara, *Biomaterials*, **2001**, 22, 1883-1889.
6. S. I. Yusa, K. Fukuda, T. Yamamoto, K. Ishihara, Y. Morishima, *Biomacromolecules*, **2005**, 6, 663-670.
7. C. E. de Castro, C. A. S. Ribeiro, A. C. Alavarse, L. J. C. Albuquerque, M. C. C. da Silva, E. Jager, F. Surman, V. Schmidt, C. Giacomelli, F. C. Giacomelli, *Langmuir*, **2018**, 34, 2180-2188.
8. Z. H. Zhang, Y. D. Xue, P. C. Zhang, A. H. E. Muller, W. A. Zhang, *Macromolecules*, **2016**, 49, 8440-8448.
9. Y. Xu, K. He, H. Wang, M. Li, T. Shen, X. Liu, C. Yuan, L. Dai, *Micromachines* **2018**, 9, 258.
10. H. Yuan, K. Luo, Y. S. Lai, Y. J. Pu, B. He, G. Wang, Y. Wu, Z. W. Gu, *Mol Pharmaceut*, **2010**, 7, 953-962.
11. K. O. Kim, B. S. Kim, I. S. Kim, *Journal of Biomaterials and Nanobiotechnology* **2011,** 2 (3), 201-206.
12. S. Chatterjee, T. Ooya, *Langmuir*, **2018**, DOI: 10.1021/acs.langmuir.8b01588.
13. S. Chatterjee, T. Matsumoto, T. Nishino, T. Ooya, *Macromol Chem Phys*, **2018**, 219.
14. K. Huber, S. Bantle, P. Lutz, W. Burchard, *Macromolecules*, **1985**, 18, 1461-1467.
15. L. Tao, J. W. Chan, K. E. Uhrich, *J Bioact Compat Pol*, **2016**, 31, 227-241.
16. Q. Xu, Y. X. Liu, S. S. Su, W. Li, C. Y. Chen, Y. Wu, *Biomaterials*, **2012**, 33, 1627-1639.
17. C. Y. Gong, Y. M. Xie, Q. J. Wu, Y. J. Wang, S. Y. Deng, D. K. Xiong, L. Liu, M. L. Xiang, Z. Y. Qian, Y. Q. Wei, *Nanoscale*, **2012**, 4, 6004-6017.

Chapter 7

R-POSS and 2-(Methacryloyloxy)ethyl phosphorylcholine-based copolymers as a simple modifier for liposome

7-1. Introduction

7-2. Experimental Section

7-2.1 Liposome preparation

7-2.2 Transmission electron microscopy (TEM)

7-2.3 Particle size and zeta potential measurement

7-2.4 Differential scanning calorimetry

7-2.5 Cellular Uptake

7-2.6 Flow cytometry

7-3. Results and discussion

7-3.1 Characterization of liposome

7-3.2 Stability of liposome

7-3.3 Effect of copolymer on the phase transition temperature of liposome membrane

7-3.4 Uptake study

7-3.4.1 Qualitative uptake study

7-3.4.2 Quantitative uptake study

7-4. Conclusion

Reference

7-1. Introduction

Liposome has high potential as a carrier of bioactive molecules due to its biocompatibility, low toxicity, low antigenicity[1,2]. Liposomes can carry both hydrophilic and hydrophobic drug and protect them from the surrounding environment. The major limitations of its wide application are lack of mechanical and chemical stability. The instability of the liposome leads to leakage of bioactive molecules entrapped in the inner water phase[2]. Different approach has been investigated to improve the stability of liposome such as polymerization of phospholipid with diene or acrylate moiety[3-5], combination with polymer[6-9], ionic complexation with natural polyelectrolyte[6], introduction of hydrophobic group in water soluble polymer as anchor[7-9] etc. A poly(ethylene glycol)-modified liposome was investigated to achieve the long term circulation in the body[7]. It was assumed that PEG on the liposome surface attract the water shell which provide a steric barrier against the recognition by the cells of mononuclear phagocyte system. The major limitation PEGylated liposomes systems are that second dose of PEGylated liposomes intravenous injection causes extensively accumulate in liver. This phenomenon is known as "accelerated blood clearance (ABC) phenomenon"[10]. Different liposomal surface coating approach has been reported to improve its stability. The polysaccharide having cholesterol moiety has been reported for liposome coating. The cholesterol moiety act as anchor for fixation of polysaccharide on the liposomal surface which improve the stability and cell-specific targeting[9]. The hydroxyapatite (HA) has been used for liposome coating which helps in reducing the release rate of hydrophobic drug indomethacin[11]. Hyaluronic acid coated liposomal formulation has been studied for paclitaxel delivery. The study showed that hyaluronic acid electrostatically attracted to the liposome surface and provide better antitumor efficacy[12]. Poly(MPC-*co*-BMA) has been studied for coating the liposome surface. The results of the study indicated that MPC molecules interact with the liposome surface and enhanced its stability in physiological environment[2]. Interpenetration of hydrophobic group in liposomal membrane induced instability in some cases.

Random and di-block copolymers using MPC and alkylated POSS, which were synthesized in **Chapter 2 (Figure 7-1)**, have shown excellent biocompatibility and form highly stable micelle in aqueous environment. The R-group of hydrophobic POSS moiety was located on the surface and induced surface hydrophobicity. The micelles composed of the copolymers, uptake by the cell due to the affinity of the MPC molecule toward specific receptor located in cell membrane. The study revealed that amount of phospholipid adsorption increases with increase in MPC molecules on MPC-based polymer surface. Based on the fact that MPC polymers have an affinity for phospholipid, MPC and POSS copolymers were subjected for investigating of stabilization of liposomes. This hypothesis in this study was that the alkylated POSS moieties act as an anchor to liposomal membrane for fixation of the copolymers on the surface of liposome. Also, the hydrophilic MPC will remain on the surface and provide stability, bio- and hemocompatibility. The DSPE-PEG-2000 modified liposome was parallelly investigated as a control sample to compare the results.

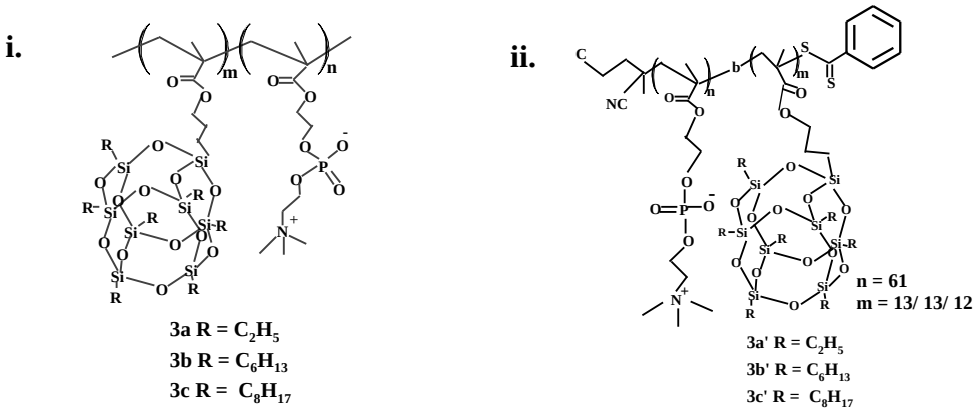

Figure 7-1. Structure of MPC and R-POSS based copolymers i) random copolymer **(3a-c)** ii) di-block copolymer **(3a'-c')**

7-2. Experimental Section

7-2.1 Liposome preparation

Liposomes consisting of L-α-phosphatidylcholine (HSPC) and cholesterol were prepared by thin-film hydration method. HSPC (228 mg, 300 μmol) and cholesterol (77.3 mg,

200 μmol) were dissolved in chloroform (10 ml) and transferred in an eggplant flask. The solvent was removed under reduced pressure using rotary evaporator. Equal amount of D-PBS was added and sonicated for 30 min. The extrusion was performed using Avanti Lipid miniextruder (100 nm polycarbonate membrane filter, 21 times) to prepare liposome with narrow size distribution.

To entrap the doxorubicin, 255 mM (pH 5.25, 9.5 ml) $(NH_4)_2SO_4$ was added instead of D-PBS and hydrated at 65 ℃ for 30 min. This is followed by same extrusion process and then the solvent was replaced to D-PBS by passing through the column. Unmodified liposome suspension (14 ml) and DOX (13.88 mg) aqueous solution (1 ml) (solvent- D-PBS) were mixed and incubated at 65 ℃ for 1 h. The unencapsulated DOX was removed by gel filtration column chromatography.

To prepare the coated liposome equal volumes of liposomal suspension and 1 % w/v concentration copolymer solution (in D-PBS) were slowly added. The mixtures were stirred for 1 h at room temperature. The surface modification of liposome by DSPE-PEG-2000 was carried out following the similar procedure except stirring at 65 ℃. The modified liposomes (liposome containing DOX coated with copolymer and DSPE-PEG-2000) was separated by passing through the chromatographic column.

7-2.2 Transmission electron microscopy (TEM)

Transmission electron microscopy (TEM) images were collected using JEOL JEM-ARM200F at an accelerating voltage of 200 kV. Samples were prepared using 200 mesh copper grids. Before the measurements, the samples were vacuum dried and kept overnight *in vacuo*. An energy-dispersive X-ray analysis (EDS) attached to the scanning TEM-high angle annular dark field (STEM-HAADF) was performed.

7-2.3 Particle size and zeta potential measurement

Dynamic light scattering (DLS) measurements were carried out to determine the average hydrodynamic diameter and size distribution of both with or without DOX-loaded copolymers and DSPE-PEG-2000 modified liposome. The zeta potential of both with or without DOX-loaded copolymers and DSPE-PEG-2000 modified liposome were also measured in D-PBS

and 1 : 1 D-PBS and FBS mixed solution. The measurement was performed using a light scattering instrument (Malvern, EXSTER DSC600) with 90° as a scattering angle. The stability measurement was performed after standing the sample at 37 ℃ for 0, 1, 3 and 8 days (copolymer-modified DOX encapsulated liposomes). The DLS measurement was performed at 25 ℃ in the water of 1 mg/ml concentration sample. Every samples were measured three times to analyse the mean diameter and zeta potential.

7-2.4 Differential scanning calorimetry

The phase transition temperature (T_c) of liposomal bilayer membranes represents the rippled gel-liquid crystalline phase transition and can be measured using DSC apparatus (EXSTAR 6000/DSC6200, Seiko Instruments Inc., Japan). The 6-7 mg lipid samples were weighted in aluminium pan and 20 µl of 2.5 mg/ml copolymers and DSPE-PEG-2000 aqueous solution was added. The pan was then hermetically sealed. The scan rate was considered 5 °C min^{-1} (1^{st} cooling, 2^{nd} cooling, 1^{st} heating and 2^{nd} heating) within the temperature range between 20 and 80 °C. The T_c was evaluated from DSC thermograms of 2^{nd} heating cycle. The empty aluminium pan was used as reference[1].

7-2.5 Cellular Uptake

HeLa cells were seeded into a 24-well plate with a cell density of 10,000 cells/ well in 1 ml DMEM media supplemented with 10% FBS and incubated overnight at 37℃ before the experiment. After 24 h incubation, the growth media removed and the cells were treated with serum free medium containing unmodified liposome, copolymers modified liposome and DSPE-PEG-2000 modified liposome (DOX concentration 10 µg/ml) for 2, 6 h. The media were removed and washed with D-PBS for 3 times. The cellular uptake was observed and imaged immediately (each well containing 0.5 ml D-PBS) using a fluorescence inverted microscope (EVOS Digital Inverted Microscope, Life Technologies, Carlsbad, CA, USA).

7-2.6 Flow cytometry

Cellular uptake of modified liposomes was further quantified by flow cytometry using BD FACS Canto II flow cytometer (CA, U.S.A.). The experimental procedure was similar to cellular uptake experiment except that after 2 and 6 h of incubation the cells were collected, washed three times with D-PBS and resuspended in D-PBS for the measurement. 10,000 events were collected for each experiment and acquisitions were perform in triplicate.

7-3. Results and discussion

7-3.1 Characterization of liposomes

The particle size of copolymer-modified liposome was measured by DLS in D-PBS (pH7.4) at 25℃, and the z-average diameters were 230-270 nm with PDI of 0.40-0.57 in D-PBS **(Figure 7-2 (i))**. The results represented that modified liposome had little bigger size (**3a**, **3c**, **3a'** and **3b'**) in comparison with non-mollified liposome (241 nm). The MPC is a hydrophilic molecule which uptake water and swell in aqueous environment. Zeta potential is known as a factor of surface electrostatic charge of particles. After modification with copolymers the surface of liposomes showed little increase in negative charge (non-modified liposome ζ-potential= -2, modified liposome ζ-potential= -3).

TEM images of the obtained liposomes were subjected to investigate the morphology of the liposomes **(Figure 7-2 (ii))**. The images represented that the modified liposomes were spherical in shape with aggregation. After modification with **3a**, **3b**, **3a'** and **3b'** smooth and more compact surface morphology was observed. The size of particles observed from TEM image was less than the hydrodynamic size observed from DLS measurements. This inconsistency might be due to the TEM image taken in dry state whereas the DLS measurement was taken in aqueous solution of D-PBS. The swelling may be the reason for higher size being observed in DLS measurement.

i.

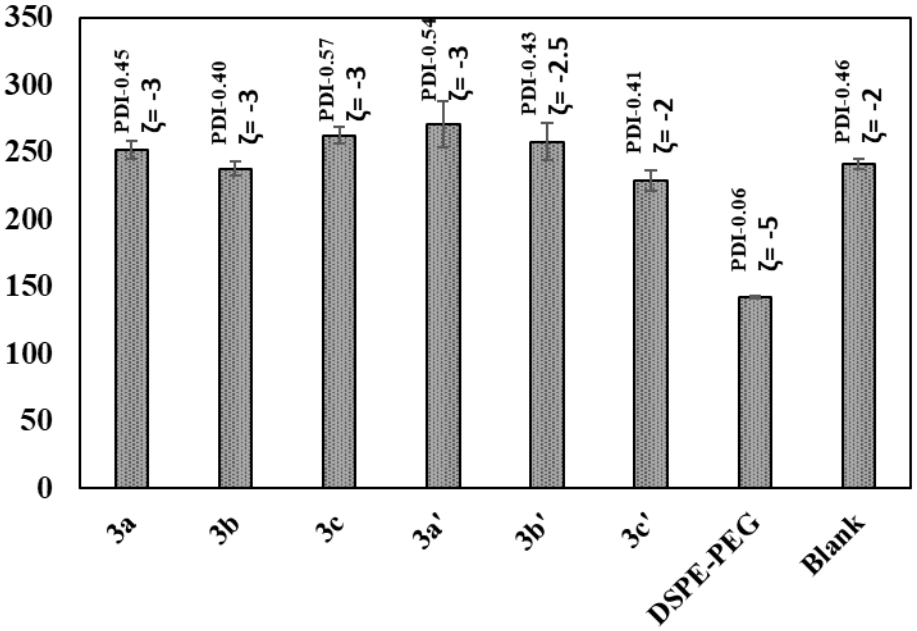
350
300
250
200
150
100
50
0
PDI-0.45 ζ= -3
PDI-0.40 ζ= -3
PDI-0.57 ζ= -3
PDI-0.54 ζ= -3
PDI-0.43 ζ= -2.5
PDI-0.41 ζ= -2
PDI-0.06 ζ= -5
PDI-0.46 ζ= -2
3a
3b
3c
3a'
3b'
3c'
DSPE-PEG
Blank

ii.

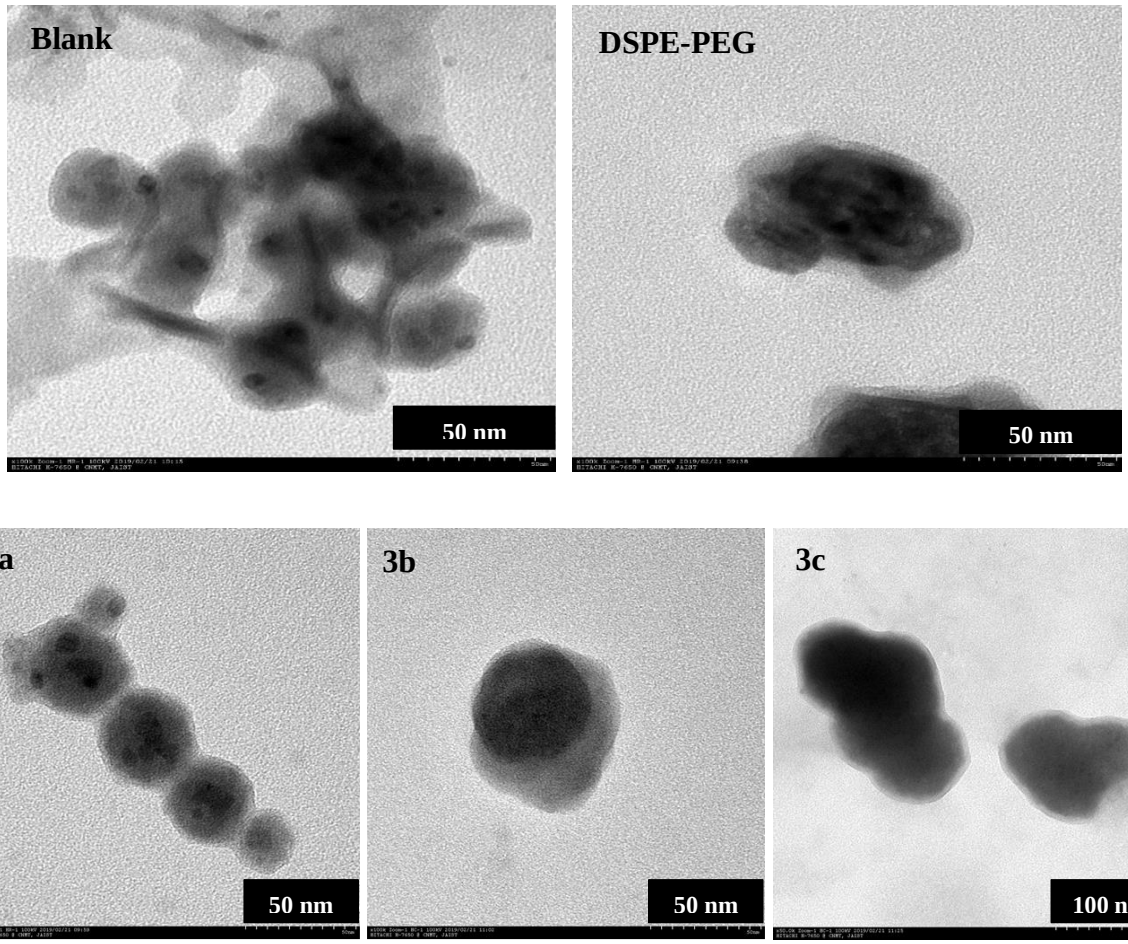
Blank
50 nm
DSPE-PEG
50 nm
3a
50 nm
3b
50 nm
3c
100 nm

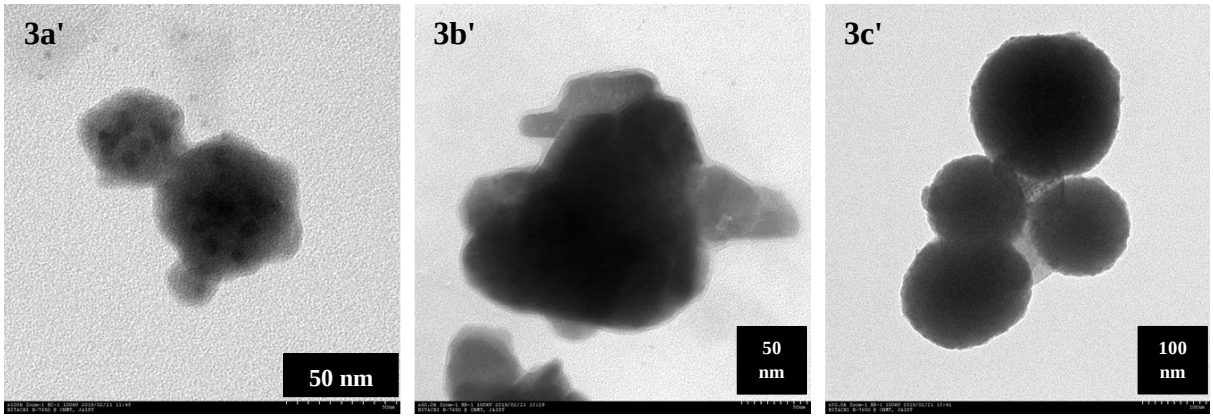

Figure 7-2 (i) Particle size (Z-average diameter) of the modified liposomes in D-PBS (pH7.4) at 25℃ **(ii)** TEM images of copolymer-modified liposomes

The distribution of copolymers on DOX encapsulated liposome surface in dry state was determined by high-resolution dark field STEM/EDS observation (**Figure 7-3)**. In case of **3b** and **3c'**, the element analysis results indicated that the surface was mainly covered by the phosphorous (P) molecule in dry state. In the case of **3a**, **3c**, **3a'** and **3b'**, the carbon (C), oxygen (O) and phosphorous (P) are observed. These oxygen and carbon might have come from the copolymer.

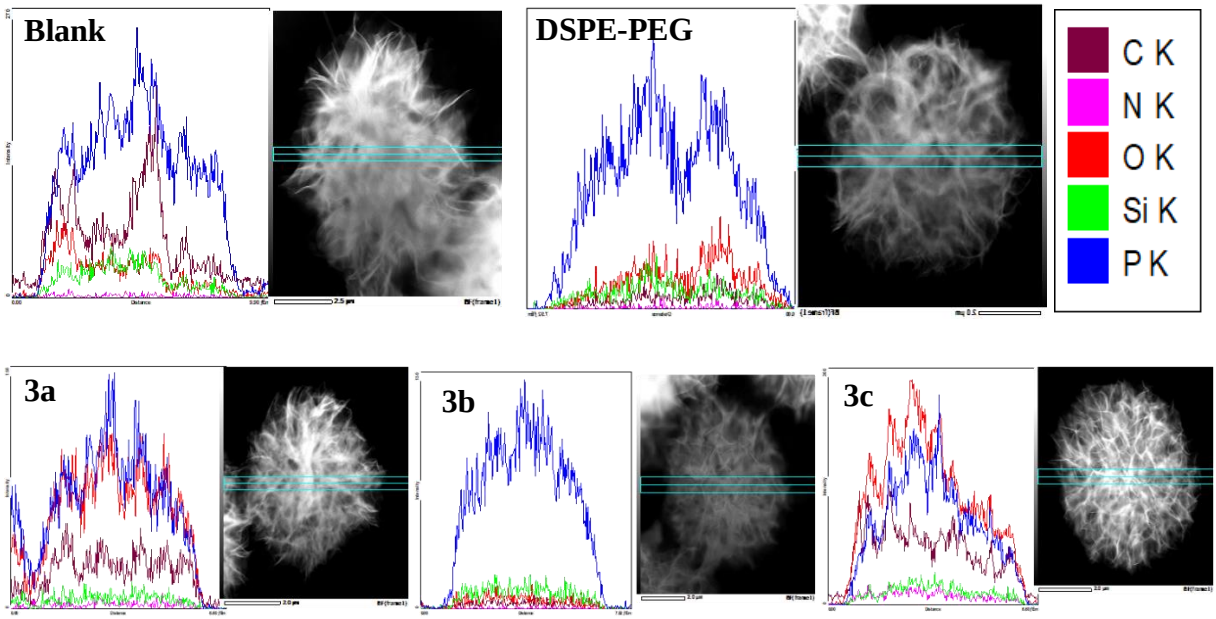

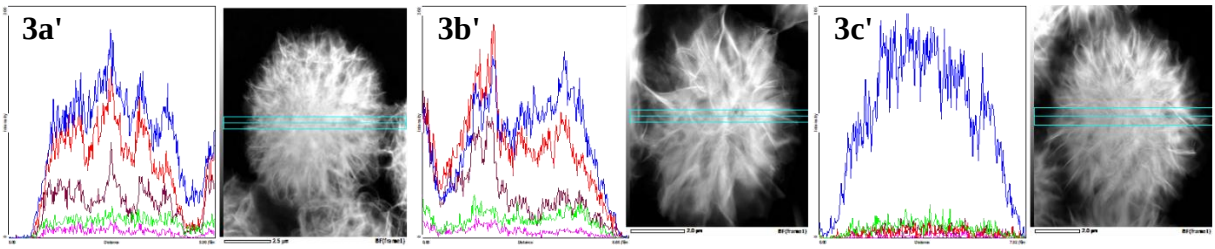

Figure 7-3. STEM images and component analysis results (by EDS measurement) of modified liposome surface

7-3.2 Stability of liposomes

The stability of copolymer coated liposomes (DOX encapsulated and without DOX) and uncoated liposomes (DOX encapsulated and without DOX) were investigated using particle size and ζ –potential measurement after keeping the samples at 37 ℃ for 3 and 6 days (1, 3 and 8 days for DOX encapsulated liposomes) in 1:1 D-PBS and serum mixed solution (**Figure 7-4)**. The particle size of copolymer **3a**, **3b** and **3c**-coated liposomes (without DOX) showed very little change after 3 and 6 days (not significantly different from the day 0) in 1:1 D-PBS and serum mixed solution, suggesting that the coating enhances the stability of the liposomes. In the case of **3a'** and **3c'** coated liposomes, the particle size decreased after 6 days, indicating closely packed structure (**Figure 7-4 (i))**. This close packing reduces the tendency of aggregation. In the case of the copolymer-coated DOX encapsulated liposome the particle size increased slowly (135 to 168 nm) over 8 days (**Figure 7-4 (iii))**.

The zeta potential of the copolymer-coated liposomes (DOX encapsulated and without DOX) and uncoated liposomes (DOX encapsulated and without DOX) were monitored (**Figure 7-4 (ii) & (iv))**. The zeta potential of the coated liposomes was increased after 1 days (DOX encapsulated) (**Figure 7-4 (iv))** and 3 days (without DOX encapsulated) (**Figure 7-4 (ii))**. The adsorption of copolymers on the surface of the liposomes might increases the zeta potential. The zeta potential value was observed to be stable after 3 days in case of **3a'** and **3b'** indicating the equilibrium state of adsorption (**Figure 7-4 (ii))**.

i.

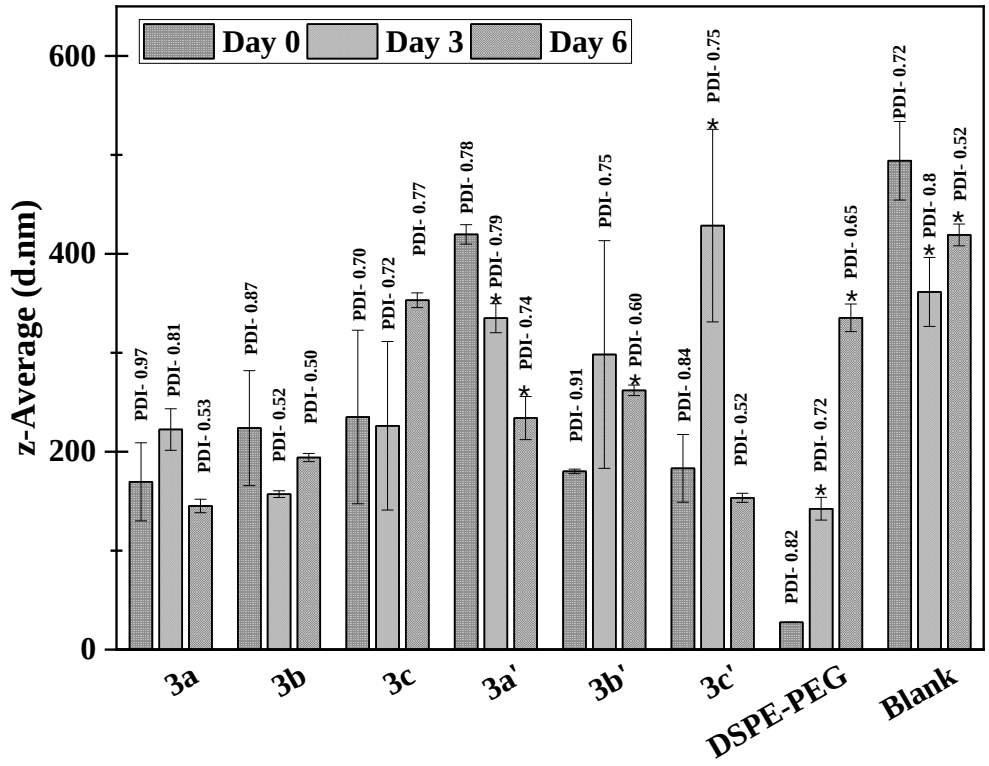
Day 0
Day 3
Day 6
z-Average (d.nm)
600
400
200
0
PDI- 0.97
PDI- 0.81
PDI- 0.53
PDI- 0.87
PDI- 0.52
PDI- 0.50
PDI- 0.70
PDI- 0.72
PDI- 0.77
PDI- 0.78
PDI- 0.79
PDI- 0.74
PDI- 0.91
PDI- 0.75
PDI- 0.60
PDI- 0.84
PDI- 0.75
PDI- 0.52
PDI- 0.82
PDI- 0.72
PDI- 0.65
PDI- 0.72
PDI- 0.8
PDI- 0.52
3a
3b
3c
3a'
3b'
3c'
DSPE-PEG
Blank

ii.

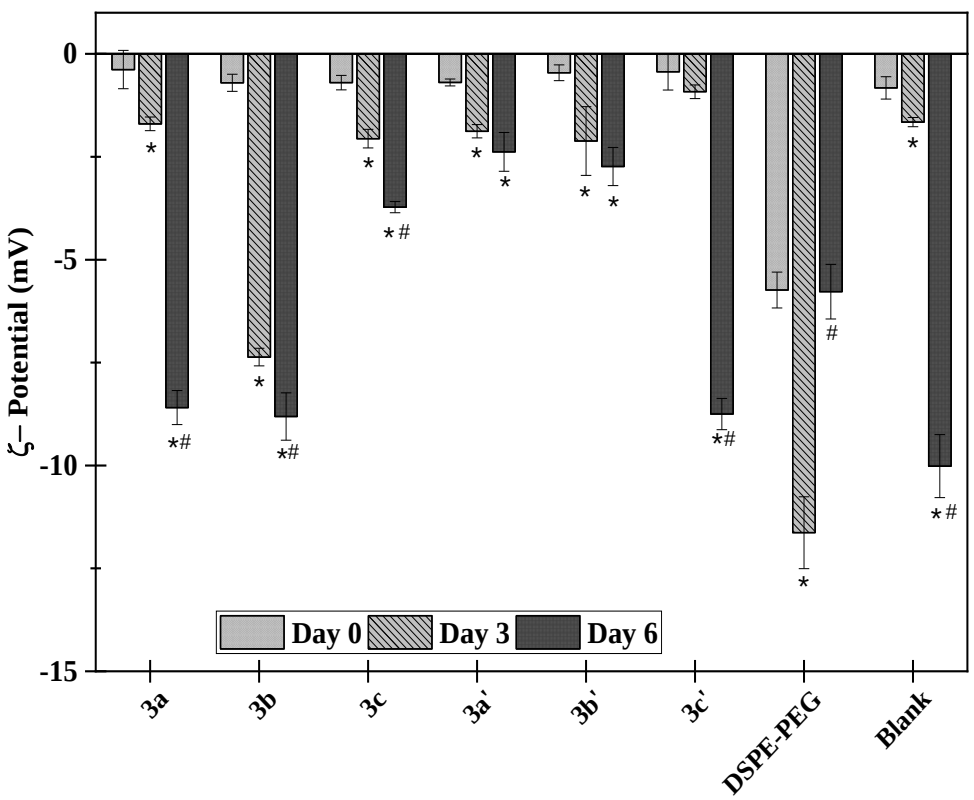
ζ– Potential (mV)
0
-5
-10
-15
Day 0
Day 3
Day 6
3a
3b
3c
3a'
3b'
3c'
DSPE-PEG
Blank

iii.

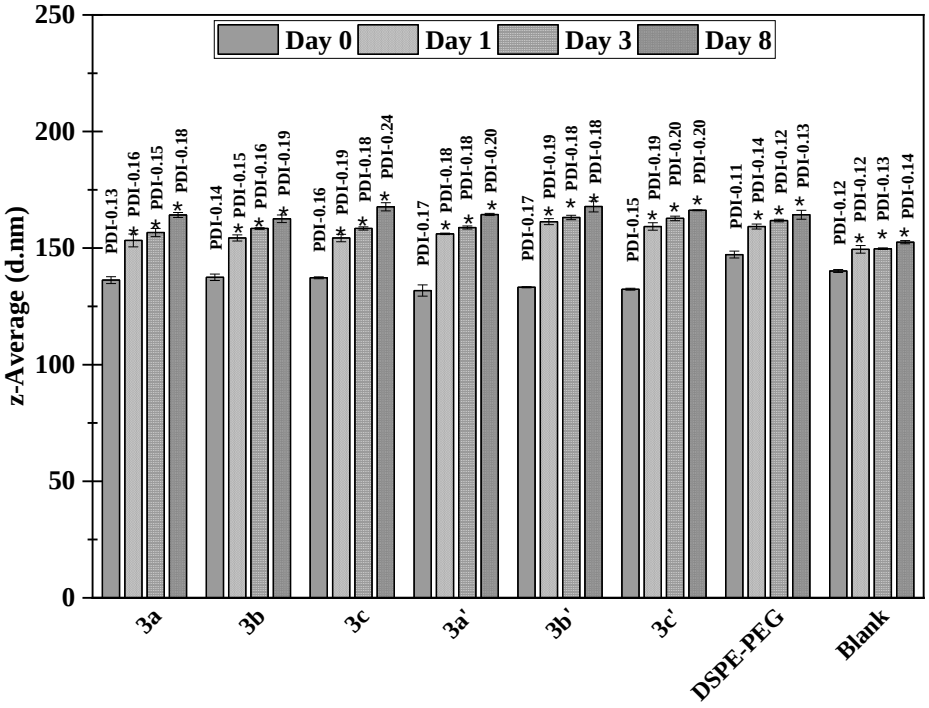

iv.

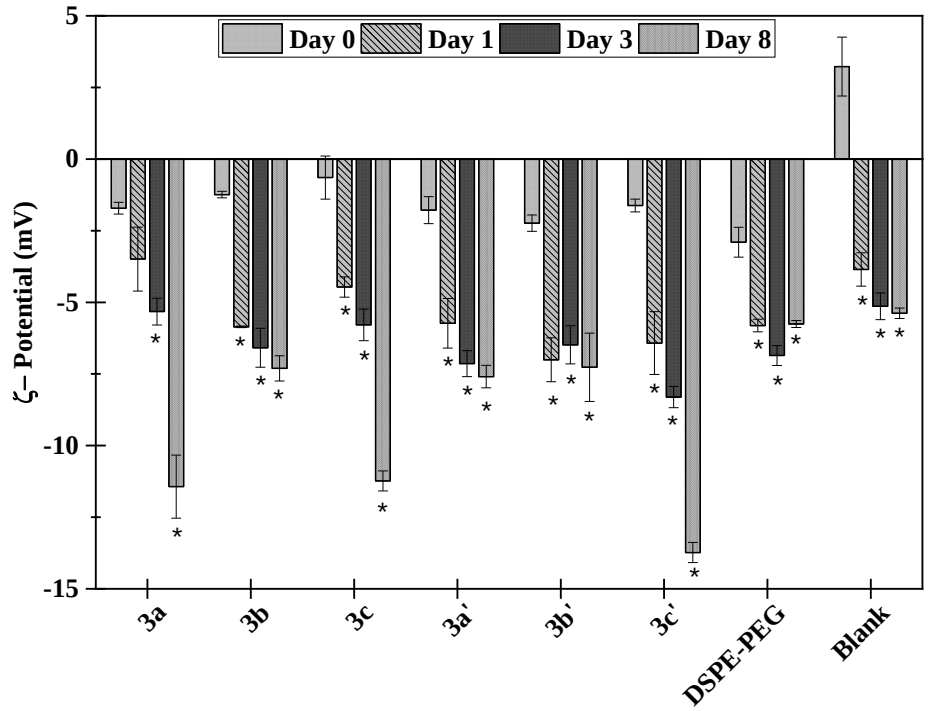

Figure 7-4. Results of stability measurement- **(i)** particle size (z-average value), **(ii)** ζ- potential of copolymer modified liposomes (without DOX) after 0, 3 and 6 days, **(iii)** particle size (z-average value), **(iv)** ζ- potential of copolymer-modified DOX encapsulated liposomes after 0, 1, 3 and 8 days keeping at 37 ℃ in 1: 1 D-PBS and serum mixed solution. (*) Statistically

significant different compared to Day 0 and (#) statistically significantly different compared to Day 3 [only in case of Fig. (ii)].

7-3.3 Effect of copolymers on the phase transition temperature of liposome membrane

The endothermic peak at about 53.3 °C corresponds to the gel-liquid crystalline phase transition temperature of HSPC[1] **(Figure 7-5 (i))**. After the addition of copolymers **3a-c**, the phase transition temperature shifted upward, indicating the liposome membrane become thermostable. The shift of the main phase transition temperature (53.3 °C) to a higher temperature side indicates miscibility and cooperative interaction between the liposome (HSPC) and the copolymers. The addition of **3c'** with liposomal system reduces the enthalpy (5.03 to 3.89 mJ/mg) of the phase transition. This phenomenon indicates that **3c'** limit the cooperativity of phospholipid structure in liposome. The **3c'** might act as membrane sealer and stabilize the membrane (low permeability). Addition of **3c'** helps in enhancing the stability against leakage of encapsulated molecules[1].

The **3c'** copolymer addition to the liposome decreases the ΔH but sharp endotherm appeared (**Figure 7-5 (ii)**). This abnormal behaviour might be due to the following reasons, a) **3c'** form copolymer rich micro-domain (which are although not detectable in endotherm) at water-lipid interface, b) the copolymer form micelle (not detectable under DSC) with phospholipid of the lipid bilayer, c) the accumulation of copolymer at bilayer surface (undetectable by DSC) disrupt the hydrogen bonding at the surface between the lipid molecule by diminishing the intermolecular interaction. In case of the other copolymer-coated liposomes (**3a**, **3b**, **3c**, **3a'** and **3b'**), the increase in ΔH might be due to an ordering effect of copolymer in forcing part of the molecule to align into the bilayer interior[13].

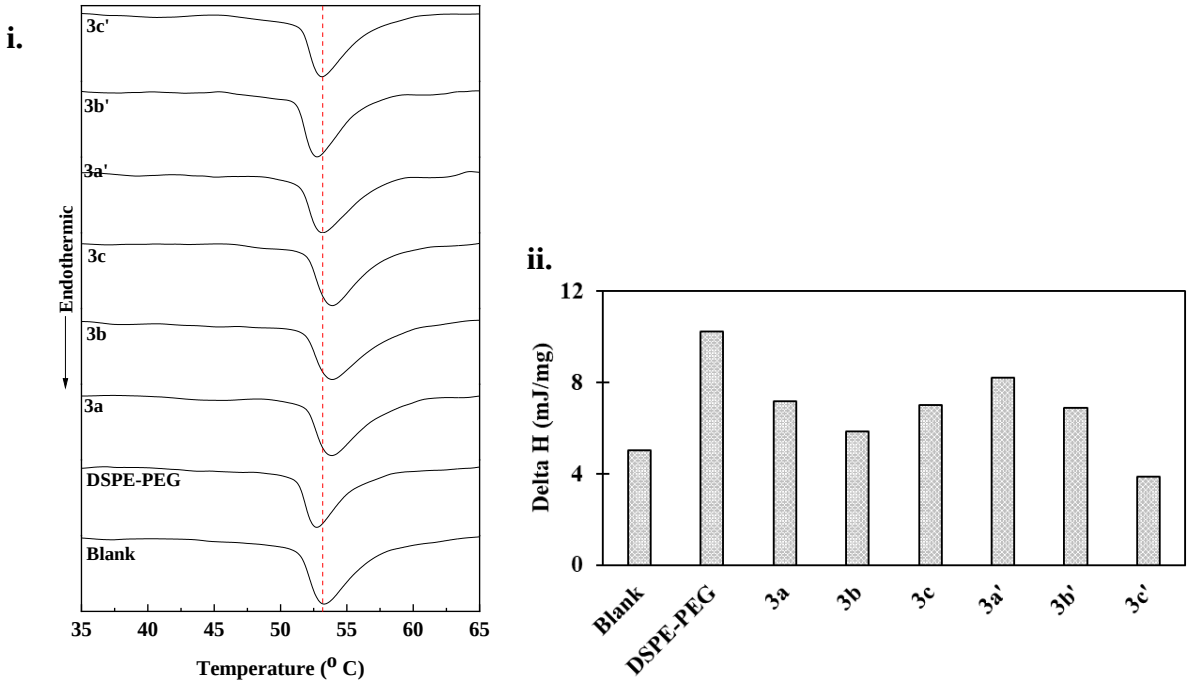

Figure 7-5. Results of liposome membrane stability measurement **(i)** DSC thermogram and **(ii)** ΔH value of the copolymer-modified liposomes (without DOX)

7-3.4 Uptake study

7-3.4.1 Qualitative uptake study

The *in vitro* intracellular localization of modified (coated with copolymers) DOX encapsulated liposomes in comparison to free DOX and blank (DOX encapsulated liposomes) was studied in HeLa cell line after 2 and 6 h incubation (**Figure 7-6 (i) & (ii)**). The red fluorescence intensity (red fluorescence signal) correspond to the free DOX. After 2 h, all the modified liposome (copolymer coated and DSPE-PEG-2000 modified liposome) samples showed weak fluorescent signal (**Figure 7-6 (i)**). The free DOX-treated liposome showed strong fluorescent intensity inside the cell. This phenomenon can be described by different cell penetration mechanism of free DOX. The free DOX molecule are hydrophobic and penetrate into the cell by slow and simple diffusion after dissolution in cell membrane. Diffusion is a kind of concentration gradient which mainly depends on the difference of free DOX concentration in and outside of cell membrane[12]. The modified liposome penetrates the cell by endocytosis mechanism. After six hours, the fluorescent intensity inside the cell was

observed to increase which indicates the increase in concentration of DOX inside the cell (copolymer **3b**, **3a'**, **3b'** and **3c'** modified liposome) (**Figure 7-6 (ii)**).

i.

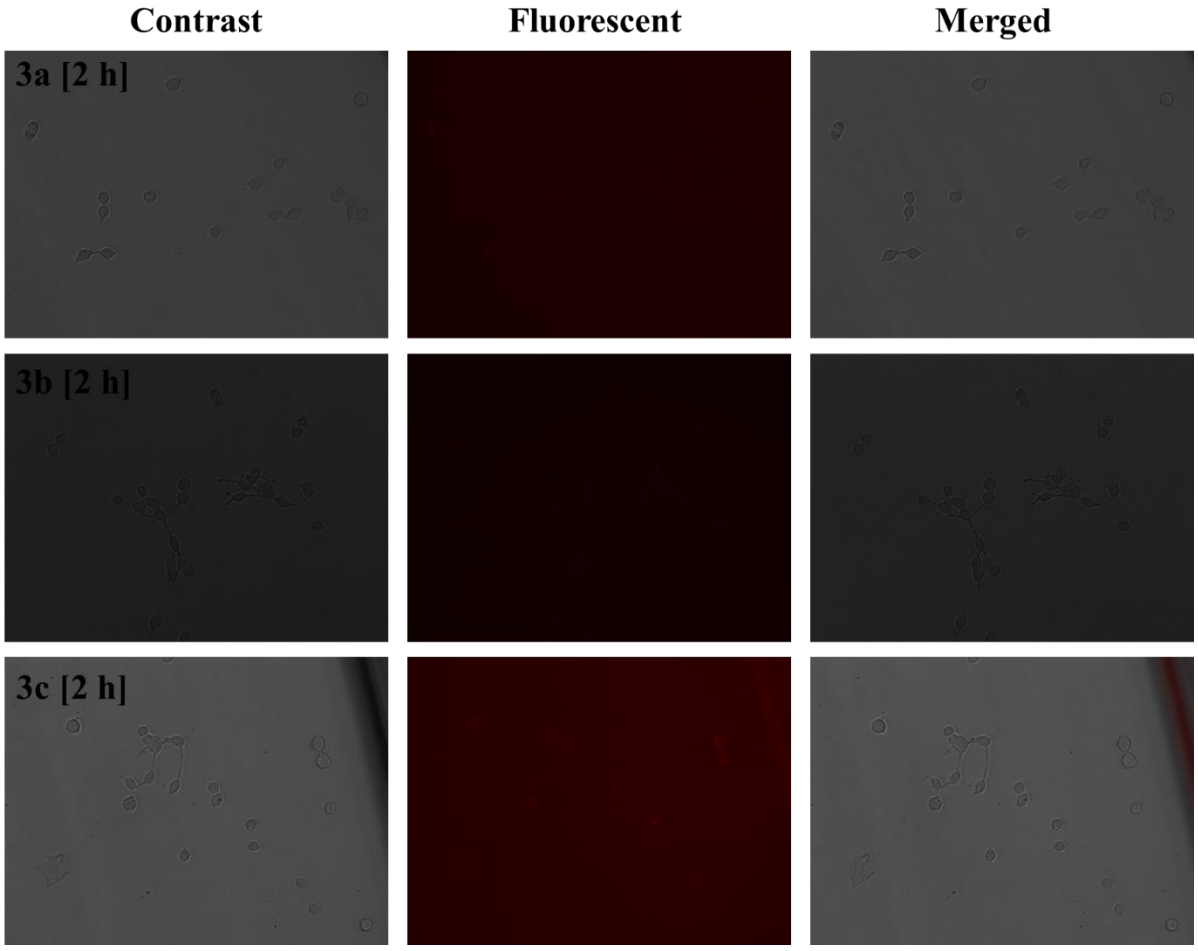

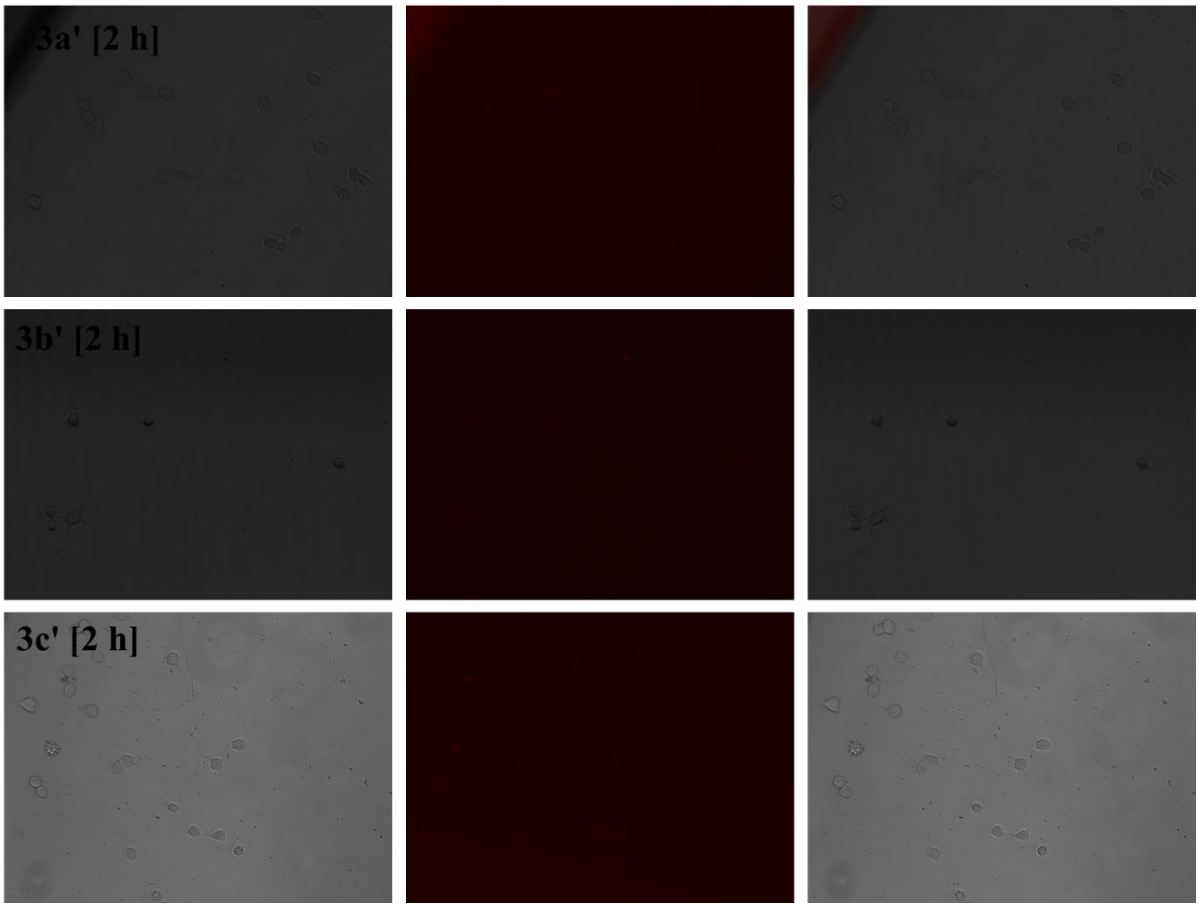
3a' [2 h]
3b' [2 h]
3c' [2 h]

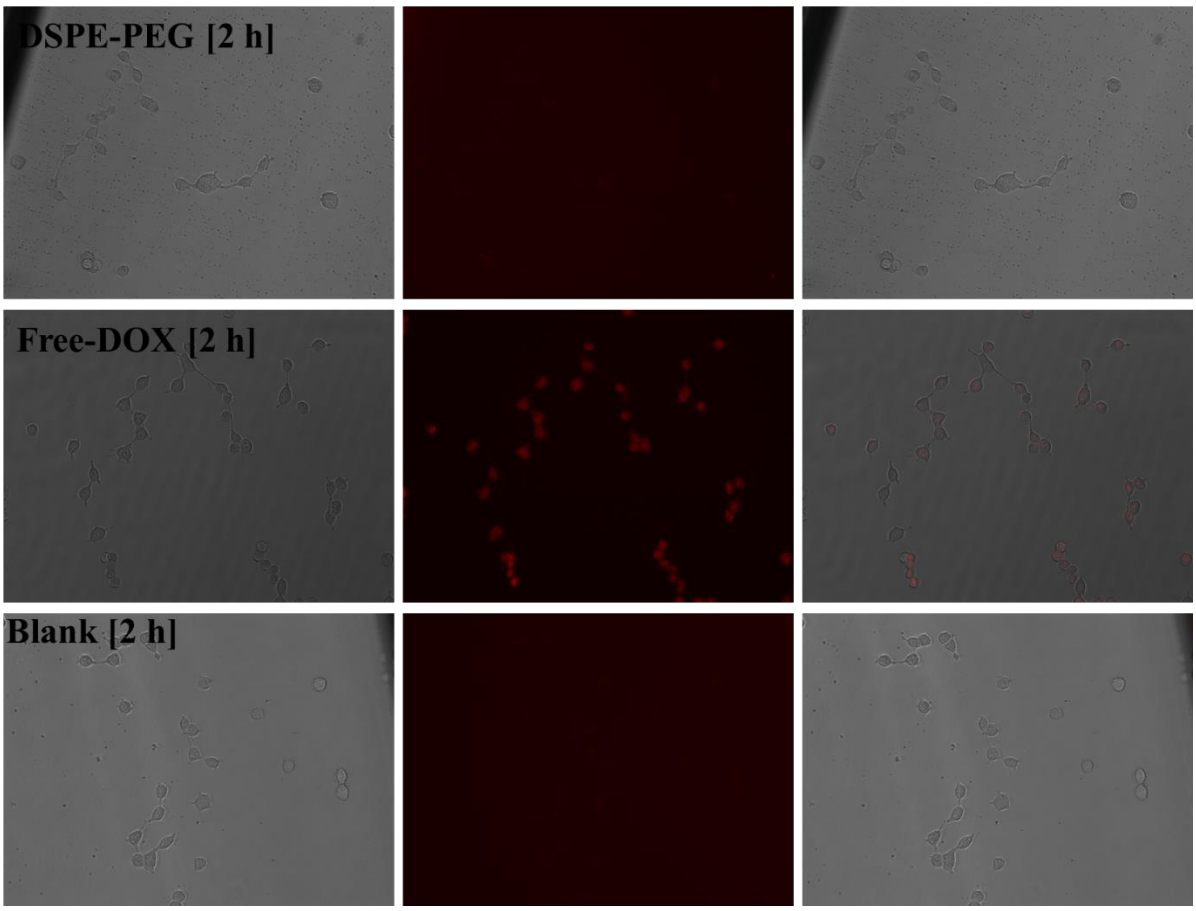
DSPE-PEG [2 h]
Free-DOX [2 h]
Blank [2 h]

ii.

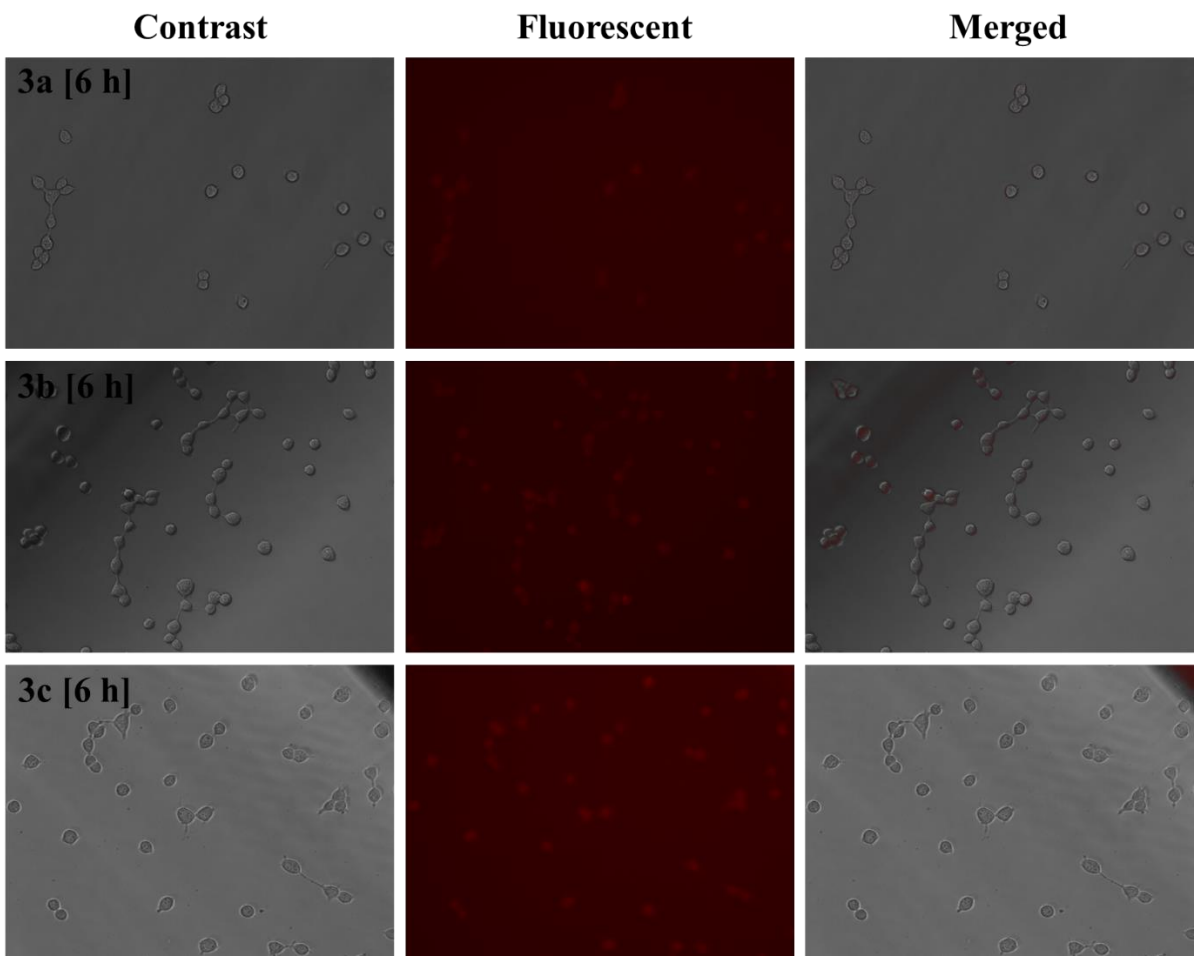

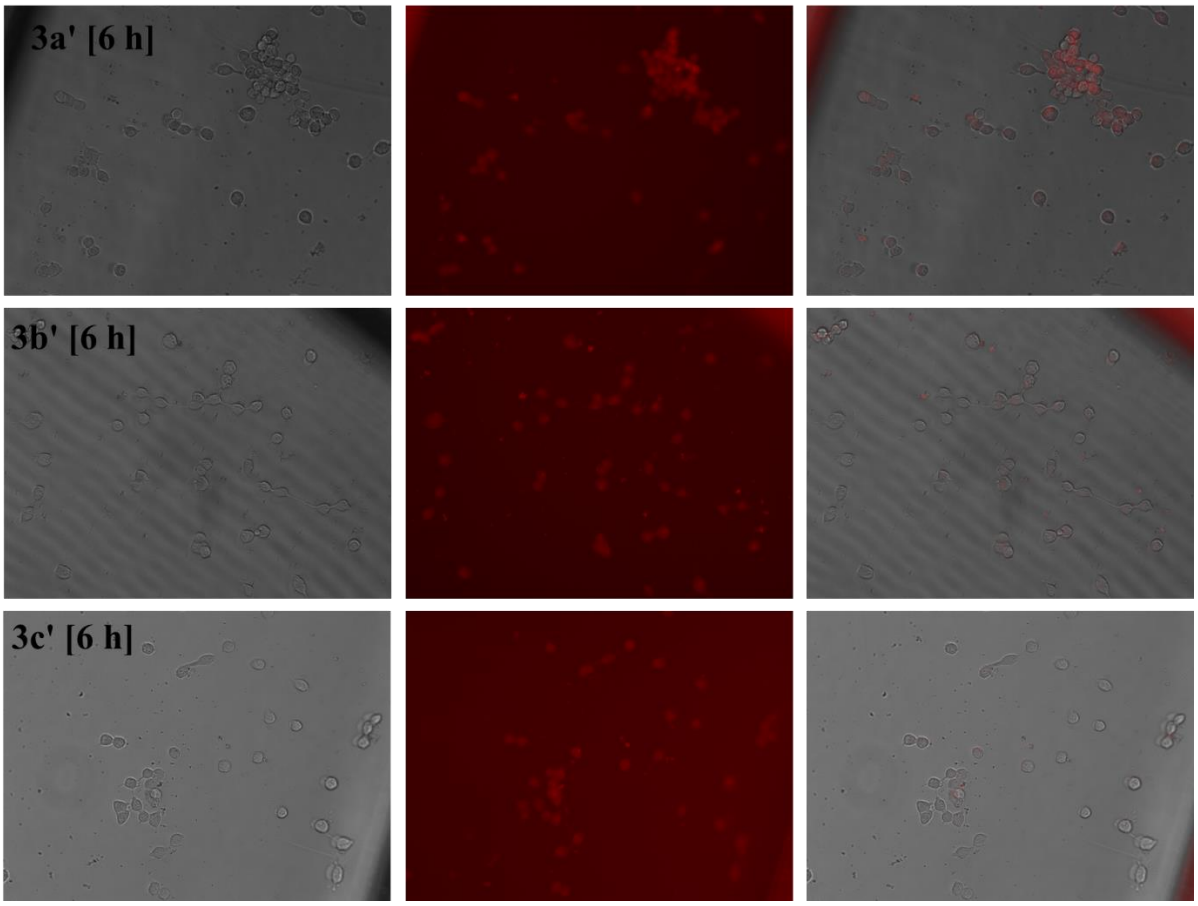
3a' [6 h]
3b' [6 h]
3c' [6 h]

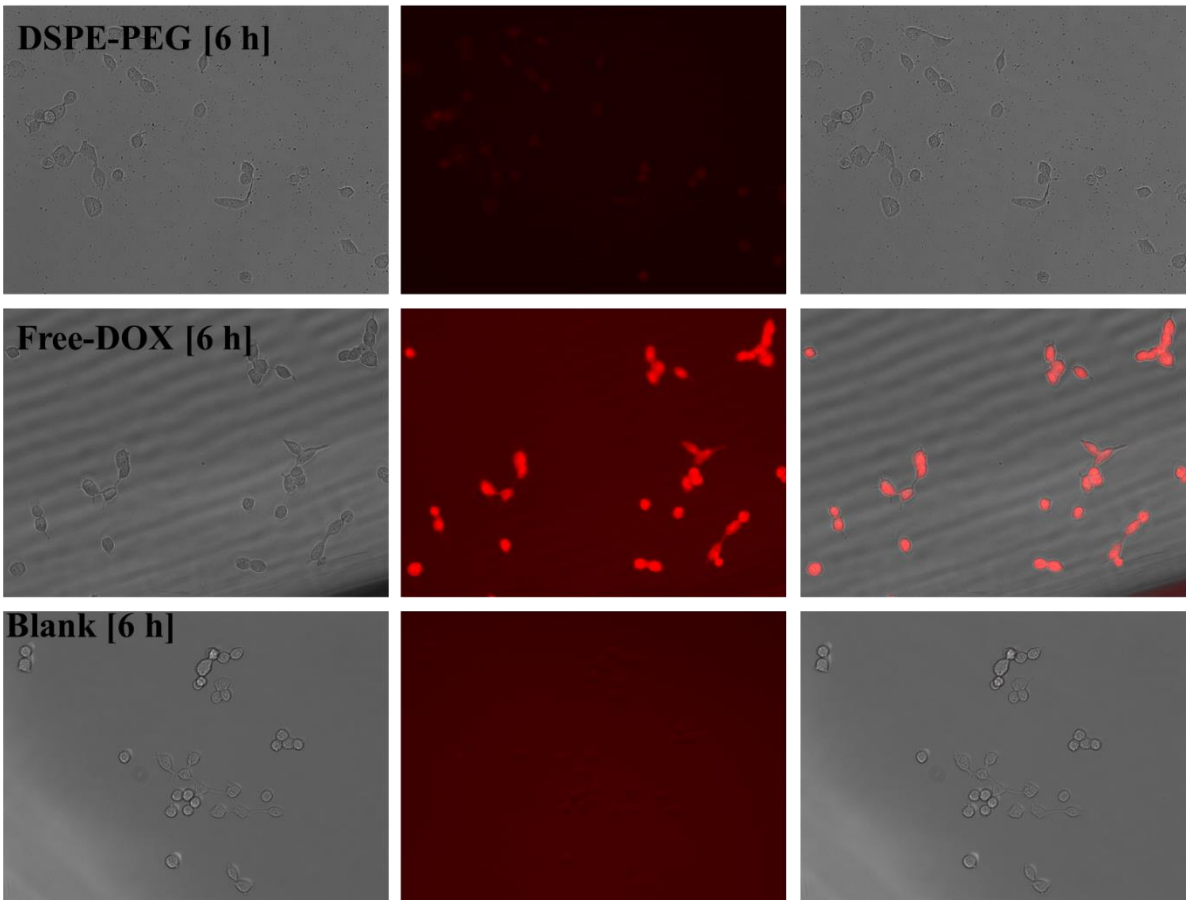

Figure 7-6. The Fluorescence microscopy images of HeLa cells treated with medium without a fluorescent probe containing liposome, free DOX and copolymer modified DOX encapsulated liposomes (DOX concentration 10 μg/ml seeded cell plate) after **(i)** 2 h and **(ii)** 6 h incubation.

7-3.4.2 Quantitative uptake study

The flow cytometry analysis was performed to measure the cellular uptake of modified (coated with copolymers) DOX encapsulated liposomes (**Figure 7-7**). The flow cytometry results are consistent with the visualization results. The free DOX showed strong fluorescent intensity than the modified liposomes due to different uptake mechanisms. Cellular uptake goes down for larger particles. The size of the liposomes was in the range of 230 to 270 nm. This might be the reasons for overall reduction of the cellular uptake of liposomes. Among the modified (coated with copolymers) DOX encapsulated liposomes, **3c**, **3a'**, **3b'** and **3c'**

copolymer-modified liposomes showed a little bit greater cellular uptake than DSPE-PEG-2000-modified liposome after 6 h, but there were no significantly different (**Figure 7-7 (iii)**). The copolymer contains MPC molecules, which have some affinity towards specific receptors expressed by most of the cells due to the phosphorylcholine group. Therefore, MPC molecules present on the surface of modified liposomes might contribute to the cellular uptake. However, the extent of the effect of MPC molecules on the liposomes seems to be not so strong.

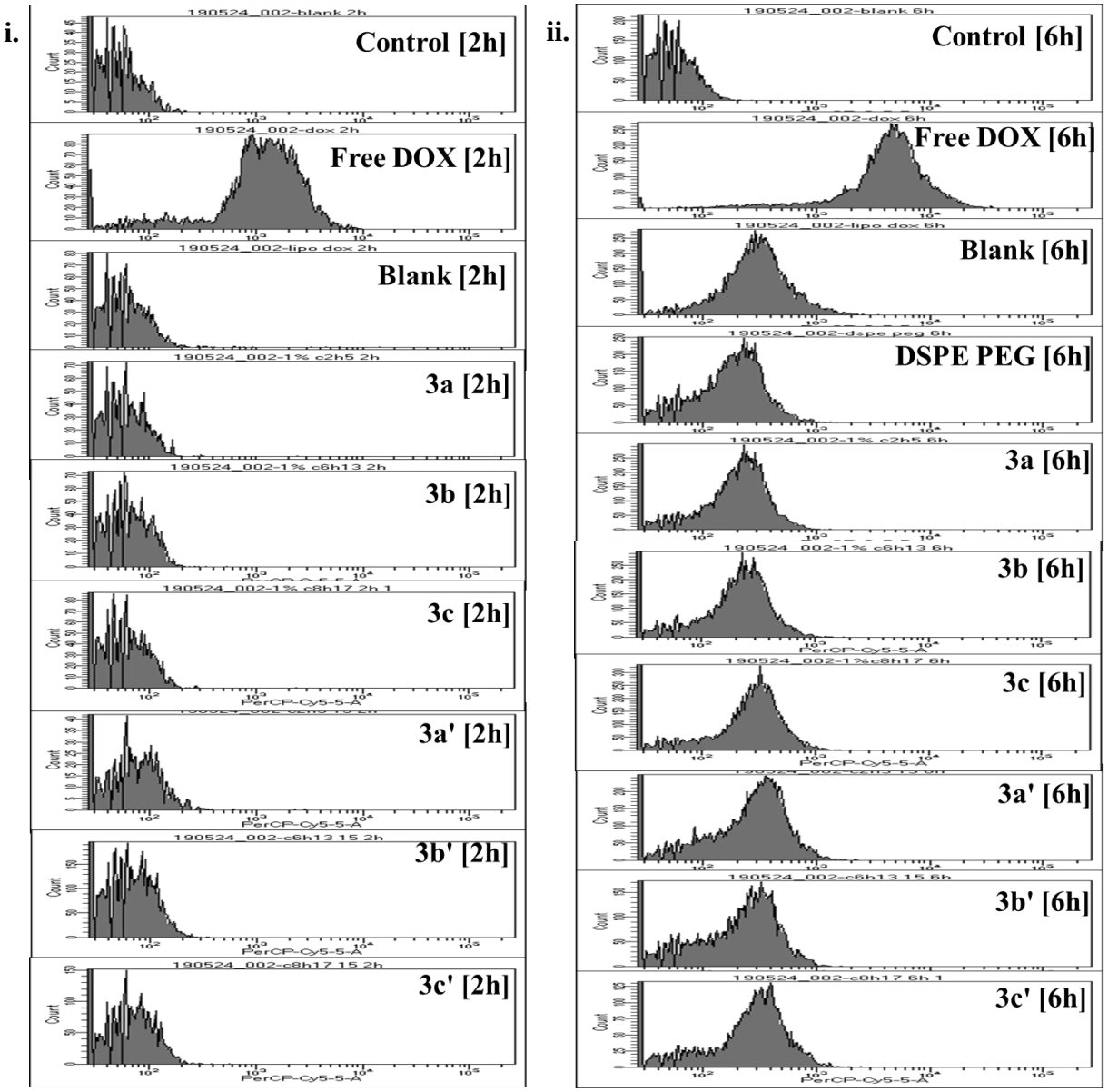

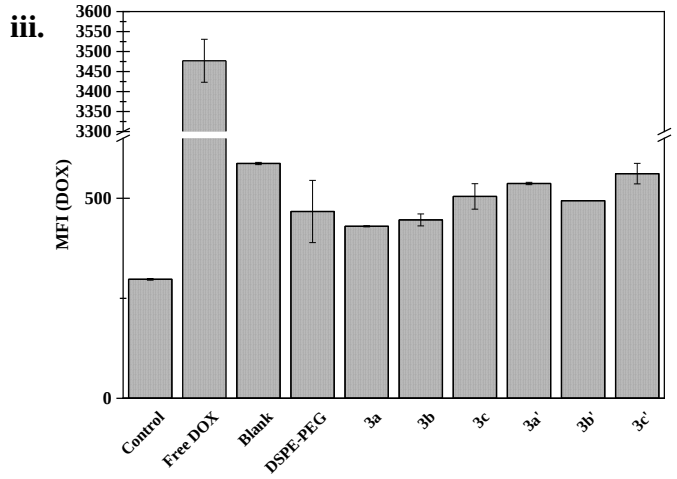

Figure 7-7. Flow cytometry data of **(i)** histograms (count vs fluorescence intensity) results of 2 h **(ii)** histograms (count vs fluorescence intensity) results of 6 h and **(iii)** mean fluorescent intensity for DOX encapsulated modified liposome (DOX concentration 10 μg/ml seeded cell plate) in HeLa cells after 6 h incubation. The mean fluorescence intensity was calculated by total 10000 events.

7-4. Conclusion

In this study, the HSPC/cholesterol liposome surface was modified by amphiphilic random and di-block copolymers containing MPC and POSS which was synthesized in **Chapter 2**. The liposomes modified with **3a**, **3a'** and **3c'** copolymers increased the stability of liposome for 6 days in 1:1 D-PBS and serum mixed solutions. The copolymer **3a-c** increased the thermal stability of the liposomes, and **3c'** helps in enhancing the stability against leakage of encapsulated molecules. The cellular uptake after 6 h was observed to be more in case of **3c**, **3a'**, **3b'** and **3c'** copolymer modified liposome than DSPE-PEG-2000 modified liposome. The MPC and POSS based random and di-block copolymers could be a good amphiphilic surface modifier of liposome for advancement of liposomal drug delivery, and further study can be done to investigate the potential as a replacement of DSPE-PEG-2000 modified liposome in future.

References

1. S. Petralito, R. Spera, S. Pacelli, M. Relucenti, G. Familiari, A. Vitalone, P. Paolicelli, M.A. Casadei, *Reactive & Functional Polymer,***2014,** 77, 30-38
2. K. Ishihara, R. Tsujino, M. Hamada, N. Toyoda, Y. Iwasaki, *Colloids and Surfaces B: Biointerfaces,* **2002,** 25, 325-333.
3. S. L. Regen, S. Aingh, G. Oehme, M. Singh, *J. Am. Chem. Soc.,***1982,** 104, 791.
4. H. H. Hub, B. Hupfer, H. Koch, H. Ringsdorf, *Angew. Chem. Int. Ed. Engl.,* **1982,** 19, 938.
5. H. Lamparski, Y. S. Lee, T. D. Sells, D. F. O'Brien, *J. Am. Chem. Soc.,***1993,** 115, 8096.
6. C. Dong, J. A. Rogers, *J. Controlled Release,***1991,** 17, 217.
7. M. C. Woodle, D. D. Lasic, *Biochim. Biophys. Acta,***1992,** 1113, 171.
8. H. Hayashi, K. Kono, T. Takagishi, *Biochim. Biophys. Acta,***1996,** 1280, 127.
9. J. Sunamoto, T. Sato, M. Hirota, K. Fukushima, K. Hiratani, K. Hara, *Biochim. Biophys. Acta,***1987,** 898, 323.
10. T. Ishida, H. Kiwada, *International Journal of Pharmaceutics,* **2008,** 354, 56–62
11. Q. Xu, Y. Tanaka, J. T. Czernuszka, *Biomaterials,* **2007**, 28, 2687–2694.
12. F. Ravar, E. Saadat, M. Gholami, P. Dehghankelishadi, M. Mahdavi, S. Azami, F. A. Dorkoosh, *Journal of Controlled Release*, **2016**, 229, 10-22.
13. S. Ali, S. Minchey, A. Janoff, E. Mayhew, *Biophysical Journal*, **2000**, 78, 246-256.

Chapter 8

General Conclusion

The purpose of this study is to design and develop amphiphilic copolymer with element block R-POSS methacrylate as stable hydrophobic domain and zwitterionic MPC molecule as a hydrophilic domain with improved thermal and mechanical properties which can be applied in the coating of biomaterial surface and enhancement of the encapsulation and delivery of the hydrophobic drug molecules. The new approach of designing and synthesis of element block (R-POSS) as hydrophobic domain, help in enhancing and tuning the properties of MPC based copolymers and extend their range of biomedical applications. The scientific and biological evaluation of R-POSS and MPC-based copolymers revealed the interesting feature which is highly motivating requisite for its application in various field of pharmaceutical science.

In **Chapter 2**, the results of the study indicated the successful design and synthesis of R-POSS and MPC based copolymer following free radical and RAFT polymerization techniques to obtain random and di-block copolymer respectively. The solubility of random copolymers in a polar solvent (water, methanol and ethanol) reduced abruptly due to the strong interaction of R-POSS moiety with phosphorylcholine (PC) group which is responsible for water solubility. All three random copolymers have shown remarkable improvement in T_g and thermal stability. The results also indicated no crystallization phase of R-POSS moiety in the randon copolymer. The RAFT polymerization could lead to controlling the sequence of R-POSS and MPC. The degree of polymerization of the di-block copolymer was calculated to be 12-13 (R-POSS), which was governed by the same monomer/initiator ratio. The molecular weight of copolymers (random) is in the range of 10^5 whereas in case of the di-block copolymer (RAFT) it is in 10^4 range. The control over the molecular weight, molecular weight distribution and site-specific functionality was the advantage of RAFT polymerization technique over the free radical polymerization. The successful design, synthesis and investigation of the properties of R-POSS and MPC-based copolymer (synthesized following two different polymerization technique) help in understanding the contribution of hydrophobic moiety R-POSS in the copolymer for it various field of application.

In **Chapter 3**, the synthesized random copolymer was studied focusing their application in the field of polymeric material for coating of cardiovascular implant fabrication and their coating. The promising results confirmed their high need in this particular area. The mechanical strength of the copolymer composed of C_2H_5-POSS improved due to the even distribution of C_2H_5-POSS moiety on polymer matrix and restricted mobility of the polymer chain. The hydrophobic C_2H_5-POSS moiety restricted the mobility of MPC molecule and increased the surface hydrophobicity at water polymer interface. The C_2H_5-POSS moiety disrupted the hydration layer surrounding the phosphorylcholine (PC) group which was responsible for resistance to the protein adsorption and cell adhesion on the surface. The hydrophobic C_2H_5-POSS moiety uniformly dispersed in MPC polymer matrix and support controlled protein adsorption, cell attachment and cell spreading on the surface. Therefore, the C_2H_5-POSS and MPC random copolymer fulfill all requisite characteristics for its application especially as coating material of the cardiovascular implant.

In **Chapter 4**, the synthesized random copolymer was studied focusing its application for solubilization of hydrophobic anti-cancer drugs like paclitaxel and their delivery as a carrier molecule due to its amphiphilic nature. The R-POSS and MPC random copolymers could form a stable association structure (size 65 – 80 nm) in the aqueous environment due to hydrophobic interaction of R-POSS moiety. The C_2H_5-POSS and MPC random copolymer observed highly biocompatible and effectively solubilized the poorly water-soluble drug paclitaxel forming a stable association. The paclitaxel solubility was concentration dependence and found in the order of $C_2H_5 > C_6H_{13} > C_8H_{17}$. The hydrophobic C_2H_5-POSS moiety strongly interacted with paclitaxel and controlled its release rate in an aqueous environment. The results obtained from the cell viability study in presence of paclitaxel solubilized C_2H_5-POSS based MPC random copolymer and in vitro paclitaxel release (from paclitaxel solubilized C_2H_5-POSS based MPC random copolymer association) study supported the phenomenon. The cell viability was observed 87 ± 24 % after 24 h incubation at pH 7 and in vitro paclitaxel release was observed around 30% in 24 h. The C_2H_5-POSS based MPC random copolymer was internalized by the cells through cellular uptake mechanism. Therefore, C_2H_5-POSS and MPC based copolymer possess promising characteristics as polymeric biomaterials for enhancing the solubility and delivery of poorly water-soluble component like a drug, imaging probs etc.

In **Chapter 5**, the solid formulation of paclitaxel was prepared using C_2H_5-POSS and MPC based random copolymer as amphiphilic solubilizer and PVP as hydrophilic carrier

molecule of paclitaxel. The solid formulation containing C_2H_5-POSS and MPC based random copolymer formed single phase homogeneous formulation and enhance the dissolution rate of paclitaxel. The C_2H_5-POSS and MPC based random copolymer improved wettability and facilitated the rapid and complete release of paclitaxel (~ 90%) within 40 min. The C_2H_5-POSS and MPC based random copolymer interacted with PTX and reduced the mobility of amorphous PTX, which help in the enhancement of the dissolution. Therefore, C_2H_5-POSS and MPC based random copolymer could be a promising amphiphilic solubilizing material to enhance the dissolution of the poorly water-soluble drug from the solid formulation.

In **Chapter 6**, the synthesized di-block copolymer was studied focusing its application in delivery and encapsulation of poorly soluble drug forming stable micelle system. The R-POSS and MPC based di-block copolymer formed micelles (size 26-43 nm) in an aqueous environment and the aggregation ability in the order of C_2H_5 > C_6H_{13} > C_8H_{17}. The size distribution of C_2H_5-POSS based di-block copolymer was extremely small and the results indicated the formation of the tightly packed association. The C_2H_5-POSS and C_8H_{17}-POSS based di-block copolymer were highly stable even after drug loading. The drug loading capacity and efficiency of the polymeric micelles were highly dependent on the structure of drug molecules. The drug-containing long aliphatic chain compatible with aliphatic core region of the polymeric micelles due to strong hydrophobic interactions. The strong interaction between the drug molecule and polymeric micelles leads to the negligible release of drug as most of the drug remains inside the micelles. The cell viability was almost 90 % in all the PTX-loaded di-block copolymers after 24 h, and around 50 % after 48 h of incubation. These results supported the phenomenon of negligible drug release. The cellular uptake of C_2H_5-POSS based di-block copolymer was significantly smaller than C_6H_{13}-POSS, C_8H_{17}-POSS and free drug due to its tightly packed association state and relatively harder morphology. The cellular uptake of R-POSS and MPC based di-block copolymer was governed by the strong affinity of MPC molecules towards specific cell membrane receptors. Therefore, the R-POSS and MPC based di-block copolymer could be a promising candidate for controlled stable micelle formation and selective hydrophobic drug encapsulation and drug delivery.

In **Chapter 7**, study on stability enhancement of liposome by surface modification using synthesized random and di-block copolymers was performed. The obtained results suggested the enhancement in the stability of liposome by maintaining the size for 6 days and also stability against leakage of encapsulated molecules. Overall, the random copolymers were preferable

for the liposome coating in terms of the stability. The cellular uptake of copolymer modified liposome was observed to be comparable with that of DSPE-PEG-2000 modified liposome after 6 h. The cellular uptake was governed by the affinity of MPC molecule towards cellular membrane. Therefore, the modification of liposome using POSS-MPC-based random and di-block copolymer could be a promising approach for enhancing the stability of liposome.

Overall, the effect of the alkyl chain length of the vertex R-groups [ethyl (C_2H_5), hexyl (C_6H_{13}), octyl (C_8H_{17})] of R-POSS methacrylate in both types of the R-POSS and MPC-based copolymer (random and di-block) were systemically studied. The molecular weight and association behavior of R-POSS and MPC based di-block copolymer was found to be controlled in a better way by controlling the degree of polymerization than that in R-POSS and MPC-based random copolymer where the control over the molecular weight and also the association behavior is difficult. This control on molecular weight and association behavior leads to formation of micelles from di-block copolymer in an aqueous environment with size range of 26-43 nm which is maintained even after drug loading. Thus, higher cellular uptake could be obtained from R-POSS and MPC based di-block copolymer which additionally showed encapsulation of the hydrophobic drug in the core of the tightly packed associated micelle leading to negligible drug release. The application of the copolymers can be extended for the stabilization of liposome by surface modification. This can be considered as a good alternative for DSPE-PEG-2000 modified liposome which has shown limitations in the clinical applications.

The innovative biomaterial for the advancement of medical treatment and diagnosis is the urgent need in the medical and pharmaceutical field. The advancement of medical diagnosis and treatment will improve the quality of human life. The systemic study in this thesis revealed that element block R-POSS as a hydrophobic domain is highly promising to improve bulk and solution properties of polymeric material. The proper selection and modification of R-group in the POSS cage could develop the biomaterial for advanced application. The element block R-POSS in combination with MPC has the potential to develop new polymeric biomaterial which will improve the quality of the medical and pharmaceutical system. The author firmly believes that R-POSS and MPC-based polymeric biomaterial will be explored more for the development of advanced biomaterial in the future.

Appendix

List of Publications and Presentations

1. List of Publication:

1. **S. CHATTERJEE**, T. Matsumoto, T. Nishino and T. Ooya, Tuned Surface and Mechanical Properties of Polymeric Film Prepared by Random Copolymers consisting of Methacrylate- POSS and 2-(Methacryloyloxy) ethyl Phosphorycholine, *Macromol. Chem. Phys.* **2018**, *219*, 1700572.
   DOI: https://doi.org/10.1002/macp.201700572

2. **S. CHATTERJEE** and T. Ooya, Hydrophobic Nature of Methacrylate-POSS in Combination with 2-(Methacryloyloxy) ethyl Phosphorylcholine for Enhanced Solubility and Controlled Release of Paclitaxel, *Langmuir*, **2019**, *35* (5), 1404–1412.
   DOI: 10.1021/acs.langmuir.8b01588

3. **S. CHATTERJEE** and T. Ooya, Amphiphilic Copolymer of Polyhedral Oligomeric Silsesquioxane (POSS) Methacrylate for Solid Dispersion of Paclitaxel, *Materials* **2019**, *12*, 1058.
   DOI: 10.3390/ma12071058

4. **S. CHATTERJEE**, M. Oshio, S. Yusa and T. Ooya, Controlled Micelle Formation and Stable Capture of Hydrophobic Drugs by Alkylated POSS Methacrylate Block Copolymers, *ACS Applied Polymer Materials* **2019**. (**Accepted**)

   DOI: 10.1021/acsapm.9b00412

5. **S. CHATTERJEE** and T. Ooya, Poly[2-(Methacryloyloxy)ethyl Phosphorylcholine]-modified (PMPCylated) liposome Comparing with PEGylated liposome, **2019**, (**To be Submitted**)

2. List of Presentation:

2.1 Oral Presentation

1. **S. CHATTERJEE**, T. Matsumoto, T. Nishino and T. Ooya, POSS 2- (Methacryloyloxy) ethyl Phosphorycholine (MPC)) based copolymers for controlling surface and bulk properties, Presentation in The Society of Polymer Science, Japan (SPSJ), July'2018, Kobe, Japan.

2. **S. CHATTERJEE** and T. Ooya, Synthesis and Characterization of Element block based 2- (Methacryloyloxy) ethyl Phosphorycholine (MPC) copolymers for biomedical applications, Paper Presentation, 6th Asian Biomaterial Congress, October'2017, India.

3. **S. CHATTERJEE**, M. Oshio, S. Yusa and T. Ooya Novel Amphiphilic Copolymers of Methacrylate-POSS in Combination with MPC monomer for Pharmaceutical Applications, Presentation in 68th SPSJ Annual Meeting, May'2019, Osaka, Japan.

4. **S. CHATTERJEE** and T. Ooya, Amphiphilic Copolymer of MPC and Polyhedral Oligomeric Silsesquioxane (POSS) Methacrylate as a Simple Modifier for Liposome, Presentation in The 65th Kobunshi Kobe, July '2019, Kobe, Japan.

2.2 Poster Presentation

1. **S. CHATTERJEE** and T. Ooya, Study on Solubility of Paclitaxel using Element Block Methacrylate-POSS-based 2-(Methacryloyloxy) ethyl Phosphorylcholine (MPC) Copolymer, Poster Presentation in APSMR, Hokkaido, July'2018, Hokkaido, Japan.

2. **S. CHATTERJEE** and T. Ooya, Approach to modulation of surface and bulk properties using an Element Block Copolymer, Poster Presentation, Frontier Workshop for Young Student of Kobe University, December'2017, Kobe, Japan.

Doctoral Dissertation, Kobe University

"Study on Polyhedral Oligomeric Silsesquioxane (POSS) Methacrylate-based copolymers for biomedical applications", 184 Pages

Submitted on 07/17/2019